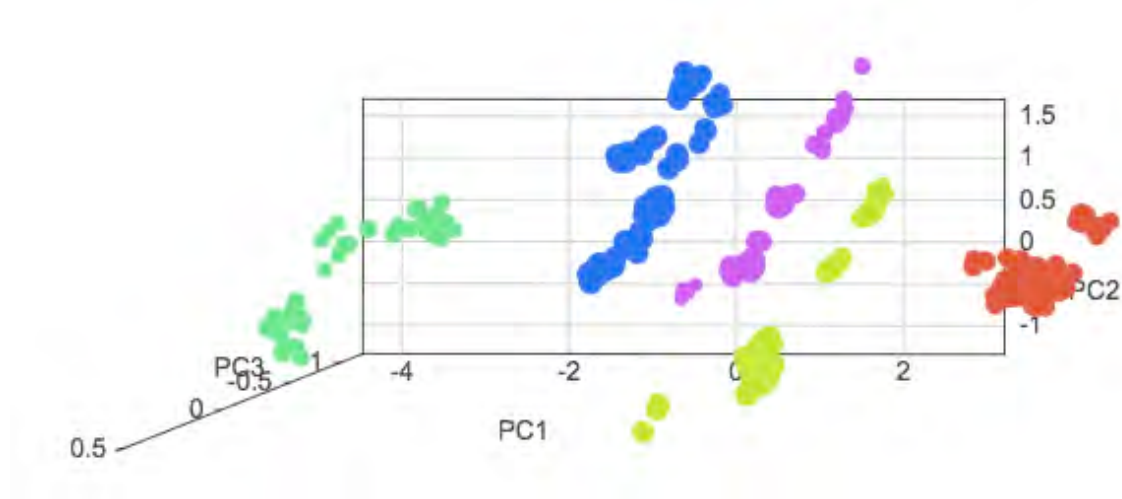




DEPARTMENT OF CONSERVATION

# SCANDINAVIAN ROCK ART PIGMENTS AND THEIR PREPARATION

-A Pilot Study on the Use of *SCiO* in Heritage  
Science



**Ingrid Sogaard**

Degree project for Master of Science with a Major in Conservation  
2018, 30 HEC  
Second Cycle  
2018:24





# **Scandinavian Rock Art Pigments and Their Preparation**

- A Pilot Study on the Use of *SCiO* in Heritage Science

Ingrid Søgaaard

Supervisor: Jacob Thomas, PhD

Degree project for Master of Science with a Major in Conservation

UNIVERSITY OF GOTHENBURG  
Department of Conservation  
P.O. Box 130  
SE-405 30 Gothenburg, Sweden

<http://www.conservation.gu.se>  
Fax +46 31 7864703  
Tel +46 31 7864700

Master's Program in Conservation, 120 ects

Author: Ingrid Søgaaard  
Supervisor: Jacob Thomas

Title: Scandinavian Rock Art Pigments and Their Preparation - A Pilot Study on the Use of *SCiO* in Heritage Science

#### ABSTRACT

This Master's thesis focuses on firing, aging and provenance of ochres and ochreous soils. It investigates which preparation methods are most significant as separation factors when near infrared (NIR) spectra of prepared pigments are statistically processed. It is performed from a rock art and heritage science perspective. One of the aims of this project is to serve as a pilot study on the application of *SCiO*®- a commercial, pocket-size NIR spectrometer - for pigment examinations. An experimental research outline sheds light on the studied objects: six soil samples from Denmark and Sweden and three artistic pigments were fired at 300°C, 600°C and 900°C for different periods of time. The pigments were applied on a rock surface with water and blood as binding media. One sample was prepared for natural outdoor exposure. All samples were analysed with *SCiO*. Principal component analyses (PCA) and cross-validation models based on *SCiO*-spectra were used to find patterns of statistical separation. Some samples were complementarily analysed with scanning electron microscopy-energy-dispersive X-ray spectroscopy. Literature studies were inspirational for the experimental setup and enable interpretation of the results. The Swedish Tumlhed rock painting is included as a case study where the results from the experiment are related back to the rock painting. *SCiO*'s spectral range is limited (700-1100nm) but some information can still be derived from the spectra of prepared pigments. PCA-plots and models show that firing temperature can separate samples from the same location. Samples can, to some extent, be ascribed to main provenance groups ('Denmark', 'Sweden' or 'other') regardless of heating temperature; although, firing is necessary. Iron content differences between Swedish samples are plausible explanations for PCA separation. Age (or exposure) seems to make some separations, also in terms of the type of binding media. When making a PCA-plot with *SCiO*-scans from Tumlhed rock painting, a noticed separation is visible between water related figures and a deer figure. Suggestions for this separation are either that the pigments have been fired at different temperatures (or same temperature for different time periods) or that the wavy patterns and a fish have been painted with pigment sourced from an aqueous environment (such as a stream) whereas the pigment for painting the deer is derived from ochreous soils. Sample set size, and the limitations of *SCiO* and the software that is supplied with the *SCiO* most definitely have negative impact on the results. *SCiO* is, without calibration, mostly suitable as a screening tool.

Title:

Language of text: English

Number of pages:

3-5 Keywords: NIR, red earth, ochre, PCA, SEM-EDX

ISSN 1101-3303

ISRN GU/KUV—18/24 — SE



## Table of Contents

<b>Preface</b> .....	<b>7</b>
<b>1. Introduction</b> .....	<b>9</b>
<b>1.1 Background</b> .....	<b>9</b>
1.1.1 Near Infrared Spectroscopy and Swedish Rock Paintings .....	9
1.1.2 The Starting Point of The Master’s Project.....	10
<b>1.2 Research Question</b> .....	<b>10</b>
<b>1.3 Purpose and Aim</b> .....	<b>10</b>
<b>1.4 Methodology</b> .....	<b>11</b>
1.4.1 Analytical Methods .....	11
<b>1.5 Limitations</b> .....	<b>13</b>
<b>1.6 Theoretical Setting</b> .....	<b>14</b>
<b>1.7. Ethical Statement</b> .....	<b>14</b>
<b>1.8 Previous Research</b> .....	<b>14</b>
1.8.1 The Formation of Some Iron Oxides.....	14
1.8.2. Near infrared spectroscopy for analysis of ochre pigments and ochreous soils.....	15
1.8.3 Pigment Preparation and Heating .....	17
1.8.4 Ageing and Binding Media .....	21
1.8.5 Provenance Studies of Ochre and Ochreous Soils .....	23
<b>1.9 Hypotheses</b> .....	<b>25</b>
<b>2. Material and Methods</b> .....	<b>26</b>
<b>2.1 Materials</b> .....	<b>26</b>
2.1.1 Ochreous Soil Samples.....	26
2.1.2 Manufactured and Received Pigments .....	29
2.1.3 Rock Surfaces.....	30
2.1.4 Binding Media .....	30
2.1.5 Tumlhed Rock Painting .....	30
<b>2.2 Sample Preparation</b> .....	<b>31</b>
2.2.1 Aging Experiment .....	31
2.2.2 Grinding and Sieving.....	32
2.2.3 Firing Experiments .....	33
2.2.4 Preparing the New Rock Slabs.....	35
2.2.5 SEM-EDX Sample Preparation.....	35
<b>2.3 Methods</b> .....	<b>35</b>
2.3.1. SEM-EDX – Execution and Instrument Settings .....	35
2.3.2 SCiO and the Accompanying Web Software .....	36
<b>3. Results and Discussion</b> .....	<b>39</b>
<b>3.1 Visual Colour</b> .....	<b>39</b>
<b>3.2 Chemical Composition – SEM-EDX with Backscattered Electrons</b> .....	<b>40</b>
<b>3.3 Crystal Morphology – SEM-EDX with secondary electrons</b> .....	<b>41</b>
<b>3.4 The ‘Hidden’ Information in SCiO-spectra</b> .....	<b>46</b>
3.4.1 Separating the Paint Layer from the Background .....	46
3.4.2 All Samples and SNV.....	47
3.4.3 Temperature.....	47
3.4.4 Age and Binding Media.....	54
3.4.5 Provenance .....	57
3.4.6 Tumlhed Spectra.....	62
<b>3.5 Only Rock Art?</b> .....	<b>64</b>
<b>4. Conclusions</b> .....	<b>65</b>

<b>5. Summery .....</b>	<b>66</b>
<b>5.1 Summarised Introduction .....</b>	<b>66</b>
<b>5.2 Summarised Materials and Methods .....</b>	<b>66</b>
<b>5.3 Summarised Results and Discussion .....</b>	<b>67</b>
<b>5.4 Summarised Conclusions .....</b>	<b>68</b>
<b>List of Figures.....</b>	<b>69</b>
<b>List of Tables .....</b>	<b>72</b>
<b>References .....</b>	<b>73</b>
<b>Unpublished.....</b>	<b>73</b>
<b>Electronic sources .....</b>	<b>73</b>
<b>Published.....</b>	<b>74</b>
<b>Appendix I – Report on SCiO.....</b>	<b>I</b>
<b>Appendix II - Newspapers.....</b>	<b>XV</b>
<b>Appendix III – All Rock Slabs .....</b>	<b>XVIII</b>
<b>Appendix IV – Painted Samples on Rock.....</b>	<b>XIX</b>
<b>Appendix V – Samples on Carbon Tape.....</b>	<b>XXIV</b>
<b>Appendix VI - SEM-EDX Spectra and Images.....</b>	<b>XXVII</b>
<b>Appendix VII – Complimentary SCiO Images .....</b>	<b>XLVII</b>
<b>Appendix VIII – Å Temperature Model.....</b>	<b>LIV</b>
<b>Appendix IX – LØ3 Temperature Model .....</b>	<b>LIX</b>
<b>Appendix X – KT Temperature Model.....</b>	<b>LXIV</b>
<b>Appendix XI – Blood versus Water Model.....</b>	<b>LXIX</b>
<b>Appendix XII – 0°C Model .....</b>	<b>LXXII</b>
<b>Appendix XIII – 300°C Model.....</b>	<b>LXXVI</b>
<b>Appendix XIV – 600°C Model .....</b>	<b>LXXXI</b>
<b>Appendix XV – 900°C Model.....</b>	<b>LXXXVI</b>

## **Preface**

This Master's thesis has been an on-going process during the last couple of years. But it would not have been possible to do the project without inputs and help from other people.

Firstly, I would like to thank Leif Stark, Rune Holmberg and Christer Johansson for taking me to their red earth spots in the Swedish forests and showing great hospitality. Thank you to Niels Jørn Kristoffersen for letting me sample on his property, showing me around and providing me with useful information about the site. The staffs at ArtLab Australia have made it possible to examine artistic natural ochre, which I am also very grateful for. Without these people, I would not have had any materials to analyse and the project could not have been completed.

Rachel Popelka-Filcoff has been an aid in the initial stages by giving me useful feedback on my project outline; and a thank you to Allan Pring for establishing the contact.

I would also like to thank the staff at the Department of Conservation at University of Gothenburg for guidance in different matters. Especially, Jacob Thomas for great supervision during the entire Master's project. He has been bringing a lot of ideas to our meetings, challenging me and making me think outside the box. His comments have indeed contributed and made the thesis turn out the way it did.

During my stay in London in the autumn of 2017, I was hosted both by the Institute of Archaeology and the Institute of Sustainable Heritage at University College London. I have appreciated my time there a lot and would especially thank Natalie Brown for devoting some of her time so I could get familiar with other near infrared instruments.

Finally, a thank you to my partner Jesper Petersén and my mother Else Najbjerg for reading and commenting on the written thesis. It means a lot that the people close to me want to read a thesis so far away from their own academic fields.







## 1. Introduction

Many rock paintings represent a culture and a people that do no longer exist. We want to know more about this people because they eventually became us.

Paintings without an archaeological context can be difficult to interpret and even date (Lødøen & Mandt 2005, pp. 15-26). Scientific analyses of the paint can be a way to understand the creation of the paintings better. There are only 44 known rock paintings from prehistory in Sweden (Gjerde 2010, p.178), and it is therefore necessary to think about what analytical methods to use in order to save as much of this rare material.

### 1.1 Background

Rock paintings are known from many places on Earth, for instance in Australia, Africa and the Lascaux painting(s) in France. The most significant colours are red and yellow ochre, but the palettes also include white and black from e.g. calcium and charcoal (Stuart & Thomas 2017, pp.1f.; Di Lernia, S. 2012; Mauriac 2011).

There are also documented rock paintings in Scandinavia (Norway and Sweden) and Finland (Gjerde 2010, p.178). Little is known about the Scandinavian rock painting pigments, but the red colour is most likely due to the use of hematite (Linderholm 2015, p.227; Lahelma 2008, p.18) perhaps originating from iron rich earth pigments generally called ochre. No yellow, black or white motifs are exemplified in the present Nordic countries.

#### 1.1.1 Near Infrared Spectroscopy and Swedish Rock Paintings

Near infrared (NIR) spectroscopy is a non-destructive and non-invasive analytical method, which can be used to make distinctions between different materials based on their chemical properties. Linderholm et al. (2015) have examined Stone Age rock paintings with NIR spectroscopy. Some motifs separate statistically from others, but the reason for this separation is only discussed hypothetically. An explanation could:

(...) be either that the pigments have been applied at different occasions, maybe with slightly different pigment composition (or even different painters) or that there may be a significant difference in time span between the painting events resulting in an uneven weathering process. (Linderholm et al. 2015, p.234).

Directly after, it is written that “These are of course complex questions to answer and a combination of sources of information will facilitate this work, such as adding stylistic attributes to this study, (...).” (ibid).

What could be a reason for a different pigment composition? Could the pigments used in the painting have been treated differently before being applied to the rock surface? Which of such features would be possible to determine with NIR spectroscopy?

The article by Linderholm et al. (2015) do not explain what preparation processes could have effected the chemical composition. How come? Was it because the researchers did not have experimental research to back their theories?

### **1.1.2 The Starting Point of The Master's Project**

The study by Linderholm et al. (2015) drew the student's attention, as it creates more questions than answers. It quickly became the main source of inspiration for this Master's project. Would it even be possible to approach some answers to the separation?

As part of the Master's degree, the student took a minor research course. The course was mainly meant as a way for the student to become familiarised with SCiO® ([www.consumerphysics.com](http://www.consumerphysics.com)) – a commercial NIR spectrometer. Because the Master's project was already in creation at the time of the minor research course, the study objects in the course became ochres. Using the SCiO, statistical separation was observed, but because meta-data about the samples was missing, no fulfilling discussion about the reason for separation could be made. However, the results indicated that yellow ochres, burned ochres and naturally red ochres could be a basis for separation. See report in Appendix I.

SCiO, as a semi quantitative screening tool for medical purposes, has been assessed in another study by Bickler & Rhodes (2018), but no publication introduces SCiO into a cultural heritage context.

## **1.2 Research Question**

The research question below is formulated based on the explanations put forward by Linderholm et al. 2015 and the observations from the minor research course. It will be the main question to be answered in this Master's thesis.

- Which factor(s) or different preparation methods could cause Scandinavian rock painting pigments to be statistically grouped and separated based on their near infrared spectral data?

Some sub-questions can be asked to deepen the main question:

- Does heating temperature affect the separation pattern?
- Will an aged paint show different spectral features from an un-aged?
- Is the provenance or origin of the pigment the most distinguishable factor?

## **1.3 Purpose and Aim**

The concern for this Master's thesis is the pigment preparation methods and if they can be recognised with scientific analyses.

The project presented in this thesis aims to bring new and continuous knowledge to the research conducted by Linderholm et al. (2015), described above. This thesis serves as a pilot study to investigate the possibilities of using SCiO in a cultural heritage context with an aim to determine what information that can be obtained from the spectral data detected with SCiO. While the thesis only presents the data and the models, it would be possible to construct an application using the SCiO developers' kit, which would be an asset for Scandinavian rock art research, conservation and heritage science in general.

## 1.4 Methodology

An experimental research design is key to achieve the needed data to answer the research question and sub-questions. Samples were measured and the data processed to look for statistical separation.

The project is hypothetical-deductive in its approach. Theories from the literature served as the starting point for the research design and the generation of hypotheses. The theories have been applied to a new set of material (new samples) to see if the hypotheses hold (Creswell 2013).

The main data collection method was experimentally based. Samples with known variables are required in order to answer the research question. Red earths (ochreous soils) from six sites and three artistic ochre pigments were heated at different temperatures, exposed for a period of time, and having different origins. This can lead to an understanding of these variables' importance and influence on the results. Statistical processing was used, which requires data with a quantitative character. Qualitative observation was, however, also included to support the statistical results.

In addition to the model materials described above, an authentic cultural heritage object, *Tumlehed rock painting*, is part of the data set as a case study. It was included to relate the experimental results to the complexity of reality, and as a first test of general applicability of the method outside of the laboratory.

### 1.4.1 Analytical Methods

Ocular observations of studied objects are always useful and can generate some initial information. Such information is not redundant. It has been used to establish knowledge about the samples in this Master's thesis so the results from the scientific analyses are better understood and interpreted.

NIR spectroscopy is incorporated in the research question, and it is therefore important to the project. Samples have been analysed with a NIR spectrometer and the spectra interpreted to look for patterns. Heating temperature, age and provenance are focus points, but they do not exclude other factors, which could potentially affect the spectra.

One can easily be misled by the results produced with one single instrument. It is therefore a good idea to include another analytical method. Scanning electron microscopy coupled with energy-dispersive X-ray spectroscopy (SEM-EDX) is in this Master's project used as a secondary method to back some of the observations and make the interpretations of the NIR spectra more reliable.

The NIR data has been treated statistically after processing. Principle component analysis (PCA) have been performed to make PCA-plots, in the same way as presented by Linderholm et al. (2015), described later in section 1.8.2. The plots were compared to the known preparation factors and chemical composition to see if there is any correlation in separation.

#### 1.4.1.1 Theory of SEM-EDX

A SEM uses electrons and not light to create images. Two main types of electrons can be generated when the SEM beam hits the atoms on the sample's surface, which will be detected

by two different detectors. The first are backscattered electrons. These electrons have almost the same energy as before. Images based on backscattered electrons will display differences in atomic weight for instance between specific grains in the sample. Secondary electrons on the other hand lose energy when struck by the SEM beam. This creates high-resolution images of the sample's morphology. Carbon coating, or similar, can be necessary to create clear images. When the secondary electrons are emitted, a dislocation of electrons between the shells of the atoms will happen. This produces distinctive X-rays. It is possible to determine the present elements by analysing these X-rays – however not elements with low atomic number (Stuart 2007, pp.91-95, p.99).

### **1.4.1.2 Theory of NIR spectroscopy**

NIR spectroscopy is used to investigate molecules' vibrational and electronic transitions. Molecules vibrate in different ways based on atom configuration and types of bonds. Light with a specific wavelength will be absorbed if a molecule's vibrations correspond with this specific wavelength. In NIR spectroscopy, samples are exposed to light with wavelengths in the NIR range (800-2500nm). Molecules can absorb in this region and will show specific absorption bands based on their properties. A particular molecule will always have the same absorption bands and because of this, molecules can be distinguished from each other (Ozaki 2012, p.546, Siesler 2002; Bokobza 2002).

Fe-O, Fe-OH vibrations are characteristic for hematite and goethite respectively. However, these vibrations will show in the mid-IR region and not in a NIR spectrum (Popelka-Filcoff et al. 2014, pp.1314). Vibrational bands in the NIR region are due to C-H, N-H and O-H vibrations, the latter being relevant for goethite. Overtones of mid-IR vibrations will also show in NIR spectra. All of the absorption peaks in the NIR region are very weak compared to those in the IR (and visible) region due to what has just been described, and transmitted light due to radiation in the molecules lowers the absorption even more (Ozaki 2012, p.546; Reeves 2010, p.6). NIR spectra can become very complicated, since absorptions of different kinds occur at the same wavelengths (Reeves 2010, p.6). The spectra therefore contain a lot of information that needs to be extracted. Spectral pre-processing is necessary for this reason. It can also function as a method to get rid of 'irrelevant' information, such as light scatter caused by microstructural differences e.g. surface roughness (Rinnan et al. 2009, pp.1201f.).

What causes the absorption bands of goethite and hematite in NIR are the electronic vibration transitions and excitations of valence electrons (Popelka-Filcoff et al. 2014, pp.1313f.; Cornell & Schwertmann 2003, p140), but overtones and *combination modes* are also present in the 800-1200nm range (Ozaki 2012, p.546). The samples in the context of this Master's project are most likely not pure iron oxides, and one could expect overtones from both minerals and impurities (Popelka-Filcoff et al. 2014, pp.1313f.).

### **1.4.1.3 Why NIR and not mid-IR spectroscopy?**

The main reason for choosing a NIR spectrometer is based on the data recorded by Linderholm et al. (2015), but it could be discussed whether mid-IR would have been more suitable. Most information that can be derived from mid-IR spectra is about organic and inorganic materials, such as minerals, whereas NIR is predominantly about the organic molecules, hydroxyl groups of organics and inorganics and finally water content (Reeves 2010, pp.7f.). The absorption bands of water lie above 1000nm (Bakker et al. 2012,p.66), but water-bands can be affected by the presence of other molecules, that indirectly can be characterised based on the change it causes to the absorption of water (Reeves 2010, p.9).

Mid-IR does not make any bands caused by electronic transition. It is also sensitive to quartz, which is not the case for NIR (Ozaki 2012, p.546; Reeves 2010, pp.5f.). The insensitivity towards quartz can be an essential feature when analysing the samples in this Master's project. The samples have been taken from the ground and certainly contain quartz in the form of sand (quartz grains). This is obvious when looking at and touching the samples.

Especially some of the peaks ascribed to goethite lie in the same region as quartz (see Fig. 1), which might make it complicated to make quantitative estimations of goethite.

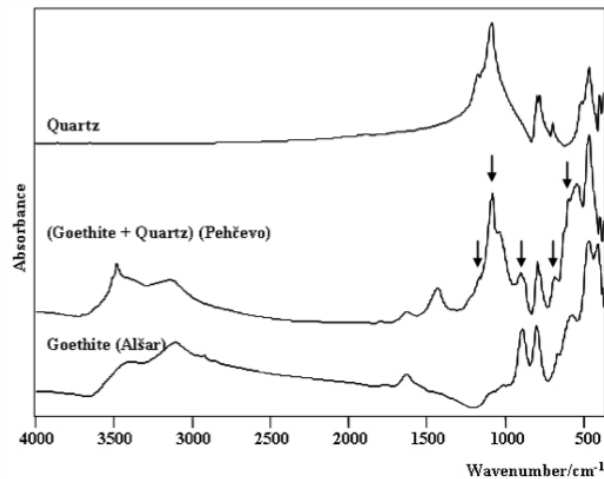


Fig. 1: Mid IR-spectra of quartz, goethite+quartz from Pehčevo and goethite from Alšar. The peaks of goethite and quartz are in the same region of the spectrum. (Jovanovsky *et al.* 2009, p.21.)

Besides what have already been mentioned, IR (in 1000-300.000nm range) can say something about the degree of crystallisation and the crystal morphology, when it comes to the iron oxides discussed in this thesis (Cornell & Schwertmann 2003, p141). The analyses in this Master's project could have benefitted from this specific feature, which would be more comprehensive with a mid-IR instrument.

## 1.5 Limitations

Some limitations of the project should be addressed. While 190 painted samples were analysed with SCiO, due to time constraints, it was not possible to examine an extended sample set, which would give more robust results. Nor was it possible to generate a fully qualitative and quantitative data set using complementary techniques to inform the interpretation. As such, the results and discussion, and hence the conclusion will reflect the limited, though still quite extensive, data set. The size of the examined groups and known classes (e.g. rock, paint, binding media etc.) have also affected the results. All classes should preferably be of the same size for the statistics to give the most reliable outcome.

Because Tumblehed rock painting was analysed with SCiO prior to the Master's project, the data set from the site is also limited. Had it been known that Tumblehed was going to be a case study in this thesis, more spectra would have been collected from the site.

A deep archaeological discussion about the knowledge and development of pigment preparation is not the point of focus. Additionally, the terminology of ochre and red earth will

not be discussed. Such a description can be found in the bachelor thesis by the same author (Ingrid Søgaaard 2016, unpublished).

Finally, it was not possible to explore the precision of SCiO compared to other established scientific near infrared (NIR) spectrometers. It also means that SCiO will only be seen in the context of the thesis, and not a lot will be said about some of the other research fields within heritage science, where SCiO might also be useful.

### **1.6 Theoretical Setting**

Within conservation and heritage science, the ethics of conservation is applied. Such are the aspect of non-destructivity and minimum intervention. Muños Viñas (2005) talks about minimum intervention and the importance of it in the field of conservation, and Muños Viñas thoughts are in line with the ICOMOS guidelines for the preservation and conservation-restoration of wall paintings: “The methods of investigation should be as far as possible non-destructive” (ICOMOS 2003, p. 38). It will however be a balancing act for the heritage scientist because, how important is the knowledge one can gain from (semi- or micro-) destructive analysis compared to the importance of preserving the required material?

### **1.7. Ethical Statement**

The preservation of objects can also be affected when analysis or treatments are carried out on historical artefacts. Some analytical methods require samples taken from the artefacts – this means loss of original material. Some treatments are not reversible, it is therefore important to think about the importance and consequences of interventions (Caple 2000, Muños Viñas 2005). This Master’s project includes experiments where samples are being manipulated and changed. It is therefore done on model materials, which are neither from historical artefacts nor from prehistoric contexts. In this way, one does not have to be a subject to the limitations of non-destructivity.

It is though important to consider how the investigated methods can be applied. If the method requires one to destroy the entire object, then the method would not be suitable for cultural heritage studies and consequently in less need of research in the conservation field.

In the case study of this Master’s project, where a cultural heritage object is analysed, no physical damage is posed on it. NIR spectroscopy is a non-destructive method that does not require sampling or consumption of small amounts of material (Ozaki 2012, p.547).

### **1.8 Previous Research**

#### **1.8.1 The Formation of Some Iron Oxides**

Ochre is simply characterized as iron oxide minerals, pure or mixed with clay minerals. Ochreous earth pigments can vary in colour from brownish to yellowish and reddish, but most commonly divided into red and yellow ochre. The yellow colour is caused by the presence of the iron oxide hydroxide goethite ( $\alpha$ -FeOOH), whereas the colours of red ochres are caused by the presence of the iron oxide hematite ( $\alpha$ -Fe<sub>2</sub>O<sub>3</sub>). These two minerals have different crystal structures that discriminates them (Cornell & Schwertmann 2003, p.14, p.29). A

detailed description of these minerals' structures is presented in the work by Cornell & Schwertmann (2003).

Goethite is the most abundant iron oxide in soils and is seen in connection with all of the other iron oxides, including hematite. In temperate and colder climate zones goethite will mainly be found in association with ferrihydrite and lepidocrocite ( $\gamma$ -FeO(OH)). The latter is orange in colour, and does not occur in calcareous soils. Ferrihydrite ( $\text{Fe}_5\text{O}_8\text{H} \cdot \text{H}_2\text{O}$ ) is reddish brown and has a low degree of crystallinity. It is not as thermodynamically stable as goethite and hematite, and will through time transform into more stable minerals. The formation of ferrihydrite happens through fast oxidation of  $\text{Fe}^{2+}$  ions in e.g. springs, groundwater borders, bogs and close to soil surfaces, especially when the amount of organic matter in the soil is high; organic matter makes it difficult for the other minerals to crystallise. The formation of ferrihydrite can oppositely be slow in the presence of silicium, hence formation of goethite and ferrihydrite will most likely happen simultaneously. Ferrihydrite can also transform into goethite under anaerobic conditions (Cornell & Schwertmann 2003, p.18, p.26, p.388, p. 423, p.441-450).

Hematite is found in soils and deposits around the world. It is formed in tropic climates under aerobic conditions. It can also be created through a heat-induced transformation of the iron oxides mentioned above (Cornell & Schwertmann 2003, p.369, p.442).

Because of the cold climate, yellow coloured soils are found in Scandinavia. These soils can, as described, contain several iron oxides in different relationships depending on the conditions of the deposit.

It would not have been difficult for prehistoric people to find pigmented material, because the iron rich soils and deposits lie close to the ground's surface. However, as visually obvious, Scandinavian rock paintings are red, indicating that hematite must have been created through (intentional or unintentional) heating.

### **1.8.2 Near infrared spectroscopy for analysis of ochre pigments and ochreous soils**

As briefly mentioned in the background section, Linderholm et. al. (2015) have completed a project. It deals with the analysis of Scandinavian rock paintings using a portable MicroNIR spectrometer (JDSU MicroNIR 1700). Some of the results from Flatruet (a rock painting site in Sweden) are discussed in the article: *Field-based near infrared spectroscopy for analysis of Scandinavian Stone Age rock paintings*. The main questions to be answered were whether it was "possible to classify and separate rock paintings and pigments from the geological background" (Linderholm et. al. 2015, p. 228) when using the MicroNIR, and if the paintings could "be analysed and differentiated by applying chemometric techniques"(ibid). Numerous rock art paintings were examined and the MicroNIR had a wavelength range from 908-1676nm when NIR-analyses were conducted. The mathematics and chemometrics were used as methods of analysis in terms of principal component analysis (PCA) after mean-centering of the spectral data and partial least squares discriminant analysis (PLS-DA). Soft independent modelling of class analogy (SIMCA) is also mentioned. The PLS-DA results could be used to separate pigments and background data if the pigment layers were not too thin. The PCA-data could on the other hand be used to make a score plot of PC1 and PC2 in which a separation between motifs in one scene: one elk stood out from the rest of the elks in the image. See Fig. 2. Also the SIMCA-models made rather good differentiations between groups.

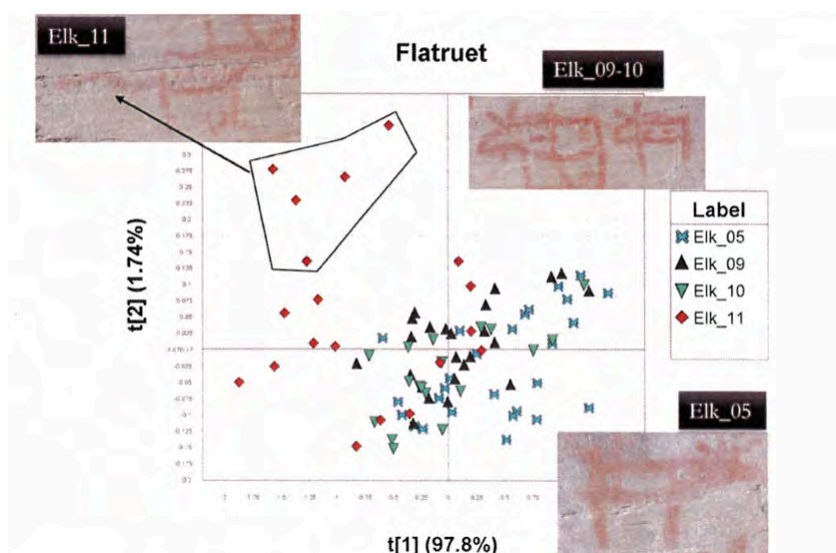


Fig. 2: PCA-plot of figures in Flatruet rock painting.  $t[1]=PC1$ ,  $t[2]=PC2$ . (Linderholm et al. 2015, p.233.)

Some possible reasons for the separation in Fig. 2 were mentioned in the background section. One theory was that the motifs had been created at separate occasions, maybe by different painters (Linderholm et al (2015, p.234). What could this actually say about the creation process of the painting? In what way would it affect the paint? Could specific pigments have been reserved for special rituals, collected at certain spots or heated at temperatures creating distinctive hues? Did painters have a personal recipe for making their paint, or is the difference just a matter of coincidence? Another theory presented by Linderholm et al (ibid.) for the separation was that the weathering process had reached different stages in the two motif groups suggesting that one motif group had been painted long after the other. Could it mean that the rock art site had been actively used through generations? What part of the paint would have been most affected; the pigments or the binding media?

Other researchers have done NIR studies on both ochre pigments and ochreous soils in other contexts. In an article by Popelka-Filcoff et al. (2014) an instrument, called HyLogger developed for the mining industry have been used to analyse and map the pigments on aboriginal artefacts. HyLogger works in the visible to shortwave infrared range, including the NIR (750-1400nm) and can do hyperspectral analyses (Popelka-Filcoff et al. 2014, p.1310). Both red and yellow ochre were identified. Characteristic bands in the NIR range is with the HyLogger instrument for hematite (red ochre) 848-906nm and for goethite (yellow ochre) 933-973nm (ibid. pp.1313f.) Scheinost et al. (1998, p.531) mention the NIR range for hematite to be 848-906 nm and for goethite to be 929-1022nm. One can see that the characteristic band for goethite is dissimilar to that in Popelka-Filcoff et al.'s article. However, as described by Popelka-Filcoff et al. (2014, p.1314), the ochres they investigated do not consist of pure hematite or goethite minerals, and the identified spectral features from their study include those impurities one can find in ochres. Since, Scandinavian ochre, or red earths, most likely have impurities as well, the observed spectral bands might not lie in the typical range of the two minerals.

Cudahy & Ramanaidou (1997) have in their study of Australian iron deposits explored the potential of using visible (vis) and NIR spectrometry (400-1000nm) as a mean to asses a hematite-goethite ratio. Scheinost et al. (1998) have also used vis-NIR spectroscopy for quantificational application possibilities when it comes to goethite, hematite and other iron oxides. Because the spectral range of the  $SCiO$  falls within this range, it should be applicable.

There are also examples of projects within the agricultural research field where vis-NIR spectroscopy has been used to predict carbon (organic matter) and moisture content in soils. Quantitative estimations of clay and mineral content and composition have been attempted as well (Viscarra Rossel et al. 2009, p.254). Viscarra Rossel et al. (2009, pp.254f.) have analysed Australian soil profiles in situ and made laboratory analyses with vis-NIR (350-2500nm) light of samples taken from the profiles. Two of the aims were to perform soil colour and mineral composition characterisations – the minerals in focus included goethite and hematite. The characteristic wavelengths used for identification of the two iron oxide minerals lie within the intervals presented by Scheinost et al. (1998). The result for Viscarra Rossel et al. (2009, p.263) showed, that X-ray diffraction (XRD)-patterns sometimes did not show signs of goethite and hematite, due to small amounts and low crystallinity of these in the soils. Vis-NIR spectra could however give quantitative estimations of mineral content in comparison to what was obtainable through XRD-analyses.

### **1.8.3 Pigment Preparation and Heating**

Mastrotheodoros, et al. (2010, pp.38f.) looks into the treatments of ochres and iron rich substances for the making of pigments in the Greek and Roman antiquity. They write:

“The antiquity arsenal of material modification practices was limited and rarely included anything beyond grinding (dry or with a liquid), mixing, heating (either in an oxidizing or in a reducing atmosphere) and interaction with a few liquids, vinegar being among the most potent and popular latter ones”(Mastrotheodoros et al. 2010, p.38).

Vinegar is mentioned in this context as a reactant to create purple-like ochres and make pigments through acidic corrosion of metals (ibid, p.39).

How have ochre pigments been prepared historically or prior to scientific analyses? And how does it show in the scientific results?

#### **1.8.3.1 Washing and Grinding**

Hansen & Jensen (1991, pp.62f.) describe the present process of cleaning ochre. Cleaning, they say, is necessary because most natural ochres contain large amounts of sand and organic material. For artistic purposes, it is favourable to have a pigment with small-grained clay particles and iron compounds. To separate impurities from the pigment, the coloured earths are finely crushed and then washed to allow heavy particles to sediment. The small clay particles and iron compounds that float around in the water can hence be filtered away and dried at room temperature.

Ochre preparation is also touched upon by Hald (1935, p.61f.). It is mentioned that natural iron rich earth should be crumbled and ground then exposed to slurry or sieving.

Grinding affects the visual expression of ochre. Goethite becomes darker and more brown when particles size is less than 0,2µm and in bigger aggregates. It is yellow between 1-2µm. Hematite becomes violet the bigger the particle size, and darker in aggregates (Cornell & Schwertmann 2003, XXII, p.133-135).

Extensive grinding can, to some degree, change the IR spectra (wavenumber 800-200cm<sup>-1</sup>) of hematite (Rendón & Serna 1981). However, grinding does not alter hematite grain size as much compared to the change in particle size (Mastrotheodoros et al. 2010, p.47, p.54). Which of these that affect the IR spectra is not elaborated. XRD patterns are on the other hand

affected by particle size (Rendón & Serna 1981).

A study by Sajó et al. (2015) investigates the possibilities of pre-processed natural red ochre from the stratigraphy of an Upper Palaeolithic site in Hungary. They suggest a ‘core-shell’ theory, where natural hematite has been added to cover a core of quartz and dolomite grains (50-150µm in diameter). Because the hematite from an untouched iron vein in the same area is of a more pure sedimentary character, it is proposed that the practice of sealing sand grains have been done post mining. In this case, as a way to make larger amounts of pigmented material as would otherwise be possible if only the pure hematite ore was used as pigment. It seems like no heating has been applied, as the ore was already hematite. However, they discuss the possibilities of a natural process for the iron oxides’ dislocation on the sand grains (ibid. p.9, pp.12f.). The process described sounds very similar to the secondary deposition of dissolved iron that, through oxidation, precipitate and can become so called bog ores or red earth soils. These are common in Sweden, but the minerals do not include hematite (Karlsson et al. 2016, p.569; Cornell & Schwertmann 2003, p.422, pp.425f., p.440).

A study of a much older site in South Africa dated to be around 100,000 years old, includes a description of a small toolkit for preparing ochre paint. Based on the excavated materials, the researchers suggest that ochre has been ground on quartzite slabs and then transferred into a shell where it was mixed with a liquid, possibly bone fat. Again, quartz grains are found within the mix of ground ochre; it could have ended there deliberately or as result of the grinding on the quartzite slabs (Henshilwood et al. 2011).

Would it be necessary to wash and or grind the pigment and soil samples used as model materials in the Master’s thesis? Based on the literature, it might not be crucial.

### ***1.8.3.2 Heating***

Heating will cause goethite to transform into hematite if a certain temperature is exceeded. Prehistoric people have, based on research, carried out this practise – especially when only yellow ochre was available. For example, Gialanella et al. (2011) have tried to look at the determination of natural or artificially made red ochre at a 13,000 BP site in Italy. Red ochre in the stratigraphy was compared to calcinated yellow ochres (transformed from yellow to red by heat) – the artificial reds were created by heating the yellow ochres for 1hr at 1000°C (Gialanella et al. 2011, pp.952f.). Based on XRD patterns, Raman spectra and scanning electron microscopy (SEM) micrographs of both archaeological samples and artificial pigments it was advocated that the ochre found on site was derived from calcination of yellow ochre. Unfortunately, no natural red ochre was included in the analyses, which could have been a contributing addition.

Goethite will transform to hematite by heating it between 260-320°C. It is due to dehydroxylation, and the temperature for transformation depends on the crystallisation and aluminium substitution in goethite (Cornell & Schwertmann 2003, p.369). Hematite created at low temperatures retain the acicular morphology of goethite, but above 600°C sintering occurs (ibid., p.370) and hematite becomes well crystallised (ibid., pp.367ff).

In a source from 315-312 BC, Theophrastus describe the process of heating natural yellow ochres. In his text, it is stated that the temperature in the oven affects the final tone of the burned red ochre (Mastrotheodoros et al. 2010, p.38). Researchers showed that if commercial natural yellow ochres were heated at 700°C, 900°C and 1100°C for 2hrs, different hues appeared depending on the temperature they were heated to. 700°C gave blood-red tints the one at 900°C went darker red and at 1100°C the hues got even deeper. See Fig. 3.



Fig. 3: Iron oxide heated at different temperatures. From left: unfired, 700°C, 900°C, 1100°C. (*Mastrotheodoros et al. 2010, p. 45.*)

It is stated that the grain size of the created hematite in the heated samples depends on the temperature – the higher the temperature and the longer the heating time, the larger the grains. (Mastrotheodoros et al. 2010, pp.45-47). The commercial pigments were not ground before firing because of the pre-processing from the manufacturer, but they were ground after heating. Heating was made in a furnace (Heraeus-Rof 7/50) under oxidising conditions. The temperature was kept for two hours; thereafter, the furnace was turned off and left to cool down to room temperature (*ibid*, pp.43f.). The amount of pigment burned in the furnace is not specified; nor is the way to maintain oxidising conditions. Would a small furnace really contain enough oxygen with the door closed during firing to oxidise the samples?

Based on the literature, there is conflicting information on time-temperature interdependence.

Increasing the heating time cannot extend the effect of low temperature heating. Raman spectroscopy shows, that the spectrum of a goethite heated at 300°C for 1hr is similar as one heated at the same temperature for 40hrs (de Faria & Lopes 2007, p.119f.). If this is also the case if goethite is heated at higher temperatures is not explained.

Other historical sources from the 17<sup>th</sup>, 18<sup>th</sup> and 19<sup>th</sup> century talk about the heating procedure when yellow ochre is transformed into red (through calcination). Some say that the ochre should be ground before heating others state that it only has to be broken into smaller pieces. Also the time of heating vary from writer to writer; it can be from 2hrs and down to a few minutes – until the right colour is obtained (Helwig 1997, p.182).

The change in molecular and crystal structure when synthetic goethite is transformed to hematite is noticeable in a Fourier transform infrared (FT-IR) microscope. Ruan et al. (2002) have done firing experiments, where synthetic goethite samples were heated between 110-300°C. The samples were observed in the furnace in intervals of 10°C (*ibid*. p.969). Different types of vibrations, e.g. bending and stretching in the bond related to the hydroxyl group in goethite changed during firing. Both the intensity and shift in characteristic FT-IR band centres had a linear relationship to the heating temperature – speaking for a gradual change depending on temperature (*ibid*. pp.969-972). How time could affect this linear relationship is not included in the study.

The impurities in the raw material, such as silicon and calcium, can affect the crystallisation process when goethite undergoes transformation (Gialanella et al. 2010). This is visible in their XRD patterns. Though there are a few examples of natural hematite with diffraction patterns similar to calcinated hematite, and XRD cannot always prove if a pigment was heated or not (Helwig 1997, p.183). Calcinated hematite will have a less ordered crystal structure than natural hematite. However, when calcinated at 900°C, disordered hematite will almost have the same diffraction pattern as naturally crystallised hematite. Grinding, biodegradation

and weathering can also be contributing factors to a higher grade of disorder observable in analysed ochre samples (de Faria & Lopes 2007, p.120).

It has only been described that goethite transform to hematite, but some other minerals present in the ochre and/or soils can also create hematite. This can be the case with Scandinavian ochreous soils (section 1.1.2). The different steps of transformation will be summarised here.

The transformation of ferrihydrite to hematite happens between 227-327°C. This is due to dehydration, dehydroxylation and reorder in the structure. The time-temperature relationship for full transformation to hematite depends on the amount of free water in ferrihydrite (ibid., pp.378-380). Lepidocrocite also transforms to hematite, but the process will go through maghemite. This reaction happens between 200-280°C (ibid., p.373). Maghemite ( $\beta\text{-Fe}_2\text{O}_3$ ) (ibid. p.32) can hereafter transform to hematite between 370-600°C (ibid., p.382). Maghemite can also be created from goethite and ferrihydrite when heated in the presence of organic matter (ibid., p.368). Ferrihydrite, on the other hand, needs to be in solution to become goethite (ibid., p.388), thus the transformation does not occur through heat-induced processes. The above reactions are mainly oxidising, but under reducing conditions will hematite transform into magnetite. Similarly, goethite and ferrihydrite can form magnetite when oxygen supply is limited and/or with high amounts of reducing agents (ibid., pp.366-368). The reaction pathways are illustrated in Fig. 4.

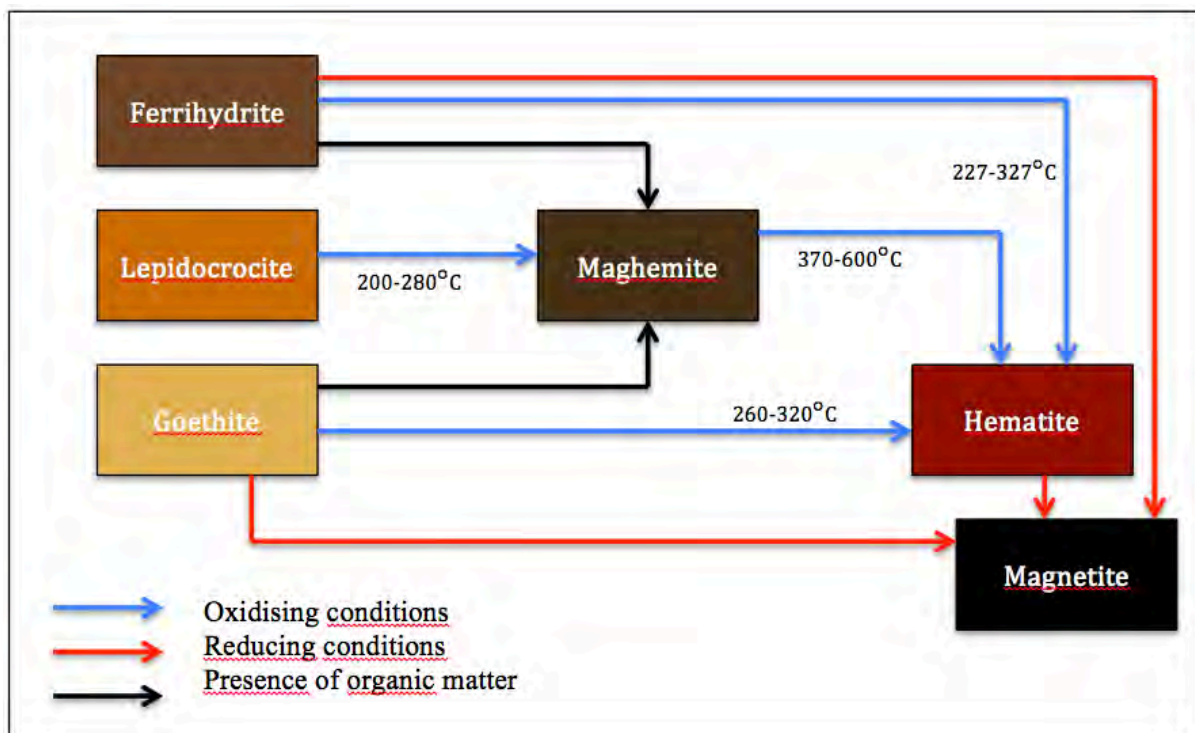


Fig. 4: The heat induced reaction pathways of ferrhydrite, lepidocrocite and goethite to hematite. (Ingrid Sogaard).

SEM-images of three temperature intervals are seen in Fig. 5. Fig. 6 shows SEM-images of samples from another project. A difference in micro-structure is definitely visible in Fig. 6, but it is less clear to see a change in Fig. 5.

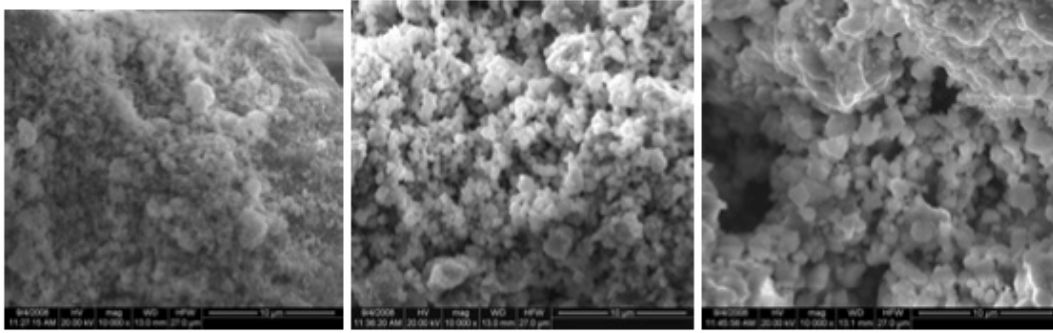


Fig 5: SEM-images of fired iron oxide at 10.000 magnification and different temperatures. From left: 700°C , 900°C, 1100°C. (Mastrotheodoros et al. 2010, p. 45.)

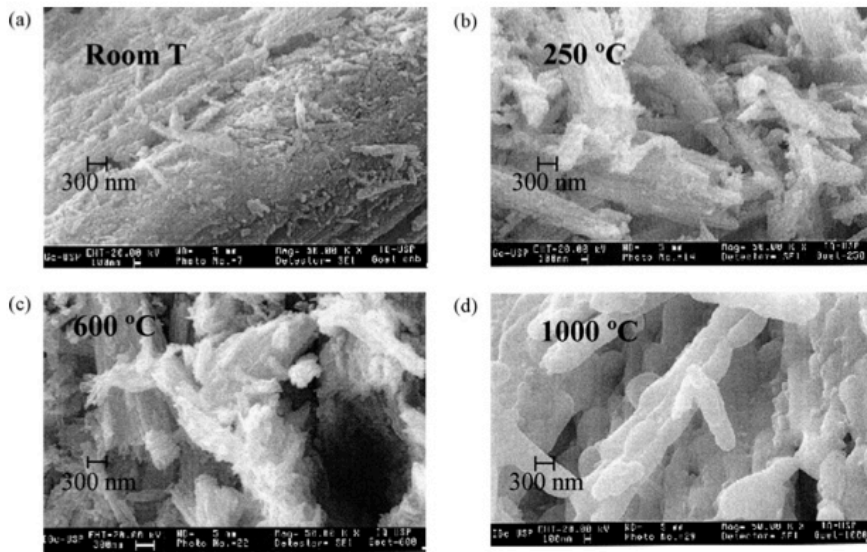


Fig 6: SEM-images of fired goethite at different temperature with 50.000 magnification. (de Faria & Lopes 2007, p.120.)

The maximal temperature in an open fire is around 750-800°C (Helwig 1997, p.182). Thus prehistoric people were actually capable of conducting most of the processes mentioned above.

As explained by Popelka-Filcoff et al. (2014), NIR can be used as a tool to differentiate between goethite and hematite pigments. In a Scandinavian Stone Age context, the heating process of goethite rich soils in a fire could have varied from time to time – which would affect the chemical (and mineralogical) composition in the pigment, mentioned by Linderholm et al. (2015). This variation could either have happened by coincidence or been a deliberate choice. Could it be that different nuances of red paint were created, by mixing and heating the pigments in distinctive ways so ‘multi-coloured’ images could be achieved? Maybe. If so, it might have impacted the paintings appearance.

#### 1.8.4 Ageing and Binding Media

Pigments are not the only substitute in paint. Usually a medium needs to be added so the pigment will adhere to the surface. Both pigments and binding media can be altered over time (Nyrén 2009).

Linderholm et al (2015, p.234) comes with several interpretations on why they see a

separation of analysed motifs in Fig. 2. One of them is, that the painting could have been executed at different stages. Theories about periodically painting sessions have been outlined in the literature, which could justify the explanation. For instance does Lahelma (2010) include the possibility of continuous use of rock art sites in Finland. Some paintings are abstract – they almost exclusively consist of one big blurred stain but with contours that looks like handprints, nearly unrecognisable. The non-figurative ochre spots are interpreted as a sign of a ritual act made by the users when touching the surface with ochre coloured hands. Repainting rock art is part of the culture of many aboriginal tribes as well. The motifs can either be repainted or new figures added to an existing picture (Bowdler 1988, pp.519f.).

How would the paint in rock paintings react through time? Ochre, both goethite and hematite, is very stable in terms of chemical degradation due to thermodynamic properties. In normal conditions, a reaction with either of the two minerals as reactants is unlikely (Cornell & Schwertmann 2003, p.3, p.6). A change in the pigments' chemistry caused by aging will therefore not be a credible factor. Loss of pigment from a rock painting would instead, expectedly, be accelerated by mechanical degradation. Aging will therefore be a more significant factor when it comes to the deterioration of binding media. But, would there even be any binding media left bearing in mind the age of Scandinavian Stone Age rock paintings?

Iron oxides absorb ultra violet light; hence to some extent ochre will protect the binding media in paint from photochemical degradation (Cornell & Schwertmann 2003, p.511). The vast majority of Finish rock paintings face west, southwest and south (Lahelma 2008, p.20), which makes them exposed to most of the sunlight on the northern latitudes. Even though the pigment has protected the binding media in the Finish rock paintings, thousands of years of light exposure must have left its mark.

Scandinavian rock paintings are partly protected from rain due to their location. They are painted on vertical rock faces, slightly tilted, and sometimes with overhanging ledges or in caves (Student's own observation; Bjerck 2012; Barnett et. al. 2006, p.445; Lødøen & Mandt 2005, pp.15-26), so the binding media might not have been washed away.

Prinsloo et al. (2013) used Raman and FTIR to study South African inspired rock art replicas. Several different mixtures of pigments, carrying agents and binding media were prepared. Included were red and yellow ochres as pigments, water, gall, saliva, plant sap and egg as carrying agents, and fat, blood, plant resin and egg as binding media. All ingredients had been chosen based on former scientific research and ethnographic studies. It have also been argued that blood could have had a ritual meaning in relation to hunting ceremonies, an the colour of the blood supplements the colour of the red ochre pigments (Prinsloo et al. 2013, pp.2981f.; Gjerde 2010, p.443). Both newly made and ten-year-old replicas were analysed; the analysis of the fresh painting gave better spectral results than the aged painting (mostly related to the organic substances) (ibid, p.2989). It does not seem like the old samples gave conflicting results.

NIR spectroscopy has been included to test its potentials as an analytical method to distinguish between binding media. Jurado-López & Castro (2004) prepared 20 binding media samples, with an organic and an inorganic pigment. They applied different algorithmic treatments (hierarchical clustering, PCA and K-nearest neighbor method) to the collected NIR spectral data of the samples. The spectra were collected between wavelengths 400-2500nm. K-nearest neighbors was best at classifying the samples by binding media, whereas hierarchical cluster analysis and PCA (in the PC1 and PC2 plane) made the biggest separation

based on pigment. In this particular study, the pigment is in two of three statistical treatments the most significant divider. However, this study only includes two very disparate types of pigments.

In both studies presented here (Jurado-López & Castro 2004 and Prinsloo et al. 2013), it is unclear how much the pigments actually affect the spectral data. How would the separation have been if, for instance, different types of red ochre were used in the study by Jurado-López & Castro (2004)?

It is a fact that certain binding media undergo chemical changes due to different types exposure e.g. UV-light and/or oxygen (Nyrén 2009, p.101-136). Blood is an example. It degrades in certain rates through oxidisation. It might be possible to distinguish between the oxidised products with NIR spectroscopy (Fouzias et al. 2011, p.741; Marrone & Ballantine 2009, pp.1-3).

### **1.8.5 Provenance Studies of Ochre and Ochreous Soils**

Pigments were needed to create the Scandinavian rock paintings, but where could they have been collected? What type of iron oxide source could have been accessible in prehistoric Scandinavia?

Iron oxides are known and have been worked with in Sweden. Iron bloomery smelting in Sweden is thought to have been an activity from 1000 BC-1800 AD (Englund 2002, p.12). In the direct bloomery process, red earths and bog ores were the raw material from which to extract iron (Buchwald 2005, pp.90-96). Maybe, it could have been used as the pigment in Scandinavian rock paintings from the Neolithic period?

Large areas of Sweden have red earth deposits (Englund 2002, pp.14f.), thus one could imagine that it was rather easy for the student to go out in the landscape and take samples for the experimental part of the Master's project. However, even though the red earth deposits are plentiful, they are most often not visible for the unaware. The earth only reveals its secrets when the topsoil with grass and mosses are removed. So, who would know where to find these red earth locations in present time?

Nowadays, bloomery iron smelting is done by e.g. hobby-blacksmiths. It takes some Google-searching and e-mailing back and forth to get in contact with some of the people, who still maintain the bloomery practise, knows where such deposits are located and are willing to show where to find them. The hobby-blacksmiths even describe some deposits as 'better' than others (Informants 1-3).

Native aboriginals have traded ochre across large distances (Stuart & Thomas 2017, p.2). Some ochres were thought of being of a better quality than others and symbolic and spiritual meaning were connected to certain quarries (Popelka-Filcoff et al. 2012, p.81). The sites for making Finnish rock paints could have been chosen for their sacredness (Lahelma 2010). Maybe the pigments for making the painting also had to come from certain places?

The sea levels in northern Scandinavia are now lower than in the Stone Age when the Fennoscandic rock paintings were created (Gjerde 2010, p.78; Ling 2008, p.102-104). Since ferrihydrite is formed in, for instance, ground water boarders (section 1.8.1), it may be difficult to locate the exact locations of the deposits prehistoric people collected ochre from.

To the student's knowledge, the literature about ochre pigments from specific Scandinavian bog ores or red earth sources is not evolving around provenance determination. Examples from other parts of the world do, however, look into the provenance of ochres, which will be elaborated in the following.

The HyLogger (described in section 1.8.2) is good at defining the mineral composition of the pigments, but in the example on aboriginal ochre no conclusion about provenance could be drawn (Popelka-Filcoff et al. 2014, p.1315). As will be presented below, the provenance of the pigments can influence the chemical composition. Therefore, it might be something worth looking at in this Master's project, even though no good results was obtained with the described HyLogger project.

Chemical analyses have shown to be useful to make statements about provenance matters. When doing provenance analyses, it is necessary to have more than just one sample, preferable 10-15 samples, from each site. Otherwise, it is not possible to make sure, if the variations between the sources are greater than the variations within each source (ibid.; Informant 4) One article by Popelka-Filcoff et al. (2012) describes the application of neutron activation analysis (NAA) on ochre from South Australian ochre sources and is an investigation of the possibility to use As in relation to Zn and Na in relation to Sb to develop plot diagrams. Distinctions between different quarries were possible when several samples from each place were taken.

A research team from the United States (Bu et. al. 2013) has completed another provenance study. They have analysed iron oxide pigments used in prehistoric rock paintings in southern Texas and potential pigment sources in the same area as the paintings. The analyses were conducted with laser ablation-inductively coupled plasma-mass spectrometry (LA-ICP-MS) and solution ICP-MS. The instruments were used to measure concentrations of possible trace or 'fingerprint' elements in the samples. This study used log plots of Mo/Fe in relation to log plots of V/Fe to establish diagrams and pigment groupings. The researchers' interpretation was conclusive that the material used to make the pigments, most likely, was not from an ochre source but instead from a siltstone source, where goethite had been extracted and heated to make red pigments.

It is hinted that ochres from the same geographical origin have similar Raman spectra (Gialanella et al. 2011, pp.953ff.) and Froment et al. (2008, p.567) implies that provenance can give visible characteristics in Raman spectra.

Methods for provenance studies, which have showed positive results, use the materials' chemical composition to determine or exclude geographical origins. Another field of research where provenance studies have been applied is within archaeometallurgy, mostly on slag and slag inclusions (Charlton 2015). Iron provenance is relevant in the context of this section because red earths can be used as a raw material source for bloomery iron smelting.

Some Scandinavian slag samples have been analysed to determine their chemical composition. Through different data treatments, it was possible to see a pattern, separating Danish slag from Norwegian and Swedish slag based on MgO, Al<sub>2</sub>O<sub>3</sub>, SiO<sub>2</sub>, K<sub>2</sub>O, CaO, TiO<sub>2</sub> and MnO content. This approach was less useful to make local differentiations, with the smelting process' alterations in mind and the chemical similarities between deposits (Charlton et al. 2012, p.2289; Buchwald 2005, Fig.253). However, this study did not look at the raw materials, but such a provenance study was attempted by Schwab et al. (2006). Several

analytical methods, ICP-MS amongst others, were used to determine chemical composition and lead isotope ratios in both bog ore samples and artefacts. The lead isotope ratios gave rather good results in terms of ascribing an artefact to a possible ore. Nevertheless, many measures need to be taken into account when dealing with metal objects, as the smelting process will have an effect on the objects' final composition and distort the ore's chemical 'fingerprint' (ibid, pp.436-439, pp.448-450).

All of the former studies in this sub-section (1.8.5) use quantitative analytical methods to determine provenance, but what about NIR spectroscopy? Parkin et al. (2013) gives an example of how NIR could be used to evaluate the building materials of historical, Scottish 'massed earth' structures. They state: "NIR is shown to be able to distinguish clearly between clay-rich blocks of different origin" (ibid. p.4574). The project was begun, so appropriate materials could be selected for repairs and conservation treatments. Experimental samples were made of clay with different content of topsoil and organic material, and analysed. Historical samples were analysed as well. A LabSpec 5000 FR Spectrometer was used. Only spectral data between 1300-2400 nm were included in the statistical data treatment, based on regions with high degrees of 'noise'. The first derivative of the spectra was created and PCA was carried out. Organic matter played a role in the study (Parkin et al. 2013), and can therefore be less characteristic when burned ochreous soils are analysed.

## **1.9 Hypotheses**

Is it possible to come up with hypotheses for the research questions in section 1.2 based on the presented previous research?

Heating temperature seems to have a big effect on both the chemistry and the crystal structure of ochre. Provenance, hence chemical composition can be separation factors, however, if Scandinavian ochres differ that much is less clear. It is not impossible that the two could be inter-correlated in such a way that chemical composition gives different products when fired.

Aging might not alter the pigments' differences; however, signs of deterioration could be observable in the NIR spectra if binding media is still present in the paint layers.

## 2. Material and Methods

### 2.1 Materials

This section is dedicated to the materials used in the experimental part of the project. It also describes the execution of the experiments prior to sample analysis.

#### 2.1.1 Ochreous Soil Samples

For the experimental part, the student has collected samples from six different locations: one in Denmark, one in northern Sweden and four from the middle part of Sweden. Three samples from each location were taken. All locations have some kind of connection to historical or archaeological contexts, in all of which the red earth/ochreous soil has been used in production processes. No rock paintings are located close to any of the sampling sites.

Sampling was only possible in summertime when the ground was not frozen.

A description of each of the sites and samples from Sweden is given in sub-sections 2.1.1.1-2.1.1.5 below. These consist of two sites in the *Tranemo*-area, two sites in the *Alvesta*-area and one close to *Los*. Samples were, as mentioned, not only taken in Sweden. A location in Denmark was found – this time not a site with red earth used for iron smelting, but a pigment mine from historic times. The Danish site is described in detail in sub-section 2.1.1.6 below.

Fig. 7 shows the locations of all Scandinavian sites marked on a geological map.



Fig. 7: The locations of sampled red earth from the Scandinavian sites; marked on a geological map. Blue colour: late Proterozoic and Phanerozoic rock types outside The Caledonides. Orange colour: Proterozoic rock types. Yellow colour: early Proterozoic rock types. (*Sveriges geologiska undersökning n.d.*)

### 2.1.1.1 Arnås (Tranemo, Sweden)

The first site close to Tranemo will be referred to as Arnås. The sampling site has the coordinates: 57°29'28.8"N 13°25'50.7"E and is marked with a red circle in Fig. 8. The location was in one corner of an open field surrounded by forest. This corner of the field was also part of an animal enclosure. Three samples were taken approximately 25m apart from each other: AÅ1, AÅ2 and AÅ3. When the samples were collected, they were air dried in open containers, marked with sample name. Then put into plastic bags again until they had to be used for sample preparation. AÅ1 was more on the outskirts of the enclosure whereas AÅ2 and AÅ3 were located in the grazing area. Soil from the Arnås-site has been used by the hobby-blacksmiths for bloomery smelting (Informants 1 and 2) and the site is in very close connection to places related to earlier bloomery production. See Fig. 8 (and for example; Riksantikvarieämbetet n.d., Tranemo 282:1).

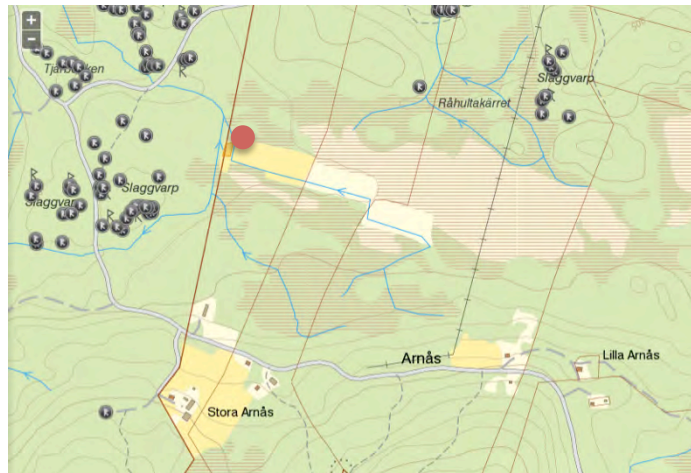


Fig. 8: The sampling site at Arnås – marked with a red dot. All black dots represent prehistoric, mostly bloomery related, sites. (Riksantikvarieämbetet n.d.)

Englund (2002, p.173-176) have made a survey of the red earth deposits in the Arnås area. One can, in Englund's doctoral thesis (2002), also find a general description of the research history of bloomery metallurgy, classification of bloomery sites in Sweden and a depiction of experimental bloomery iron production.

### 2.1.1.2 Sjöryd (Tranemo, Sweden)

Next site east of Tranemo is called *Sjöryd*, with the coordinates: 57°28'41.1"N 13°23'36.6"E. Sjöryd was an open field also with grazing cattle. Sampling was made on one hillside. Compared to Arnås, Sjöryd was not placed in the middle of a forest, but in open scenery. A farm had previously been on the hilltop (with a more recent dating) (Riksantikvarieämbetet n.d., Tranemo 282:1) but also in very close connection to earlier bloomery production sites (for example Riksantikvarieämbetet n.d., Tranemo 283:1).

The samples from Sjöryd will be named SR1, SR2 and SR3. Distance between samplings was approximately 25m. It seemed like SR3 was mostly 'regular' soil with organic material, but this was not noticed in the field.

As for the red earth from Arnås, the hobby-smiths had also tried to make bloomery iron with soil from Sjöryd. Iron extracted from the latter was however not as desired as the iron from the former location. What made this difference was unclear for the hobby-smiths, but a guess could be the composition of fluxes (Informants 1 and 2).

Several bloomery related sites without exact dating is known and registered south of *Tranemo*. Neither the *Arnås* nor the *Sjöryd* sampling sites are marked as prehistoric sites and no bloomery associated objects are known to have been unearthed at the specific spots.

### **2.1.1.3 Klasentorp (Alvesta, Sweden)**

Klasentorp is located north of Alvesta and has the coordinates: 57°02'12.8"N 14°30'10.8"E. Samples from this place will be named KT1, KT2 and KT3, and were taken with 100-200m distance between them.

It had been a while since someone collected red earth for smelting from this site, and it was rather difficult to find good spots to dig. KT1 was taken from the bed of a small brook where water was running. Iron deposits in streams are easier to locate at first sight compared to bog ores. The water in such brooks has a rusty colour from the floating iron particles. KT1 had, initially, less sandy particles and more leaves and wooden fragments from the undergrowth. KT1 contained a lot of leaves and sticks coming from the brook. KT2 had some charcoal, but also yellow-coloured pieces and KT3 is maybe mostly 'regular soil' with organic material. The latter was not noticed in the field.

Bloomery related sites are located about 4km away from Klasentorp (for example Riksantikvarieämbetet n.d., Moheda 372).

### **2.1.1.4 Sjötorp (Alvesta, Sweden)**

The other site in the Alvesta-area to be visited was Sjötorp, with coordinates: 56°46'42.5"N 14°21'54.2"E. Samples will be referred to as ST1, ST2 and ST3. These were samples very close to each other, approximately 3m, because of the limited size of the red earth deposit. The hobby-blacksmith (Informant 3) based in Alvesta had not used the red earth for smelting experiments, and said that a good red earth for iron smelting should feel a bit like chewing gum between the teeth. The soil at Sjötorp looked red and very sandy. Sjötorp was situated in the forest, but the vegetation was low. ST1 and ST2 red in colour and with a lot of organic material. ST3 was very red as well and had pieces of charcoal in it. The reason for the red colour could be because of a previous forest fire, which also fit well with the type of vegetation. The iron hydroxide would then have been partly calcinated while still being in the ground. Occurrences of naturally burned iron oxides of this kind may have helped prehistoric people understand that heat can change an otherwise yellow earth into red.

A bloomery related site is registered about 1km away from Sjötorp (for example Riksantikvarieämbetet n.d., Vislanda 54:1).

### **2.1.1.5 Holmsjön (Los, Sweden)**

The samples from Holmsjön in northern Sweden were not taken by the student, but by Informant 3 and sent to Gothenburg. 61°49'51.07"N 14°45'24.64"E is the coordinates of the site. Three samples: HO1, HO2 and HO3 were taken 8-10m apart; HO1 and HO2 close to a forest road and HO3 from an uprooted tree in the forest area. The hobby-blacksmith found the red earth from Holmsjön suitable for smelting purposes. HO3 was reddish and contained some charcoal.

Bloomery related sites are quite far away from Holmsjön, approximately 2km north. However, some prehistoric settlements are registered very close to the sampling site (with no specific dating: stone-iron age) (Riksantikvarieämbetet n.d.).

### 2.1.1.6 Løvskal (Bjerringbro, Denmark)

Løvskal was the final sampling site. Compared to the sites in Sweden, Løvskal is situated in Denmark, which has different bedrock type compared to Sweden (Fig. 7). The coordinates are: 56°27'16.5"N 9°42'00.3"E. It is not known if the red earth from Løvskal has been used for prehistoric iron production. There is only one registered Iron Age settlement 1,5km away from the sampling site (Kulturministeriet n.d.). However, it has been the raw material for ochre pigment production from 1910, when it was discovered by a coincidence, until the mine was closed in 1960. The soil was dug up and shipped to Randers, the nearest larger city. At the time the mine was active, iron content had been noted to be 36% and 50%, depending on the source of information (Appendix II and Informant 5).

Samples from this site will be named LØ1, LØ2 and LØ3. All three samples were taken with a distance of approximately 3m, because the area possible to dig in was limited as an effect of the earlier industry. All samples from this location had larger chunks of chalk and harder, yellowish brown pieces. An example of a sampling spot is seen in Fig. 9.



Fig. 9: Sampling at Løvskal. (Ingrid Søgaard 2016.)

### 2.1.2 Manufactured and Received Pigments

Two pigments were chosen from the Department of Conservation's pigment cabinet. The first one named 'hematite'. From previous XRD analyses of this pigment by university staff, the hematite was relatively pure (Informant 6). This hematite sample will be named HEM from now on. It was the intention to use a sample of pure goethite and treat it the same way as the red earth samples described above. Unfortunately, it was not possible to acquire at the time of writing. Instead a light ochre from Beckers was picked out, named LOB from now on. If this pigment is a natural ochre or if it is synthetically made (*Riksantikvarieämbetet 2003*) is not known.

One pigment from Australia was also included. Conservators at *ArtLab Australia* in Adelaide had received pigment samples from the artist Queenie McKenzie when working on one of the artist's pieces. The artist used pigments collected in the area around her home (Informant 7).

A small amount of a yellow ochre pigment was passed to the student. Further on, the sample will be referred to as YAU.

### **2.1.3 Rock Surfaces**

Thinly cut rock slabs of red granite, similar to that found on the Bohuslän coast were used for the sample support. One side of the slabs was roughly polished the other still showed signs of the cut. All rock slabs could probably have been cut from the same larger piece of granite. The unpolished side of the slabs were chosen for the experiments to serve as supportive background to apply pigments on.

### **2.1.4 Binding Media**

Egg yolk, fat, egg yolk-fat mixture and blood were chosen as binding media. It was not possible to get any pure animal fat, and therefore bones from cattle was bought in a supermarket and the fat was boiled from the bones for approximately 2hrs in water on a kitchen stove. The fat was skimmed of the water surface with a spoon, and other part from the bones, such as small pieces of meat, could possibly be in this fat layer as well. The egg yolk came from Swedish organic eggs and blood was from cattle, frozen when bought. Both blood and eggs were purchased from a grocery store.

### **2.1.5 Tumblehed Rock Painting**

The cultural heritage object used for comparison is Tumblehed rock painting. The painting is located close to the sea in northern Gothenburg, south of Bohuslän, Sweden. A deer, fish and what looks like waves adorns the vertical rock face. One needs to climb a bit to reach it, as it is now placed almost on top of a ridge. Because rock paintings are difficult to date it is only estimated that the painting is 5000 years or older. It is the nature of the figures, which leads dating back to the hunter-gatherers of prehistoric Sweden (Länsstyrelsen – Västergötaland n.d.).

The Master's student had, a year before writing this thesis, visited the rock painting in Tumblehed. At that time it was not decided that SCiO was going to be the key instrument for this Master's project. However, SCiO was in the student's backpack when visiting the rock painting. Some scans were made on site, both on the rock surface and on the paint. Meta-data was written down; for instance if it was paint or rock and what type of motif had been scanned. The scans' positions were not exactly recorded. However, three areas of interest are marked in Fig. 10 by yellow circles. The deer figure consists of both thin and thick paint layers.



Fig. 10: Tumblehed rock painting. The yellow circles mark the areas of analyses: deer, fish and waves. (*Varbergs Fornminnesforening n.d.*)

Could the paint be separated from the rock when using SCiO? And what about the thickness of the paint? Linderholm et al. (2015) had, as stated, some difficulties getting good spectra from thin paint layers.

As seen in Fig. 10, the deer motif and the rest of the figures are divided by a large crack in the rock face. It has been suggested by George Nash that the crack divides wet from dry; marine from terrestrial, with an argument about the significance of these resource in the landscape (Tilley, C. 2003, p.139). Did the crack only serve as a compositional feature or are the motifs on the left side of the crack material-wise of another matter than the deer figure on the right side of the crack?

## 2.2 Sample Preparation

This section includes a description of the different initial firing experiments that was carried out on the samples. As stated before, sample preparation was done based on and with inspiration from the previous research.

### 2.2.1 Aging Experiment

Because it was essential to get the samples out for natural aging in time, this step was executed first, and did not undergo same pre-preparation as the rest of the samples, described later on in section 2.2.

To prepare the samples for aging/exposure, a single pigment sample was chosen, LØ3, because of the sample's mass – there was more of this than the others – and because of its beautiful yellow colour. Some of LØ3 was calcined in an open pan with no controlled heating on a conventional kitchen stove.

The earth samples – heated and unheated – were ground in a ceramic mortar with some water to make two thick pastes. Each paste (a yellow and a red) was divided into five small dishes, so it was possible to make five different binding medium preparations. The first paint was only going to be with water, and the paste was hence mixed with more water until it was thin and easy to apply to the rock surface. The second paint was made by mixing the thick paste

with egg yolk in a 1:1 relationship. The third paint was made by warming up the fat in a low heated water bath and mixing it with the paste in a 1:1 relationship. To make the fourth paint, egg yolk and fat were firstly mixed in a 2:1 relationship, then, the egg-fat-mix was incorporated with the thick pigment paste in a 1:1 relationship. All measurements were made approximately by volume.

Four rock slabs were all divided into six spaces with masking tape. One space was kept clean as a 'blank', the other five were covered with the five different paints, just described. The paint was applied May 30, 2017 with a spoon in an even layer so the surfaces were fully concealed. Two slabs were covered with the paint made with unheated earth, the other two slabs with paint made with the heated earth pigment. One of each type (heated end unheated) was mounted on the supervisor's garage wall July 13, 2017 (named Y1 and R1; for yellow outside and red outside). The garage wall faced south. The other two (also one of each) were placed in a drawer in the university lab (named Y2 and R2, for yellow inside and red inside).

Y1 and R1 sat up on the garage until February 6, 2018; a total of 252 days.

The masking tape was removed from all four rock slabs in February 2018. Some glue residues adhered too well to the rock and could not be removed entirely.

Samples will be referred to as exposed and unexposed in terms of aging. Y1, Y2, R1 and R2 can be seen in Appendix III. The pictures are taken after exposure.

### **2.2.2 Grinding and Sieving**

It did not seem necessary for prehistoric people to only use very fine pigments, as grains of quartz were present in some of the excavated pigment samples (section 1.8.3.1). The washed and smoothly powdered pigments may not have been as important before as it became when smaller and more detailed paintings were being executed later on in history. Of course, the pureness of the natural deposit must also be taken into account. However, for this Master's thesis it might be less important to wash earth samples, but instead grind and sieve them to achieve a more homogenous powder.

Three ceramic mortars were used for grinding. To insure the least contamination, the mortars were sandpapered till most colour from previous use was gone. Then, the mortars were cleaned with water and put in an ultra sonic bath with demineralised water for 10 min. Afterwards they were wiped with paper to dry. This cleaning process was conducted between every sample.

The dry soil samples were ground for approximately 1min by hand, until most of the larger lumps were gone – quite homogenous by eye. Then, the ground pigment was poured through 4 sieves with mesh of 1mm, 500um, 250um and 125um and shaken by hand till completion.

The sieves were shaken, washed with soap and a dishwashing brush and dried with paper towel and a hairdryer between each sample. Note that some cross contamination could have happened in this stage.

HEM, LOB and YAU were not sieved beforehand. LOB and YAU had very fine particles that almost clogged the holes in the sieves. It can also be presumed that both HEM and LOB had been treated in a way to make them suitable for paint making.

### 2.2.3 Firing Experiments

Initial firing experiments were made to see how the samples reacted when heated at different temperatures, times and crucible composition. Two furnaces (Termolyne FB 1400) were used for firing. When the samples had been fired for the decided time, they were taken out to cool down outside the furnace.

#### 2.2.3.1 Preliminary Firing Experiments

To see if time and temperature were related, a firing experiment was required. One sample, LØ3 was chosen (based on what has previous been mentioned in section 2.2.1) and an experiment setup was made. The sample were to be heated at 900°C, 600°C and 300°C for 1hr and 2hrs. Small carbon crucibles were used. The samples heated to 600°C and 300°C became brownish red, however the sample heated at 900°C for both 1hr and 2hrs became strangely yellowish light brown – not what was expected. From literature, the yellow ochre were supposed to turn red. Could this colour change have something to do with the chemical composition of the sample? Had the samples been heated for too long or at a temperature too high? Or did the carbon crucible make the conditions too reducing? Instead, the sample was heated in ceramic crucibles at 900°C and 600°C for 1hr and for 5min at both temperatures to see if it made any change. A difference in colour could be recognised when crucibles were changed. The colour of the samples fired at 900°C were paler with a red tint, but the colour was still not as red as expected. Then, it was remembered that the landowner, of the area where the sample had been taken from, had passed on an old newspaper article describing the area and pigment production (Appendix II). It is stated that the company, from the Løvskaal soil, could produce a red pigment if it was heated at 1100°C – the temperature could therefore not be too high. The article also specified that they could make a chestnut brown and that pigment was used for painting brown train cargo cars at the time. A cargo car from 1960 (the last year the pigment mine in Løvskaal was running) is seen in Fig. 11.



Fig. 11. Cargo car build and painted in Randers 1960. (*Djurslands Jernbanemuseum n.d.*)

It suddenly did not seem like everything had went wrong with the way the samples was heated in the experiment. It could be the nature of the sample. The reducing conditions did not seem to be far out either. A change in surface area between the carbon and the ceramic crucibles could also have contributed to the rate of transformation.

After the first firing experiment, no further investigation in the composition of the samples heated in carbon crucibles were done. Only ceramic crucibles were used for the rest of the firing experiments mainly because of the amount of available ceramic crucibles compared to carbon crucibles.

For the following firing experiments, one sample from each location was used. The decision on which ones to use was made with an artistic perspective – the samples that looked most appealing were picked. The samples had the brightest colours and seemed to contain the least amount of organic material. Also samples that most likely had been heated in the ground were excluded at this point. One location (ST) however, did not have any unburned samples; therefore the chosen sample from this place was reddish from the start.

It was first decided that LØ3, KT1 and AÅ1 should be heated 15min at 900°C, 600°C and 300°C. It gave very interesting results. Especially KT1 was exciting. It turned to a chocolate brown at 600°C and light brown at 300°C but when heated to 900°C the brightest red colour occurred – none of the other samples exhibited such an intense red colour. Maybe this could be the case for LØ3? If it was only heated to higher temperatures, for instance to 1100°C as described in the newspaper (Appendix II), it might turn even more red? Firing at 1100°C was however not possible with the available furnaces. HO1, ST3, SR2, LOB and YAU were at this stage only heated at 600°C for 15min. HO1, ST3 and SR2 were not fully transformed in the centre at 600°C, and a new experiment was set up. All samples were heated at 900°C, 600°C and 300°C for 30min. The three samples which were not fully transformed in the centre at 600°C showed the same pattern after 30min, but only at 600°C. It might have something to do with the way the furnaces heated up. It could also have something to do with the higher content of organic material, or maybe that the final transformation took longer time than the other? This strange pattern cannot be answered better at the moment.

The initial firing experiments showed that red earth samples behave extremely differently. It also showed, that there is no straight way from yellow to red – the terminology therefore gets more complicated, because what is a red ochre? How red should it be to be considered red? Even though it is a yellow ochre to begin with, it is not necessary that it turns red. Many questions can be opposed based on the observations.

The experiments also made it clear that a relationship between time and temperature might not be possible to establish so it includes and covers all samples. It might describe one specific sample and/or location, but no generalisations can be made. How relevant would it be to set up experiments like this then? This question will be kept open.

XRD analyses could answer some of these questions – for instance as a technique to look for similarities in the mineral composition and crystallisation or as a tool to make quantitative analyses of the amount of goethite transformed to hematite caused by heat.

### ***2.2.3.2 The Final Firing Experiment***

Based on the preliminary firing experiments, a final sample preparation set-up was decided on. Only one furnace was used to fire all samples. LØ3 samples were fired at 900°C, 600°C and 300°C for 15min, 30min and 1hr. KT1 and AÅ1 were fired at 900°C, 600°C and 300°C for 30min and 1hr. Finally, HO1, ST3, SR2, LOB and YAU were fired at 900°C, 600°C and 300°C for 1hr.

#### **2.2.4 Preparing the New Rock Slabs**

Before seeing the exposed samples on slabs Y1 and R1, the plan was the paint only with water and no other binding media when the new rock slabs had to be made. However, what was evident was that water did not at all seem like a good choice for outdoor paintings. Almost none of the pigment was left on the surface (Appendix III). The egg yolk looked quite good on both slabs (Y1 and R1). An insect had made a nest in the bottom of the fat sample on R1 and had also been eating the paint. Taking into account that the paint sample with blood as binding media looked good after many days in wind and weather and that it was the smoothest and nicest to apply when the slabs were prepared, blood was chosen for the new paint samples as well. Having blood as a binding media could however bring some difficulties as it contains iron in the haemoglobin molecules.

The prepared samples from the final firing experiment were painted on rock surfaces (Appendix III and IV). To make sure that the paint was not mixed when applied, masking tape was used to make small squares. The tape was removed after some days when the paint had dried.

These samples will be referred to as 'new' in terms of aging.

#### **2.2.5 SEM-EDX Sample Preparation**

Samples were also prepared in powdered form and without having rock as a background. It could give other results when analysed.

A piece of carbon tape was stuck to an aluminium stub and the stub with tape was pressed by hand into a small pile of sieved soil. Due to the character of the pigments, it was not possible to cover the entire piece of carbon tape with a thick layer of pigment. Parts of the carbon tape were only covered with a dusty layer of pigment, yet enough to conduct satisfactory analyses. The samples from the final firing experiment (section 2.2.3.2) were prepared in this way. An overview of all samples on carbon tape can be seen in Appendix V.

### **2.3 Methods**

#### **2.3.1 Visual Examination**

Before doing any form of analysis, all samples, both those painted on rock and those on carbon tape were photographed. The rock slabs and pure pigments were examined by eye in room lighting.

#### **2.3.2 SEM-EDX – Execution and Instrument Settings**

No extra preparation was done to the samples prior to SEM-EDX analyses with backscattered electrons, besides being stuck unto carbon tape. LØ3, KT1, HO1, ST3, AÅ1, SR2 and HEM were inserted into the SEM instrument at one occasion. At another occasion, LOB, YAU and HEM (for the second time) were analysed. All the samples were unheated. No standard was included in any of the analyses.

The samples were carbon coated before analysis with secondary electrons. HEM, LØ3, KT1, HO1, ST3, AÅ1, SR2, LOB and YAU, unheated and heated to 900°C for 1hr, were included in this analysis step.

The instrument used for this project was a S3400N SEM (Hitachi), with an X-Max<sup>N</sup> (20) EDX detector (Oxford Instruments). The INCA software system was used to create semi-quantitative data and the mapping function with five frames was used to extract elemental composition and distribution. SEM-EDX analysis was conducted with chamber pressure <1Pa and beam energy at 20kV.

### 2.3.3 SCiO and the Accompanying Web Software

It was not possible to use the same instrument as Linderholm et al. (2015) used in their research. A SCiO (version 1.2) by Consumer Physics ([www.consumerphysics.com](http://www.consumerphysics.com)) was used instead. SCiO is made for the commercial market and is rather inexpensive, ca. 1500 SEK, compared to other scientific NIR spectrometers. It has a light source and a detector in one end, which means that no transmitted light is detected. See Fig. 12. Compared to the instrument used by Linderholm et al. (2015), SCiO's functional wavelength range is limited to 700-1100nm. As written in section 1.8.3.2, the bands for both goethite and hematite lie within the limits of SCiO.

Inside the cover of SCiO is an integrated calibration surface. A notice will appear when calibration is needed. It will be shown in the SCiO Lab developer toolkit software app, which can be run on an Android or iOS tablet or phone. The instrument is controlled through the app as well and therefore it does not need to be physically connected to a stationary computer. A small attachable chamber follows with SCiO, so the same distance between analyser and sample is kept constant and so no external light affects the signal. See Fig. 13.



Fig 12: The position of the light source and detector on SCiO. (Ingrid Sogaard 2018.)



Fig 13: Size an attachable camber for SCiO. (Ingrid Sogaard 2018.)

Data processing were performed through Consumer Physic's SCiO Lab web – an online platform where all scans and samples can be accessed through private accounts. Several spectral pre-processing methods are available: standard normal variate (SNV), log, first (1<sup>st</sup>) and second (2<sup>nd</sup>) derivative, subtraction of minimum and subtraction of average spectra. It is possible to see the spectra and the PCA plot of all scans, and models can be created. Samples can be coloured based on their meta-data, which makes it easy to look for patterns or groupings in the PCA-plots. It is also possible to filter out samples that are not desired to be included in PCA-plots or models.

Unfortunately, it is not possible to download the raw spectral data with the account settings available for this Master's project.

### **2.3.3.1 Scanning With SCiO**

The small attachable chamber was used when scanning all samples with SCiO. It was straightforward with the paint on the rock slabs, where the instrument was placed directly on top of the painted area – with the light source centred on the sample. Samples painted on rock were analysed three times at different occasions; approximately nine scans per sample each time. Between every three scans (of one sample), the spectrometer was moved slightly to obtain representative spectra of all samples.

Meta-data was written down before every new sample. A list can be seen in Appendix IV.

Scanning the aluminium stubs was a bit more difficult, because the stubs were smaller than the attachable chamber. A sample holder was made with a hole cut to fit the stub. See Fig. 14. Again, the spectrometer was moved between every three scans (nine scans per sample), but this time, samples were only scanned at one occasion. None of the scanned samples on aluminium stubs were carbon coated.



Fig 14: The scanning set-up for scanning samples on aluminium stubs. SCiO is placed on top of the sample holder. (Ingrid Søgaaard 2018.)

Obvious outlier scans were deleted from the collected spectra.

### **2.3.3.2 Statistical Data Processing**

Linderholm et al. (2015) used mean-centering to normalise the spectral data. This pre-processing method is carried out in the same way as SCiO's 'subtraction of average' method: the average-over-wavelength is subtracted from each spectrum, which makes the spectra swing between + and – in reflection or absorption (Consumer Physics n.d.). Important spectral information can however be lost during this pre-processing method (Manley et al. 2008, p.76). SCiO's main normalisation method is SNV. Here, the mean is subtracted from each spectrum, and is then divided by the standard deviation (Rinnan et al. 2009, p.1210). Scatter due to differences in particle size, surface roughness, crystalline defects etc. can be excluded by applying SNV to the spectral data (Manley et al. 2008, p.76).

Taking the derivative of a spectrum can on the other hand enhance changes in a spectrum. Without such enhancements, some spectral features would be almost invisible. For instance, the 1<sup>st</sup> derivative refers to the slope of the original spectrum; it will therefore show more distinctive peaks (Rinnan et al. 2009, p.1213; Manley et al. 2008, p.76).

Because a spectrum is a collection of measurements at several wavelengths, it can be difficult to see how two spectra differ from each other. A linear relationship between all variables in the spectra is made through PCA – a multivariate analysis method. PC1 is where most variability is present, PC2 is second most variation and so forth. The larger the distance is between the coordinates (for instance in PC1) the bigger variability (Leardi 2008; Miller & Miller 2000, pp.217f).

Samples can be coloured based on different meta-data to look for groupings. When a fairly good separation in a PCA plot is established (after applying pre-processing algorithms), it is time to create a model based on these variances.

Models in SCiO Lab web is made through cross-validation (CV) (Informant 8) of the samples picked out as foundation for the model. Here, samples are taken out of the training set to validate and test the model (Hastie et al. 2009, pp.241ff). The small number of samples in the sample set in the Master's project may affect the model's final validation and usability.

When a model has been created, it gives a table with the known classes, and how these have been classified (in percentage).

It also gives an F1 score that discloses the model's performance. F1 is defined as:

$$F1=2* \frac{\text{Recall*Precision}}{\text{Recall+Precision}}, \text{ where}$$

$$\text{Recall}=\frac{\text{Number of correct positive predictions}}{\text{Number of positive examples}} \text{ and } \text{Precision}=\frac{\text{Number of correct positive predictions}}{\text{Number of positive predictions}}$$

(Tan 2005, p.669)

If F1=1 the performance is good because all predictions have been correct, and if F1=0 the performance is bad because no right classifications has been made (Consumer Physics n.d.)

After a model has been created in SCiO Lab web, its performance can be tested on other samples with known meta-data. Samples are assigned to classes based on the random forests (RF) algorithm (Informant 8). Samples are classified according to each variable represented by classification trees. The final classification is based on what the majority of classifications have been in all trees (Hastie et al. 2009, pp.587ff.).

### 3. Results and Discussion

Analytical results are presented in this section. The results are discussed and interpreted based on observations and previous research.

#### 3.1 Visual Colour

The photo overview (Appendix IV) – mainly samples with no binding media – is used to make general descriptions of the samples. ST3 and SR2 produced red colours more or less in the same tone at all firing temperatures. The same were the case for AÅ1 fired to 300°C and 600°C, but the samples fired to 900°C are a bit richer. There is no obvious colour alteration between samples fired for 30min and 1hr. LOB fired to 600°C and 900°C and all fired YAU samples do also look quite similar. KT1 samples are a bit different. The samples fired to 300°C are light brown, the samples fired to 600°C are chocolate brown, and the samples fired to 900°C are very bright red. Again there is no difference between samples fired for shorter or longer periods of time. It is most unusual with the LØ3 samples. At 300°C and 600°C reddish colours have developed, but the 900°C samples are light and pale brown. When fired at 900°C for only 15min a hint of red is observed, making the sample pale pink.

Based on the visual colours, one is able to distinguish between the different firing temperatures of KT1, LØ1 and to some extent LOB, but YAU, AÅ1, HO1, ST3 and SR2 is more difficult to tell apart. In these cases ocular examination is not enough, compared to the example in Fig. 3, section 1.8.3.2, where it was shown how ochre turned darker the higher the heating temperature. Most of the samples in the experiment turned red, which was expected if a transformation to hematite was to have occurred. See Fig. 15.

What happened in the case of LØ3 and KT1? Why did these samples not behave as anticipated? As described in section 1.1.2, ferrihydrite is most abundant in spring water – and this is exactly where KT1 was taken from. Does it mean that there is no goethite present in KT1 samples? Based on the colour of the unfired KT1 sample it seems highly likely that goethite indeed makes up part of the sample. See Fig 15.

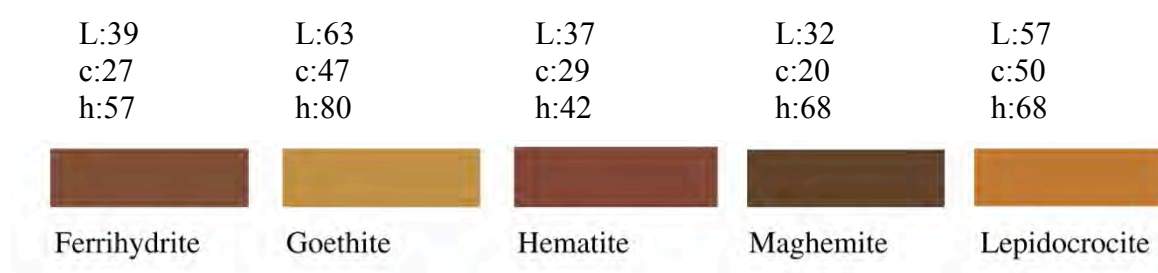


Fig. 15: The Lch colours of ferrihydrite, goethite, hematite, maghemite and lepidocrocite. Lch values are found in *Cornell & Schwertmann 2003, p.133*. The colour images are made with the software by: *Johnstone n.d.*

Other transformation mechanisms may have been happening when KT1 was fired. In section 1.8.3.2 it is said that ferrihydrite and goethite transforms into maghemite when a lot of organic matter is present during firing. This was in fact the case of KT1: a lot of organic material was observed when the sample was sieved and in the SEM images with backscattered electrons (Appendix VI). This can explain the brownish colour of KT1 samples

fired at 300°C and 600°C. The darker hue of KT1 fired at 600°C might also be explained by the presence of carbenised matter that has not been burned away entirely. See Fig. 15.

As for LØ3, there is no explanation for the transformation in the presented literature other than the creation of maghemite. Inter-reactions of minerals not identified (maybe CaCO<sub>2</sub>), might also have created the conditions that led to the final pale colour of LØ3 fired at 900°C.

Vibrations due to colour are mostly outspoken in vis-spectroscopy compared to the NIR region (Popelka-Filcoff et al. 2014, p.1313), but they can be a good indication about what minerals are present.

### 3.2 Chemical Composition – SEM-EDX with Backscattered Electrons

Elemental content of HEM, LØ3, KT1, HO1, ST3, AÅ1, SR2, LOB and YAU, all unheated, is shown in Table 1 in weight (wt)%. Because no standard were used, the results should not be seen as absolute and quantitative. The results only give an idea about what elements are present and to some extent the relative relationship between these. It is also quite certain that the percentages would change depending on where the analyses were made – based on the somewhat heterogeneous distribution in some of the samples (will be elaborated in section 3.3). Carbon content should not be regarded. It is not possible to know about the form it is in – if it is carbonates, organic matter or from the carbon tape. It could also be due to an unnoticed and unwanted instrument setting (such as lower vacuum).

Table 1: Chemical composition of unheated HEM, LØ3, KT1, HO1, ST3, AÅ1, SR2, LOB and YAU in wt%. HEM is included two times, the second time it functions a bit like a reference, as LOB and YAU were analysed at another occasion. Orange fill indicate extraordinary features compared to the other samples.

Sample name Content in wt%	LØ3	KT1	HO1	ST3	AÅ1	SR2	HEM	HEM	LOB	YAU
C	6,75	13,12	6,13	8,08	11,44	8,15	1,92			
Al	0,33	0,02	0,22	2,37	0,09	0,16	0,19		11,46	5,21
Si	3,28	0,13	1,81	13,64	0,26	1,13	0,49		19,90	31,41
Fe	32,34	34,17	56,37	26,62	43,93	51,92	71,01	77,73	24,50	17,84
O	38,86	48,95	34,91	47,48	43,78	38,31	26,24	22,27	40,60	45,54
Na				0,31						
Mg	0,11			0,1						
K				0,53					1,15	
P	0,29	0,05				0,09				
S					0,17	0,08				
Ca	17,45	0,01	0,24	0,19		0,18	0,15		0,55	
Ti				0,3						
Mn	0,42		0,33	0,37	0,22					
Cu	0,16	0,03			0,12					
Ba L									1,44	
Total	100	100	100	100	100	100	100	100	100	100

One can see that ST3 is very unlike the Swedish and Danish samples on many levels. There is a lot of Si in relation to Fe. Moreover, ST3 contain elements not present in any of the other samples, though in small amounts. LØ3 is also different from the rest with its high amount of Ca. HEM is extremely clean, with Fe as the main constituent. LOB and YAU, in particular, have a high content of Si and Al.

If observations from the backscattered SEM-images are included (see Appendix IV), KT1 looks very different compared to the others, with almost a 'stick-like' appearance – which could indicate a lot of organic material (wood fragments etc.). LØ3 is heterogeneous with separation between Ca and Fe. ST3 has big Si-grains. The distribution of Fe is in all samples, excluding LØ3, more or less homogenous. The grain shape and size of AÅ1 is also notable. Together with KT1, AÅ1 has the smallest grains/crystals.

In conclusion, LØ3, KT1 and ST3 stand out from the rest of the Scandinavian samples. However, the three remaining samples are not totally similar either. Maybe it is difficult to talk about some samples being different from others, when the sample set is so limited? LOB and YAU are contrasting all Scandinavian samples, and HEM is in its own league.

### 3.3 Crystal Morphology – SEM-EDX with secondary electrons

Since it was not possible to do XRD analyses, another method other than colour estimation would be useful as an indicator for goethite and hematite presence and transformation. SEM-EDX with secondary electrons could be a possible method for this, by looking at the main habits of the goethite and hematite crystals.

Secondary electron-SEM-images of HEM, LØ3, KT1, HO1, ST3, AÅ1, SR2, LOB and YAU, unheated and heated to 900°C for 1hr can be seen in Fig. 16-32.

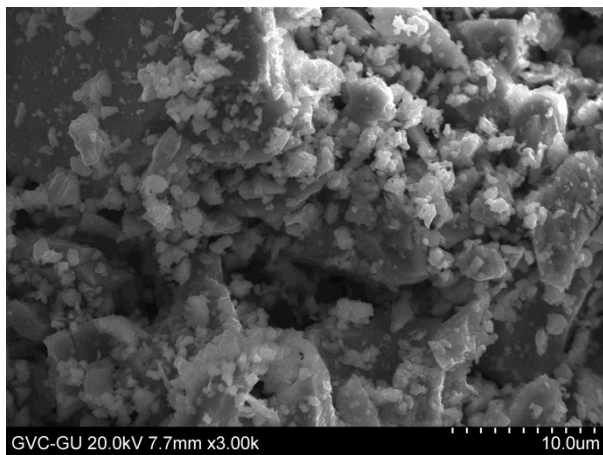


Fig. 16: Secondary electron-SEM-image of HEM.

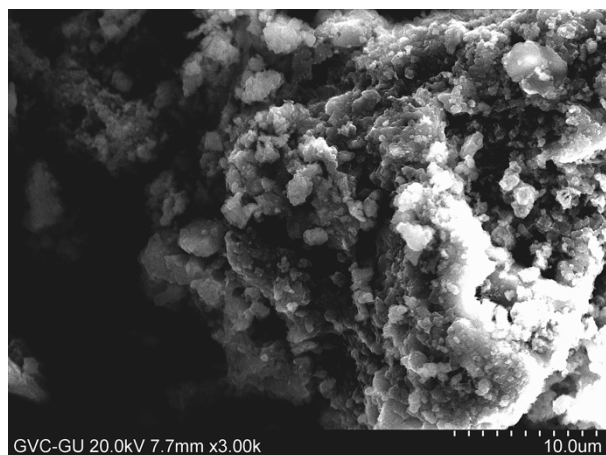


Fig. 17: Secondary electron-SEM-image of LØ3 0°C

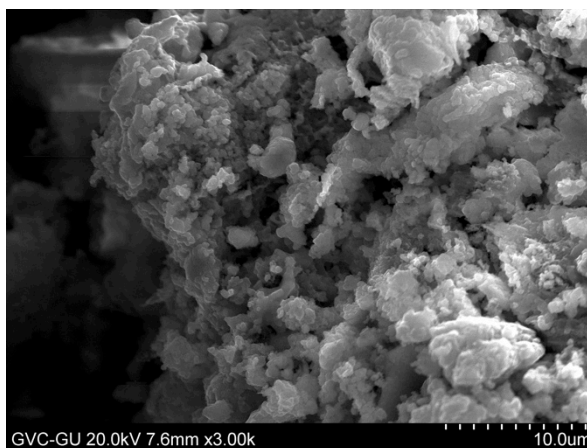


Fig. 18: Secondary electron-SEM-image of LØ3 900°C

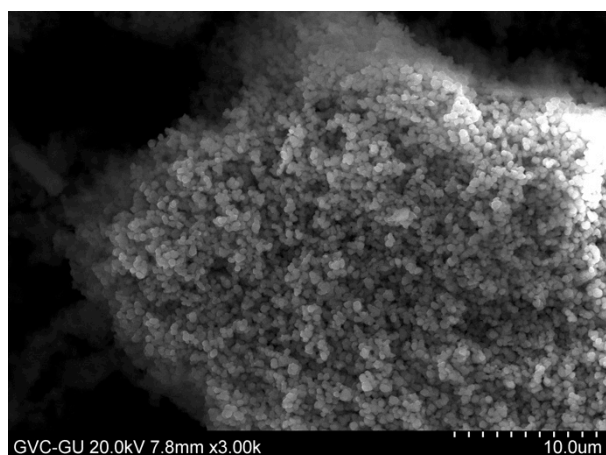


Fig. 19: Secondary electron-SEM-image of KT1 0°C

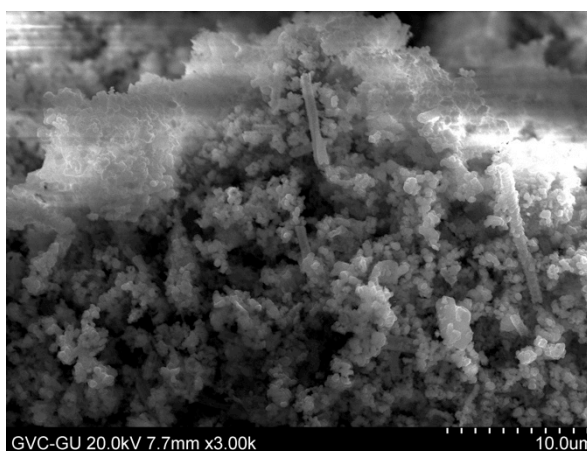


Fig. 20: Secondary electron-SEM-image of KT1 900°C

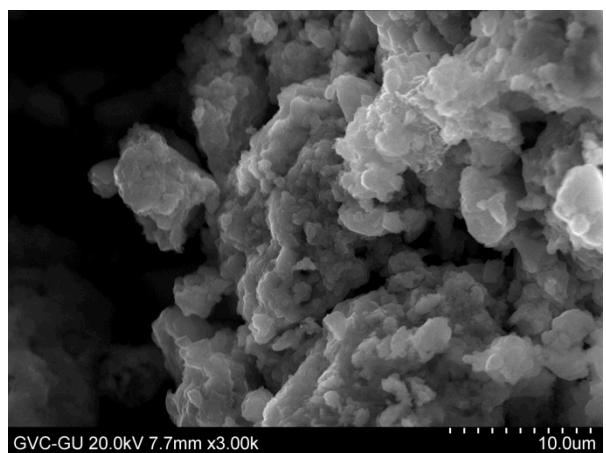


Fig. 21: Secondary electron-SEM-image of HO1 0°C

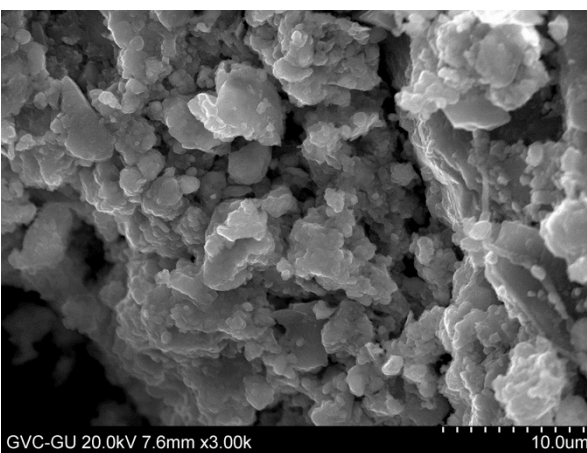


Fig. 22: Secondary electron-SEM-image of HO1 900°C

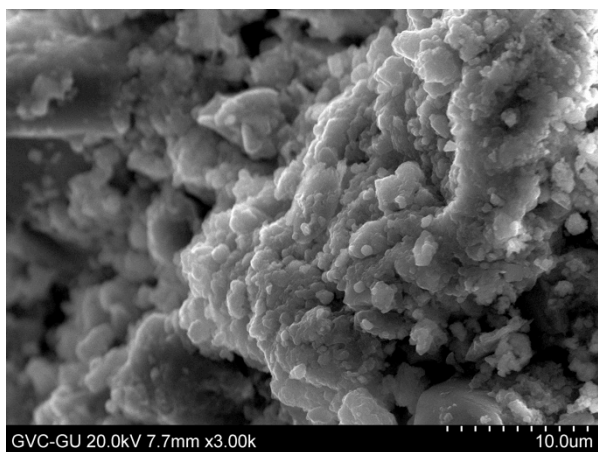


Fig. 23: Secondary electron-SEM-image of ST3 0°C

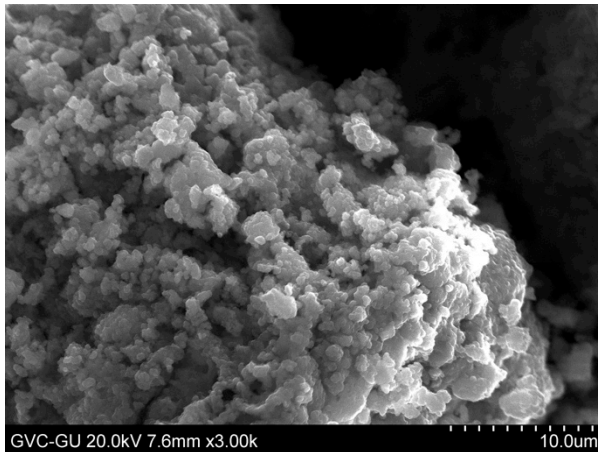


Fig. 24: Secondary electron-SEM-image of ST3 900°C

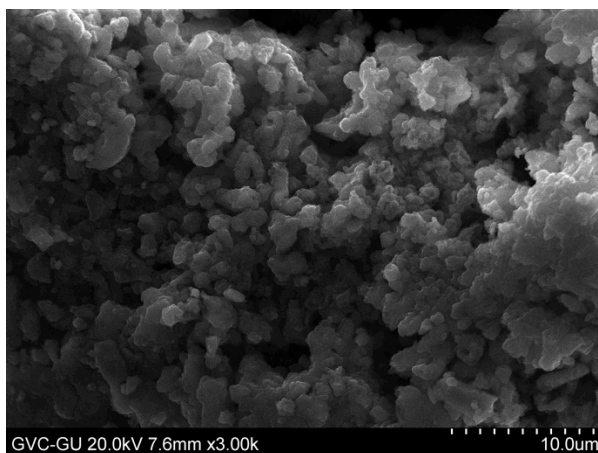


Fig. 25: Secondary electron-SEM-image of AA1 0°C

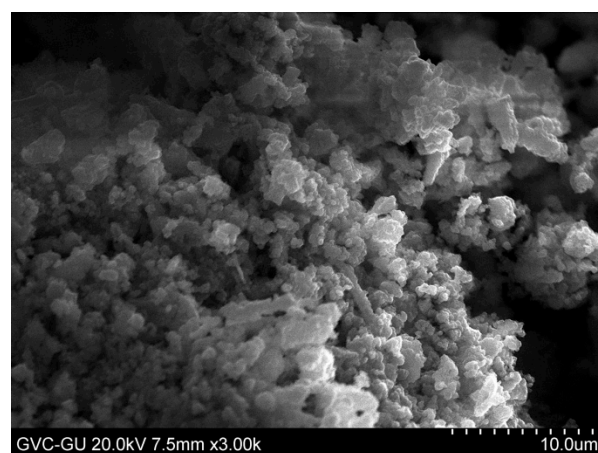


Fig. 26: Secondary electron-SEM-image of AA1 900°C

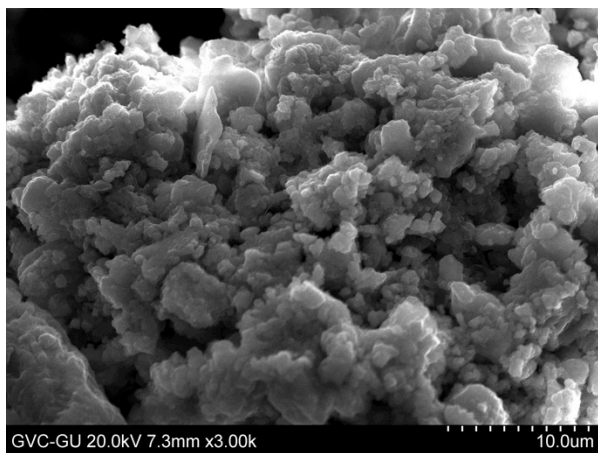


Fig. 27: Secondary electron-SEM-image of SR2 0°C

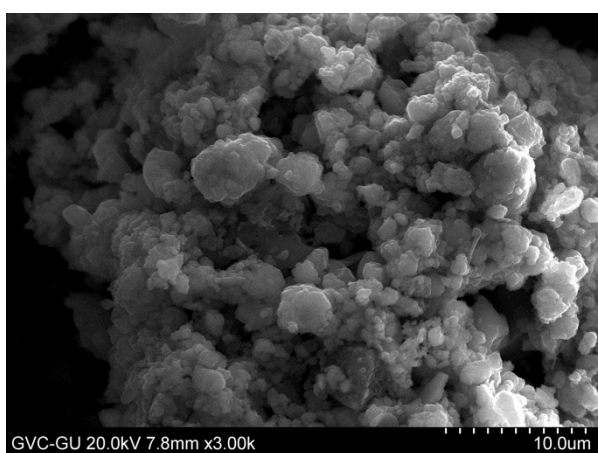


Fig. 28: Secondary electron-SEM-image of SR2 900°C

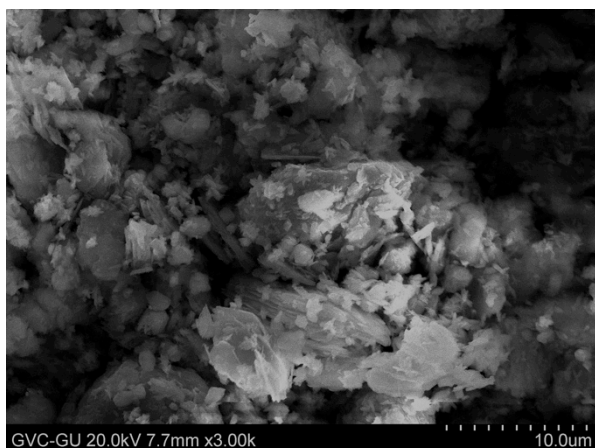


Fig. 29: Secondary electron-SEM-image of LOB 0°C

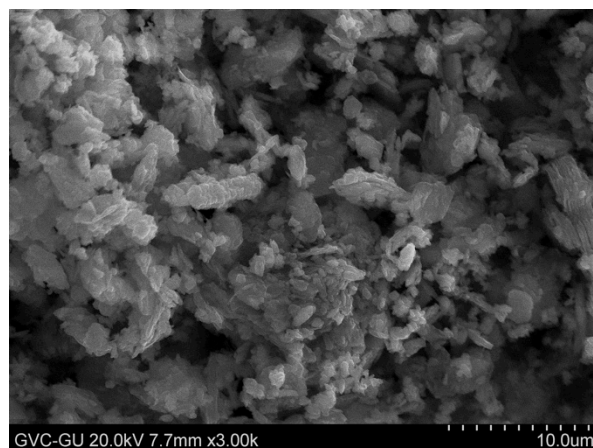


Fig. 30: Secondary electron-SEM-image of LOB 900°C

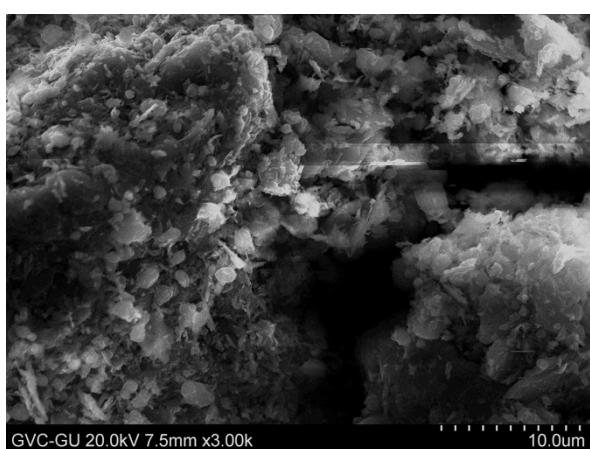


Fig. 31: Secondary electron-SEM-image of YAU 0°C

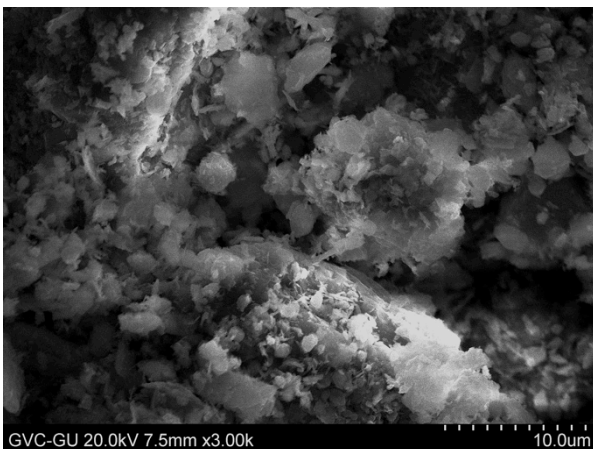


Fig. 32: Secondary electron-SEM-image of YAU 900°C

The HEM sample consists of angular crystals, but no other general crystal shape is seen.

The unheated LOB sample shows almost pointy elongated crystals, some of which almost aggregate in layers. The crystals in the 900°C sample have more rounded edges compared to the 0°C sample, maybe speaking of developed sintering. Layers are somewhat visible here as well.

The YAU 0°C and 900°C samples look quite the same. The crystals are pointy, a bit like the LOB 900°C, but no layering seems to appear in the YAU samples.

LØ3, HO1, ST3, AÅ1 and SR2 samples, both unheated and heated, are more or less the same. Small globules are seen scattered evenly in the images. Some of the globules stand out as little spheres others seem to have emerged together to form aggregates which are more angular but still rounded. The globules and the aggregates are covering bigger grains.

KT stands out from the rest of the soil samples from Sweden and Denmark. It only consists of the small globules, which are all almost the same size. These spheres also cover the surface of bigger grains. As with the other samples, no noticeable difference is visible between the heated and the unheated sample.

Since there is no eye-catching alteration between un-heated and heated samples, investigation of the heating time's effect on crystal morphology were not taken any further with the SEM.

The different crystal habits of the common iron oxides can be seen in Table 2. YAU and LOB fit the description of goethite crystal habits very well and looks a bit similar to the ochre samples in Fig. 6 in section 1.8.3.2. The Swedish and Danish samples, especially KT, fit the description of ferrihydrate, which is in line with the description about the samples' origin. The conditions for crystallisation could have been better for LØ3, HO1, ST3, AÅ1 and SR2 – were several iron oxide could have crystallised – in contrast to KT1 where only the poorly crystallised ferrihydrite could be formed. LØ3, HO1, ST3, AÅ1 and SR2 have some similarities with what is seen in Fig. 5 in section 1.8.3.2 as well.

Table 2: The crystal habits of the common iron oxides. (Cornell & Schwertmann 2003, p.64.)

Oxide	Principle habits	Other habits
Goethite	Acicular	Stars (twins), hexagons, bipyramids, cubes, thin rods
Lepidocrocite	Laths	Tablets, plates, diamonds, cubes
Akaganéite	Somatoids, Rods	Stars, crossed (twins), hexagons, prisms*
Schwertmannite	“Hedge-hog” aggregates	
$\delta$ -FeOOH	Plates	Thin, rolled films
Feroxyhyte	Plates	Needles
Ferrihydrite	Spheres	
Hematite	Hexagonal plates Rhombohedra	Spindles, rods, ellipsoids, cubes, discs, speres, double ellipsoids, stars, bipyramids, peanuts
Magnetite	Octahedra	Intergrown octahedral (twins), rhombic dodecahedra, cubes, spheres, bullets
Maghemite	Laths or cubes**	Plates, spindles
* Only reported, no micrographs available	** Adopts the morphology of its precursor	

On the other hand, would there not be goethite present in KT1? The colour of KT1 (augmented in section 3.1) definitely suggests it. Could the spheres be representing goethite instead? Goethite can in fact make globular aggregates, and an example of this can be seen in Fig. 33. The image shows a 20000 years old sand deposit from Denmark, where goethite has aggregates on quartz grains (Cornell & Schwertmann 2003, p.421).

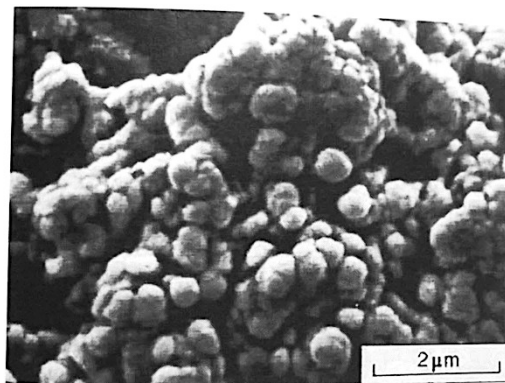


Fig. 33: Globular aggregates of goethite on quartz grains from a 2000 years old sand deposit in Karup, Denmark. (Cornell & Schwertmann 2003, p.421.)

The natural deposition of goethite around the quartz grains in Fig. 33 seems very similar to the core-shell structure of pigments described by Sajó et al. (2015) in section 1.8.3.1. Fig. 33 could definitely speak for a natural rather than an intentional process in the Upper Palaeolithic example from Hungary.

This could suggest that the difference between KT1 and LØ3, HO1, ST3, AÅ1 and SR2 is based on the degree of crystallinity of goethite and/or the type of aggregation.

Why are there no difference between the heated and the unheated samples? Based on the literature in section 1.8.3.2, goethite heated to 900°C should give well-ordered and well-crystallised hematite. Could it be that the crystal structure has changed but not the shape of the aggregates? Lack of distinguishable features between fired and unfired samples in the SEM-images cannot be explained any further in this thesis.

### **3.4 The ‘Hidden’ Information in SCiO-spectra**

Some of SCiO’s advantages and disadvantages will be presented before the analytical results. These are the experiences of the student after using SCiO and its accompanying software.

SCiO is affordable, portable and takes up little space. Making one scan takes around ten seconds and it is easy to do simple statistics without a lot of expert knowledge. When the spectral data is processed, one can find correlations with PCA-plots. It is all done through an intelligible interface of SCiO Lab web. However, all the simplified features do also bring undesirable elements. The spectral range is limited and it is not possible to get the raw data unless paying a larger fee. Because no statistical expertise is needed, it can be more difficult to interpret the data. One can be left with the question: what is exactly happening?! There is no control over the statistics, other than picking an algorithm from a list – the things that happen ‘behind the scenes’ are invisible. The layout of for instance the PCA-plot is also unchangeable. The units on PC1 can in some cases be unrelatable to those on the PC2.

The advantages have made it possible for the student to use SCiO in the Master’s project, and in some way helped the student to get familiar with statistical processing in a visual way. The limitations have on the other hand affected the interpretations. When there is no control, one can fail to notice important changes in how the data is processed. A lot more could be discussed here, but will not be extended.

It is instead time to move forward with the presentation of the results from the SCiO analyses. The figures in the following subsections are screen-shots from SCiO Lab web. They are this study’s ‘raw data’, because it is not possible to download the raw NIR spectra. All processing and model making is executed on the full spectral range collected by SCiO.

#### **3.4.1 Separating the Paint Layer from the Background**

Before looking deeper into aging, temperature, provenance (and other), it seems relevant to see if paint and background can be separated, as was the case in the Linderholm et al. (2015) project. The best result for this is done with the pre-processing SNV. Model 1 is created with only background scans from the rough side of the rock surfaces and paint on rock slabs. See Fig. 34.



Fig. 34: Model 1 made with SNV-processing on background scans from the rough side of the rock surfaces (b) and paint on rock slabs (p).

One can see that some background scans mistakenly are classified as paint. Some of the misclassifications could be attributed to the fact that some of the paint layers with water as binding media are very thin. This could have moved the ‘grouping border’ resulting in painted scans overlapping rock scans. Due to the relatively small number of background samples compared to paint samples, the result might look differently if samples were more evenly distributed between the two groups (known classes). It is also possible to make models only with subtraction of average, which also gives a  $F1=0,995$ , see Appendix VII, Fig. A.

### 3.4.2 All Samples and SNV

An initial examination of the data-set was done by applying SNV to all the spectral data of this Master’s project without any further processing (and no averaging of scans), PCA-plots are shown in Appendix VII, Fig. B-D, together with an image of the raw spectra of all samples (Appendix VII, Fig. E). They are all the same PCA-plots, but the samples are coloured differently to match the research questions for this thesis (heating temperature, aging and provenance).

The PCA-plots coloured by temperature and provenance gives some kind of grouping but the PCA-plot based on aging show no signs of obvious grouping. It is noteworthy that the unheated samples do not mix with heated samples. KT samples do furthermore spread out quite a lot compared to the other earth samples, particularly the KT samples heated to 300°C and 600°C. The reason for KT to spread out in that extent can have something to do with its iron oxide composition and the maghemite possibly produced in during firing (Fig. 4, section 1.8.3.2).

The rock surfaces do not differ that much from the painted samples, which may be because of the nature of the red granite as it can also contain hematite, hence its red colour (Platou 1970, p.106).

Could it be possible to extract more information or to obtain models and more clear PCA-plots if some samples are were filtered out?

### 3.4.3 Temperature

When a model (2) is created based on all samples with meta-data about heating temperature, samples are classified fairly well, with an  $F1=0,843$ . See Fig. 35. An almost similar model

with  $F1=0,823$  could be achieved when using ‘subtraction of average’ as normalisation (Appendix VII, Fig. F). Samples with unknown heating temperature are not included in the model, because the number of samples in these ‘known’ classes are too small compared to the rest. Neither are HEM samples for the same reason and because classes need to contain at least 5 samples before being included in models. Scans of the background is furthermore not included in model 2.

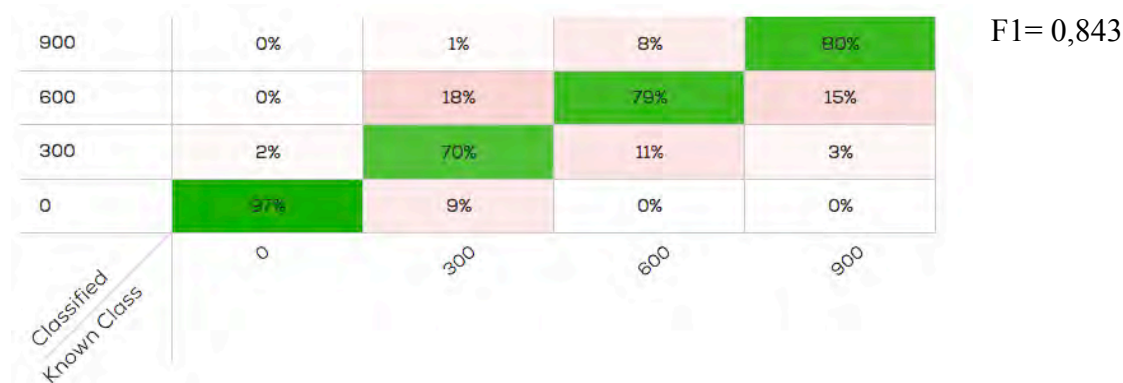


Fig. 35: Model 2 made with SNV-processing on all painted samples, excluding samples with unknown heating temperature and HEM samples.

Model 2 classify unheated samples very well but have problems with the fired samples. If the misclassifications are caused by the presence of certain minerals (e.g. maghemite), the difference in provenance, thin paint layer, binding media etc. is not to say – there are simply too many variables included in the model.

SNV is applied to the spectra of pigment samples on carbon tape in Fig. 36 to eliminate the effect of binding media, and KT samples are filtered out to exclude the big variance it brings to the PCA. The samples are coloured by heating temperature. The same PCA-plot is seen in Fig. 37, with samples coloured by provenance instead.

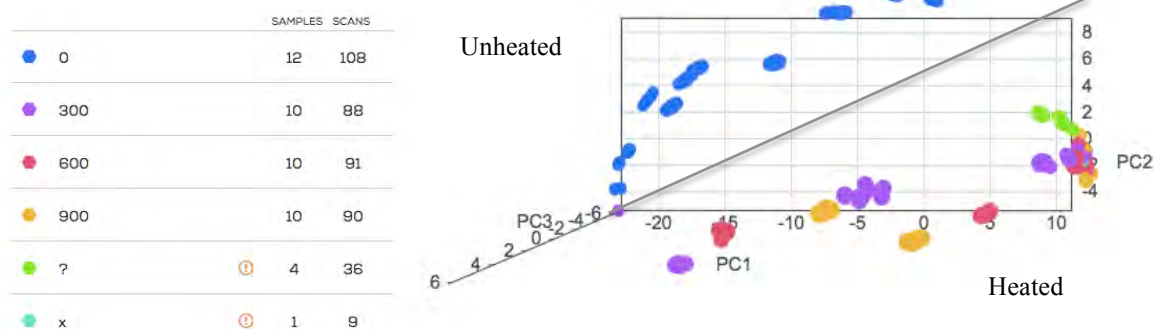


Fig. 36: PC1-PC2-plot of samples on carbon tape (excluding KT) with SNV-processing. The samples are coloured by heating temperature; Blue/ 0 represents unheated, green/? represents unknown heating temperature and turquoise/x represents HEM.

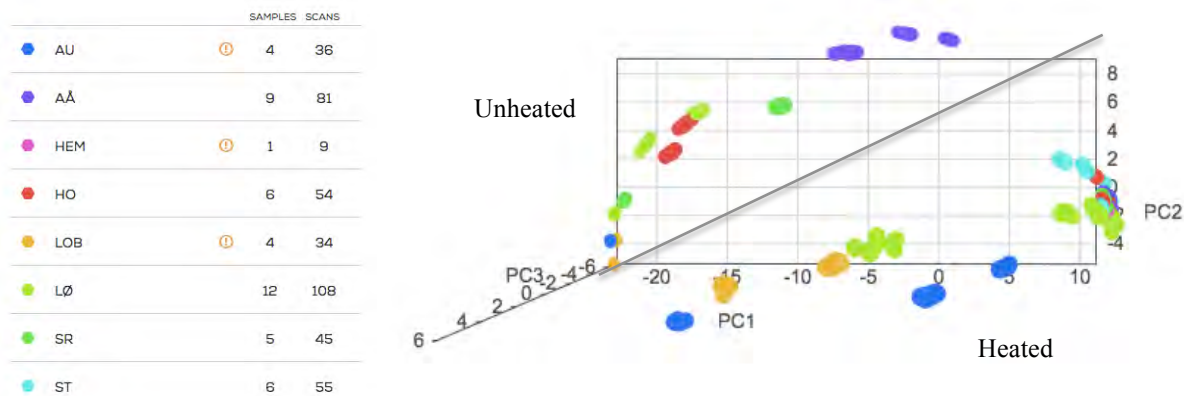


Fig. 37: PC1-PC2-plot of samples on carbon tape (excluding KT) with SNV-processing. The samples are coloured provenance.

Unheated samples can be separated from heated samples in Fig 36, but the heated samples are mixing together in the PCA-plot. Fig. 37 shows how the samples spread out on PC1 due to the provenance. It is evident that several factors, other than heating temperature, are still contributing to the PCA.

To eliminate even more variables, the spectra from a single location, AÅ with SNV, is plotted in a PCA and coloured based on heating temperature. See Fig. 38.

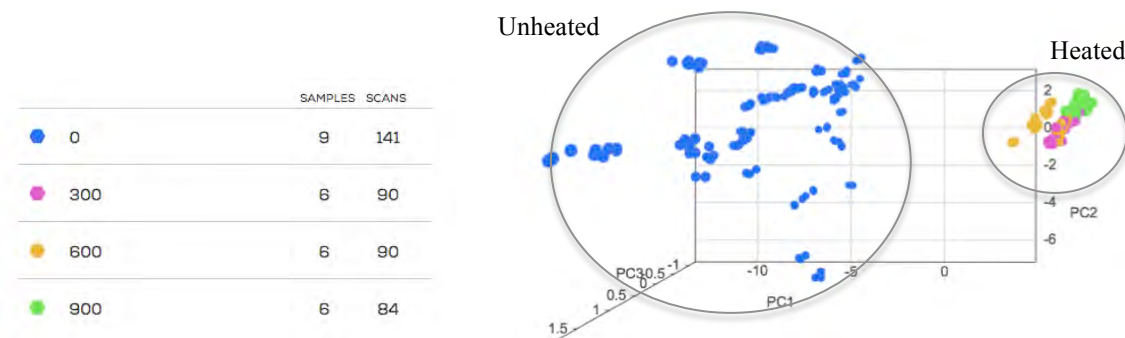


Fig. 38: PC1-PC2-plot of AÅ spectra with SNV-processing. The samples are coloured by heating temperature; 300°C - 900°C, blue/0 represents unheated samples.

The unheated samples are scattered out in the negative part of PC1 and all heated samples cluster in the positive part of PC1. The PC1 could in this case indicate the presence of hematite, but the presence of hematite does not explain why the unheated samples cover such a large area in the PCA-plot. Could grain size and/or degree of crystallisation be another variation factor? Based on the previous research in section 1.8.3.2, it makes sense that the iron oxide crystals in the unheated samples are much more diverse in terms of size and/or less crystallised than newly formed hematite crystals.

Unheated samples have been filtered out in Fig. 39 to explore the variance between samples heated at different temperatures.

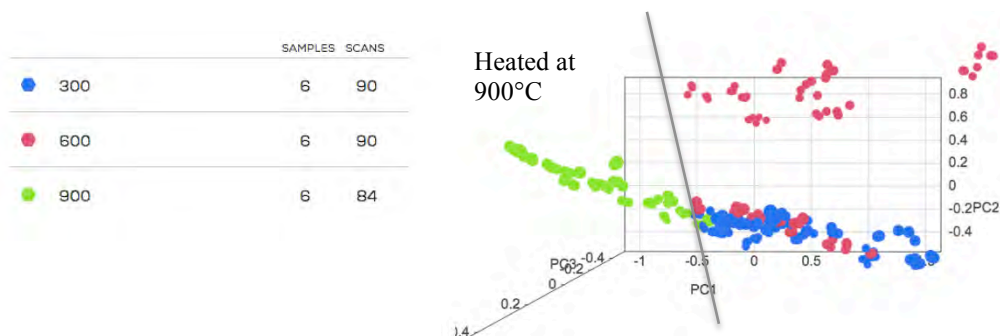


Fig. 39: PC1-PC2-plot of AÅ spectra with SNV-processing. The samples are coloured by heating temperature; 300°C - 900°C.

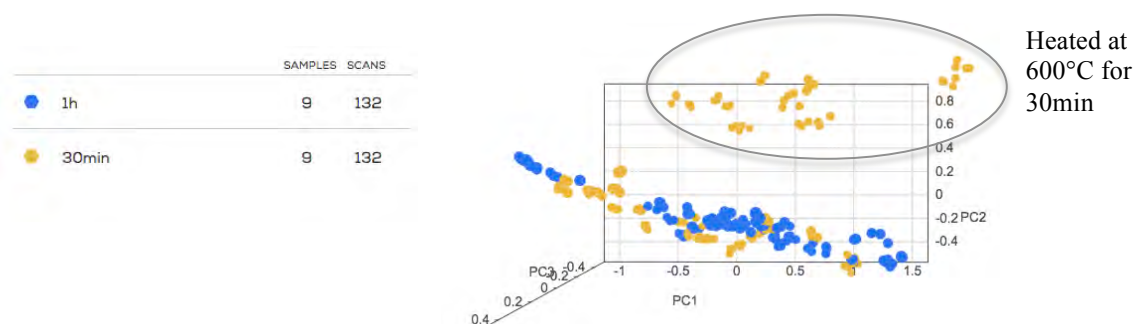


Fig. 40: PC1-PC2-plot of AÅ spectra of samples heated at 300°C, 600°C and 900°C with SNV-processing. The samples are coloured by heating time; 1hr and 30min.

Samples heated to 900°C separate well from samples heated to 300°C and 600°C in PC1, Fig. 39. Could this suggest that samples with a negative PC1 in Fig. 39 have a higher (maybe more well-crystallised) hematite content? Again, the literature speaks for this interpretation.

What about the samples heated to 600°C that separates on PC2? In Fig. 40, one will notice that samples in the positive side of PC2 has only been heated for 30min in contrast to the others fired for 1hr. It could be possible to make arguments about this separation based on the creation of hematite from maghemite. The process happens between 370-600°C and might require longer time for hematite to be well crystallised compared to the hematite producing processes that happens at 300°C.

The spectral data above have only been treated with SNV-processing. Different combinations of processing methods with and without normalisation were applied to the data set to see if the difference in heating temperature could be distinguished better.

Three different models were created based on heating temperature: all AÅ samples, all LØ3 samples with blood and water as binding media and all KT samples. The reason for only choosing these three sample groups were that the amount of samples from the other locations is not large enough to create these types of models with. In each model, the sample scans were averaged and processing and normalisation methods applied:  $\log \rightarrow 1^{\text{st}} \text{ derivative} \rightarrow \text{SNV}$ . The models (3-5) derived from all three sample groups gave relatively good results, despite the low number of samples used in each model. See Fig. 41-43.

An example of the PCA-plot with AÅ samples used as a basis for making model 3 can be seen in Appendix VII, Fig. G. In the figure, heated samples cluster on the negative side of PC1 whereas unheated are located on the positive side. Fig. H in Appendix VII shows another

PCA-plot of heated AÅ samples and how they separate on PC2, in terms of heating temperature, maybe based on the degree of transformation from goethite to hematite.

900	0%	0%	0%	91%	F1= 0,963
600	0%	0%	91%	8%	
300	0%	100%	8%	0%	
0	100%	0%	0%	0%	
Classified Known Class	0	300	600	900	

Fig. 41: AÅ samples. Model 3 made with log → 1<sup>st</sup> derivative → SNV-processing of AÅ samples. The scans have been averaged.

900	0%	0%	0%	100%	F1= 0,985
600	0%	0%	100%	0%	
300	7%	100%	0%	0%	
0	92%	0%	0%	0%	
Classified Known Class	0	300	600	900	

Fig 42: LØ samples. Model 4 made with log → 1<sup>st</sup> derivative → SNV-processing of LØ3 samples with known heating temperature. The scans have been averaged.

900	0%	0%	0%	100%	F1= 0,921
600	0%	16%	100%	0%	
300	0%	66%	0%	0%	
0	100%	16%	0%	0%	
Classified Known Class	0	300	600	900	

Fig 43: KT samples. Model 5 made with log → 1<sup>st</sup> derivative → SNV-processing of KT samples. The scans have been averaged.

F1=0,963 for the AÅ-model, F1=0,985 for the LØ3 model and F1=0,921 for the KT model. The classification seen in the models can be due to loss of bound water from the goethite crystal structure and ferrihydrite. The KT-model (5) seems to have difficulties in the classification of samples heated at 300°C. It is not possible to see which samples cause the wrong classifications. How each of these three models performs when tested on the rest of the data set will be discussed in section 3.4.3.1.

When looking at the Å spectra when SNV→1<sup>st</sup> derivative has been applied obvious differences are visible: heated samples have a y-axis value of 0 at approximately 855 nm wavelength, while the spectra of the unheated samples cross the same line a bit above 900nm. See Fig. 44. As the characteristic NIR bands for hematite is in the range: 848-906 nm and for goethite: 929-1022nm mentioned in section 1.8.2, it fits quite well with what is observed in Fig. 44. The spectra for KT-samples and LØ samples do not give the same clear result. See Fig. 45 and Fig. 46.

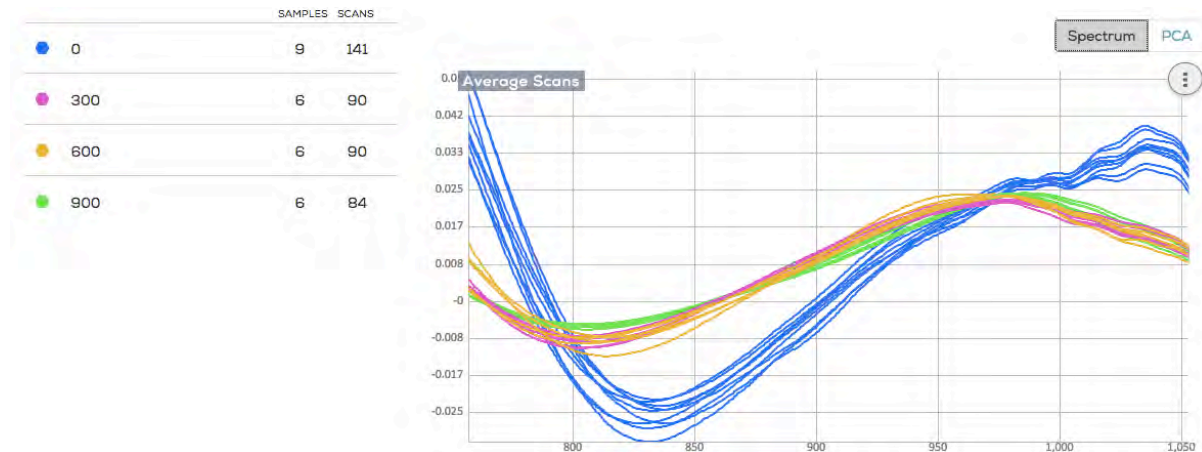


Fig. 44: Å spectra with SNV→1<sup>st</sup> derivative-processing. The samples are coloured by heating temperature; 0°C - 900°C and scans have been averaged.

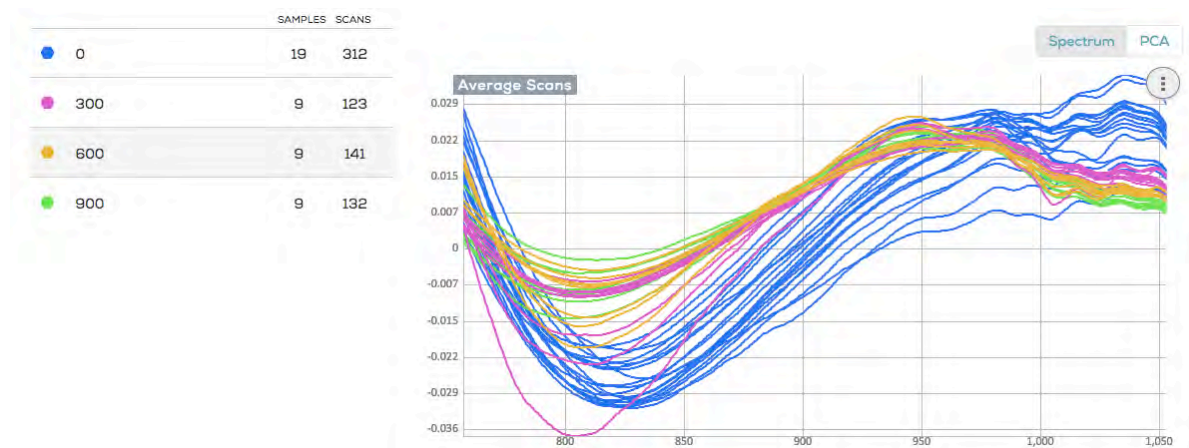


Fig 45: LØ spectra with SNV→1<sup>st</sup> derivative-processing. The samples are coloured by heating temperature; 0°C - 900°C and scans have been averaged.

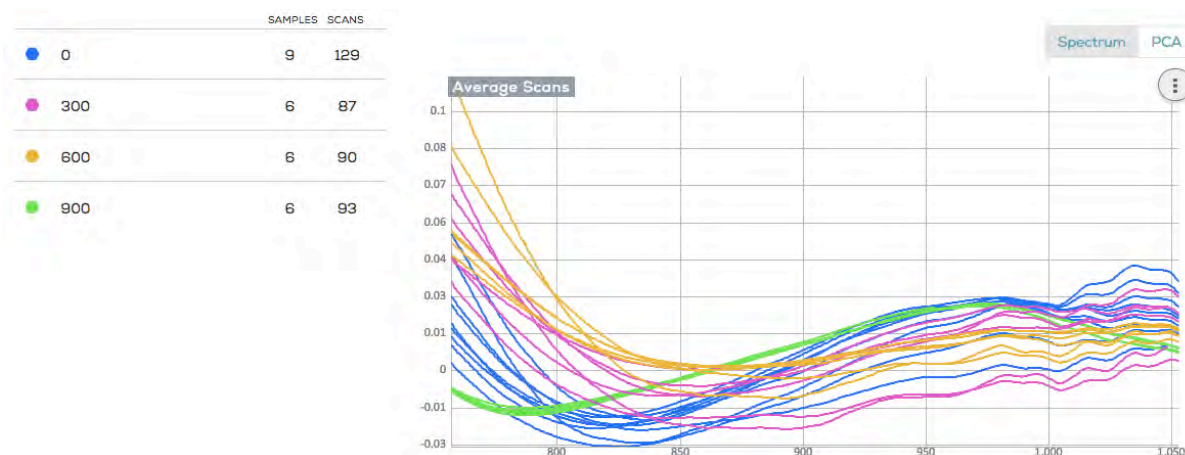


Fig 46: KT spectra with SNV  $\rightarrow$  1<sup>st</sup> derivative-processing. The samples are coloured by heating temperature; 0°C - 900°C and scans have been averaged.

The heterogeneous character of LØ3 (shortly presented in section 3.3) can have affected the collected spectra and be the basis for spreading between spectra in Fig. 45. However, it could again have something to do with the mineralogical transformation steps. For KT, the reaction might not have gone straight from goethite and ferrihydrate to hematite at the lower temperatures, but instead to maghemite (Fig. 4, section 1.8.3.2). Only the spectra of the 900°C KT samples cuts the y-axis at 0 very precisely around 855nm, which corresponds well with the bright red colour of the same samples.

#### 3.4.3.1 Samples and Heating Temperature: Model Testing

To examine the applicability of models 3-5 on the rest of the samples, three tests have been run, one for each model. The samples that had been used to make the model were in each case excluded when calculating the F1-scores, as well were samples with unknown heating temperature. None of the model tests came out with good F1-scores (see Appendix VIII, IX and X). To gain more information about the models and how usable they are at making predictions about heating temperature of other samples, the individual F1-scores for every heating temperature could be considered. See Table 3.

Table 3: F1-scores speaking of model 3's, model 4's and model 5's performance to classify heating temperature on the remaining samples.

Model 3 (AÅ)		Model 4 (LØ3)		Model 5 (KT)	
0°C F1=	0,833	0°C F1=	0,760	0°C F1=	0,876
300°C F1=	0,476	300°C F1=	0,413	300°C F1=	0
600°C F1=	0,379	600°C F1=	0,064	600°C F1=	0
900°C F1=	0,666	900°C F1=	0,454	900°C F1=	0,521

As it can be seen, the models are all better at classifying unheated samples correctly than heated samples. The KT F1-scores for 300°C and 600°C in Table 3 also show, that no other samples seem to fit the variables of the KT samples. It supports the idea about maghemite over hematite in these KT samples. The LØ3 F1-score for 900°C samples seem to classify some samples correctly. It could mean that LØ3 900°C samples contain some hematite or, that the other correctly classified samples contain maghemite (or something else) that causes LØ3 900°C samples to exhibit their colour. Based on Table 3 and the discussed results in section 3.4.3, it could be proposed that AÅ samples go through a classic conversation from goethite to hematite, whereas LØ3 and KT include more complex transformation processes.

The attentive reader may have noticed, that the temperature of LØ3 samples with unknown heating temperature has not been specified. At the time of writing, the temperature on the pan where samples for the aging experiment were heated has not been tested. Could model 4 maybe be used to determine the temperature they had been heated at? Most of the exposed samples are classified as 600°C, whereas only the un-exposed sample with fat as binding media is classified as 600°C (see Appendix IX). Either 300°C or 600°C do not appear as an unexpected temperatures a pan can reach on a kitchen stove. Both exposure and binding media does, based on this test, affect how samples from the same location and fired at the same temperature classify. The effect of age and binding media will be further elaborated in the next section.

### 3.4.4 Age and Binding Media

The model (6) in Fig. 47, based on aging (including new scans), did not perform well even though F1 is relatively high. This can be due to the size of the groups/known classes. Especially the ‘new samples’ category is far bigger then the exposed and unexposed sample groups.

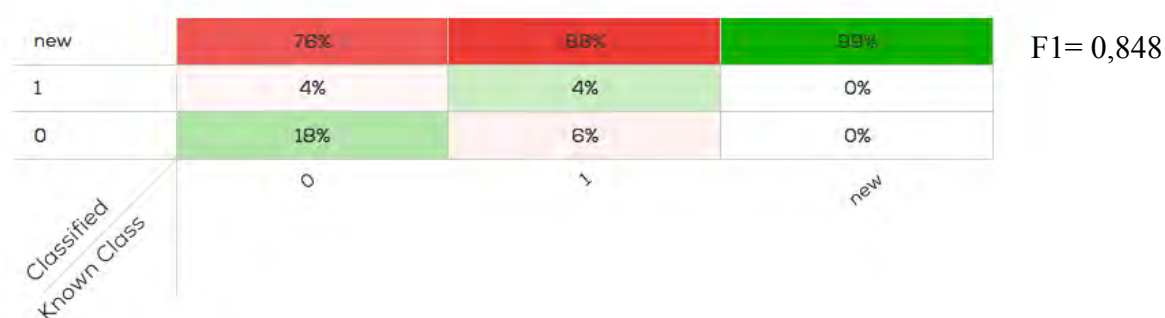


Fig. 47: Model 6 made with SNV-processing on all samples. – represents background/rock scans, 0 represents unexposed samples and 1 represents exposed samples.

The overrepresentation of the ‘new’ samples can be circumvented by excluding these. Fig. 48 shows a PCA-plot of the exposed and unexposed heated samples after applying ‘subtraction of average’. The same PCA-plot where samples have been coloured by binding media is shown in Fig. 49.; the PC1-PC3-plot is also included.

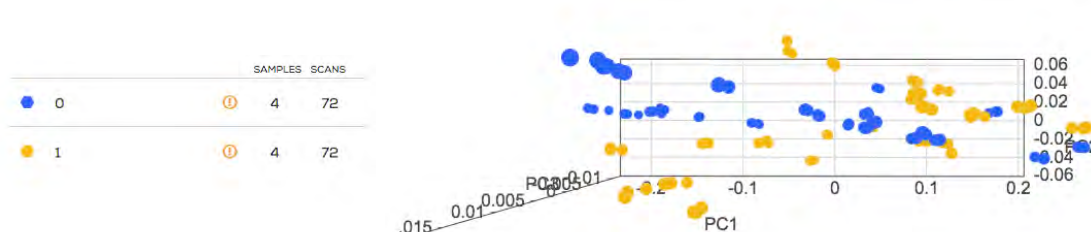


Fig. 48: PC1-PC2-plot of exposed and unexposed heated samples with ‘subtraction of average’-processing. Samples are coloured by aging. Blue/0 represents unexposed samples and yellow/1 represents exposed samples.

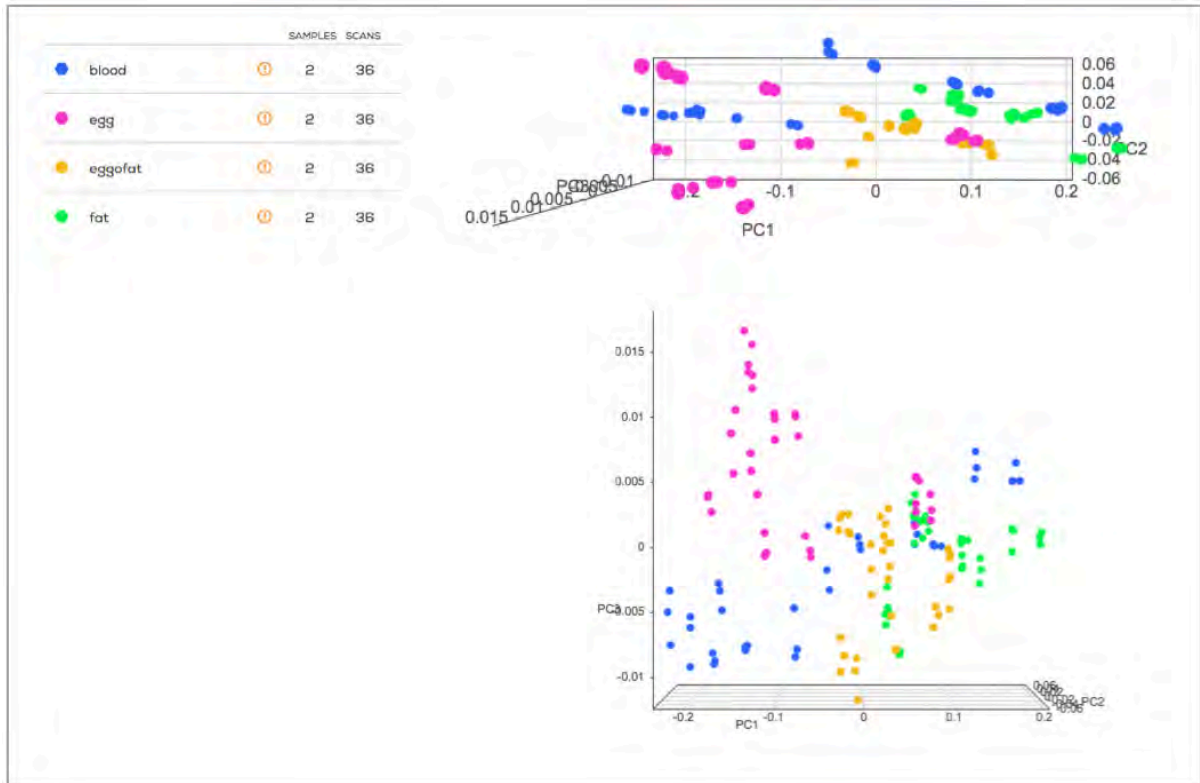


Fig. 49: PC1-PC2 and PC1-PC3-plots of exposed and unexposed heated samples with 'subtraction of average'-processing. Samples are coloured by binding media. Yellow/eggofat represents egg and fat-mixture.

Fig. 48 does not depict the effect of aging in general, but when Fig. 49 is used to establish a relationship between aging and binding media, it is apparent that all types binding media do not age in the same way. Exposed and unexposed egg samples and egg and fat-mixture samples are more or less within the same area of each other on PC1 regardless of aging. Exposed and unexposed fat samples separate a bit on PC1, whereas the blood samples separate to most on PC1 with unexposed samples in the negative part of PC1 and exposed samples in the positive part. Some types of binding media seem to be effected by exposure more than others.

Clustering of the four types of binding media is slightly visible in the PC1-PC3-plot in Fig. 49, but is even enhanced in the PC1-PC3-plot in Fig. 50, illustrating only the unexposed samples. A PC1-PC2 of the same PCA is also presented in Fig. 50. Three groups can be identified: a protein-based binding media group with blood samples, a protein and fat-based group with egg and egg-fat samples, and a fat-based group with fat samples, divided by diagonal lines in the PC1-PC2 plot. Both PCA-plots in Fig. 50 demonstrate that different types of binding media can be detected with SCiO.

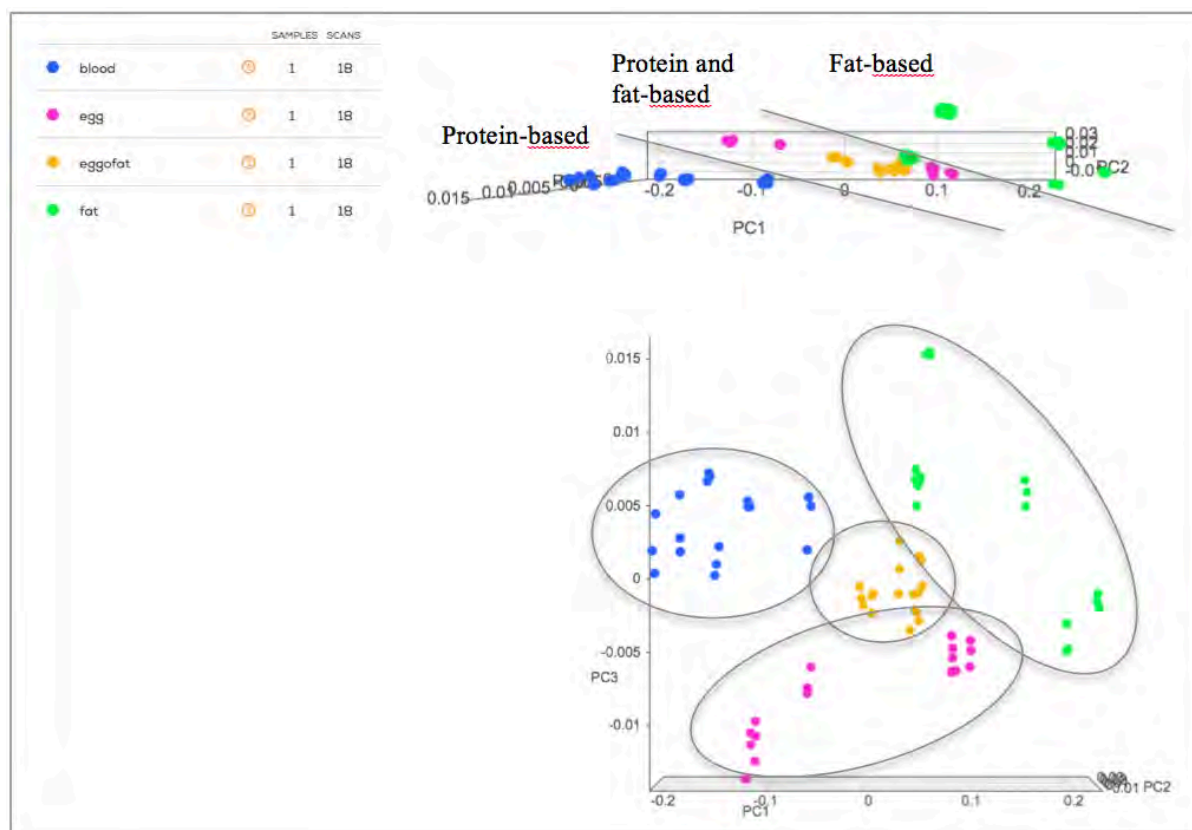


Fig. 50: PC1-PC2 and PC1-PC3-plots of unexposed heated samples with ‘subtraction of average’-processing. Samples are coloured by binding media. Yellow/eggfat represents egg and fat-mixture.

It is discovered that, by only taking the logarithmic (log) value of the spectra of painted samples, a separation based on the presence of binding media emerges along PC1. The animal based binding media is more or less located on the negative part of PC1 whereas samples with no binding media (on carbon tape) and samples mixed with water on the positive part of PC1. See Fig. 51. A model (7) was created based on samples applied with either blood or water. See Fig. 52.

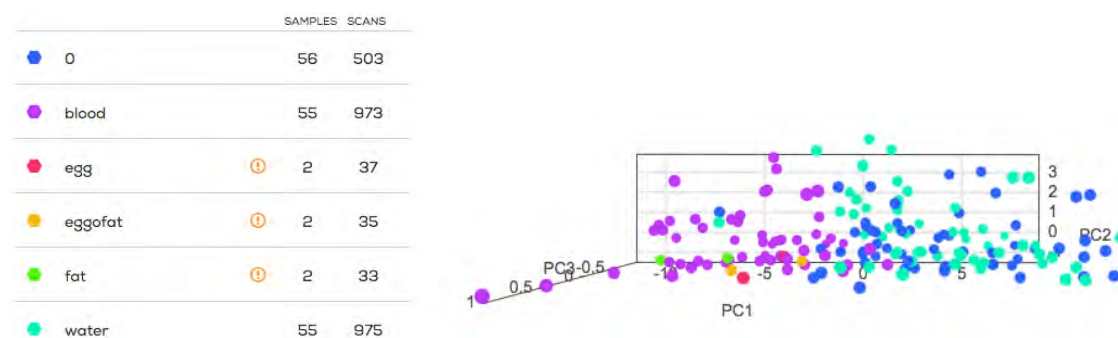


Fig. 51: PC1-PC2-plot of all painted samples with log-processing and averaged scans. The samples are coloured by binding media. Blue/0 represents samples on carbon tape. Yellow/eggfat represents samples painted with the egg yolk-fat mix.



Fig. 52: Model 7 made with all painted samples with blood and water as binding media and log-processing. The scans have been averaged.

Model 7 gives a good classification with  $F1=0,91$ . Because no normalisation is carried out on the spectra, scattered light is not eliminated. The separation seen in Fig. 51 can hence be due to the difference in surface roughness. Pigments with animal based binding media have been incorporated in a smooth film whereas pigments applied with water lies on the surface as pure grains. It does not seem like the different types of animal based binding media can be separated with this method.

#### 3.4.4.1 Blood and Water: Model Testing

Model 7 was tested on the rest of the sample set: the other animal based binding media and carbon tape samples. How samples have been classified can be seen in Appendix XI. The fact that carbon tape-samples are classified as water-samples does not seem strange, as the water has obviously evaporated after application, and therefor must be comparable to the samples where no liquid had been added. It is also logical that the animal based binding media are classified as blood-samples. It is now possible to calculate the performance of the model on the new set of samples that were not included in the creation of model 7. F1 have been calculated under the conditions that no binding media (samples on carbon tape) = water; and egg, fat and egg mixed with fat = blood. Regular averaged  $F1=0,820$  and weighed averaged  $F1=0,880$ , where group size is taken into account. The F1-scores suggest that model 7 works quite well on other samples not included in the model.

#### 3.4.5 Provenance

A model (8), focused on provenance, based on all samples (excluding HEM samples) gives a  $F1=0,713$ . See Fig. 53. There are a percentage of almost all known samples that are classified as LØ, especially HO, which also classifies with a lot of the other locations. Besides the false LØ classifications, LOB and AU have most in common with each other, SR have most in common with HO, and ST have most in common with AÅ. Compared to the SEM-EDX results presented above, there is no clear, recurrent pattern applicable to all sample cases. From model 8, it can also be derived that the background scans, for most incidences, separate from the rest of the samples.

## Results and Discussion

ST	0%	0%	1%	5%	1%	0%	1%	0%	62%
SR	0%	0%	1%	22%	0%	0%	0%	63%	0%
LØ	4%	10%	6%	25%	20%	4%	64%	8%	13%
LOB	1%	23%	0%	0%	1%	73%	0%	0%	0%
KT	0%	1%	0%	1%	75%	2%	2%	2%	0%
HO	0%	0%	7%	23%	0%	0%	4%	21%	3%
AA	0%	0%	63%	21%	0%	0%	2%	3%	18%
AU	1%	61%	0%	0%	0%	15%	1%	0%	0%
-	32%	2%	0%	0%	0%	3%	2%	0%	0%
Classified Known Class	-	AU	AA	HO	KT	LOB	LØ	SR	ST

F1= 0,713

Fig. 53: Model 8 made with SNV-processing on all painted samples, excluding HEM samples. – represents background/rock scans.

Continuously, four different models were created: one for every heating temperature: 0°C (unheated), 300°C, 600°C and 900°C. The classification is based on provenance. Because it is not possible to make classifications targeting all locations – due to a low number of samples in some sample groups – the provenance categories are instead ‘Denmark’, ‘Sweden’ and ‘others’. All painted samples are included and  $\log \rightarrow 1^{\text{st}}$  derivative is applied to the spectra. The models (9-12) are presented in Fig. 54-57. Models 9-12 have been tested on the rest of the data set. Results are described in section 3.4.5.1.

s	42%	50%	79%
o	0%	41%	0%
d	57%	8%	20%
Classified Known Class	d	o	s

F1= 0,678

Fig 54: Model 9 made with all unheated samples (excluding HEM) and  $\log \rightarrow 1^{\text{st}}$  derivative-processing. The scans have been averaged. d represents Denmark, o represents other and s represents Sweden.

s	11%	0%	95%
o	0%	100%	0%
d	88%	0%	4%
Classified Known Class	d	o	s

F1= 0,944

Fig 55: Model 10 made with all samples heated to 300°C and  $\log \rightarrow 1^{\text{st}}$  derivative-processing. The scans have been averaged. d represents Denmark, o represents other and s represents Sweden.

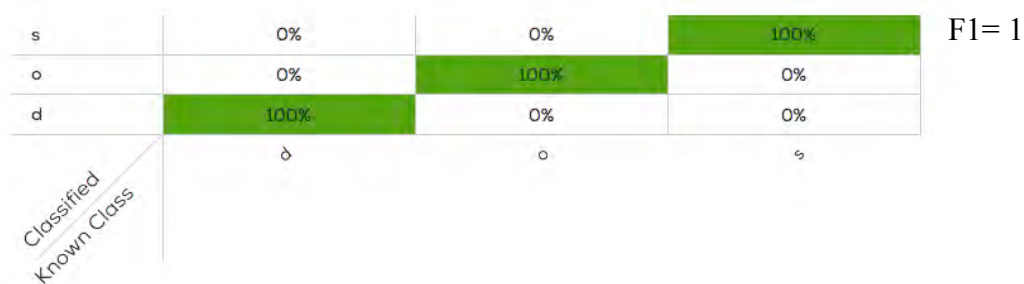


Fig 56: Model 11 made with all samples heated to 600°C and log → 1<sup>st</sup> derivative-processing. The scans have been averaged. d represents Denmark, o represents other and s represents Sweden.

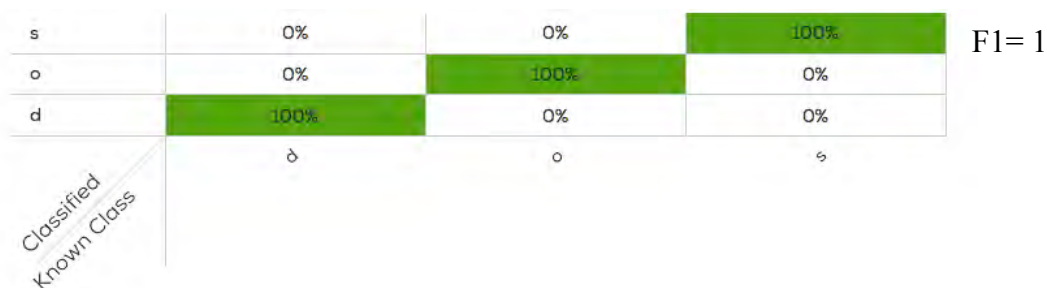


Fig 57: Model 12 made with all samples heated to 900°C and log → 1<sup>st</sup> derivative-processing. The scans have been averaged. d represents Denmark, o represents other and s represents Sweden.

The low number of samples in each model must have affected the final F1 scores. For both 600°C and 900°C, the models gives an F1=1, which means that all samples have been classified correctly in relation to their known class. Model 10, for samples heated to 300°C, the classifications are less precise, but still excellent with F1=0,944. The model with unheated samples perform poorest with F1=0,678; these samples seem difficult to separate from each other. Conclusively, samples can be ascribed to their overall area of origin when, whereas they cannot when unheated.

An example of PCA-plot of samples heated to 600°C is seen in Fig. 58. The PCA was used to construct model 11.

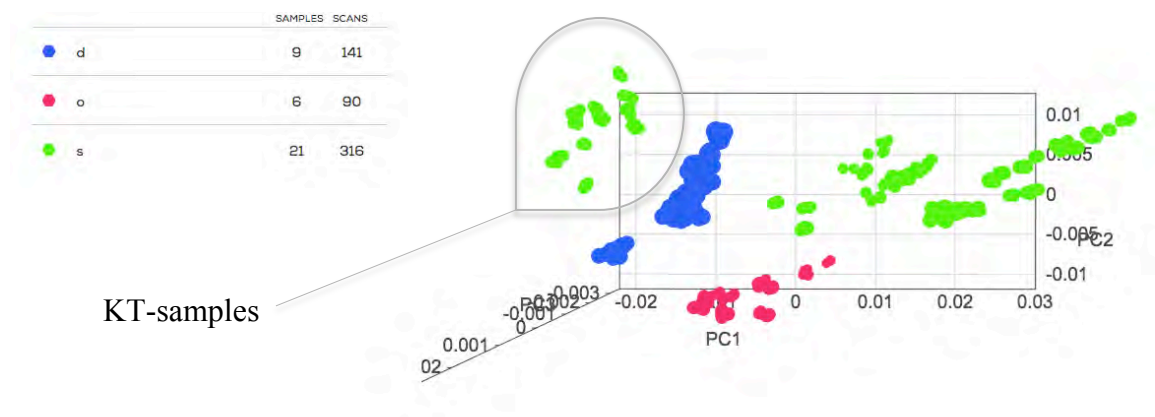


Fig 58: PC1-PC2-plot of painted samples heated to 600°C with log → 1<sup>st</sup> derivative-processing. Samples have not been averaged and are coloured by overall origin. d represents Denmark, o represents other and s represents Sweden. KT samples group away from the other Swedish samples.

One can see, that the PCA is not based on big variances in the variables – the plots only differ on a 0,01 scale. Even though KT separates from the rest of the Swedish samples in Fig. 58, they are still classified as Swedish samples. This is a good illustration of the complexity in the cross-validation method – all variances are included in the creation of models.

The reason for the Danish samples to separate for themselves and not with the Swedish samples could be motivated by the SEM-EDX result in section 3.2, where the LØ3 sample contain Ca, something none of the other samples do. KT samples may again separate in Fig. 58 based on the content in maghemite. No normalisation has been applied in models 9-12 or Fig. 58. The difference in particle size or crystalline defects that dominates the variation between unheated samples and to some extent samples heated to 300°C, are reduced or eliminated when hematite crystallisation is initiated. The chemical composition will instead be major ground for variation in fired samples. The SEM-images (Fig. 16-32) does not speak for a huge change in particle size (aggregates), so crystalline defects or differences in grain size in unheated samples seem more credible.

Because only one sample is available from Denmark, it cannot be concluded if the separation between the Danish and the Swedish samples also have something to do with the difference in bedrock type. Fig. 7 shows quite nicely that the Danish site is located in late Proterozoic and Fanerozioc region. On the other side, all Swedish samples are somewhat in the borderline between Proterozoic and early Proterozoic bedrock types. As stated in section 1.8.5, main bedrock type differences may be the only way the discriminate between otherwise similar raw materials in terms of slag.

If only the Swedish samples heated to 900°C are plotted in a PCA with  $\log \rightarrow 1^{\text{st}}$  derivative  $\rightarrow$  SNV, the variance is bigger. See Fig. 59. The 900°C samples were selected to avoid the influence of the brown KT1 samples on the variance. The samples spread out on PC2 in terms of binding media. See Fig. 60.

	SAMPLES SCANS	
AA	6	84
HO	3	46
KT	6	93
SR	3	43
ST	3	45

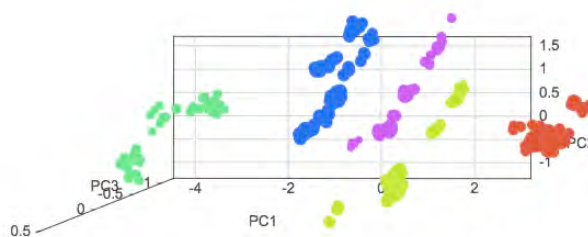


Fig. 59: PC1-PC2-plot of all Swedish samples heated to 900°C with  $\log \rightarrow 1^{\text{st}}$  derivative  $\rightarrow$  SNV-processing. Scans have not been averaged and samples are coloured by location.

	SAMPLES SCANS	
0	7	63
blood	7	122
water	7	126

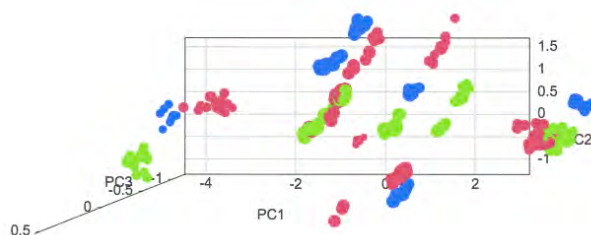


Fig. 60: PC1-PC2-plot of all Swedish samples heated to 900°C with  $\log \rightarrow 1^{\text{st}}$  derivative  $\rightarrow$  SNV-processing. Scans have not been averaged and samples are coloured by binding media. Blue/0 represent samples on carbon tape.

It is more uncertain what PC1 represents, especially because the SEM-EDX results cannot be compared to a standard unit. One explanation can be the hematite content – consequently the Fe content as well. The samples in the positive part of PC1 could contain the highest amount of hematite, with the hematite concentration being lower as PC1 goes negative. Based on the SEM-EDX result, KT1 is mostly Fe, O and C. After all carbon has burned away in the 900°C hot furnace, one can assume that there is not much more left than iron in the sample and all iron minerals have been transformed to hematite. Something that could support this interpretation, besides the SEM-EDX results, is the information that was given about the ST location. The hobby-blacksmith had never made bloomery iron with red earth from this place, most likely because it did not have the ‘desired’ qualities. The reason for the lack of quality was not known by the hobby-blacksmith, but iron content could definitely be a possibility. KT1 comes from a stream where natural sedimentation has occurred – only the fine particles have been deposited on the brook bed.

Fig. 59 might be the basis for future quantification investigations. The student could in retrospect have wished that more effort had been put into quantification measurements of the samples – including the heated samples.

When the HEM samples are included, they plot between KT and SR, and not with KT or further away. See Fig 61; observe that PCA units are mirrored in contrast to Fig. 59.

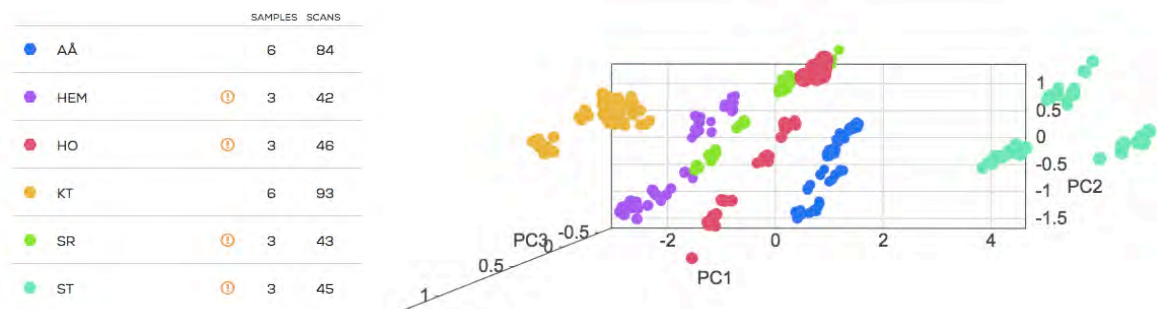


Fig. 61: PC1-PC2-plot of all Swedish samples heated to 900°C and HEM with log → 1<sup>st</sup> derivative → SNV-processing. Scans have not been averaged and samples are coloured by location.

If hematite content is represented in Fig. 59, HEM would be expected to contain most hematite and therefore plot farthest away from ST, but this is not the case. Other factors, for example particle and/or grain size, or the samples’ homogeneity, must therefore be contributing the PCA. At this point, it is not possible to come any closer to a conclusion about Fig. 59 and Fig 61.

#### 3.4.5.1 Heating Temperature for Provenance Determination: Model Testing

Models 9-12 have separately been tested on the rest of the sample set, which means that model 9 is tested on samples heated to 300°C, 600°C and 900°C, model 10 is tested on unheated samples and samples heated 600°C and 900°C, and so on. This was done to see if temperature makes any difference to the provenance classification. Regular averaged F1 and weighed averaged F1 were calculated for all four models’ performances (Appendixes XII-XV). Model 9 (0°C): regular averaged F1=0,267 and weighed averaged F1=0,401, model 10 (300°C): regular averaged F1=0,727 and weighed averaged F1=0,766, model 11 (600°C): regular averaged F1=0,598 and weighed averaged F1=0,691 and model 12 (900°C): regular averaged F1=0,627 and weighed averaged F1=0,667. These F1 values do not seem to be good in respect of the models’ performances, however, that is because the performance on specific

groups will not show. For this, it is necessary to examine each classification and compare it to the meta-data of each sample. Model 10 (300°C) has problems classifying some of the unheated samples and some samples heated to 900°C. However, all samples heated to 600°C classified correctly (Appendix XIII). Model 11 (600°C) classifies most 300°C and 900°C samples (except a few of both), while it has problems with unheated samples (Appendix XIV). Model 12 (900°C) classifies all 600°C samples (except one), and are having problems with unheated samples and a few 300°C samples (Appendix XV).

Three of the models (10-12) predict overall place of origin, regardless of heating temperature. Place of origin may in this context be about chemical composition, especially Ca for the Danish versus the Swedish samples.

### 3.4.6 Tumlehed Spectra

The raw spectra of the Tumlehed scans can be seen in Appendix VII, Fig. I. By applying  $\log \rightarrow 1^{\text{st}} \text{ derivative} \rightarrow \text{SNV}$  to the spectra collected from the Tumlehed rock painting, it is possible to separate paint from rock background on PC1. See Fig. 62.

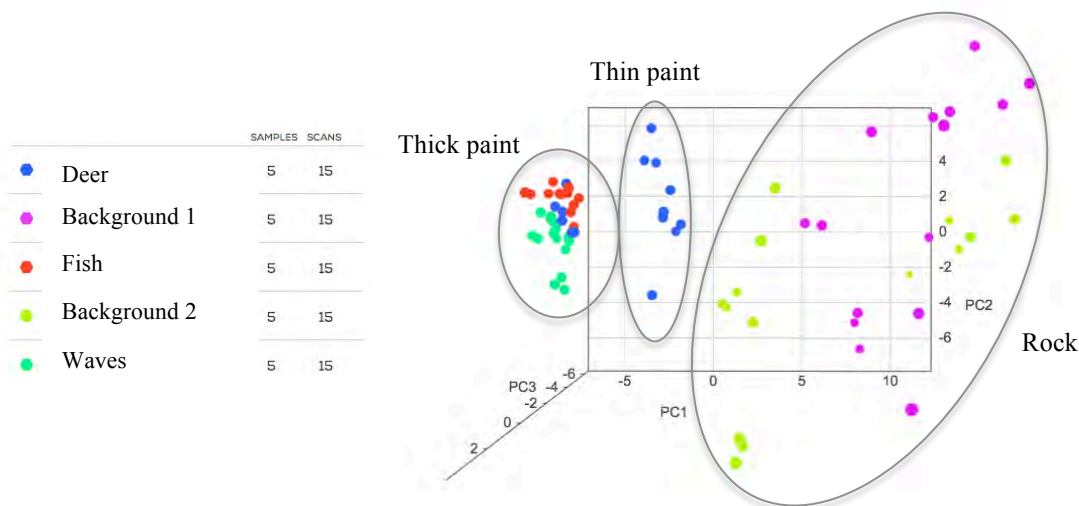


Fig. 62: PC1-PC2-plot of Tumlehed scans with  $\log \rightarrow 1^{\text{st}} \text{ derivative} \rightarrow \text{SNV}$ -processing. Samples are coloured by type of motif. Background 1 is from the rock surface around the deer figure, background 2 from is around the fish and waves.

Samples on the positive PC1 are background; negative PC1 equals paint. The rock scans are spread out on PC1 and PC2, owing big diversity and heterogeneity of the rock surface. It can also be noticed that some of the deer samples lie between the rest of the paint samples and  $\text{PC1}=0$ . The reason for this can be based on the thinner paint layer at the specific spots, as these scans were made on the head, front leg and body of the deer. Seen in Fig. 10, section 2.1.5, both the fish, the waves and the back part of the deer are redder in colour than the front part of the deer.

When all painted samples are compared with only SNV applied, the waves separate quite nicely from both the fish and the deer motifs. See Fig. 63. When a model (13) is made, based on the limited amount of samples available from Tumlehed  $F1=0,967$ , when classification is made between animal motifs versus wave motif. See Fig. 64.

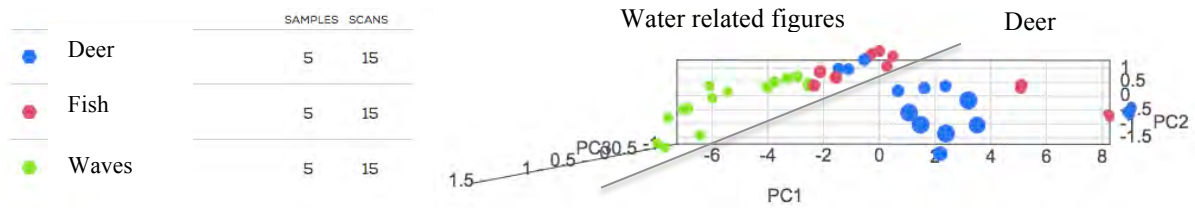


Fig. 63: PC1-PC2-plot of Tumlehed scans with SNV-processing. Scans are coloured by type of motif.



Fig 64: Model 13 made with scans from Tumlehed with SNV-processing. d represents animal figures, h represents waves.

Is it possible to make any interpretations of the Tumlehed rock painting based on the results obtained in this Master's project?

As stated in section 3.4.3.1, both exposure and binding media has an effect on the predicted temperature (in the specific case). However, the analysis was conducted on un-exposed versus exposed samples and not samples exposed at different time periods. Furthermore, the time of exposure was quite short in this investigation, and cannot at all be considered comparable to the 5000 years the Tumlehed rock painting has been exposed for. On the other hand, it can be discussed how much of the original binding media is left in the Stone Age paint – and hence the effect of binding media (and age) on the NIR spectra.

No satisfactory results are achieved when the models above are tested on the Tumlehed spectra. Even model 1 cannot separate paint from background in the Tumlehed rock painting. This might be due to the fact that model 1 is mainly created with newly made samples. If more exposed samples had been included in the experiment, it might have ended up with a more general model that could suit the Tumlehed spectra. The rock surfaces' different characters may also be causing trouble. Tumlehed rock painting is executed on a weathered rock face whereas the painted samples from the experiment are applied to a cut rock surface.

If the effect of age and binding media is disregarded in the Tumlehed case, it might be possible to make some propositions of Fig. 63.

It is known from the literature (section 1.8.3.2) that an open fire can reach temperatures of 750-800°C. Pigments containing sintered hematite could therefore have been a possibility, as the process happens above 600°C. AÅ1 seems most representable for the Swedish samples. Based on the PCA-plots of AÅ1 (Fig. 41-43 with same pre-processing method as presented in Fig. 63) the pigments from Tumlehed could have been heated at different temperatures:  $\leq 600^\circ\text{C}$  and/or  $\geq 600^\circ\text{C}$ , or heated at the same temperature for different time periods. This would mean that pigments might have been prepared in different batches. The batches could either have been fired at one occasion or at two separate occasions. Does it mean that only a

limited amount of paint and/or pigment could be made in each batch? A spiritual factor could also have played a role: did the production of paint for animal figures and nature elements have to be disconnected acts?

Another way of interpreting the data could be that the pigments in Tumlehed were taken from two different types of sources; not saying that these locations had to be hundreds of kilometres apart. AÅ1 and KT1 heated at 900°C are both red in colour, but the starting composition are unlike (with higher Fe content for the latter). The appearance of the raw material is also distinctive: one is dug out of the ground, the other found in a flowing stream. Would it be surprising if pigment for painting water related motifs were collected from aqueous sources, and that the paint body making up the lines of deer figure originated from 'Mother Earth'? Arguably, it would not be incomprehensible, especially if the idea of hunting magic is taken into account (see Gjerde 2010, pp.61f, p.159)

A model made with the data from the experimental part, and tested on the Tumlehed data set does not support this interpretation. Yet, so many factors seem to affect the outcome – the right variables have just not been identified in the experimental part of the Master's project.

However, effects of environmental exposure and binding media are explored too little in this Master's project. The size of the sample set is as well extremely limited, which makes it impossible to distinguish between individual and general differences. The discussion about Tumlehed rock painting can therefore only be hypothetical. No final conclusions can be made based on the obtained results. The circumstances would be the same when interpreting Flatruet rock painting, presented by Linderholm et al. (2015).

### **3.5 Only Rock Art?**

Even though this Master's project has been focussing on pigments in rock paintings, it does not exclude that SCiO could be applied in the analysis in other cultural heritage contexts. Since ochres are such widespread pigments used in so many art forms, it could definitely be interesting to expand the research to other fields within conservation and heritage science. The possibilities of using SCiO with other types of pigments and in situations where knowledge about clay content is desirable is not to disregard.

As this Master's thesis showed, the prospect of recording the degradation in binding media seems promising. It may not only be relevant to natural or traditional materials but also applicable in terms of other contemporary materials such as plastics. Because SCiO is small and portable, it can potentially be used in the field, in storage rooms or on objects with limited access for larger instruments.

## 4. Conclusions

Many results have been presented in the previous section, but a final conclusion to the research question should be made. The main research question was: *Which factor(s) or different preparation methods could cause Scandinavian rock painting pigments to be statistically grouped and separated based on their near infrared spectral data?* with heating temperature, aging, and provenance in focus.

The results suggest that heating temperature could be a major separation factor when it comes to the pigments in rock art. It is possible to discriminate between pigments heated to 300°C, 600°C and 900°C, respectively. However, this separation is most apparent if samples from the same location (fundamentally similar) are compared. The provenance can also, to some extent, be read in the data of heated ochreous soils, whereas unheated samples show weaker separation patterns. The provenance does, in this respect, refer to the chemical composition, type of mineral aggregate habits or hematite (and hence iron) content. Some of these mentioned discriminants can be connected to the character of the pigment source; for instance can red earths have mineralogical ‘impurities’ compared to the ferrihydrite substance found in streams. Aging (or exposure) seemed to affect the types of binding media in different ways, for instance did the blood-based paint change a lot more due to aging than the binding media with egg. The unexposed samples did also show distinct groupings of the four types of binding media. How this is relatable to rock paintings, which are several thousand years old, is uncertain.

Other factors not part of the sub-questions in section 1.2 were also investigated. It is possible to distinguish between samples with binding media and samples lightly stuck to a surface with water as a carrier. In this case, the distinction is probably based on the surface roughness more than the chemistry in the binding media. Painted samples can also be separated from the rock background.

The results fit very well with the hypotheses in section 1.9. However, all suggestions from this Master’s project are mostly hypothetical. The limited, but still extensive, amount of samples seems to affect the statistical data processing and therefore the possibility to make general conclusions.

Because SCiO is the main analytical tool in the project, and no other published studies about its application in heritage science are available, one can discuss the suitability of the instrument for these types of investigations. When financial resources are limited, SCiO could most definitely be an alternative instrument to turn to. Though, this Master’s project has shown that many variables can affect the results accessible in SCiO Lab web. If SCiO were to be used in another pigment or heritage context to make correct and predictive estimations, a lot of work has to be done calibration-wise. It might be too comprehensive to map all variables. Instead, one could see SCiO as a screening tool that highlights overall differences, which can open up for further research.

SCiO do also work out well in a context of learning. It makes it possible for the inexperienced to understand statistics visually and scientifically investigate and work with cultural heritage objects in a simple and risk-free way.

## 5. Summery

### 5.1 Summarised Introduction

Inspiration to the Master's project came after reading Linderholm et al.'s (2015) article about the statistical separation of motifs in a Swedish rock painting using a near infrared (NIR) spectrometer. The researchers posed some reasons for the separation, but how these features are actually visible on pigments treated experimentally is not mentioned. Based on a preliminary study by the Master's student on ochre pigments and the reasons stated by Linderholm et al., a main research question for the Master's thesis was made:

- Which factor(s) or different preparation methods could cause Scandinavian rock painting pigments to be statistically grouped and separated based on their near infrared spectral data?

Three sub-questions were also asked:

- Does heating temperature affect the separation pattern?
- Will an aged paint show different spectral features from an un-aged?
- Is the provenance or origin of the pigment the most distinguishable factor?

An experimental research design was constructed to answer the research questions. Red earths (ochreous soils) and ochre pigments were heated at 300°C, 600°C and 900°C, exposed and kept unexposed, and were collected from different places. A case study of a Swedish rock painting has also been included.

Previous research is presented, and is used to construct the experiment and interpret the obtained results.

SCiO® (from Consumer Physics), a commercial NIR spectrometer is the main analytical instrument. Because no published studies describe the use of SCiO in a cultural heritage context, the Master's project is also a pilot study in the particular setting. NIR spectroscopy is non-destructive and is therefore favourable when analysing cultural heritage objects.

### 5.2 Summarised Materials and Methods

Ochreous soil from five sites in Sweden, one site in Denmark and three artistic pigments (HEM, LOB and YAU) were the main materials to be studied. An unheated sample and a heated sample from Denmark were initially painted on rock slabs with water, egg yolk, animal fat, egg yolk-fat mixture and blood as binding media. Two rock slabs were hung on an open-air wall for exposure, the other kept unexposed. All samples were later ground and sieved (<125nm), and included in a firing experiment. Different heating temperatures and heating time was tried out. All samples were in the end fired to 300°C, 600°C and 900°C, some for 15 minutes, some for 30 minutes and all of them for 1 hour. The fired pigments were painted on rock slabs with water and blood as binding media. The samples were also applied to pieces of carbon tape. SCiO was used to scan the entire sample set. Photographs of all samples were also taken.

The case study is Tumlhed rock painting, which is predicted to be at least 5000 years old. Both animal figures and wavy patterns can be seen in the composition. Several scans were made of both rock and painted figures.

The NIR spectra ranging from 700-1100nm and collected with SCiO were treated statistically in the web-based software created for SCiO data processing. The following processing methods are available with SCiO: standard normal variate (SNV), log, first and second derivative, subtraction of minimum and subtraction of average spectra. PCA-plots can be made and models created through cross-validation. The models can be tested on other samples through the random forests algorithm.

An unheated and a heated sample from each location were analysed with SEM-EDX with backscattered and secondary electrons.

### 5.3 Summarised Results and Discussion

The visual colour of the unheated samples implies that goethite is present. Heated samples are mostly red, which suggests the presence of hematite. One sample collected in a stream turned brown when heated to 300°C and 600°C. The brown colour may be caused by maghemite created when organic matter is present.

All artistic pigments have high content of iron, and LOB and YAU high content of aluminium and silicon. One Swedish sample also contains a lot of silicon, but the rest of Scandinavian samples do not have high contents of either aluminium or silicon. Soil from the Danish location contains a lot of calcium. SEM-images created with secondary electrons show crystal/aggregate variations between ochreous soil pigments and HEM, LOB and YAU.

PCA-plots and models were made with various types of pre-processing of the spectra.

Rock background and painted samples on these can be separated with SNV.

With  $\log \rightarrow 1^{\text{st}} \text{ derivative} \rightarrow \text{SNV}$  on spectra from one location, it is possible to distinguish between heating temperatures. The degree of transformation from goethite to hematite (or just the presence of certain minerals) can be causing this separation. Models based on one location can to some extent determine unfired samples from other locations, but not the heating temperature of fired samples. Exposure does, in this context, alter the samples' spectra, meaning that exposed samples are classified differently than unexposed samples. It may be changes in the binding media's chemistry that causes this alteration.

When the spectra of aged samples are treated with 'subtraction of average', a difference between the binding media types is visible. Blood-based paint, for instance, seem to be affected more by exposure than egg-based paint. Clustering of the types of binding media is also noticeable. Taking only the log of spectra can show if the pigments are incorporated in some kind of binding media, which is not water. This may be due to the difference in surface roughness of the paint layers.

By applying  $\log \rightarrow 1^{\text{st}} \text{ derivative}$  to all painted samples heated at the same temperature, one can find a separation between Danish, Swedish and artistic samples – the separation is best

expressed in heated samples. Models made for each heating temperature, can to some extent predict the origin of samples heated at other temperatures. The separation may be caused by chemical differences between the heated samples, whereas no separation is seen in unheated samples, maybe due to variation in crystal defects/particle size. However, the variance between PC values is not that big. If all Swedish samples are compared after  $\log \rightarrow 1^{\text{st}}$  derivative  $\rightarrow$  SNV-processing, a separation between samples emerges, which may be based on the hematite (and hence iron) content in the samples.

The models created from the experiment give inadequate results when applied to the Tumblehed rock painting scans. Paint and rock background can, however, be separated in a PCA-plot when  $\log \rightarrow 1^{\text{st}}$  derivative  $\rightarrow$  SNV is applied to the Tumblehed spectra. Thin paint layers lie between rock scans and thick paint layer scans in PC1. SNV-processing can separate painted motifs in terms of deer figure and water related motifs. Explanations for this separation, based on the experimental results, are that pigments have either been heated at different temperatures or collected from different sources – resulting in different iron content. Would it be that incomprehensible to collect pigments from the bed of a stream for painting waves and fishes?

#### **5.4 Summarised Conclusions**

SCiO can to some extent be used to distinguish between heating temperatures of samples from the same origin. Aging (or exposure) seem to make statistical separation, as do the different types of binding media, especially when unexposed. The presence of a binding media can also be extracted from the spectral data. Provenance determination is in some cases possible, but may be due to chemical composition rather than geographical origin.

More calibration work can be done, as hematite (hence iron) content might cause some separation as well. The character of the pigment source can be interpreted based on such estimations.

Information about the pigment and their preparation and type of source can help interpreting rock art painting, though these interpretations (in this Master's project) can only be hypothetical.

SCiO is a relevant screening tool and is also useful for the inexperienced researcher in conservation and heritage science. The instrument is a good alternative to other more scientific instruments with access to raw data, but a lot of work needs to be done if SCiO should be used for precise predictions.

## List of Figures

Fig. 1: Mid IR-spectra of quartz, goethite+quartz from Pehčevo and goethite from Alšar. The peaks of goethite and quartz are in the same region of the spectrum. (Jovanovsky et al. 2009, p.21.)	13
Fig. 2: PCA-plot of figures in Flatruet rock painting. $t[1]=PC1$ , $t[2]=PC2$ . (Linderholm et al. 2015, p.233.)	16
Fig. 3: Iron oxide heated at different temperatures. From left: unfired, 700°C, 900°C, 1100°C. (Mastrotheodoros et al. 2010, p. 45.)	19
Fig. 4: The heat induced reaction pathways of ferrihydrite, lepidocrocite and goethite to hematite. (Ingrid Søgaard).	20
Fig 5: SEM-images of fired iron oxide at 10.000 magnification and different temperatures. From left: 700°C , 900°C, 1100°C. (Mastrotheodoros et al. 2010, p. 45.)	21
Fig 6: SEM-images of fired goethite at different temperature with 50.000 magnification. (de Faria & Lopes 2007, p.120.)	21
Fig. 7: The locations of sampled red earth from the Scandinavian sites; marked on a geological map. Blue colour: late Proterozoic and Phanerozoic rock types outside The Caledonides. Orange colour: Proterozoic rock types. Yellow colour: early Proterozoic rock types. (Sveriges geologiska undersökning n.d.)	26
Fig. 8: The sampling site at Arnås – marked with a red dot. All black dots represent prehistoric, mostly bloomery related, sites. (Riksantikvarieämbetet n.d.)	27
Fig. 9: Sampling at Løvskaal. (Ingrid Søgaard 2016.)	29
Fig. 10: Tumblehed rock painting. The yellow circles mark the areas of analyses: deer, fish and waves. (Varbergs Fornminnesforening n.d.)	31
Fig. 11. Cargo car build and painted in Randers 1960. (Djurslands Jernbanemuseum n.d.)	33
Fig 12: The position of the light source (Ingrid Søgaard 2018.)	36
Fig 13: Size an attachable camber for SClO. and detector on SClO. (Ingrid Søgaard 2018.)	36
Fig 14: The scanning set-up for scanning samples on aluminium stubs. SClO is places on top of the sample holder. (Ingrid Søgaard 2018.)	37
Fig. 15: The Lch colours of ferrihydrite, goethite, hematite, maghemite and lepidocrocite. Lch values are found in Cornell & Schwertmann 2003, p.133. The colour images are made with the software by: Johnstone n.d.	39
Fig. 16: Secondary electron-SEM-image of HEM.	41
Fig. 17: Secondary electron-SEM-image of LØ3 0°C	42
Fig. 18: Secondary electron-SEM-image of LØ3 900°C	42
Fig. 19: Secondary electron-SEM-image of KT1 0°C	42
Fig. 20: Secondary electron-SEM-image of KT1 900°C	42
Fig. 21: Secondary electron-SEM-image of HO1 0°C	42
Fig. 22: Secondary electron-SEM-image of HO1 900°C	42

## List of Figures

---

Fig. 23: Secondary electron-SEM-image of ST3 0°C _____	43
Fig. 24: Secondary electron-SEM-image of ST3 900°C _____	43
Fig. 25: Secondary electron-SEM-image of AÅ1 0°C _____	43
Fig. 26: Secondary electron-SEM-image of AÅ1 900°C _____	43
Fig. 27: Secondary electron-SEM-image of SR2 0°C _____	43
Fig. 28: Secondary electron-SEM-image of SR2 900°C _____	43
Fig. 29: Secondary electron-SEM-image of LOB 0°C _____	44
Fig. 30: Secondary electron-SEM-image of LOB 900°C _____	44
Fig. 31: Secondary electron-SEM-image of YAU 0°C _____	44
Fig. 32: Secondary electron-SEM-image of YAU 900°C _____	44
Fig. 33: Globular aggregates of goethite on quartz grains from a 2000 years old sand deposit in Karup, Denmark. (Cornell & Schwertmann 2003, p.421.) _____	45
Fig. 34: Model 1 made with SNV-processing on background scans from the rough side of the rock surfaces (b) and paint on rock slabs (p). _____	47
Fig. 35: Model 2 made with SNV-processing on all painted samples, excluding samples with unknown heating temperature and HEM samples. _____	48
Fig. 36: PC1-PC2-plot of samples on carbon tape (excluding KT) with SNV-processing. The samples are coloured by heating temperature; Blue/ 0 represents unheated, green/? represents unknown heating temperature and turquoise/x represents HEM. _____	48
Fig. 37: PC1-PC2-plot of samples on carbon tape (excluding KT) with SNV-processing. The samples are coloured provenance. _____	49
Fig. 38: PC1-PC2-plot of AÅ spectra with SNV-processing. The samples are coloured by heating temperature; 300°C - 900°C, blue/0 represents unheated samples. _____	49
Fig. 39: PC1-PC2-plot of AÅ spectra with SNV-processing. The samples are coloured by heating temperature; 300°C - 900°C. _____	50
Fig. 40: PC1-PC2-plot of AÅ spectra of samples heated at 300°C, 600°C and 900°C with SNV-processing. The samples are coloured by heating time; 1hr and 30min. _____	50
Fig. 41: AÅ samples. Model 3 made with log → 1 <sup>st</sup> derivative → SNV-processing of AÅ samples. The scans have been averaged. _____	51
Fig 42: LØ samples. Model 4 made with log → 1 <sup>st</sup> derivative → SNV-processing of LØ3 samples with known heating temperature. The scans have been averaged. _____	51
Fig 43: KT samples. Model 5 made with log → 1 <sup>st</sup> derivative → SNV-processing of KT samples. The scans have been averaged. _____	51
Fig. 44: AÅ spectra with SNV→1 <sup>st</sup> derivative-processing. The samples are coloured by heating temperature; 0°C - 900°C and scans have been averaged. _____	52
Fig 45: LØ spectra with SNV→1 <sup>st</sup> derivative-processing. The samples are coloured by heating temperature; 0°C - 900°C and scans have been averaged. _____	52

Fig 46: KT spectra with SNV→1 <sup>st</sup> derivative-processing. The samples are coloured by heating temperature; 0°C - 900°C and scans have been averaged.	53
Fig. 47: Model 6 made with SNV-processing on all samples. – represents background/rock scans, 0 represents unexposed samples and 1 represents exposed samples.	54
Fig. 48: PC1-PC2-plot of exposed and unexposed samples with ‘subtraction of average’-processing. Samples are coloured by aging. Blue/0 represents unexposed samples and yellow/1 represents exposed samples.	54
Fig. 49: PC1-PC2 and PC1-PC3-plots of exposed and unexposed samples with ‘subtraction of average’-processing. Samples are coloured by binding media. Yellow/eggofat represents egg and fat-mixture.	55
Fig. 50: PC1-PC2 and PC1-PC3-plots of unexposed samples with ‘subtraction of average’-processing. Samples are coloured by binding media. Yellow/eggofat represents egg and fat-mixture.	56
Fig. 51: PC1-PC2-plot of all painted samples with log-processing and averaged scans. The samples are coloured by binding media. Blue/0 represents samples on carbon tape. Yellow/eggofat represents samples painted with the egg yolk-fat mix.	56
Fig. 52: Model 7 made with all painted samples with blood and water as binding media and log-processing. The scans have been averaged.	57
Fig. 53: Model 8 made with SNV-processing on all painted samples, excluding HEM samples. – represents background/rock scans.	58
Fig 54: Model 9 made with all unheated samples (excluding HEM) and log → 1 <sup>st</sup> derivative-processing. The scans have been averaged. d represents Denmark, o represents other and s represents Sweden.	58
Fig 55: Model 10 made with all samples heated to 300°C and log → 1 <sup>st</sup> derivative-processing. The scans have been averaged. d represents Denmark, o represents other and s represents Sweden.	58
Fig 56: Model 11 made with all samples heated to 600°C and log → 1 <sup>st</sup> derivative-processing. The scans have been averaged. d represents Denmark, o represents other and s represents Sweden.	59
Fig 57: Model 12 made with all samples heated to 900°C and log → 1 <sup>st</sup> derivative-processing. The scans have been averaged. d represents Denmark, o represents other and s represents Sweden.	59
Fig 58: PC1-PC2-plot of painted samples heated to 600°C with log → 1 <sup>st</sup> derivative-processing. Samples have not been averaged and are coloured by overall origin. d represents Denmark, o represents other and s represents Sweden. KT samples group away from the other Swedish samples.	59
Fig. 59: PC1-PC2-plot of all Swedish samples heated to 900°C with log → 1 <sup>st</sup> derivative → SNV-processing. Scans have not been averaged and samples are coloured by location.	60
Fig. 61: PC1-PC2-plot of all Swedish samples heated to 900°C and HEM with log → 1 <sup>st</sup> derivative → SNV-processing. Scans have not been averaged and samples are coloured by location.	61
Fig. 62: PC1-PC2-plot of Tumblehed scans with log → 1 <sup>st</sup> derivative → SNV-processing. Samples are coloured by type of motif. Background 1 is from the rock surface around the deer figure, background 2 from is around the fish and waves.	62
Fig. 63: PC1-PC2-plot of Tumblehed scans with SNV-processing. Scans are coloured by type of motif.	63
Fig 64: Model 13 made with scans from Tumblehed with SNV-processing. d represents animal figures, h represents waves.	63

## List of Tables

Table 1: Chemical composition of unheated HEM, LØ3, KT1, HO1, ST3, AÅ1, SR2, LOB and YAU in wt%. HEM is included two times, the second time it functions a bit like a reference, as LOB and YAU were analysed at another occasion. Orange fill indicate extraordinary features compared to the other samples. _____	40
Table 2: The crystal habits of the common iron oxides. (Cornell & Schwertmann 2003, p.64.) _____	45
Table 3: F1-scores speaking of model 3's, model 4's and model 5's performance to classify heating temperature on the remaining samples. _____	53

## References

### Unpublished

Informant 1: Leif Stark, hobby-blacksmiths, Tranemo, Sweden. Personal communication 2016.

Informant 2: Rune Holmberg, hobby-blacksmiths, Tranemo, Sweden. Personal communication: 2016.

Informant 3: Christer Johansson, hobby-blacksmith, Alvesta, Sweden. Personal communication: 2016.

Informant 4: Rachel Popelka-Filcoff, Doctor at School of Chemistry and Physical Sciences, Flinders University. E-mail correspondence: 2016.

Informant 5: Niels Jørn Kristoffersen, landowner, Løvsdal Denmark. Personal communication: 2016.

Informant 6: Zareen Abbas, Docent at Department of Chemistry and Molecular Biology, University of Gothenburg. Personal communication: 2018.

Informant 7: Eugene Taddeo, paintings conservator at ArtLab Australia. Personal communication: 2015.

Informant 8: Consumer Physics support. E-mail correspondence: 2018.

Ingrid Søgaard, *Karakteristika og identifikation af okker – samt dets anvendelse som pigment i ældre skandinavisk helle- og kalkmaleri*. Unpublished bachelor thesis (2016), University of Gothenburg. Available: <http://hdl.handle.net/2077/44600> [09.05.2018].

### Electronic sources

Consumer Physics. *SCiO Developers Online Guide*. [www.dev.consumerphysics.com](http://www.dev.consumerphysics.com) (only accessible with developer login). [01.05.2018]

Johnstone, D. (n.d.) *Lch and Lab Colour and Gradient Picker*. [www.davidjohnstone.net/pages/lch-lab-colour-gradient-picker](http://www.davidjohnstone.net/pages/lch-lab-colour-gradient-picker). [07.05.2018].

Kulturministeriet (n.d.). *Fund og Fortidsminder* (Database). [www.kulturarv.dk/fundogfortidsminder](http://www.kulturarv.dk/fundogfortidsminder). [07.05.2018].

Riksantikvarieämbetet (n.d.). *Fornsök* (Database). [www.fmis.raa.se/cocoon/fornsok/search.html](http://www.fmis.raa.se/cocoon/fornsok/search.html). [07.05.2018].

Varbergs Fornminnesforening (n.d.). *Tumlehed*

[http://www.varbergsforminnesforening.se/bilder/2002\\_Lodose/images/tumlehed\\_01.JPG](http://www.varbergsforminnesforening.se/bilder/2002_Lodose/images/tumlehed_01.JPG) [02.05.2018].

Sveriges geologiska undersökning (SGU) (n.d.). *Sveriges Berggrund*. [www.sgu.se/om-geologi/berg/sveriges-berggrund](http://www.sgu.se/om-geologi/berg/sveriges-berggrund) [19.04.2018].

Djurslands Jernbanemuseum (n.d.). *Lukket godsvogn Gs*. [www.djbm.dk/aktivside.php?fid=30](http://www.djbm.dk/aktivside.php?fid=30) [19.04.2018].

Länsstyrelsen – Västergötaland (n.d.). *Tumlehed*. [www.lansstyrelsen.se/VastraGotaland/Sv/samhallsplanering-och-kulturmiljo/historia-plats/tumlehed/Pages/default.aspx](http://www.lansstyrelsen.se/VastraGotaland/Sv/samhallsplanering-och-kulturmiljo/historia-plats/tumlehed/Pages/default.aspx). [22.04.2018].

## Published

Bakker, A., Smith, B., Ainslie, P. & Smith, K. (2012) Near-infrared spectroscopy. In: (eds.) Ainslie, P. *Applied Aspects of Ultrasonography in Humans*. Pp. 65-88.

Barnett, J.R., Miller, S. & Pearce, E. (2006) Colour and art: A brief history of pigments, *Optics and Laser Technology*, 38(4), pp. 445-453.

Bickler M.P. & Rhodes L.J. (2018) Accuracy of detection of carboxyhemoglobin and methemoglobin in human and bovine blood with an inexpensive, pocket-size infrared scanner. In: *PLoS ONE* 13(3), DOI: <https://doi.org/10.1371/journal.pone.0193891>. Pp.1-12.

Bjerck, H.B. (2012) On the outer fringe of the human world: Phenomenological perspectives on anthropomorphic cave paintings in Norway. In: Bergsvik, K.A. & Skeats, R. (eds.). *Caves in Contexts: The Cultural Significance of Caves and Rock Shelters in Europe*. Oxford: Oxbow Books. Pp. 48–64.

Bokobza, L. (2002) Origin of near infrared absorption bands. In: Siesler, H.W. (eds) *Near-infrared Spectroscopy: Principles, Instruments, Applications*. Weinheim: Wiley-VCH, pp. 11-39.

Bowdler, S. (1988) Repainting Australian rock art. In: *Antiquity* 62(236), pp.517-523.

Bu, K., Cizdziel, J.V & Russ, J. (2013) The source of iron-oxide pigments used in Pecos River style rock paints. *Archaeometry*, 55(6), pp. 1088–1100.

Buchwald V.F. (2005) *Iron and Steel in Ancient Times*, København: Det Kongelige Danske Videnskabernes Selskab.

Caple, C. (2000) *Conservation Skills: Judgement, Method and Decision Making*, London, Routledge.

Charlton M.F., Blakelock, E., Martínón-Torres, M. & Young, T. (2012) Investigating the production provenance of iron artifacts with multivariate methods In: *Journal of Archaeological Science* 39. Pp. 2280-2293.

- Charlton M.F. (2015) The last frontier in ‘sourcing’: the hopes, constraints and future for iron provenance research. In: *Journal of Archaeological Science* 56. Pp. 210-220.
- Cornell, R. M. & Schwertmann, U. (2003) *The Iron Oxides: Structure, Properties, Reactions, Occurrences and Uses* 2. udg., Weinheim: Wiley-Vch Verlag.
- Creswell, J.W. (2013) *Research Design: Qualitative, Quantitative, and Mixed Methods Approaches*. Los Angeles: Sage Publication.
- Cudahy, T.J. & Ramanaidou, E.R. (1997) Measurement of the hematite:goethite ratio using field visible and near-infrared reflectance spectrometry in channel iron deposits, Western Australia. In: *Australian Journal of Earth Sciences*, 44(4), pp.411-420.
- Di Lernia, S. (2012). Thoughts on the rock art of the Tadrart Acacus Mts., SW Libya. *Adoranten*, 19-37.
- Englund, L. (2002) Blästbruk – Myrjärnshanteringens förändringar I ett långtidsperspektiv. Jernkontorets Berghistoriska Skriftserie nr 40. Jerkontoret: Stockholm.
- de Faria, D.L.A. & Lopes, F.N. (2007) Heated goethite and natural hematite: can Raman spectroscopy be used to differentiate them? In: *Vibrational Spectroscopy* 45(2), pp.117-121.
- Fouzas, S., Priftis, K.N. & Antrhocopoulos, M.B. (2011) Pulse oximetry in Pediatric Practice. In: *Pediatrics* 128(4) pp.740-752.
- Froment, F., Tournié, A. & Colombar, P. (2008) Raman identification of natural red to yellow pigments: ochre and iron-containing ores. In: *Journal of Raman Spectroscopy*, 39(5), pp. 560–568.
- Gialanella, S., Girardi, F., Ischia, G., Lonardelli, D., Mattarelli, M. & Montagna, M. (2010) On the goethite to hematite phase transformation. In: *Journal of Thermal Analysis and Calorimetry*, 102(3), pp. 867-873.
- Gialanella, S., Belli, R., Dalmeri, G., Lonardelli, D., Mattarelli, M., Montagna, M. & Toniutti, L. (2011) Artificial or natural origin of hematite-based red pigments in archaeological contexts: the case of Riparo Dalmeri (Trento, Italy). In: *Archaeometry*, 53(5), pp.950–962.
- Gjerde, J. M. (2010) *Rock art and landscapes: studies of Stone Age rock art from northern Fennoscandia*, Doktorafhandling, Tromsø: Tromsø universitet, Fakultet for humaniora, samfunnsvitenskap og lærerutdanning.
- Hald, P. (1935) *Maleriets Teknik*. København: Jul. Gjellerups Forlag.
- Hansen, F. & Nyrén, O.I., 1991. *Farvekemi: Uorganiske Pigmenter*, København: Gad.
- Hastie, T., Tibshirani, R. & Friedman, J. (2009) *The Elements of Statistical Learning – Data mining, Inference and Prediction*. 2<sup>nd</sup> edition. New York: Springer

Helwig, K. (1997) A note on burnt yellow earth pigments: documentary sources and scientific analysis. In: *Studies in Conservation*, 42(3), pp.181-188.

Henshilwood, C.S., d'Errico, F., van Niekerk, K.L., Coquinot, Y., Jacobs, Z., Lauritzen, S., Menu, M. & García-Moreno, R. (2011) A 100,000-Year-Old Ochre-Processing Workshop at Blombos Cave, South Africa. In: *Science* 334(6053), pp. 219-222.

ICOMOS (2003) *ICOMOS Principles for the Preservation and Conservation-Restoration of Wall Painting*, International Council of Monuments and Sites (ICOMOS). Paris: ICOMOS. [http://www.icomos.org/charters/wallpaintings\\_e.pdf](http://www.icomos.org/charters/wallpaintings_e.pdf). Available: [08.05.2018].

Jovanovsky, G., Makreski, P., Kaitner, B. & Šoptrajanov, B. (2009) Minerals from Macedonia. X-ray powder diffraction vs. vibrational spectroscopy in mineral identification. In: *Contributions, Sec. Math. Tech. Sci.* pp.7-34. Available from: [https://www.researchgate.net/publication/243464792\\_Minerals\\_from\\_Macedonia\\_X-ray\\_powder\\_diffraction\\_vs\\_vibrational\\_spectroscopy\\_in\\_mineral\\_identification](https://www.researchgate.net/publication/243464792_Minerals_from_Macedonia_X-ray_powder_diffraction_vs_vibrational_spectroscopy_in_mineral_identification). Available: [06.05.2018].

Jurado-López, A. & Castro, M.D.L (2004) Use of near infrared spectroscopy in a study of binding media used in paintings. In: *Analytical and Bioanalytical Chemistry*, 380(4), pp.706–711.

Karlsson, J., Rydberg, J. Segerström, U., Nordström, E., Thöle, P., Biester, H. & Bindler, R. (2016) Tracing a bog-iron bloomery furnace in an adjacent lake-sediment record in Ängersjö, central Sweden, using pollen and geochemical signals. In: *Vegetation History and Archaeobotany* 25(6), pp. 569-581.

Lahelma, A. (2008) *A Touch of Red: Archaeological and Ethnographic Approaches to Interpreting Finnish Rock Paintings*, Published Ph.D thesis, Helsinki: Suomen muinaismuistoyhdistys.

Lahelma, A. (2010) Hearing and touching rock art: Finnish rock paintings and the non-visual. In: Goldhahn, J., Fuglestedt, I. & Jones A, (eds.), *Changing Pictures: Rock Art Traditions and Visions in Northern Europe*. Oxford: Oxbow Books, pp. 48- 59.

Learidi, R. (2008) Chemometric methods in food authentication. In: Sum, D. (eds.) *Modern Techniques for Food Authentication*. Amsterdam: Elsevier.

Linderholm, J., Geladi, P. & Sciuto, C. (2015) Field-based near infrared spectroscopy for analysis of Scandinavian Stone Age rock paintings. *Journal of Near Infrared Spectroscopy*, 23, pp. 227-236.

Ling, J. (2008) *Elevated Rock Art. Towards a Maritime Understanding of Rock Art in Northern Bohuslän, Sweden*. Gothenburg: Gotarc Serie B. Archaeological Thesis 49.

Lødøen, T. & Mandt, G. (2005) *The Rock Art of Norway*. Oxford: Oxbow books.

Mauriac, M. (2011). Lascaux: The history of the discovery of an outstanding decorated cave. *Adoranten*, pp. 5-25.

Manley, M., Downey, G. & Baeten, V. (2008) Spectroscopic technique: Near infrared (NIR) spectroscopy. In: Sum, D. (eds.) *Modern Techniques for Food Authentication*. Amsterdam: Elsevier.

Marrone, A. & Ballantyne (2009) Changes in dry state hemoglobin over time do not increase the potential for oxidative DNA damage in dried blood. In: *PLoS ONE* 4(4) pp.1-8. doi:10.1371/journal.pone.0005110

Mastrotheodoros, G., Beltsios, K.G. & Zacharias, N. (2010) Assessment of the production of antiquity pigments through experimental treatment of ochres and other iron based precursors. In: *Mediterranean Archaeology and Archaeometry*, 10(1), pp. 37-59.

Miller, J.N. & Miller, J.C. (2000) *Statistics and Chemometrics for Analytical Chemistry*. 4<sup>th</sup> edition. Essex: Pearson Education Limited.

Muños Viñas, S. (2005). *Contemporary Theory of Conservation*, Oxford: Elsevier ButterworthHeinemann.

Navasaitis, J., Selskienė, A. & Žaldarys, G. (2010) The study of trace elements in bloomery iron. In: *Materials Science (Medžiagotyra)* 16(2). Pp. 113-188.

Nyrén, O.I. (2009) *Målningar Ändrar Färg*. Stockholm: Raster Förlag

Ozaki, Y (2012) Near-infrared spectroscopy - Its versatility in analytical chemistry. In: *Analytical Sciences* 28(6) pp.545-563.

Parkin, S.J., Adderley, W.P., Young, M.E. & Kennedy, C.J. (2013) Near infrared (NIR) spectroscopy: a potential new means of assessing multi-phase earth-built heritage. In: *Analytical Methods* 18(5). Pp. 4574-4579.

Platour, S.W. (1970) The Svaneke granite complex and the gneisses on East Bonholm. In: *Bulletin of the Geological Society of Denmark* 20(2), pp.93-133.

Popelka-Filcoff, R.S., Lenehan, C.E., Walshe, K., Bennett, J.W., Stopic, A., Jones, P., Pring, A., Quinton, S. & Durham, A. (2012) Characterisation of Ochre Sources in South Australia by Neutron Activation Analysis (NAA). Roberts, A & Pate, F.D., ed., *Journal of the Anthropological Society of South Australia* (Special Edition, Archeological Science) 35, pp. 81-90.

Popelka-Filcoff, R. S., Mauger, A., Lenehan, C. E., Walshed, K. & Pringe, A. (2014) HyLoggerTM near-infrared spectral analysis: a non-destructive mineral analysis of Aboriginal Australian objects, *Analytical Methods*, 6(5), ss. 1309-1316. DOI: 10.1039/c3ay41436a.

Prinsloo, L.C., Tournié, A., Colomban, P., Paris, C. & Basset, S.T. (2013) In search of the optimum Raman/IR signatures of potential ingredients used in San/Bushman rock art paint. In: *Journal of Archaeological Science*, 40(7), pp.2981–2990.

- Reeves (2010) Near- versus mid-infrared diffuse reflectance spectroscopy for soil analysis emphasizing carbon and laboratory versus on-site analysis: Where are we and what needs to be done? In: *Geoderma* 158(1), pp.3-14.
- Rendón, J.L. & Serna, C.J. (1981) IR spectra of powder hematite: Effects of particle size and shape. In: *Clay Minerals* 16(4), pp.375-381.
- Riksantikvarieämbetet (2003) Pigment Ockra*. Visby: Riksantikvarieämbetet. Available from: <http://www.raa.se/app/uploads/2015/02/Ockra-uppdatt1.pdf>. [03.05.2018].
- Rinnan, Å., van den Berg, F. & Engelsen, S.B. (2009) Review of the most common pre-processing techniques for near infrared spectra. In: *Trends for Analytical Chemistry* 28(10). Pp.1201-1222.
- Sajó, I.E., Kovács, J., Fitzsimmons, K.E., Jäger, V., Lengyel, G., Viola, B., Talamo, S. & Hublin, J. (2015) Core-shell processing of natural pigment: Upper Palaeolithic red ochre from Lovas, Hungary. In: *PloS one*, 10(7), pp.1-18.
- Scheinost, A.C., Chavernas, A., Barron, V. & Torrent, J. (1998) use and limitations of second-derivative diffuse reflectance spectroscopy in the visible to near-infrared range to identify and quantify Fe oxide minerals in soils. In: *Clay and Clay Minerals*, 46(5), pp.528-536.
- Schwab, R., Heger, D., Höppner, B. & Pernicka, E. (2006) the provenance of iron artefacts from Manching: A multi-technique approach. In: *Archaeometry*, 48(3), pp.433–452.
- Siesler, H.W. (2002) Introduction. In: Siesler, H.W. (eds) *Near-infrared Spectroscopy : Principles, Instruments, Applications*. Weinheim: Wiley-VCH, pp. 1-10.
- Stuart, B.H. (2007) *Analytical Techniques in Materials Conservation*, Chichester: John Wiley & Sons.
- Stuart, B.H & Thomas, P.S. (2017) Pigment characterisation in Australian rock art: a review of modern instrumental methods of analysis. In: *Heritage Science* 5(10), pp. 1-6.
- Tan, S. (2005) Neighbor-weighted K-nearest neighbour for unbalanced text corpus. In: *Expert Systems with Applications* 28. Pp. 667-671.
- Tilley, C. (2003) Landscape and Rock Art: European Landscapes of Rock-art, eds by Nash G. & Chippindale, C. Review in *Cambridge Archaeological Journal*, 13(1), 138-139.
- Viscarra Rossel, R.A., Cattle, S.R., Ortega, A. & Fouad, Y. (2009) In situ measurements of soil colour, mineral composition and clay content by vis-NIR spectroscopy. In: *Geoderma* 150(3), pp.253-266.





## **Appendix I – Report on SCiO**

### **Report on the use of SCiO as a near infrared spectrometer to examine ochre and earth pigments**

By Ingrid Søgaaard  
University of Gothenburg, Department of Conservation  
May-June 2017  
Individual Course supervised by Jacob Thomas

#### **Introduction**

This report describes the application of near infrared (NIR) spectrometry when studying ochres and earth pigments, mostly reds and yellows, but also a few brown ochres are included. All used materials will be listed later. The reason for this study to be conducted is to investigate the potentials of SCiO, an affordable NIR spectrometer, from a conservation scientific point of view. The method is non-destructive and therefore suitable when examining cultural heritage objects. In the following text, instrumentation, preparation and procedure will be presented, including possible interpretations of the gained results.

NIR spectrometry has been used in other studies to analyse hematite and goethite containing materials. These two minerals are contributing to the red and yellow colours in ochres and earth pigments and are hence central to look at when studying natural red and yellow earth pigments. The word “ochre” is used as synonym for the wide variety of iron oxide/hydroxide earth pigments.

Popelca-Filcoff et al. (2014) have tried to identify minerals used as pigments on Indigenous Australian objects. The research team used an instrument operating in the wavelength range 380nm-3000nm. For identification, characteristic bands for hematite and goethite were used to distinguish. Bands in the NIR spectra lies at 848-906nm (for hematite) and 933-973nm (for goethite). Another research group, Cudahy & Ramanidou (1997), have looked at the hematite-goethite ratio in Australian channel iron deposits using Vis-NIR spectroscopy. For this purpose, they refer to specific crystal field absorption for the two minerals. These are around 860nm for hematite and 915nm for goethite. Scheinost et al. (1998) used Vis-NIR diffuse reflectance spectroscopy to identify and quantify iron oxide minerals in soils. In the NIR wavelength range, they mention the characteristic field band positions of hematite and goethite: 877nm (848-906nm) and 953nm (929-1022nm), respectively.

Based on the presented literature above, wavelength intervals can be made to describe the two minerals. Hematite could potentially give characteristic bands between 848-906nm and goethite between 915-1022nm.

#### **Samples and preparation**

Pigment samples were taken from a pigment cabinet at the Department of Conservation, University of Gothenburg. A total of 42 pigments were chosen for this study, based on their colour and written etiquette. Iron oxides and earths were preferred.

All pigments were sampled. Each sample was prepared in two ways – 1) pressed into a pellet at 5 ton and 2) un-pressed powder form – and fixated with carbon tape on aluminium stubs. This resulted in a total of 84 samples. Some un-pressed pigments did not stick as nicely on the tape, which resulted in sparsely distributed pigment grains where some of the black carbon tape background was visible through the pigment powder.

A list of samples and meta-data can be seen in Appendix A, Table 1. Believed matter attributes were given based on label, colour and texture. Shortenings of these: Yellow ochre (YO), Yellow ochre, synthetic (YO(S)), Red ochre (RO), Red ochre, burned (RO(B)), Red bolus (RB), Brown ochre (BO), Yellow, not ochre (Y?) and Iron oxide, hematite IO(H).

## Instrumentation

For this study, two different instrumentations were used: a NIR spectrometer called SCiO and scanning electron microscopy with energy dispersive x-ray spectroscopy (SEM-EDX).

SCiO is a cheap portable NIR spectrometer compared to regular NIR spectrometers used for scientific purposes (Consumer Physics n.d.) It has a light source and a light detector in one end, a button on the side - pressed to start a scan- and a charging input in the other end. It functions in the wavelength range 700-1100nm and the light detector measures the reflected light returning from the sample and the raw generated spectra are reflectance spectra. The small instrument has a cover with a calibration surface and the provided software gives notice, when the instrument needs to be calibrated again. Latest version (1.2) was used.

SCiO Lab developer toolkit software, on an iPad (as app) and through an online Internet browser account, has been used through the analyses and data treatment.

The SEM-EDX analyses were executed in a Hitachi S3400N SEM, with EDX detector, a X-Max<sup>N</sup> (20) model from Oxford Instruments. INCA was the software program for data treatment.

## Analyses

All 84 pigment samples and a blank carbon tape piece were analysed with SCiO. Each sample was scanned 3 times in a row at two different occasions (not all samples were scanned under the same conditions because of difference in time), and each scan did not take any longer than 10 seconds or so. The SCiO was placed approximately 5mm above the samples while trying to direct the SCiO light source towards the centre of the samples. See Fig. 1. Meta data was kept written and updated before and between scans.

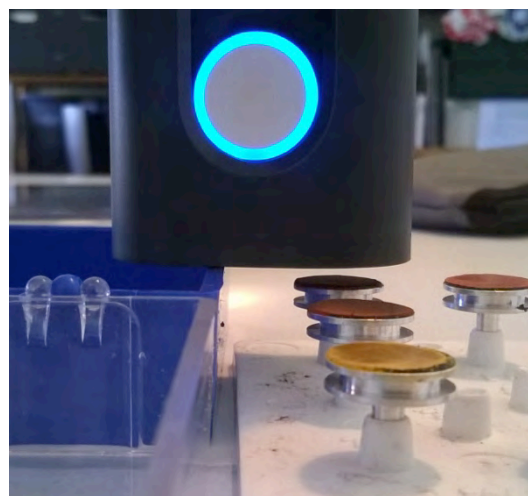


Fig. 1: The scanning procedure setup.

40 of the pressed pellets were analysed with SEM-EDX equipment. Not all 42 pressed samples went through analyses because of limited time. Only 12 samples could fit in the instrument at once. Furthermore, all samples were not analysed the same day, which meant that the conditions and settings changed between analyses. Data obtained consisted of SEM images at a magnification of approximately 3k and EDX mapping of elements made in the same area as the SEM image.

## **Data treatment**

### ***SCiO***

With the developer web software, it was possible to select between different pre-processing methods and wavelength ranges – a minimum range of 50nm is required. *(log(R))'* & *Normalized* was chosen as processing method for this study. The software can both create a spectrum and a PCA model with PC1, PC2 and PC3. Samples can be filtered out if wanted and/or treated based on their meta-data attributes. PCA is suitable for this study because it helps one to find correlations and groupings between samples; for instance can one choose that all pressed samples are shown in one colour and all un-pressed samples are shown in another colour. It is hence possible to see if the given meta-data and premade groupings (yellow ochre, red ochre etc.) fit the groupings made through the processing treatment.

Furthermore, models can be created and these models can be tested on another data set with unknown samples. When making models – also PCA models – the software asks for at least five samples in each category the analysis is based on. This study does not have enough samples in all categories and models will hence not be truly reliable.

The carbon tape spectra were filtered out. R-OB was also filtered out because the material could not give strong spectra when analysed.

### ***SEM-EDX***

Mapped elements from EDX analyses were listed in an Excel document, including a short description of the structure seen on the SEM image.

## **Results and Discussion**

### ***SCiO***

Firstly, the full wavelength range was used: 778-1033nm (with *log(R))'* & *Normalized* method) and the samples treated (coloured) based on their *Believed Matter* where *Object name* was taken into account (e.g. R-TM). This gave quite a clear distinction on the PC1. See Fig. 2. The red samples positioned in the positive part of PC1 and the yellows in the negative part.

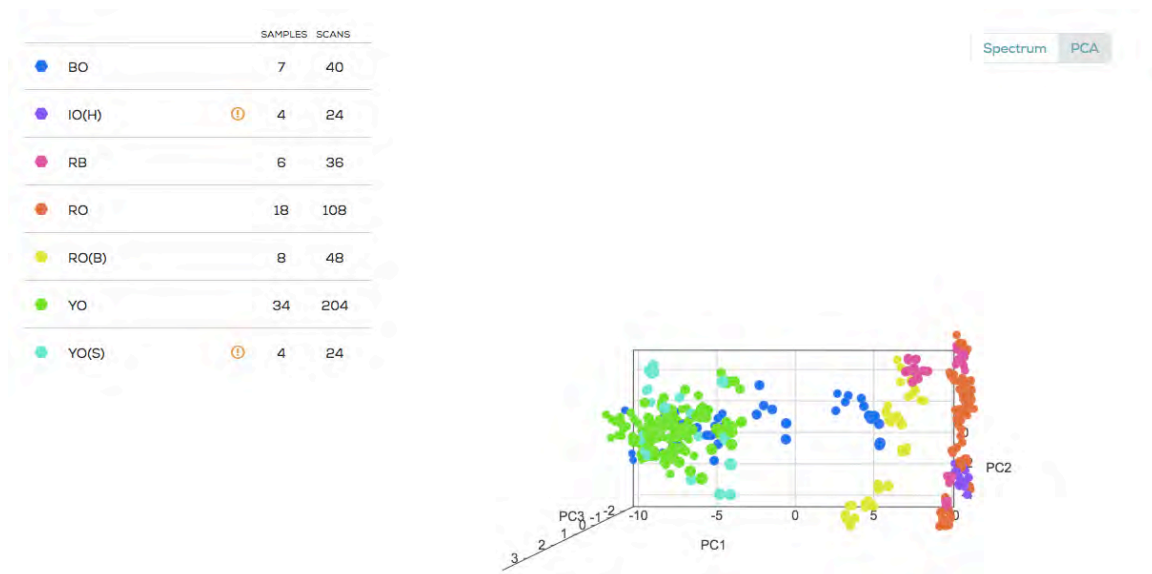


Fig. 2: PCA model of spectra treated with  $\log(R)$ ' & Normalized. Wavelength 788-1033nm. PC1 vs. PC2. Pressed and un-pressed samples visible, Y-OR filtered out. Coloured by *Believed matter*.

Y-OR was in the negative part but positioned as an outlier. By looking at the SEM-EDX results it could be confirmed that Y-OR was not an iron based pigment because no iron was present in the sample. Based on this finding, Y-OR was filtered out to give a better separation between existing samples.

After this first separation, decreased wavelength ranges were chosen corresponding to the characteristic bands mentioned in the literature. Neither of the two gave good separation in the PCA model, so it was decided to use the entire spectra for further data treatments. It was however noticed that the spectra separated nicely in yellow and red in the wavelength range 780-810nm, a little bit lower than the characteristic wavelength range ascribed to hematite (848-906nm). See Fig. 3.

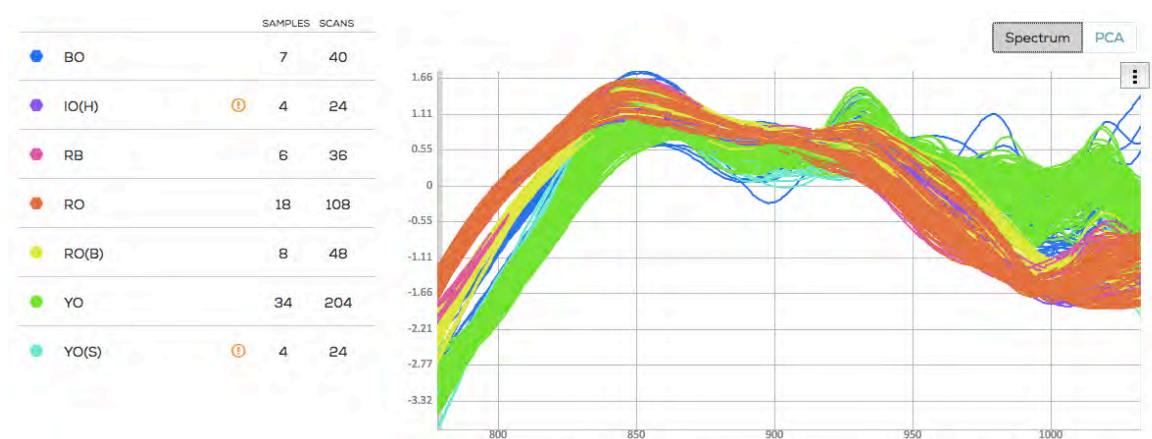


Fig. 3: Spectra treated with  $\log(R)$ ' & Normalized. Wavelength 788-1033nm. Pressed and un-pressed samples visible, Y-OR filtered out. Coloured by *Believed matter*.

When coloured based on *Believed matter* (Fig. 2), it is also possible to see that the samples cluster in three separated groups: 1) one with IO(H) and RO, 2) one with RO(B), and 3) one

with YO, where 1) is the most negative and 3) is the most positive on the PC1. The RB is both in the group 1) and 2), BO is divided in group 2) and 3), and YO(S) lies within group 3).

Based on the two observations above, it can be suggested that differentiation on PC1 illustrate the goethite content in the material. The reason why RO and RO(B) split in two groups can be based on the degree of transformation from goethite to hematite upon heating. Samples within RO(B) could contain less crystallised hematite with goethite traits. This splitting might also be expressed for RB and BO. For instance is the R-BR samples clustering with RO(B) more reddish in colour than the two others (Y-BR and Y-RE).

Goethite can transform into hematite when heated above 260-300°C. Put forward by Helwig (1997), X-ray diffraction (XRD) patterns of red earths can be more or less sharp and intense and is due to the crystallisation of hematite. Earths containing goethite heated at high temperatures gives low disordered hematite crystals whereas earths containing goethite heated at low temperatures gives high disordered hematite crystals. XRD can be used as a method to confirm if the clustering and separation on PC1 is caused by the degree of disorder in hematite and hence different heating temperatures.

The samples also differ on PC2 and PC3. If the samples are coloured by *Object name*, one can see that sample scans spread out on PC3. See Fig. 4. It could mean that differences between each scan are represented on PC3.

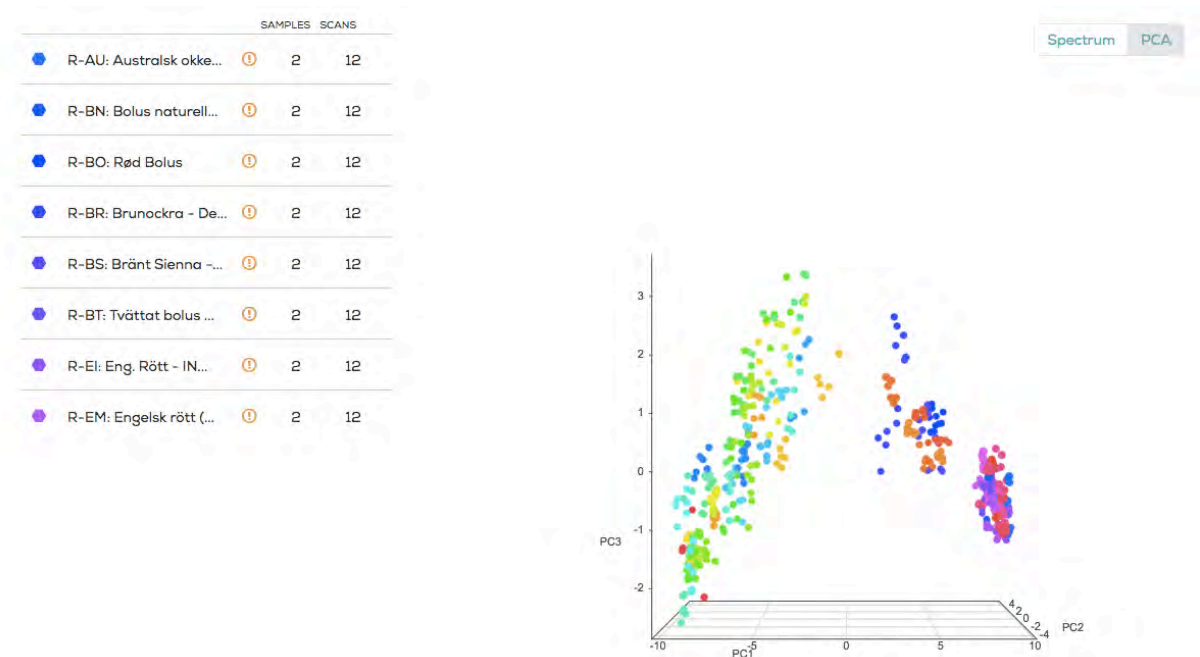


Fig. 4: PCA model of spectra treated with  $\log(R)''$  & Normalized. Wavelength 788-1033nm. PC1 vs. PC3. Pressed and un-pressed samples visible, Y-OR filtered out. Coloured by *Object name*.

Pressed and un-pressed samples lie within the same main groups (1), 2) and 3)) but when grouped by first *Preparation* and hence *Object name* one can see a differentiation between un-pressed and pressed in all PCA directions. Further on, only pressed samples will be treated. OBS: When un-pressed samples are filtered out, it is worth noticing, that the yellows suddenly cluster in the positive part of PC1 and the reds cluster in the negative part. See Fig.

5. The elemental characterisation from the SEM-EDX analyses will be used to suggest the differentiation pattern on PC2.

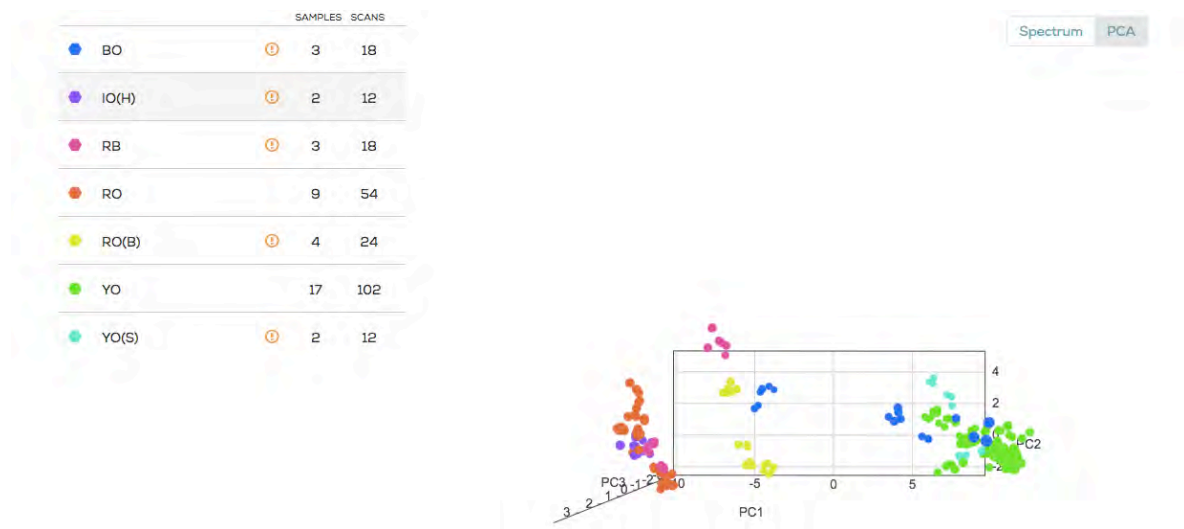


Fig. 5: PCA model of spectra treated with  $\log(R)$ '' & Normalized. Wavelength 788-1033nm. PC1 vs. PC2. Only pressed samples visible, Y-OR filtered out. Coloured by *Believed matter*.

### ***SEM-EDX and SCiO***

When looking at the elements represented in the EDX-mapping, no clear pattern, significant for all sample spreading on PC2, emerge. See Table 2 in appendix. However if samples within group 2) (in the middle) are examined, it is possible to find resemblances between samples in the negative part of PC2 compared to the samples in the positive part. R-BO and R-BS contain Na and R-BR contains both Na and S compared to R-RÖ, R-TM and R-TS. This distinction is not as clear in the other groups (1) and 3)), however, if samples are coloured based on *Contains S and/or Na*, the majority of samples, which contain either of these are located in the positive part of PC2 and the majority of samples, which do not contain S and/or Na, are located in the negative part of PC2. No samples in group 1) contain Na. It can consequently not be definitely concluded that PC2 represent S and/or Na content, because samples both with and without S and/or Na are located oppositely relative to this hypothesis.

What S and/or Na means and in what way it affect earth pigments and ochres are not clear. This will need further studies.



Fig. 6: PCA model of spectra treated with  $\log(R)$ ' & Normalized. PC1 vs. PC2. Only pressed samples visible, Y-OR filtered out. Coloured by *Containing S and/or Na*.

The structures seen on the SEM images (not included) do not explain the differentiation clearly. It must therefore be implied that structure and grain size does not contribute or affect the NIR spectra.

## Model creation

The PCA models above show classifications based on *Believed matter* and *Containing S and/or Na*. To investigate the PCA models, classification models can be created where all samples are classified in relation to each other. This gives a chart with given percentages and an analysis result (F1). Models of the two groupings can be seen in Fig. 7 and Fig 8. The rather good distribution is noticeable in Fig. 7. No other samples than those categorised to be IO(H) fall in the IO(H) group. Also, the yellow ochres separate quite nicely from the rest, only the brown ochres, which in fact could be just yellow ochres but named brown ochre because of a slightly browner colour, fall into the YO group. Fig. 8 shows how unreliable the *Containing S and/or Na* classification actually is compared to how it looks in the PCA model (Fig. 6).

As stated before, more samples should have been used to create better models.

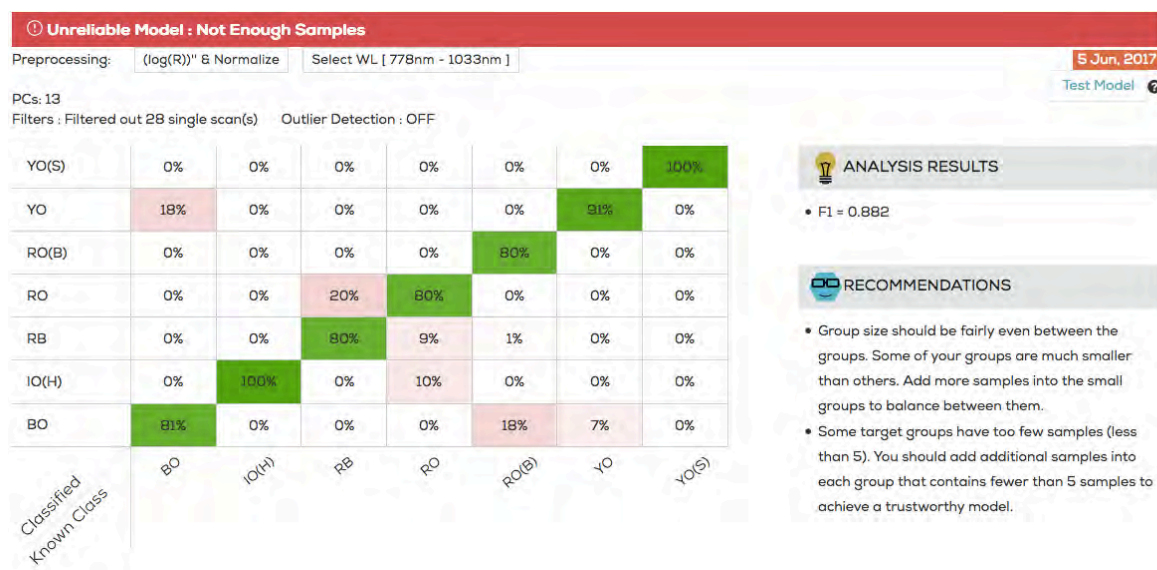


Fig. 7: Classification model based on *Believed matter* groupings. Spectra treated with  $\log(R)$ ''& *Normalized*. Only pressed samples visible, Y-OR filtered out.



Fig. 8: Classification model based on *Containing S and/or Na* groupings. Spectra treated with  $\log(R)$ ''& *Normalized*. Only pressed samples visible, Y-OR filtered out.

## Conclusion

Separation based on visual colour was possible to make using PCA modelling (in PC1) when both red, yellow and brown earth pigments were analysed with the NIR spectrometer SCiO. Another type of clustering also appeared through data treatment, which might illustrate the degree of heating an earth pigment has undergone to become a red earth. Even though the red pigments visually look quite the same in colour, SCiO could separate heated red earths from pure iron dioxide and ochres with a presumably normal hematite crystallisation order. The theory seems promising, however, to confirm this, other methods, such as XRD, has to be used.

It is less clear if SCiO can be used to distinguish between S and/or Na containing pigments compared to pigments with none of these elements. The separation in PC2 is not as clear and apparent as the one in PC1.

Some final things can be said about SCiO in this context: it is a fast and cheap method that may or may not give readable results beyond what is visible by the human eye. Even though it to some extent is non-destructive, some limitations should be considered into more detail. If powdered pigments need to be pressed into pellets, a part of the non-destructiveness and fast examination time is lost. However, this study has not examined pigments used on objects and therefor it is not known if pressed or un-pressed pigments are to be preferred when studying real objects. Powdered pigment in a container might also give better result than the amount of pigment grains that can stick to a piece of carbon tape.

## References

- Consumer Physics (n.d.) (<https://www.consumerphysics.com/myscio/scio/>). [01.06.2017].
- Cudahy, T.J. & Ramanaidou, E.R. (1997) Measurement of the hematite:goethite ratio using field visible and near-infrared reflectance spectrometry in channel iron deposits, Western Australia. In: Australian Journal of Earth Sciences 44(4). Pp. 411-420.
- Helwig, K. (1997) A note on burnt yellow earth pigments: documentary sources and scientific analysis. In: Studies in Conservation 42(3). Pp. 181-188.
- Popelka-Filcoff, R.S., Mauger, A., Lenehan, C.E., Walshe, K. & Pring, A. (2014) HyLogger™ near-infrared spectral analysis: a non-destructive mineral analysis of Aboriginal Australian objects. In: Analytical Methods 6(5). Pp. 1309-1316.
- Scheinost, A.C., Chavernas, A., V. Barron, V. & J. Torrent, J. (1998) use and limitations of second-derivative diffuse reflectance spectroscopy in the visible to near-infrared range to identify and quantify Fe oxide minerals in soils. In: Clays and Clay Minerals 46(5). Pp. 528-536.

**Appendix A**

Table 1: List of samples and meta-data (Sample name = scan number) exported from the browser based data treatment software.

Sample name	Object Name	Believed Matter	Preparation	Contains S and/or Na
2	R-JÄ: Järnoxid (Hematit)	IO(H)	Pressed 5 ton	no
4	R-RÖ-: Rödockra (gulockra bränt 850°C)	RO(B)	Pressed 5 ton	no
5	R-BO: Röd Bolus	RB	Pressed 5 ton	Na
6	R-ER: Engelsk Rött	RO	Pressed 5 ton	S
7	R-BS: Bränt Sienna - Verona 44I	RO(B)	Pressed 5 ton	Na
8	R-TS: Terra Di Sienna - bränt - Beckers	RO(B)	Pressed 5 ton	no
9	Y-FA: Fransk ockra A (Handwritten label)	YO	Pressed 5 ton	no
11	Y-FB: Fransk ockra B	YO	Pressed 5 ton	no
12	Y-LJ: Ljusockra - Beckers	YO	Pressed 5 ton	no
13	Y-RS: Rå Sienna	YO	Pressed 5 ton	no
15	Y-BR: Brunockra	BO	Pressed 5 ton	Na and S
16	Y-TG: Terra Gialla	YO	Pressed 5 ton	S
17	Y-FB: Fransk ockra B	YO	Powder	no
18	Y-FA: Fransk ockra A (Handwritten label)	YO	Powder	no
19	R-BO: Röd Bolus	RB	Powder	Na
20	R-BS: Bränt Sienna - Verona 44I	RO(B)	Powder	Na
21	R-ER: Engelsk Rött	RO	Powder	S
22	R-JÄ: Järnoxid (Hematit)	IO(H)	Powder	no
23	R-RÖ-: Rödockra (gulockra bränt 850°C)	RO(B)	Powder	no
24	R-TS: Terra Di Sienna - bränt - Beckers	RO(B)	Powder	no
25	Y-BR: Brunockra	BO	Powder	Na and S
26	Y-LJ: Ljusockra - Beckers	YO	Powder	no
27	Y-RS: Rå Sienna	YO	Powder	no
28	Y-TG: Terra Gialla	YO	Powder	S
29	R-ID: Indisk rött - no. 651 - Schmincke	RO	Powder	no
30	R-JM: Järnmönja	RO	Powder	S
32	R-BR: Brunockra - Dekorima	BO	Powder	Na and S
33	R-OB: Oxid - brunt - Held & Schyberg	BO	Powder	no
34	R-TM: Tranemo mix - bränt på panna	RO(B)	Powder	no
36	Y-TM: Tranemo mix	YO	Powder	no
37	Y-RB: Rehbrant - 39 D	YO	Powder	Na
38	Y-MG: Marsgult - järnoxidhydroxyd-kalciumsulfat - framställt här	YO(S)	Powder	no
39	Y-CC: C. C. Verdaccio	YO	Powder	no
40	Y-OR: Orlena	Y?	Powder	no
41	Y-OT: Obränt terra	YO	Powder	no
43	R-OR: Oxidrött	RO	Powder	no
44	R-JJ: Järnmönja - järnoxid	RO	Powder	S
45	R-EI: Eng. Rött - INEX	RO	Powder	no

## Appendix I

46	R-JR: Järnoxidrött - Nestor	RO	Powder	no
47	R-EM: Engelsk rött (mörk) - Dekorima	RO	Powder	no
48	R-AU: Australsk okker - rød	RO	Powder	no
49	Y-AU: Australsk okker - gul	YO	Powder	no
50	Y-MF: Marsgult no. 31 - Ferrario Color	YO(S)	Powder	S
51	Y-GD: Guldockra - Dekorima	YO	Powder	?
52	Y-GI: Gulockra - INEX	YO	Powder	?
53	Y-GO: Guldockra	YO	Powder	no
54	Y-LO: Light ocher - Schmincke	YO	Powder	no
55	Y-GU: Guldocker	YO	Powder	no
56	Y-LS: Ljusockra - Schmincke	YO	Powder	no
57	Y-RE: Rehn brunt	BO	Powder	Na and S
58	Y-OC: Obränt terra - no. 46 - Credo	YO	Powder	Na
59	Blank - carbon tape	Black carbon tape		no
60	Y-GU: Guldocker	YO	Pressed 5 ton	no
61	Y-LS: Ljusockra - Schmincke	YO	Pressed 5 ton	no
62	Y-RE: Rehn brunt	BO	Pressed 5 ton	Na and S
63	Y-OC: Obränt terra - no. 46 - Credo	YO	Pressed 5 ton	Na
64	R-OR: Oxidrött	RO	Pressed 5 ton	no
65	R-JJ: Järnmönja - järnoxid	RO	Pressed 5 ton	S
66	R-EI: Eng. Rött - INEX	RO	Pressed 5 ton	no
68	R-JR: Järnoxidrött - Nestor	RO	Pressed 5 ton	no
69	R-EM: Engelsk rött (mörk) - Dekorima	RO	Pressed 5 ton	no
70	R-AU: Australsk okker - rød	RO	Pressed 5 ton	no
71	Y-AU: Australsk okker - gul	YO	Pressed 5 ton	no
72	Y-MF: Marsgult no. 31 - Ferrario Color	YO(S)	Pressed 5 ton	S
73	Y-GD: Guldockra - Dekorima	YO	Pressed 5 ton	?
74	Y-GI: Gulockra - INEX	YO	Pressed 5 ton	?
75	Y-GO: Guldockra	YO	Pressed 5 ton	no
76	Y-LO: Light ocher - Schmincke	YO	Pressed 5 ton	no
77	R-ID: Indisk rött - no. 651 - Schmincke	RO	Pressed 5 ton	no
78	R-JM: Järnönja	RO	Pressed 5 ton	S
79	R-JO: Järnoxid N. 7053 - Chematex-Bro AB	IO(H)	Pressed 5 ton	no
80	R-BR: Brunockra - Dekorima	BO	Pressed 5 ton	Na and S
81	R-OB: Oxid - brunt - Held & Schyberg	BO	Pressed 5 ton	no
82	R-TM: Tranemo mix - bränt på panna	RO(B)	Pressed 5 ton	no
83	Y-TM: Tranemo mix	YO	Pressed 5 ton	no
84	Y-RB: Rehbrant - 39 D	YO	Pressed 5 ton	Na
85	Y-MG: Marsgult - järnoxidhydroxyd-kalciumsulfat - framställt här	YO(S)	Pressed 5 ton	no
86	Y-CC: C. C. Verdaccio	YO	Pressed 5 ton	no
87	Y-OR: Orlena	Y?	Pressed 5 ton	no
88	Y-OT: Obränt terra	YO	Pressed 5 ton	no
89	R-JO: Järnoxid N. 7053 - Chematex-Bro AB	IO(H)	Powder	no
90	R-BN: Bolus naturell - bolus rød -Held &	RB	Powder	S

## Appendix I

---

	Schyberg			
91	R-BT: Tvättat bolus 1N	RB	Powder	S
92	R-BN: Bolus naturell - bolus röd -Held & Schyberg	RB	Pressed 5 ton	S
93	R-BT: Tvättat bolus 1N	RB	Pressed 5 ton	S

Appendix I

Table 2: Elements mapped through EDX analyses and summed in Excel.

Sample	F e	C	O	Na	Mg	Al	Si	S	P	Cl	K	a	Ti	V	Mn	B	a	Z	W	n	C	e	Sb	Structure
R-JA	X	X	X			X	X				X													Big seperated grains
R-RO	X		X			X	X		X		X	X												Mixture of small and big grains, with star-like cristals
R-BO	X	X	X	X	X	X	X				X	X												Mixture of small and big grains
R-ER	X	X	X				X	X			X				X	X								small grains
R-BS	X	X	X	X	X	X	X		X		X	X	X											Mixture of small and big grains
Y-FA	X	X	X		X	X	X		X		X	X	X											Mixture of small and big grains, with star-like cristals
Y-FB	X	X	X		X	X	X		X		X	X	X											Mixture of small and big grains, with star-like cristals
Y-LJ	X	X	X		X	X	X		X		X	X	X											Mixture of small and big grains, with star-like cristals
Y-RS	X	X	X		X	X	X		X		X													Mixture of small and big grains
Y-TG	X	X	X		X	X	X	X			X								X					Mixture of small and big grains, with star-like cristals
Y-BR	X	X	X	X	X	X	X	X	X		X	X	X		X									Mixture of small and big grains
R-TS	X		X		X	X	X		X		X	X	X	X	X									Mixture of small and big grains
R-ID	X		X				X																	small grains
R-JM	X		X		X	X	X	X			X	X						X						Mixture of small and big grains
R-JO	X	X	X			X	X																	Big seperated grains
R-BR	X	X	X	X	X	X	X	X	X		X	X	X		X									Mixture of small and big grains
R-OB	X	X	X																					small grains
R-TM	X	X	X			X	X		X		X													small grains
Y-TM	X	X	X				X																	small grains
Y-RB	X		X	X	X	X	X		X	X	X	X			X									small grains
Y-MG	X	X	X			X	X		X		X	X												Mixture of small and big grains
Y-CC	X	X	X		X	X	X				X	X								X				Mixture of small and big grains
Y-OT	X	X	X		X	X	X				X													small grains
Y-OR		X	X								X													VERY BIG seperated grains
R-BN	X	X	X		X	X	X	X			X	X												Mixture of small and big grains
R-BT	X	X	X		X	X	X	X			X	X												small grain
Y-GU	X		X		X	X	X		X		X	X	X											small grains
Y-LS	X	X	X			X	X		X		X	X	X											Mixture of small and big grains, with star-like cristals
Y-RE	X	X	X	X	X	X	X	X	X		X	X	X		X									Mixture of small and big grains, with star-like cristals
Y-OC	X		X	X	X	X	X		X	X	X	X			X									small grains
R-OR	X	X	X			X	X																	small grains
R-JJ	X		X		X	X	X	X			X	X	X									X		Mixture of small and big grains
R-EI	X	X	X				X				X												X	Mixture of small and big grains
R-JR	X	X	X			X	X		X															small grains
R-EM	X	X	X			X	X																	small grains

## Appendix I

R-AU	X	X		X	X			X	small grains
Y-AU	X	X		X	X	X	X	X	Mixture of small and big grains, with star-like crystals
Y-MF	X	X	X	X		X			small grains, with star-like crystals
Y-GO	X	X	X	X	X	X	X	X	Mixture of small and big grains, with star-like crystals
Y-LO	X	X	X	X	X	X	X	X	Mixture of small and big grains

## Appendix II - Newspapers

Articles from newspapers

There are no sources on these articles. They were collected and kept by the landlord of the former Løvskaal ochre mine. Since words in the Danish language is correctly written with 'å' instead of 'aa' from 1948 and onwards, these articles are most likely before 1948 (Brink, L. & Jastrup, P.O. (n.d.) Å, å. In: *Den Store Danske*. Gyldendal. Available from 22.04.2018, <http://denstoredanske.dk/index.php?sideId=31147> ).

735

## FARVER GRAVES OP AF DANSK JORD

**N**U graver man Farver op af den danske Jord, Farver til Kalkning og Malning, Naturfarver, der saa at sige er født med de to Egenskaber, man altid spørger efter, naar det drejer sig om Farver: Lyseghed og Holdbarhed. Vi maa aabenbart til at revidere vore tilvante Begreber om, at den danske Jord skulde være saa fattig og gold, at den ikke kan give Raastoffer til Landets Produktion. Vi skal dog ikke ved denne Lejlighed fordybe os i Raastof-Problemet, men her blot fortælle, at der er paabegyndt en hjemlig Jordfarvefabrikation af Y/S Color, hvis Leder er Ingeniør E. R. Licht.

Fabrikken er gemt i Glostrup, saa godt endda, at den ikke har faaet Telefon. Dette, siger Ingeniør Licht med et Smil, skyldes dog vor Beskedenhed. Vi vil ikke slaa for stort op, men hellere begynde smaat og vokse sold. Men naar Fabrikken er lagt i Glostrup i det aabne Land, er det af Hensyn til de Ulemper, som Røg fra Farvebrændingen og Støv kan medføre.

Det er forstaaeligt, naar man ser det gul-brune Støv, der har lejet sig paa Gulve og Fremspring i Fabrikken, og en Arbejder, der er ved at fryde Farvepulveret i Sække, ser ud, som skulde han aske Frymte i en Solbrænd-hedskonkurrence.

— Vi graver dog ikke Farven op hende i Glostrup, fortsætter Ingeniør Licht. Ganske vist findes paa Sjælland et Par Forekomster af den jernholdige Jord, der drejer sig om Men det er for maa Klatter. Paa Stevns Klint er den ogsaa sporet, men der er for kostbart at udvinde den, naar man skal rydde 10 Tons Kalk for hver Haandfuld, man faar. I Jylland

føroverrig Tale om, at man vilde udvinde Jernet, men det blev ikke til Alvor. Nu laver vi altsaa Farve deraf. Vi købte Jordstykket i 1934 og begyndte Eksperimenterne frem og tilbage, indtil vi maade et tilfredsstillende Resultat. Vi var saa heldige at finde en stor Afgrø, som erklærede, at hvis vi blot kunde lave noget brugbart, vilde han købe, fordi han ikke brød sig om at anvende udenlandsk, saafremt han kunde faa dansk Arbejde. Desværre er det ikke alle — mærker vi — som har den Indstilling.

Ved Okkergraven har vi opført et Slømmeri, hvor Masser renses og slømmes til en sanden Fuldhed, at der ikke bliver noget til Rest i en Sigt, der har henvend 17 000 Masker paa hver Kvadrat-Centimeter. Saa tørrer Pulveret og transporteres til Fabrikken i Glostrup, hvor det i forskellige Møller finmøles og yderligere siges, og saa har vi et Materialiale, der giver en mørk Okkerfarve.

Efter mange Genforsøg og Forsøg har vi nu ogsaa fremstillet rødlig og røde Farver. Vi putter Materialiet, der er knust og slømmet til Grynslørrøse, i en Rotator og brænder det ved en Temperatur omkring 1 000 Grader. Derved siges Jernindholdet, som giver den rødlig Tone. Men vi skal nu



En Okkergrav.

derimod, mellem Randers og Viborg, ligger et stort Leje af Okker i ca. 4 Meters Dybde.

— Hvorledes er det opstaaet?

— En populær Forklaring gaar ud paa, at der er faldet en Meteorsten engang i Istiden. Den har ikke smeltet sig helt igennem Isen, men er ført med paa Vandringen, indtil den har lejet sig her i Jylland. Aflejringerne indeholder ca. 50 pct. Jern. Under Krigen var der

som er udmærket anvendelig til Linn- og Kalkfarver.

Efter mange Genforsøg og Forsøg har vi nu ogsaa fremstillet rødlig og røde Farver. Vi putter Materialiet, der er knust og slømmet til Grynslørrøse, i en Rotator og brænder det ved en Temperatur omkring 1 000 Grader. Derved siges Jernindholdet, som giver den rødlig Tone. Men vi skal nu

at vi ikke kommer for højt op i Varmegrafterne, for saa brænder vi det helt til Jern. Det Jern, der dannes under Processen i Rolvervnen, udskiller vi bagetter ved at lade det brændte Materiale passere over en roterende Magnet.

Ved at variere Temperaturerne kan vi fremstille forskellige røde Nuancer. I Øjeblikket fremstiller vi 7 Farver til Lm og Kalk og 4, som er gode til Ohmaling. Vi forsætter imidlertid Forsøgene. Vi vil gerne lave en lysere rød Farve og en violet Farve. Den sidste kan vi faa ved at gaa et Stykke op over de 1000 Grader ved Brændingen.

Megen Glæde har vi haft af en kastaniobrun Farve, den. De kender fra Jernbane-Godsvogne. Statsbanerne, som jo prøver deres Varer meget nøje, har købt af den og været udmærket tilfreds med den.

— Hvor stor er Fabriken's Produktion?

— Af den mørke Okker kan vi med de nuværende Maskiner fremstille ca. 150 Tons aarlig, og af de rødlige Farver kan det Ovrnarlæg

og Mølleri, vi i Øjeblikket har, fremstille ca. 120 Tons aarlig. Denne nye Industri kan, hvis Produktionen anbringes paa det hjemlige Marked, overflødigøre for ca. 60 000 Kr. Import fra Ulandet.

— Hvorledes er Prisforholdene?

— Vi sælger vore Varer i Konkurrence med de udenlandske og maa indrette vore Priser derefter.

## Centralisering af Oste Eksporten.

EN TANKKE, som »Dansk Arbejde« tidligere har været inde paa, synes nu at have Ud-sigt til Virkeliggørelse. I Morgen, den 16. Oktober, holdes i Odense et Møde mellem 5—600 Repræsentanter for osteproducerende Mejerier for at drøfte en Systematisering af Oste-Eksporten og en Centralisering gennem et Fælles-Ostelager.

Der foreligger et Forslag, hvorefter samtlige

Mejerier, der producerer Ost, skulde forpligte sig til at levere til Fælles-Lageret 25 pCt. af deres Fabrikation i den bedste Kvalitet, saaledes at der opnaaedes Garanti for en ensartet, god Vare til Eksport. I Tilknytning til Fælles-Lageret skulde efter Planen oprettes en Fabrik for Smelte-Ost, d. v. s. Ost uden Skorpe, f. Eks. de bekendte smaa Trekanter.

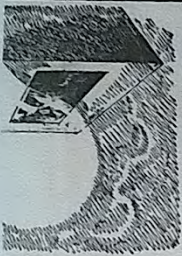
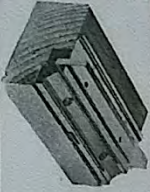
Naar man nu paa dette Tidspunkt rejser dette Centralisations-Spørgsmaal paany, hænger det sammen med den stærke Udvikling, der har været i den danske Oste-Eksport. Den plejer at beløbe sig til 4—5 Mill. Kr. om Aaret, medens Hjemmemarkedet aflægger for godt en Snos Mill. Kr. I Aar har der i de 8 Maanedere til 1. September været eksporteret for 6,6 Mill. Kr. mod 3,9 i samme Tidrum i Fjor, saaledes at det tegner til en Fordobling af Eksportværdien i 1936.

— Nu skulde vi blot ogsaa »opfinde« en special dansk Ostetype, som kunde sendes paa Markedet Side om Side med vore udmærkede Oste-Kopier, saa var vi inde paa det helt rigtige.

Kan en

## Kähler

Vase glæde Dem?



## B. F. Kjellsson <sup>1/5</sup>

Tagensvej 97, København N.  
Telefon 8949 · Taga 3553

B. F. K.-Karme, Butiksarme i alle Metaller, modviker Dug-dennelse, uundværlig i ethvert Forretningsvindue  
Løvrigt alt Smedearbejde i Jern og Metaller efter Opsave



HELLESSENS  
TØR-ELEVENT

den danske Malm.

Mine-Drift har vel aldrig været det store Sus i Danmark. I vore Nabolande, Tyskland, Norge og Sverige, brydes Kul og Malm i store Mængder, men Danmark har maattet klare sig med Kullene paa Bornholm, Brunkul, Torv, Kalk, Myremalm, Kiselgur og fleje andre Ting. I Ogsaa har Torv og Brunkul haft meget at betyde for Landet, men under normale Forhold kan Produktion i helt stor Stil ikke betale sig. Men taget under eet har Mine-Driften dog ikke saa lidt at betyde for Danmark, men kan blot tænke paa Kryolitbruddene paa Grønland. Indtil 1840 kunde Kalkbruddene ved Mariager næsten hele Danmark med brændt Kalk, men Gruberne i Mønsied og Daugbjerg ved Viborg aflost Mariagers Kalkbrud som Stor-Leverandør, og fra Gruberne i Mønsied, der ejes af Aktieselskabet »De jyske Kalkværker«, leveres hvert Aar store Mængder.

Ogsaa paa Randers-Egnen findes en Form for Mine-Drift. Ved Hollerup mellem Langaa og Ulstrup brydes Kiselgur, det Stof, som Nobel i sin Tid anvendte, da han opfandt Dynamitten ved at lade Nitroglycerin opsuge i Kiselgur. I Nærheden af Løvskaal brydes Myremalm, og paa Egnen omkring Ulstrup graves store Mængder Støbesand, der forsendes over Ulstrup Station, hvor Stationsforstander Madsen har bygget en speciel Rampe, som de store Lastbiler kan køre op paa, saaledes at Malmen og andre Ting kan hældes lige ned i Jernbanevognene. Mine-Driften paa Egnen betyder meget for Stationens Omsætning, — og det er kun naturligt, at vi yder den bedst mulige Service,« siger Stationsforstanderen.

#### Opdaget ved Brøndboring.

Kiselgur-Lejerne ved Hollerup ejes af Ingeniør Børge Simonsen. Svejbæk, der fortæller, at man begyndte at udnytte Lejerne i 1892. Lejerne blev formodentlig opdaget ved, at man borede efter Vand, og derved fik Kiselgur op fra Boringen. En Ingeniør ved Navn Janzen var klar over, hvad der var Tale om, og han erhvervede Jorden for at udnytte Lejerne. For ca. 8 Aar overtog Ingeniør Simonsen Virksomheden, og han fortæller, at der hvert Aar graves ca. 1000 Tons Kiselgur.

De øverste Lag er finest.

Vi har aflagt et Besøg paa Virk-

somheden, der er omgivet af en særpræget Lugt. — Bestyrer Aage Kristiansen fortæller, at Lugten stammer fra de mange Miler, hvor man gløder Planteresterne ud af Kiselguren, der ligger omkring Lagerbygningen i store Stabler. Kiselguren er »støbt« i lange Rør, men efter Brændingen knuses den og forsendes i store Sække.

Kiselgurværket beskæftiger ca. 15 Mand om Sommeren, og om Vinteren 6—7 Mand. Raastoffet brydes i store Udgravninger i Bakkerne, hvor man maa fjerne Overjord paa flere Meters Tykkelse. Overjorden fjernes med Transportører, — og øverst finder man den fineste Kiselgur, som er betydelig mere værd end den dybliggende, der er meget forurenset af Planterester.

#### Mange Anvendelsesmuligheder i den kemiske Industri.

Ingeniør Simonsen fortæller, at Kiselguren er dannet langt tilbage i Fortiden af Kiselalger. Stoffet består af disse Algers »Skeletter«, og Tallet paa de Alger, der danner blot 1 Kilogram Kiselgur, er saa stort, at man næppe kan forestille sig det. Kiselguren er meget let, og da Stoffets Opsugningsevne er meget stor, har det mange Anvendelsesmuligheder i den kemiske Industri. Før i Tiden brugtes det meste til Isolation, men i Dag bruges det navnlig som Katalysator og som Hjelpe-Materiale ved Fremstilling af andre Stoffer. Det kan

vejer saaledes kun 150 Kilo. Lejerne ved Hollerup er meget store, og Brydningen kan fortsættes mange Aar endnu. Værket har adskillige faste Aftagere, og ca. 90 Procent af Produktionen eksporteres.

#### 36 Procent Jern i Danmarks tykkeste Lag Myremalm

Minedriften paa Randersegnen skaber Arbejde til mange Hænder — maaske ikke netop direkte, men i høj Grad indirekte. Kiselgur og Støbesand betyder Beskæftigelse for mange Mennesker i de Virksomheder, der anvender disse Stoffer, og det samme gælder Myremalmen. Det tykkeste Lag Myremalm i Danmark findes i Løvskaal. Det store Leje, der ejes af en Grosserer i Odense, blev i 1916 opdaget af et Jagtselskab. En af Jægerne havde Kendskab til Malmforekomster, og han fik en Klump, som han havde fundet, undersøgt. Under den første Verdenskrig, da der var stor Mangel paa Raastoffer, udnyttedes Lejet, hvor Jernet findes sammen med Okker, som farver alting og alle paa Stedet.

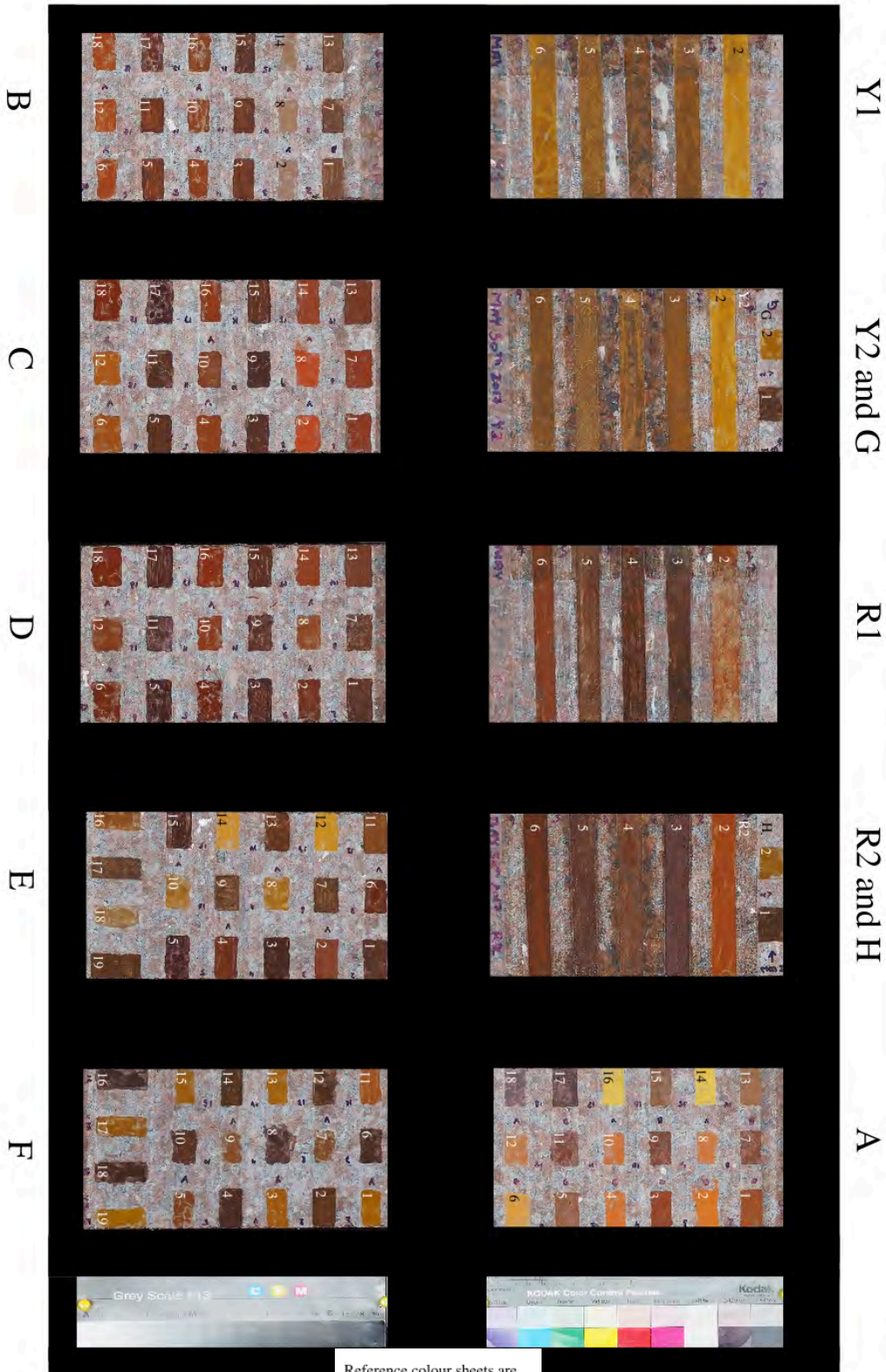
Der er op til 36 Procent Jern i den grusagtige Masse, man graver op, og det er altsaa nok til, at Udnyttelse kan betale sig. I gamle Dage blev Malmen fragtet bort ad Aaen til Randers, fortæller Lærer Einar Poulsen, Løvskaal Skole, der er godt inde i Egnens Historie.

Myremalmen fra Løvskaal anvendes ikke til Jernfremstilling, men til Rensning af Gas. Traktorer, der er forsynet med store Skovle, køre Malmen til Lastbiler, og disse kører derpaa til Ulstrup Station, hvorfra Malmen sendes ud til de forskellige Aftagere. Det er interessant at følge Arbejdet med Myremalmen, og det er nemt nok at finde ud til Lejet. Okkeren i Malmen har næsten farvet hele Vejen fra Løvskaal til Lejet rød.

vico.

### Appendix III – All Rock Slabs

All samples on rock slabs. I description of their meta-data and close-up images is found in Appendix IV. Y1, Y2, R1, R2, A-H is the name of rock slabs/part of rock slabs. Small number refers to the individual number on the rock slab. For instance will the first sample (to right) be referred to as Y1-2.



Reference colour sheets are misscoloured due to reflection

## Appendix IV – Painted Samples on Rock

All samples on rock slabs. See meta-data of these in the table below.

Row No.	1	2	3	4	5	6	7	8	9	10	11	12	13	14	15	16	17	18	19	20	21	22
	Y1-2	Y2-2	R1-2	R2-2	Backgr.	A19		E13	F12	E19	F6	F18	B5	B11	B19	C5	C19	D5	D11	E5		
	Y1-3	Y2-3	R1-3	R2-3	Backgr.	A18		E14	F13	E8	F9	F19	B6	B12	B18	C6	C18	D6	D12	E6		
	Y1-4	Y2-4	R1-4	R2-4		A15		E15	F14	E9	F8	G1	B3	B9	B15	C3	C15	D3	D9	E3		
	Y1-5	Y2-5	R1-5	R2-5		A16		E16	F15	E10	F9	G2	B4	B10	B16	C4	C16	D4	D10	E4		
	Y1-6	Y2-5	R1-6	R2-6		A11		E19	F16	E11	F10	H1	B1	B9	B13	C1	C13	D1	D9	E1		
						A12		E18	F19	E12	F11	H2	B2	B8	B14	C2	C14	D2	D8	E2		
						A9																
						A10																
						A9																
						A8																



Reference colour sheets are misscoloured due to reflection

Appendix IV

Table: Meta-data of all samples on rock slabs. This meta-data was also written into SCiO Lab web.

Row No.	Name	Location	Local area	Heating temperature in *C	Heat-ing time	Area	Bind-ing media	Aging	Paint or back-ground	Rock slab No	DK SE or other
1	y1-2	LØ3	LØ	0	0	dk	water	1	p	y1	d
1	y1-3	LØ3	LØ	0	0	dk	egg	1	p	y1	d
1	y1-4	LØ3	LØ	0	0	dk	fat	1	p	y1	d
1	y1-5	LØ3	LØ	0	0	dk	eggof at	1	p	y1	d
1	y1-6	LØ3	LØ	0	0	dk	blood	1	p	y1	d
2	y2-2	LØ3	LØ	0	0	dk	water	0	p	y2	d
2	y2-3	LØ3	LØ	0	0	dk	egg	0	p	y2	d
2	y2-4	LØ3	LØ	0	0	dk	fat	0	p	y2	d
2	y2-5	LØ3	LØ	0	0	dk	eggof at	0	p	y2	d
2	y2-6	LØ3	LØ	0	0	dk	blood	0	p	y2	d
3	r1-2	LØ3	LØ	?	?	dk	water	1	p	r1	d
3	r1-3	LØ3	LØ	?	?	dk	egg	1	p	r1	d
3	r1-4	LØ3	LØ	?	?	dk	fat	1	p	r1	d
3	r1-5	LØ3	LØ	?	?	dk	eggof at	1	p	r1	d
3	r1-6	LØ3	LØ	?	?	dk	blood	1	p	r1	d
4	r2-2	LØ3	LØ	?	?	dk	water	0	p	r2	d
4	r2-3	LØ3	LØ	?	?	dk	egg	0	p	r2	d
4	r2-4	LØ3	LØ	?	?	dk	fat	0	p	r2	d
4	r2-5	LØ3	LØ	?	?	dk	eggof at	0	p	r2	d
4	r2-6	LØ3	LØ	?	?	dk	blood	0	p	r2	d
5	Rock	-	-	-	-	-	-	-	b	Rock	-
5	Rock	-	-	-	-	-	-	-	b	Rock	-
5	a13	LOB	LOB	0	0	?	blood	new	p	a	o
5	a14	LOB	LOB	0	0	?	water	new	p	a	o
5	a5	LOB	LOB	300	1h	?	blood	new	p	a	o
5	a6	LOB	LOB	300	1h	?	water	new	p	a	o
5	a3	LOB	LOB	600	1h	?	blood	new	p	a	o
5	a4	LOB	LOB	600	1h	?	water	new	p	a	o
5	a1	LOB	LOB	900	1h	?	blood	new	p	a	o
5	a2	LOB	LOB	900	1h	?	water	new	p	a	o
6	a17	HEM	HEM	x	x	?	blood	new	p	a	o
6	a18	HEM	HEM	x	x	?	water	new	p	a	o

Appendix IV

6	a15	YAU	AU	0	0	au	blood	new	p	a	o
6	a16	YAU	AU	0	0	au	water	new	p	a	o
6	a11	YAU	AU	300	1h	au	blood	new	p	a	o
6	a12	YAU	AU	300	1h	au	water	new	p	a	o
6	a9	YAU	AU	600	1h	au	blood	new	p	a	o
6	a10	YAU	AU	600	1h	au	water	new	p	a	o
6	a7	YAU	AU	900	1h	au	blood	new	p	a	o
6	a8	YAU	AU	900	1h	au	water	new	p	a	o
7	e7	LØ1	LØ	0	0	dk	blood	new	p	e	d
7	e8	LØ1	LØ	0	0	dk	water	new	p	e	d
7	e9	LØ2	LØ	0	0	dk	blood	new	p	e	d
7	e10	LØ2	LØ	0	0	dk	water	new	p	e	d
7	e11	LØ3	LØ	0	0	dk	blood	new	p	e	d
7	e12	LØ3	LØ	0	0	dk	water	new	p	e	d
8	e13	KT1	KT	0	0	ms	blood	new	p	e	s
8	e14	KT1	KT	0	0	ms	water	new	p	e	s
8	e15	KT2	KT	0	0	ms	blood	new	p	e	s
8	e16	KT2	KT	0	0	ms	water	new	p	e	s
8	e17	KT3	KT	0	0	ms	blood	new	p	e	s
8	e18	KT3	KT	0	0	ms	water	new	p	e	s
9	f12	AA1	AA	0	0	ms	blood	new	p	f	s
9	f13	AA1	AA	0	0	ms	water	new	p	f	s
9	f14	AA2	AA	0	0	ms	blood	new	p	f	s
9	f15	AA2	AA	0	0	ms	water	new	p	f	s
9	f16	AA3	AA	0	0	ms	blood	new	p	f	s
9	f17	AA3	AA	0	0	ms	water	new	p	f	s
10	e19	HO1	HO	0	0	ns	blood	new	p	e	s
10	f1	HO1	HO	0	0	ns	water	new	p	f	s
10	f2	HO2	HO	0	0	ns	blood	new	p	f	s
10	f3	HO2	HO	0	0	ns	water	new	p	f	s
10	f4	HO3	HO	?	?	ns	blood	new	p	f	s
10	f5	HO3	HO	?	?	ns	water	new	p	f	s
11	f6	ST1	ST	?	?	ms	blood	new	p	f	s
11	f7	ST1	ST	?	?	ms	water	new	p	f	s
11	f8	ST2	ST	?	?	ms	blood	new	p	f	s
11	f9	ST2	ST	?	?	ms	water	new	p	f	s
11	f10	ST3	ST	?	?	ms	blood	new	p	f	s
11	f11	ST3	ST	?	?	ms	water	new	p	f	s
12	g1	SR2	SR	0	0	ms	blood	new	p	y2	s

## Appendix IV

12	g2	SR2	SR	0	0	ms	water	new	p	y2	s
12	h2	SR3	SR	0	0	ms	water	new	p	r2	s
12	h1	SR3	SR	0	0	ms	blood	new	p	r2	s
12	f18	SR1	SR	0	0	ms	blood	new	p	f	s
12	f19	SR1	SR	0	0	ms	water	new	p	f	s
13	b5	LØ3	LØ	300	15min	dk	blood	new	p	b	d
13	b6	LØ3	LØ	300	15min	dk	water	new	p	b	d
13	b3	LØ3	LØ	600	15min	dk	blood	new	p	b	d
13	b4	LØ3	LØ	600	15min	dk	water	new	p	b	d
13	b1	LØ3	LØ	900	15min	dk	blood	new	p	b	d
13	b2	LØ3	LØ	900	15min	dk	water	new	p	b	d
14	b11	LØ3	LØ	300	30min	dk	blood	new	p	b	d
14	b12	LØ3	LØ	300	30min	dk	water	new	p	b	d
14	b9	LØ3	LØ	600	30min	dk	blood	new	p	b	d
14	b10	LØ3	LØ	600	30min	dk	water	new	p	b	d
14	b7	LØ3	LØ	900	30min	dk	blood	new	p	b	d
14	b8	LØ3	LØ	900	30min	dk	water	new	p	b	d
15	b17	LØ3	LØ	300	1h	dk	blood	new	p	b	d
15	b18	LØ3	LØ	300	1h	dk	water	new	p	b	d
15	b15	LØ3	LØ	600	1h	dk	blood	new	p	b	d
15	b16	LØ3	LØ	600	1h	dk	water	new	p	b	d
15	b13	LØ3	LØ	900	1h	dk	blood	new	p	b	d
15	b14	LØ3	LØ	900	1h	dk	water	new	p	b	d
16	c5	KT1	KT	300	30min	ms	blood	new	p	c	s
16	c6	KT1	KT	300	30min	ms	water	new	p	c	s
16	c3	KT1	KT	600	30min	ms	blood	new	p	c	s
16	c4	KT1	KT	600	30min	ms	water	new	p	c	s
16	c1	KT1	KT	900	30min	ms	blood	new	p	c	s
16	c2	KT1	KT	900	30min	ms	water	new	p	c	s
17	c11	KT1	KT	300	1h	ms	blood	new	p	c	s
17	c12	KT1	KT	300	1h	ms	water	new	p	c	s
17	c9	KT1	KT	600	1h	ms	blood	new	p	c	s
17	c10	KT1	KT	600	1h	ms	water	new	p	c	s
17	c7	KT1	KT	900	1h	ms	blood	new	p	c	s
17	c8	KT1	KT	900	1h	ms	water	new	p	c	s
18	c17	AA1	AA	300	30min	ms	blood	new	p	c	s
18	c18	AA1	AA	300	30min	ms	water	new	p	c	s
18	c15	AA1	AA	600	30min	ms	blood	new	p	c	s
18	c16	AA1	AA	600	30min	ms	water	new	p	c	s

## Appendix IV

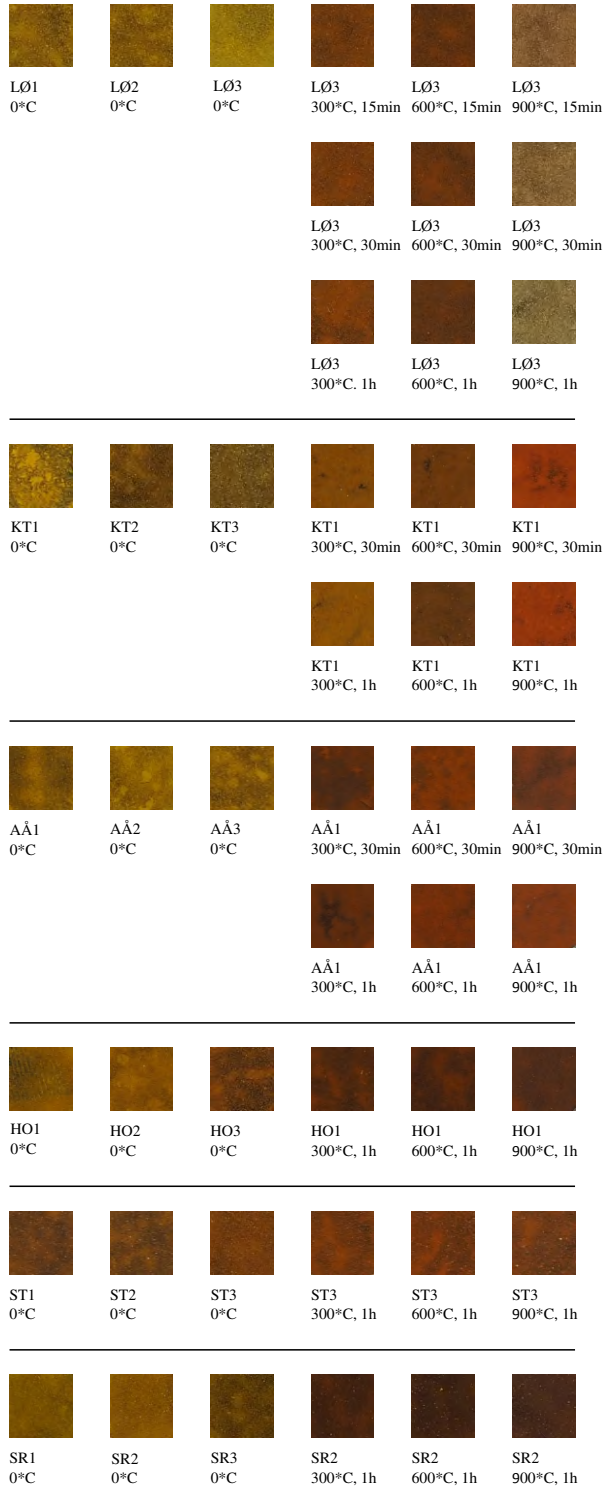
18	c13	AA1	AA	900	30min	ms	blood	new	p	c	s
18	c14	AA1	AA	900	30min	ms	water	new	p	c	s
19	d17	AA1	AA	300	1h	ms	blood	new	p	d	s
19	d18	AA1	AA	300	1h	ms	water	new	p	d	s
19	d15	AA1	AA	600	1h	ms	blood	new	p	d	s
19	d16	AA1	AA	600	1h	ms	water	new	p	d	s
19	d13	AA1	AA	900	1h	ms	blood	new	p	d	s
19	d14	AA1	AA	900	1h	ms	water	new	p	d	s
20	d5	HO1	HO	300	1h	ns	blood	new	p	d	s
20	d6	HO1	HO	300	1h	ns	water	new	p	d	s
20	d3	HO1	HO	600	1h	ns	blood	new	p	d	s
20	d4	HO1	HO	600	1h	ns	water	new	p	d	s
20	d1	HO1	HO	900	1h	ns	blood	new	p	d	s
20	d2	HO1	HO	900	1h	ns	water	new	p	d	s
21	d11	ST3	ST	300	1h	ms	blood	new	p	d	s
21	d12	ST3	ST	300	1h	ms	water	new	p	d	s
21	d9	ST3	ST	600	1h	ms	blood	new	p	d	s
21	d10	ST3	ST	600	1h	ms	water	new	p	d	s
21	d7	ST3	ST	900	1h	ms	blood	new	p	d	s
21	d8	ST3	ST	900	1h	ms	water	new	p	d	s
22	e5	SR2	SR	300	1h	ms	blood	new	p	e	s
22	e6	SR2	SR	300	1h	ms	water	new	p	e	s
22	e3	SR2	SR	600	1h	ms	blood	new	p	e	s
22	e4	SR2	SR	600	1h	ms	water	new	p	e	s
22	e1	SR2	SR	900	1h	ms	blood	new	p	e	s
22	e2	SR2	SR	900	1h	ms	water	new	p	e	s

Table 2: Shortenings

Temperature and time	Area	Aging	Paint or background	DK, SE or other
x=not relevant	dk=Denmark ms=Middle Sweden ns=Northern Sweden	1=exposed 0=not exposed	p=paint b=Background/rock	d=Denmark s=Sweden  o=Other

## Appendix V – Samples on Carbon Tape

All samples on carbon tape. The black carbon tape affects the visual colour when the pigment lay is thin.



HEM  
0°C

Appendix V

Table: Meta-data about samples on carbon tape.

Sample No.	Sample name	Location	Local area	Heating Temperature in *C	Heating time	Area	Binding media	Aging	Paint or backg.	Rock slab No	DK, SE or other
163	LØ1 powder	LØ1	LØ	0	0	dk	0	new	p	carbon tape	d
164	LØ2 powder	LØ2	LØ	0	0	dk	0	new	p	carbon tape	d
165	LØ3 powder	LØ3	LØ	0	0	dk	0	new	p	carbon tape	d
166	KT1 powder	KT1	KT	0	0	ms	0	new	p	carbon tape	s
167	HO1 powder	HO1	HO	0	0	ns	0	new	p	carbon tape	s
168	ST3 powder	ST3	ST	?	?	ms	0	new	p	carbon tape	s
169	AA1 powder	AA1	AA	0	0	ms	0	new	p	carbon tape	s
170	HEM powder	HEM	HEM	x	x	?	0	new	p	carbon tape	o
171	LØ3 powder	LØ3	LØ	300	15min	dk	0	new	p	carbon tape	d
172	LØ3 powder	LØ3	LØ	600	15min	dk	0	new	p	carbon tape	d
173	LØ3 powder	LØ3	LØ	900	15min	dk	0	new	p	carbon tape	d
174	LØ3 powder	LØ3	LØ	300	30min	dk	0	new	p	carbon tape	d
175	LØ3 powder	LØ3	LØ	600	30min	dk	0	new	p	carbon tape	d
176	LØ3 powder	LØ3	LØ	900	30min	dk	0	new	p	carbon tape	d
177	LØ3 powder	LØ3	LØ	300	1h	dk	0	new	p	carbon tape	d
178	LØ3 powder	LØ3	LØ	600	1h	dk	0	new	p	carbon tape	d
180	LØ3 powder	LØ3	LØ	900	1h	dk	0	new	p	carbon tape	d
181	LOB powder	LOB	LOB	900	1h	?	0	new	p	carbon tape	o
182	YAU powder	YAU	AU	900	1h	au	0	new	p	carbon tape	o
183	SR2 powder	SR2	SR	900	1h	ms	0	new	p	carbon tape	s
184	KT1 powder	KT1	KT	900	30min	ms	0	new	p	carbon tape	s
185	KT1 powder	KT1	KT	900	1h	ms	0	new	p	carbon tape	s
186	HO1 powder	HO1	HO	900	1h	ns	0	new	p	carbon tape	s
187	AA1 powder	AA1	AA	900	30min	ms	0	new	p	carbon tape	s
188	AA1 powder	AA1	AA	900	1h	ms	0	new	p	carbon tape	s
189	ST3 powder	ST3	ST	900	1h	ms	0	new	p	carbon tape	s
194	KT1 powder	KT1	KT	600	30min	ms	0	new	p	carbon tape	s
195	KT1 powder	KT1	KT	300	30min	ms	0	new	p	carbon tape	s
196	KT3 powder	KT3	KT	0	0	ms	0	new	p	carbon tape	s
197	KT2 powder	KT2	KT	0	0	ms	0	new	p	carbon tape	s

## Appendix V

198	KT1 powder	KT1	KT	300	1h	ms	0	new	p	carbon tape	s
199	KT1 powder	KT1	KT	600	1h	ms	0	new	p	carbon tape	s
200	HO2 powder	HO2	HO	0	0	ns	0	new	p	carbon tape	s
201	HO3 powder	HO3	HO	?	?	ns	0	new	p	carbon tape	s
202	HO1 powder	HO1	HO	300	1h	ns	0	new	p	carbon tape	s
203	HO1 powder	HO1	HO	600	1h	ns	0	new	p	carbon tape	s
204	AA2 powder	AA2	AA	0	0	ms	0	new	p	carbon tape	s
205	AA3 powder	AA3	AA	0	0	ms	0	new	p	carbon tape	s
206	AA1 powder	AA1	AA	300	30min	ms	0	new	p	carbon tape	s
207	AA1 powder	AA1	AA	600	30min	ms	0	new	p	carbon tape	s
208	AA1 powder	AA1	AA	300	1h	ms	0	new	p	carbon tape	s
209	AA1 powder	AA1	AA	600	1h	ms	0	new	p	carbon tape	s
210	ST1 powder	ST1	ST	?	?	ms	0	new	p	carbon tape	s
211	ST2 powder	ST2	ST	?	?	ms	0	new	p	carbon tape	s
212	ST3 powder	ST3	ST	300	1h	ms	0	new	p	carbon tape	s
213	ST3 powder	ST3	ST	600	1h	ms	0	new	p	carbon tape	s
214	LOB powder	LOB	LOB	0	0	?	0	new	p	carbon tape	o
215	LOB powder	LOB	LOB	300	1h	?	0	new	p	carbon tape	o
216	LOB powder	LOB	LOB	600	1h	?	0	new	p	carbon tape	o
218	YAU powder	YAU	AU	0	0	au	0	new	p	carbon tape	o
219	YAU powder	YAU	AU	300	1h	au	0	new	p	carbon tape	o
220	YAU powder	YAU	AU	600	1h	au	0	new	p	carbon tape	o
221	SR1 powder	SR1	SR	0	0	ms	0	new	p	carbon tape	s
222	SR3 powder	SR3	SR	0	0	ms	0	new	p	carbon tape	s
223	SR2 powder	SR2	SR	300	1h	ms	0	new	p	carbon tape	s
224	SR2 powder	SR2	SR	600	1h	ms	0	new	p	carbon tape	s

## **Appendix VI - SEM-EDX Spectra and Images**

The EDX-results and backscattered images of HEM, LØ3, KT1, HO1, ST3, AÅ1, SR2, LOB and YAU, all unheated, will be shown on the following pages.

## Backscattered electron images and EDX-result of HEM

14/02/2018 12:07:17

Spectrum processing :

Peaks possibly omitted : 2.630, 5.897 keV

Processing option : Oxygen by stoichiometry (Normalised)

Number of iterations = 3

Standard :

C Calcite 18-May-2017 02:38 PM

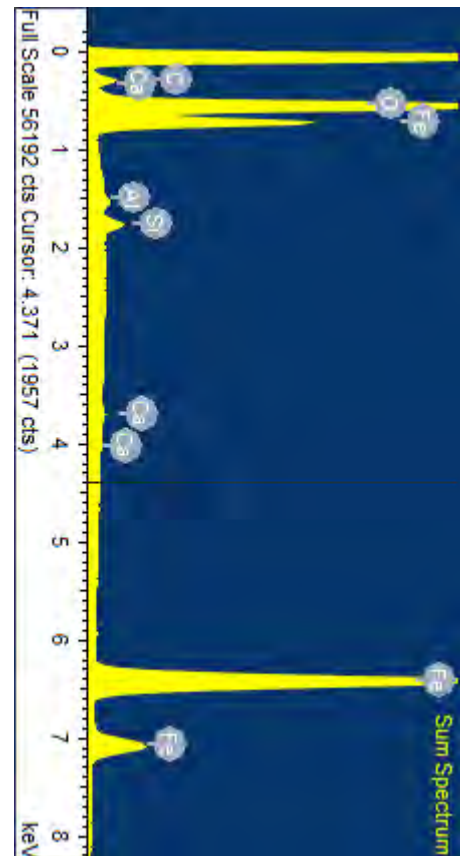
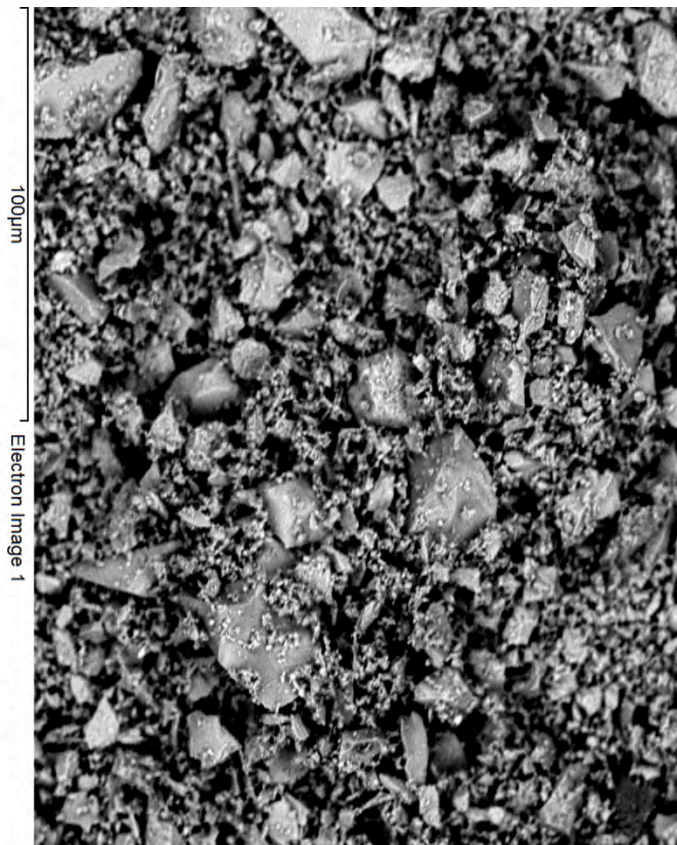
Al Corundum 15-Sep-2017 01:33 PM

Si MAC Wollastonite 15-Sep-2017 01:48 PM

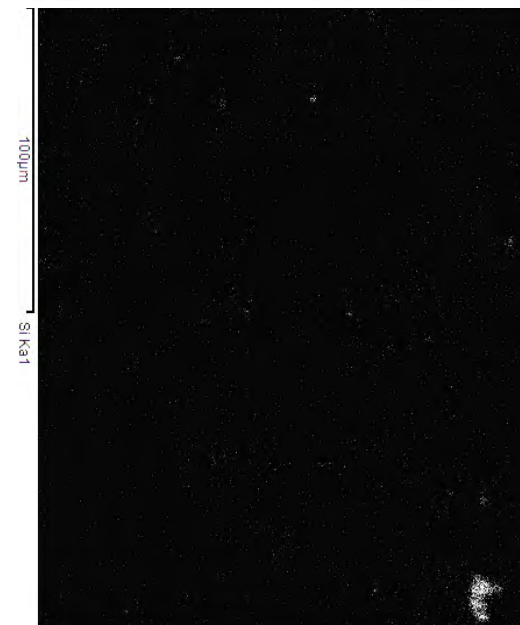
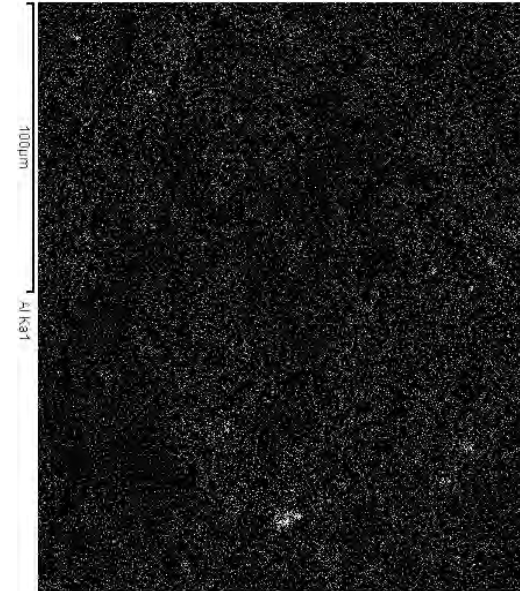
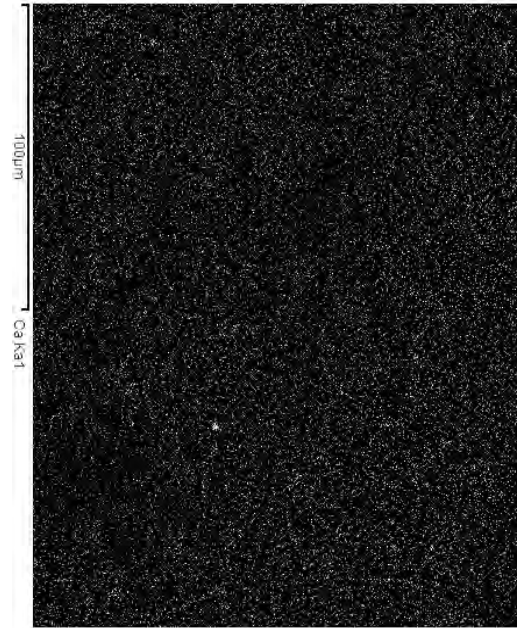
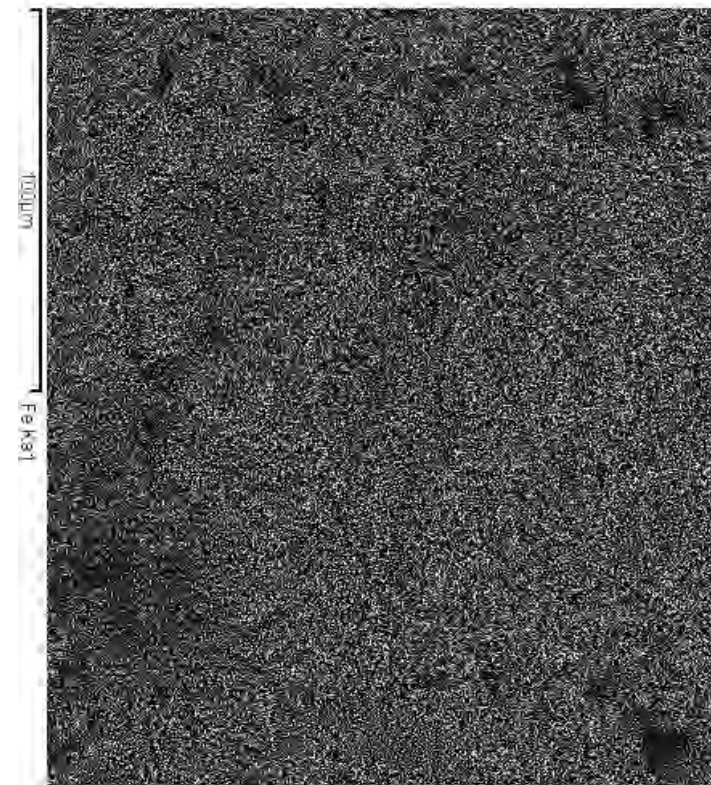
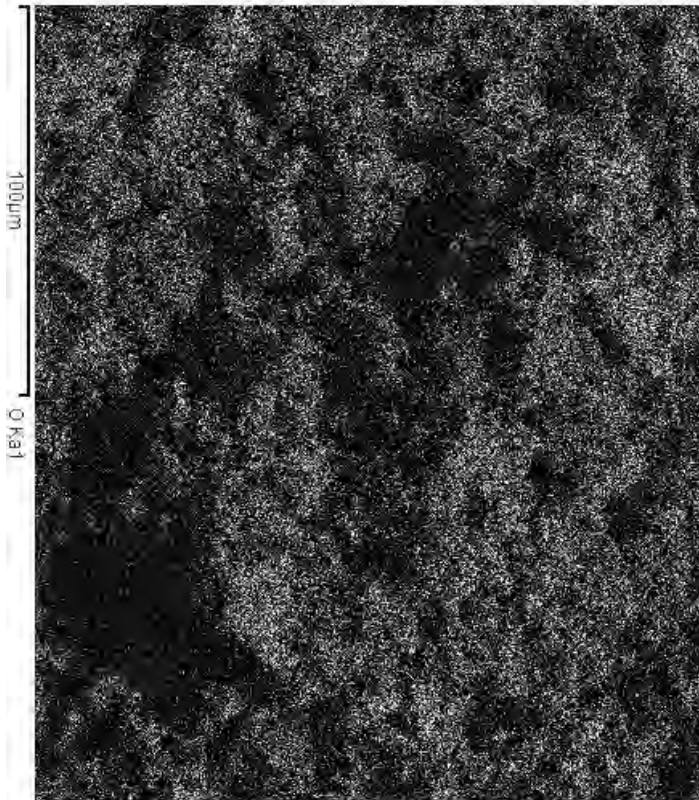
Ca MAC Wollastonite 15-Sep-2017 01:48 PM

Fe Fe Metal 15-Sep-2017 10:25 AM

Element	Weight%	Atomic%	Compd%	Formula
C K	1.92	5.15	7.02	CO <sub>2</sub>
Al K	0.19	0.23	0.37	Al <sub>2</sub> O <sub>3</sub>
Si K	0.49	0.56	1.04	SiO <sub>2</sub>
Ca K	0.15	0.12	0.21	CaO
Fe K	71.01	41.03	91.36	FeO
O	26.24	52.91		
Totals	100.00			



Elemental mapping of HEM



## Backscattered electron images and EDX-result of L03, 0°C

14/02/2018 09:36:24

Spectrum processing :

No peaks omitted

Processing option : Oxygen by stoichiometry (Normalised)

Number of iterations = 3

Standard :

C Calcite 18-May-2017 02:38 PM

Mg MgO 15-Sep-2017 02:39 PM

Al Corundum 15-Sep-2017 01:33 PM

Si MAC Wollastonite 15-Sep-2017 01:48 PM

P Apatite MAC 15-Sep-2017 02:01 PM

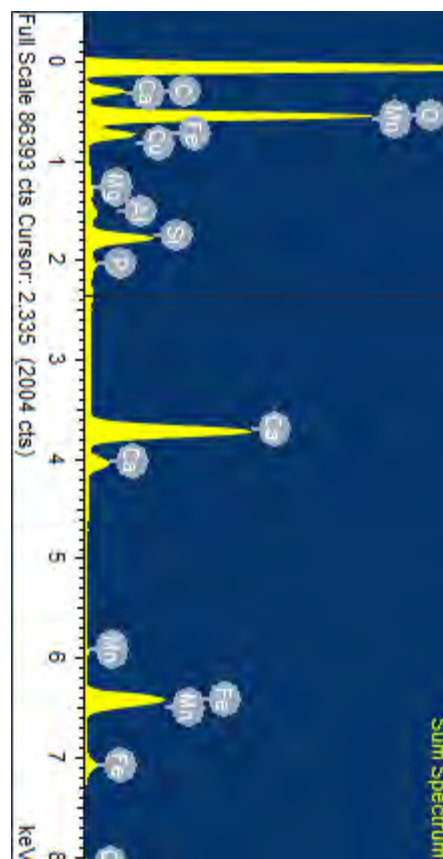
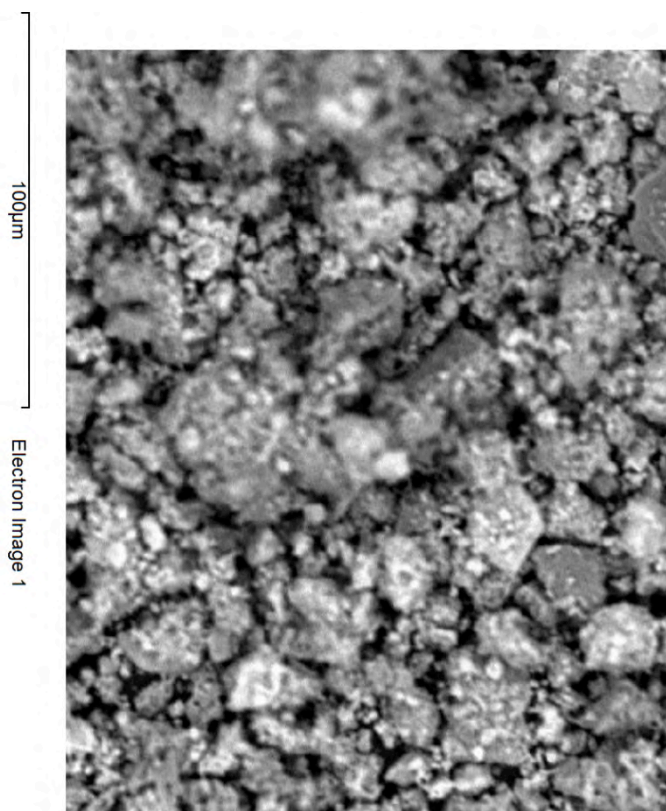
Ca MAC Wollastonite 15-Sep-2017 01:48 PM

Mn Mn Metal 15-Sep-2017 10:35 AM

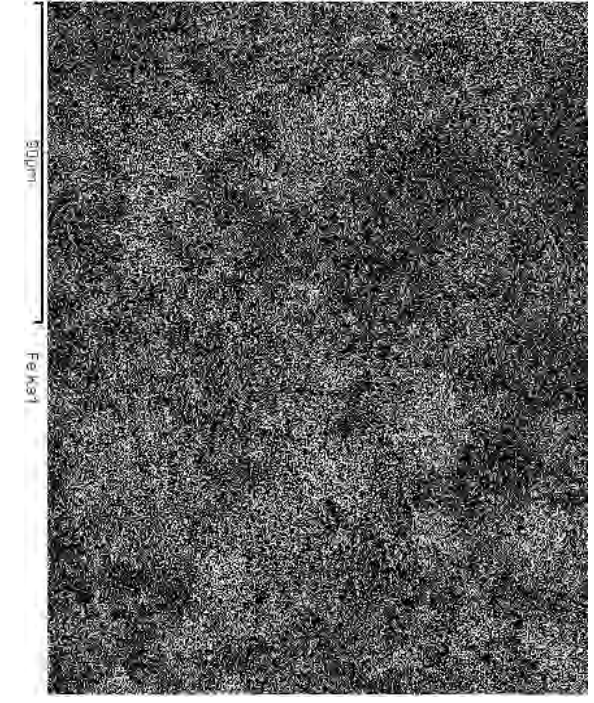
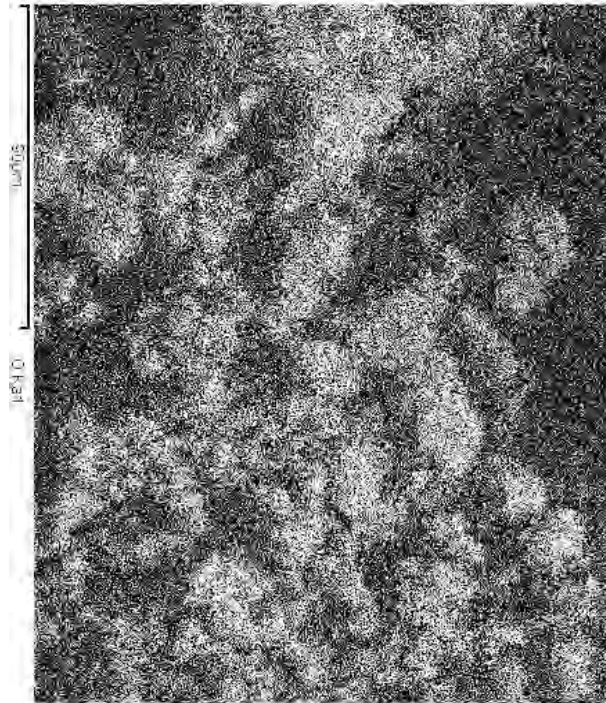
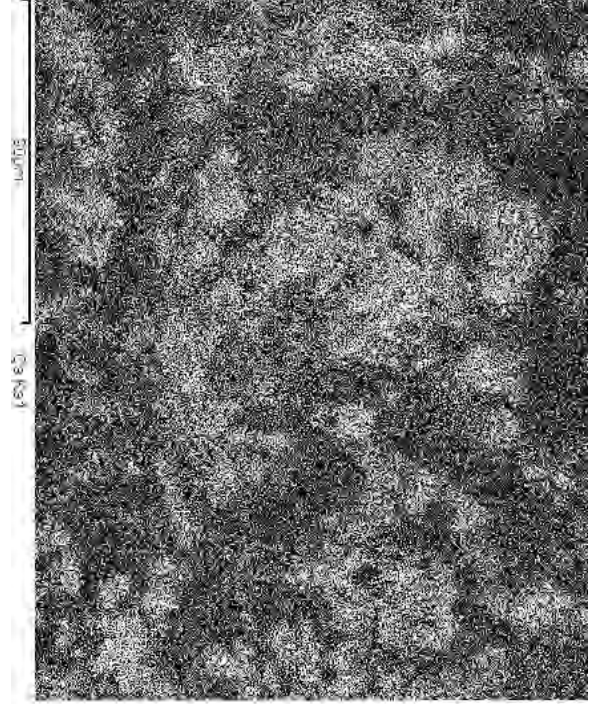
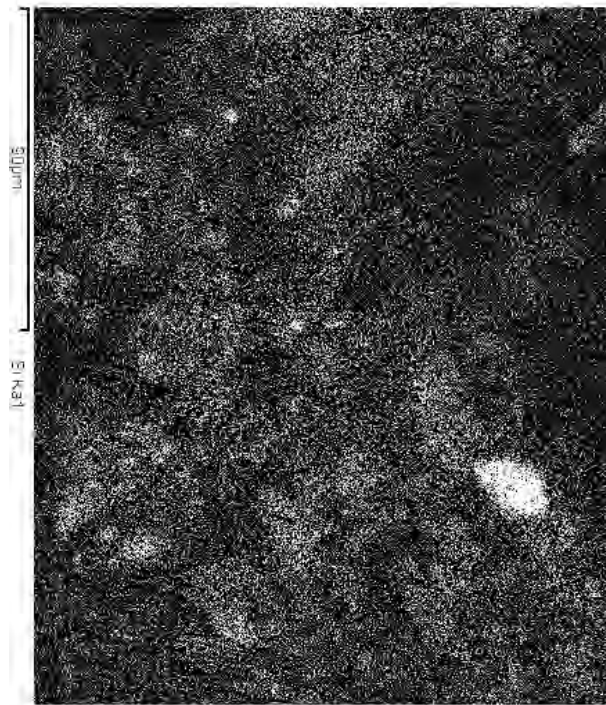
Fe Fe Metal 15-Sep-2017 10:25 AM

Cu Cu 1-Jun-1999 12:00 AM

Element	Weight%	Atomic%	Compd%	Formula
C K	6.75	13.52	24.75	CO2
Mg K	0.11	0.10	0.18	MgO
Al K	0.33	0.30	0.63	Al2O3
Si K	3.28	2.81	7.02	SiO2
P K	0.29	0.22	0.66	P2O5
Ca K	17.45	10.47	24.42	CaO
Mn K	0.42	0.18	0.54	MnO
Fe K	32.34	13.93	41.61	FeO
Cu L	0.16	0.06	0.20	CuO
O	38.86	58.41		
Totals	100.00			



Elemental mapping of LØ3



## Backscattered electron images and EDX-result of KT1, 0°C

14/02/2018 10:08:57

Spectrum processing :

No peaks omitted

Processing option : Oxygen by stoichiometry (Normalised)

Number of iterations = 4

Standard :

C Calcite 18-May-2017 02:38 PM

Al Corundum 15-Sep-2017 01:33 PM

Si MAC Wollastonite 15-Sep-2017 01:48 PM

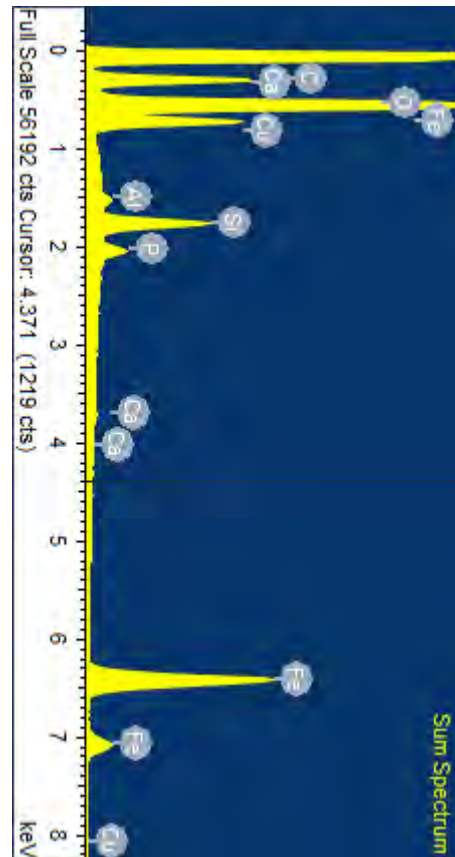
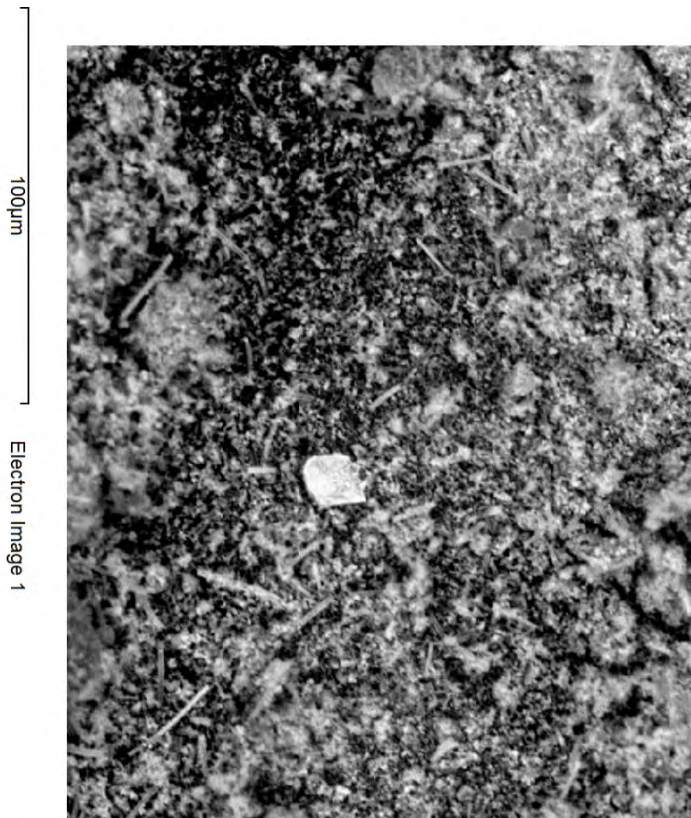
P Apatite MAC 15-Sep-2017 02:01 PM

Ca MAC Wollastonite 15-Sep-2017 01:48 PM

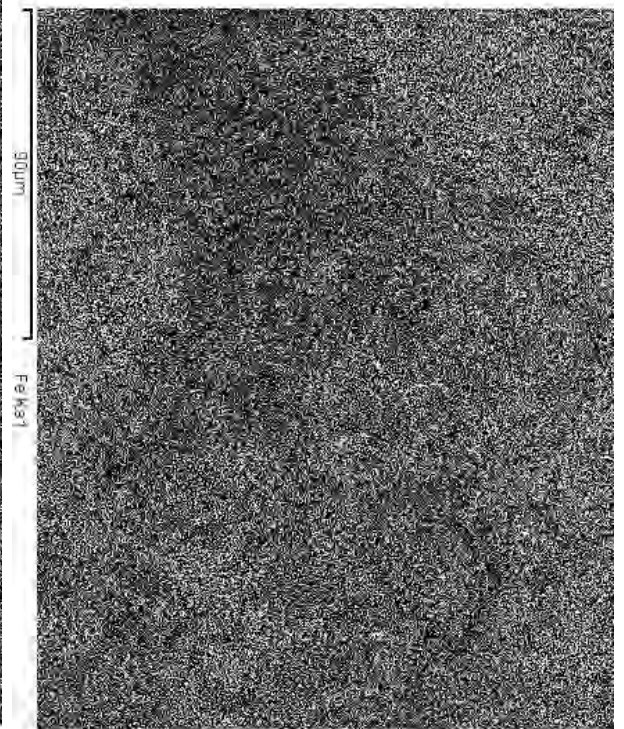
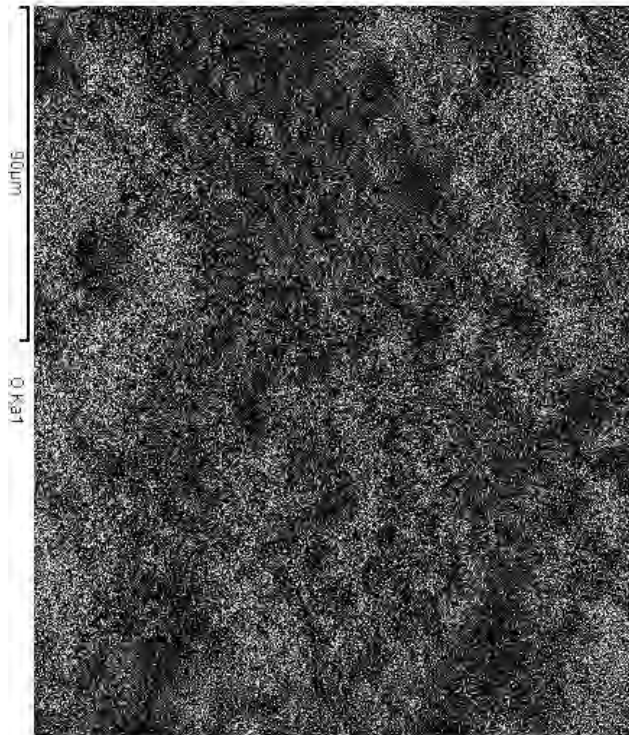
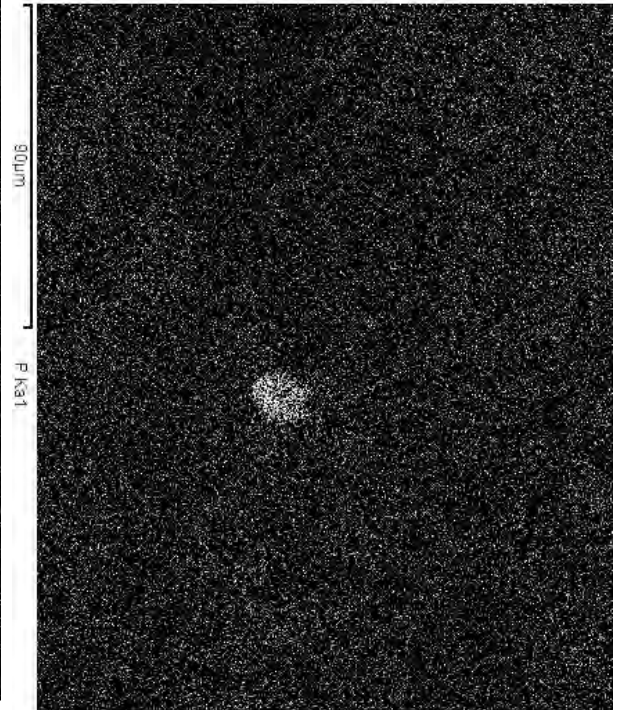
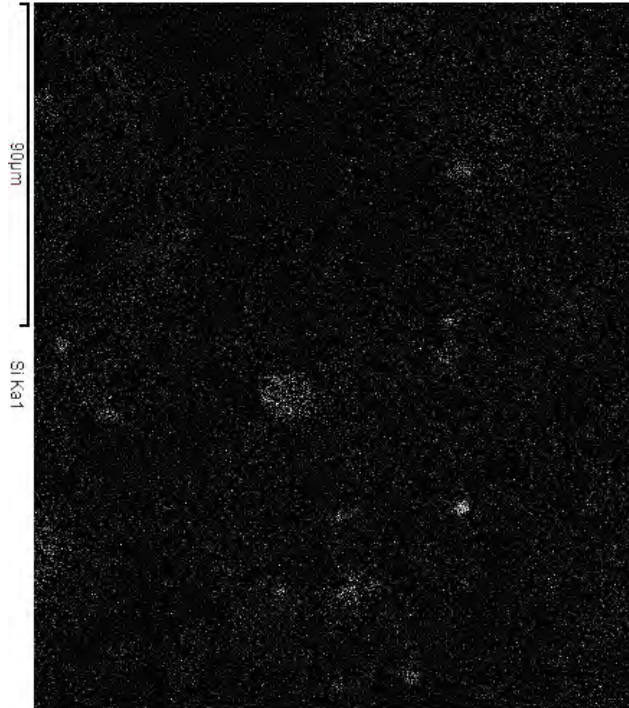
Fe Fe Metal 15-Sep-2017 10:25 AM

Cu Cu 1-Jun-1999 12:00 AM

Element	Weight%	Atomic%	Compd%	Formula
C K	13.12	22.32	48.06	CO <sub>2</sub>
Al K	0.23	0.17	0.44	Al <sub>2</sub> O <sub>3</sub>
Si K	2.63	1.92	5.63	SiO <sub>2</sub>
P K	0.73	0.48	1.68	P <sub>2</sub> O <sub>5</sub>
Ca K	0.13	0.07	0.18	CaO
Fe K	34.17	12.50	43.96	FeO
Cu L	0.03	0.01	0.04	CuO
O	48.95	62.52		
Totals	100.00			



Elemental mapping of KT1



## Backscattered electron images and EDX-result of HO1, 0°C

14/02/2018 10:35:08

Spectrum processing :

Peaks possibly omitted : 2.291, 8.060 keV

Processing option : Oxygen by stoichiometry (Normalised)

Number of iterations = 3

Standard :

C Calcite 18-May-2017 02:38 PM

Al Corundum 15-Sep-2017 01:33 PM

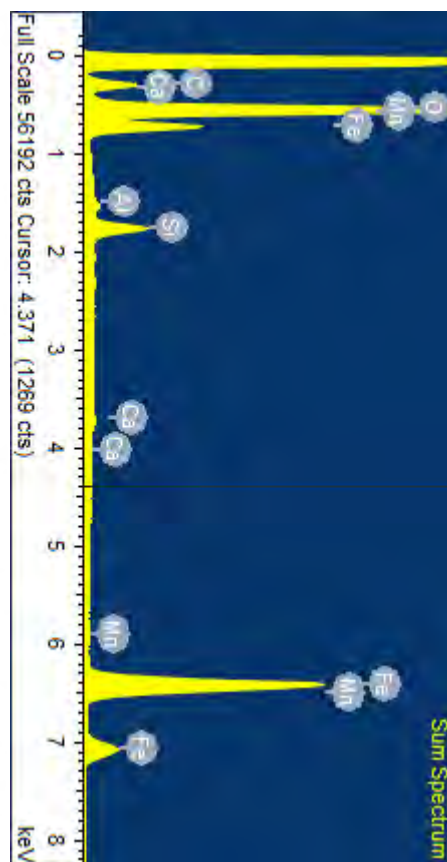
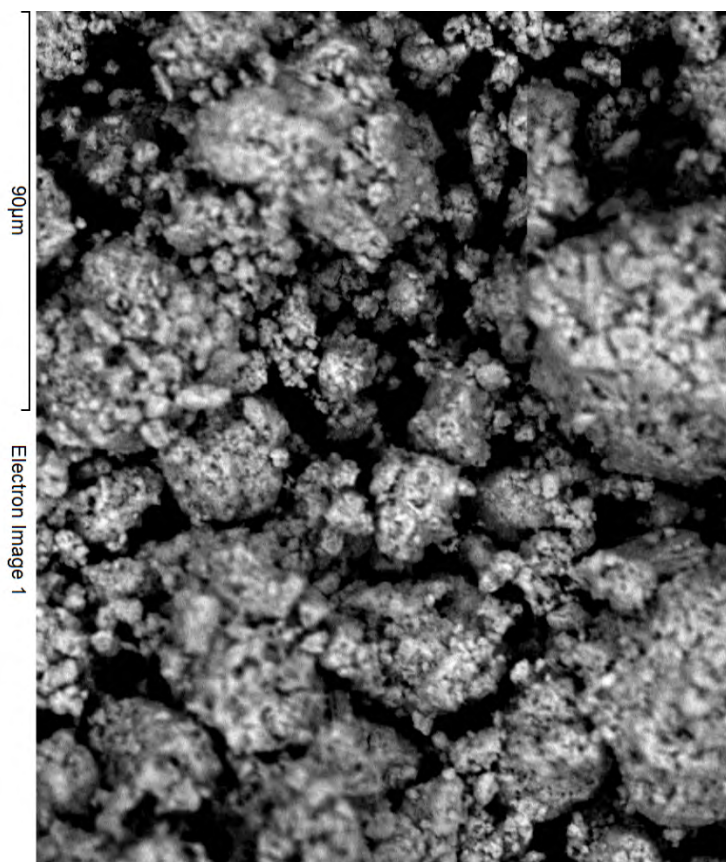
Si MAC Wollastonite 15-Sep-2017 01:48 PM

Ca MAC Wollastonite 15-Sep-2017 01:48 PM

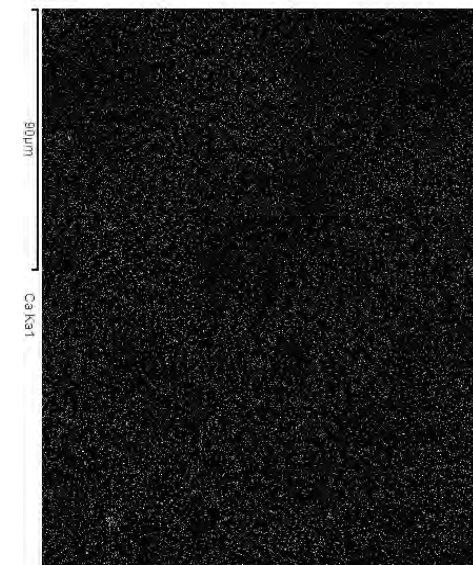
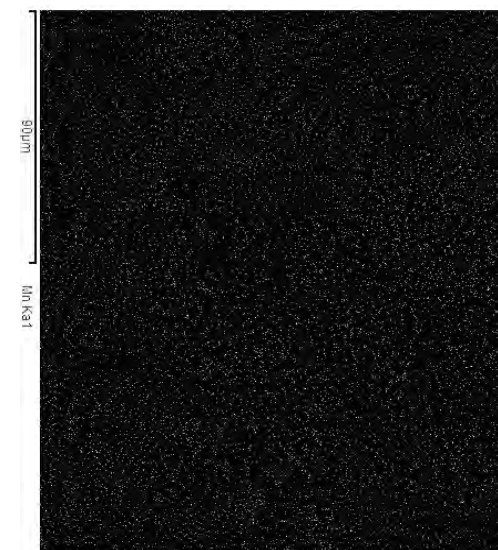
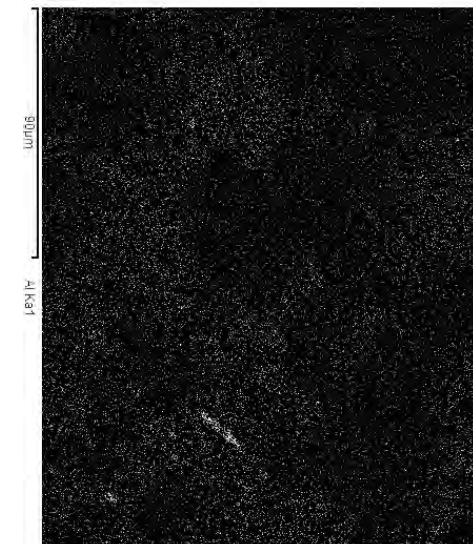
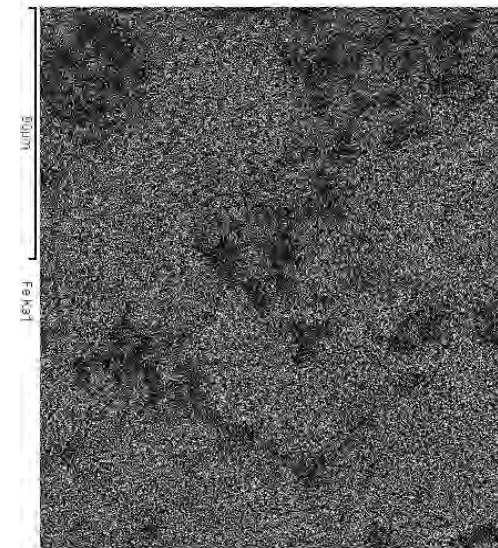
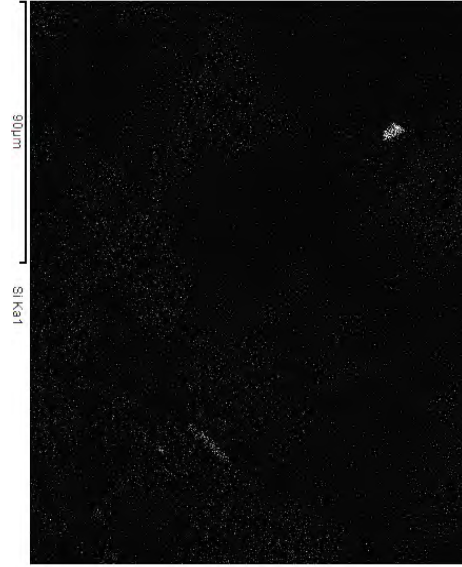
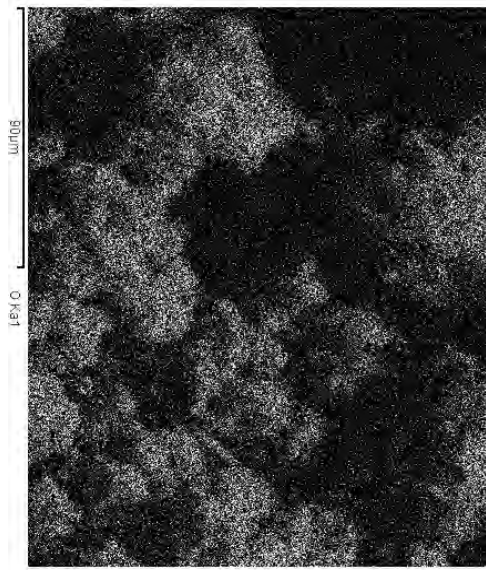
Mn Mn Metal 15-Sep-2017 10:35 AM

Fe Fe Metal 15-Sep-2017 10:25 AM

Element	Weight%	Atomic%	Compd%	Formula
C K	6.13	13.47	22.45	CO <sub>2</sub>
Al K	0.22	0.21	0.41	Al <sub>2</sub> O <sub>3</sub>
Si K	1.81	1.70	3.87	SiO <sub>2</sub>
Ca K	0.24	0.16	0.33	CaO
Mn K	0.33	0.16	0.42	MnO
Fe K	56.37	26.66	72.51	FeO
O	34.91	57.64		
Totals	100.00			



Elemental mapping of HO1



## Backscattered electron images and EDX-result of ST3 0°C

14/02/2018 10:59:46

Spectrum processing :

Peaks possibly omitted : 2.323, 8.029 keV

Processing option : Oxygen by stoichiometry (Normalised)

Number of iterations = 3

Standard :

C Calcite 18-May-2017 02:38 PM

Na Jadeite MAC 15-Sep-2017 11:04 AM

Mg MgO 15-Sep-2017 02:39 PM

Al Corundum 15-Sep-2017 01:33 PM

Si MAC Wollastonite 15-Sep-2017 01:48 PM

K MAC Orthoclase 15-Sep-2017 01:41 PM

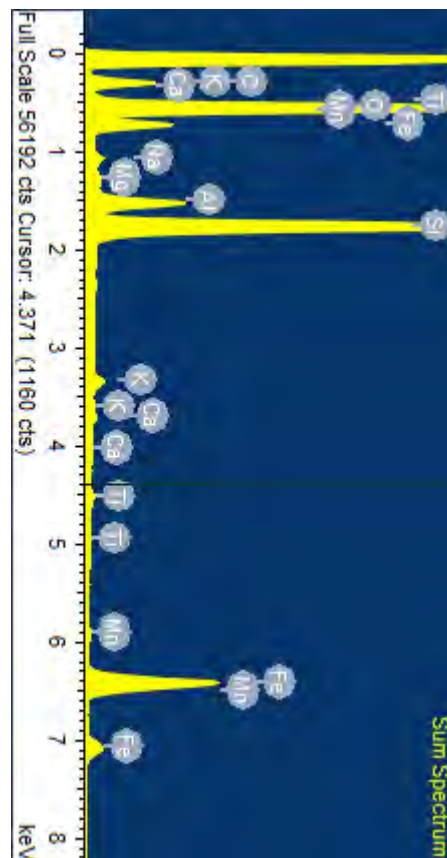
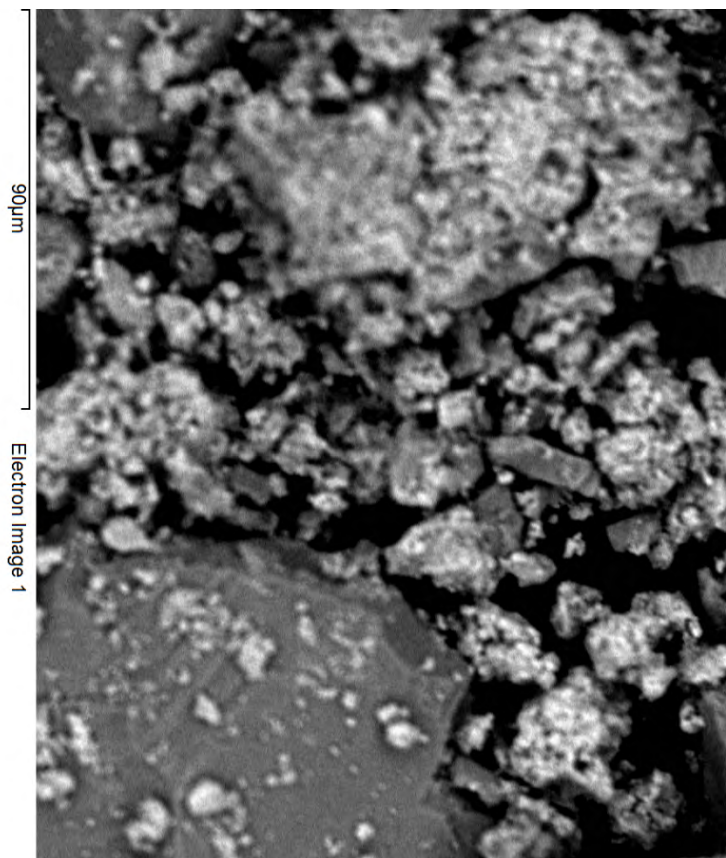
Ca MAC Wollastonite 15-Sep-2017 01:48 PM

Ti Ti metal 15-Sep-2017 10:53 AM

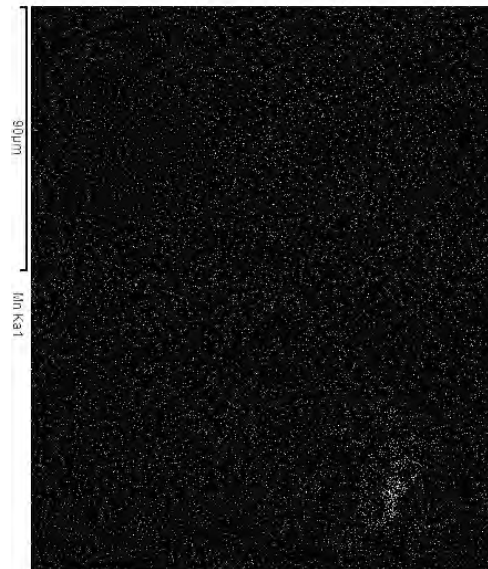
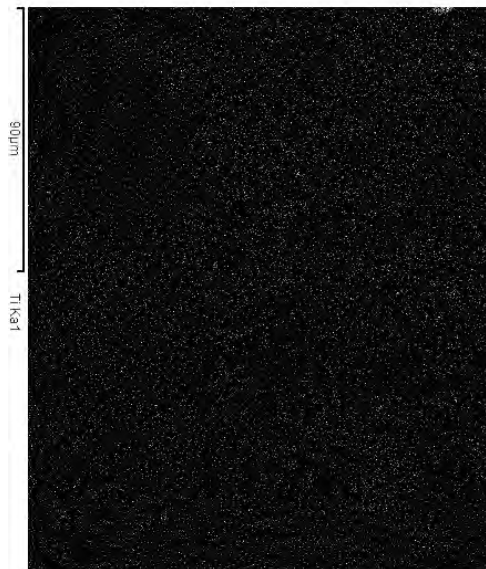
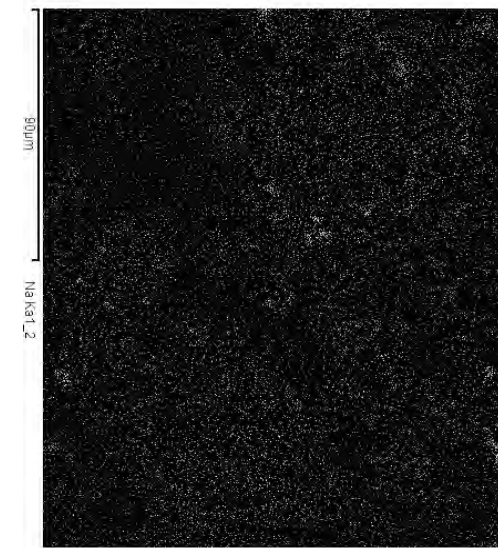
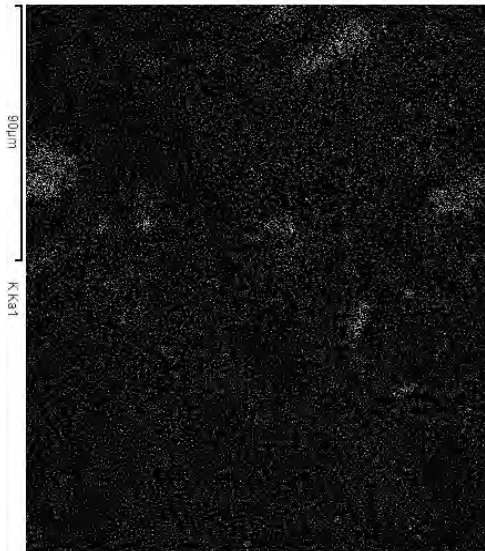
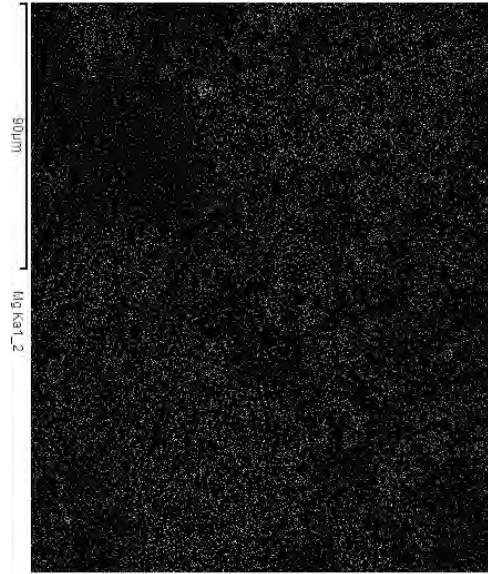
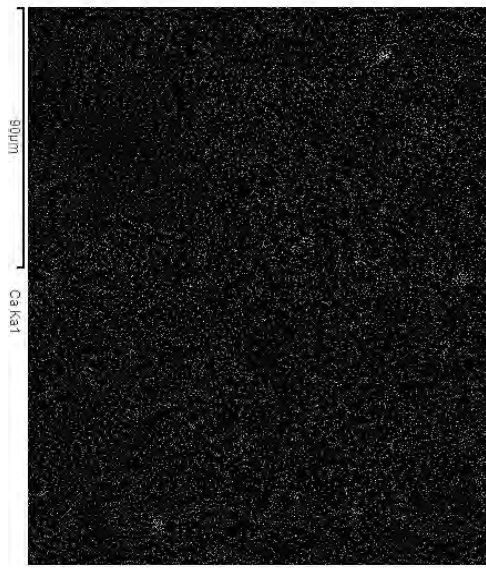
Mn Mn Metal 15-Sep-2017 10:35 AM

Fe Fe Metal 15-Sep-2017 10:25 AM

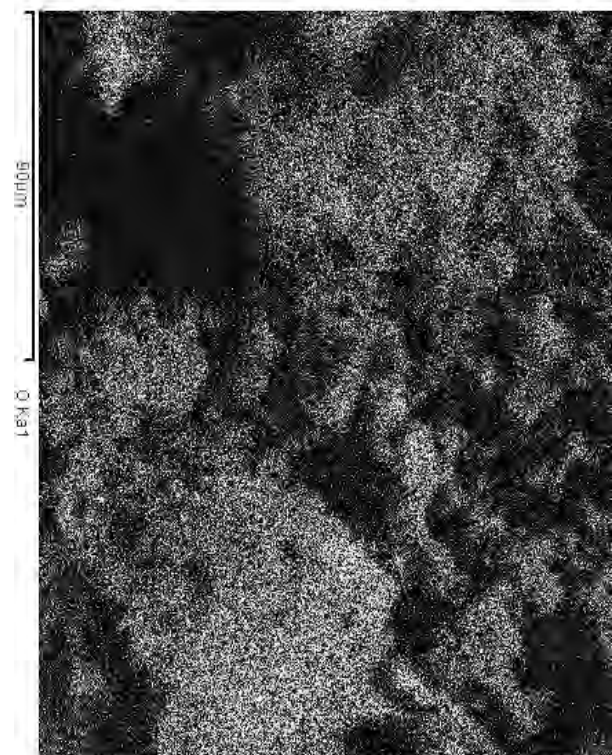
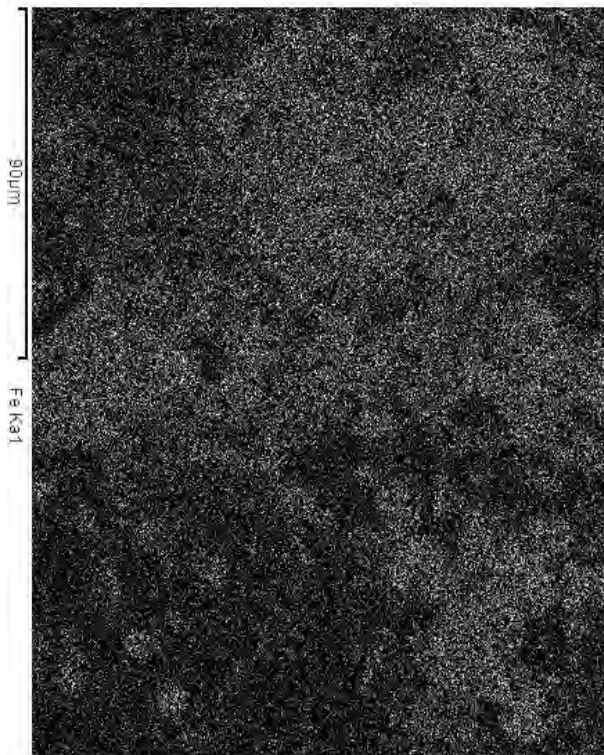
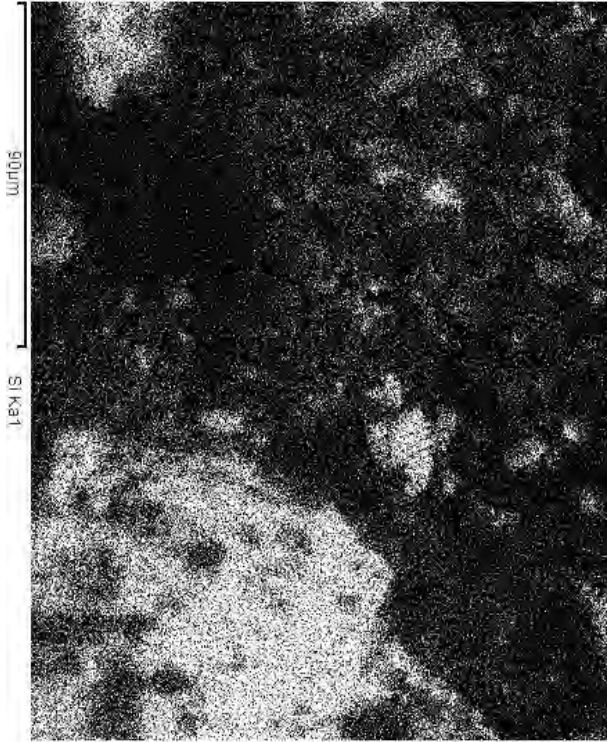
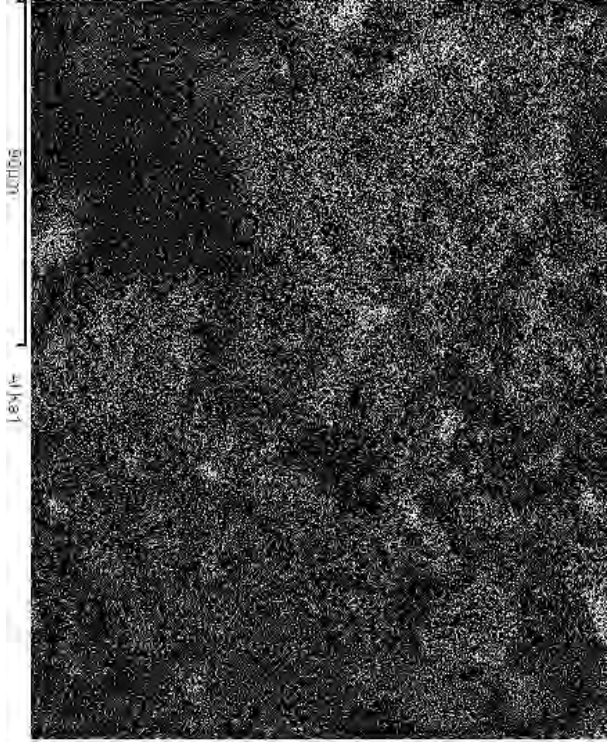
Element	Weight%	Atomic%	Compd%	Formula
C K	8.08	14.20	29.62	CO <sub>2</sub>
Na K	0.31	0.29	0.42	Na <sub>2</sub> O
Mg K	0.10	0.09	0.17	MgO
Al K	2.37	1.86	4.49	Al <sub>2</sub> O <sub>3</sub>
Si K	13.64	10.25	29.18	SiO <sub>2</sub>
K K	0.53	0.29	0.64	K <sub>2</sub> O
Ca K	0.19	0.10	0.27	CaO
Ti K	0.30	0.13	0.49	TiO <sub>2</sub>
Mn K	0.37	0.14	0.48	MnO
Fe K	26.62	10.05	34.24	FeO
O	47.48	62.61		
Totals	100.00			



Elemental mapping of ST3



Elemental mapping of ST3



## Backscattered electron images and EDX-result of AA1 0°C

14/02/2018 11:22:15

Spectrum processing :

Peak possibly omitted : 3.712 keV

Processing option : Oxygen by stoichiometry (Normalised)

Number of iterations = 4

Standard :

C Calcite 18-May-2017 02:38 PM

Al Corundum 15-Sep-2017 01:33 PM

Si MAC Wollastonite 15-Sep-2017 01:48 PM

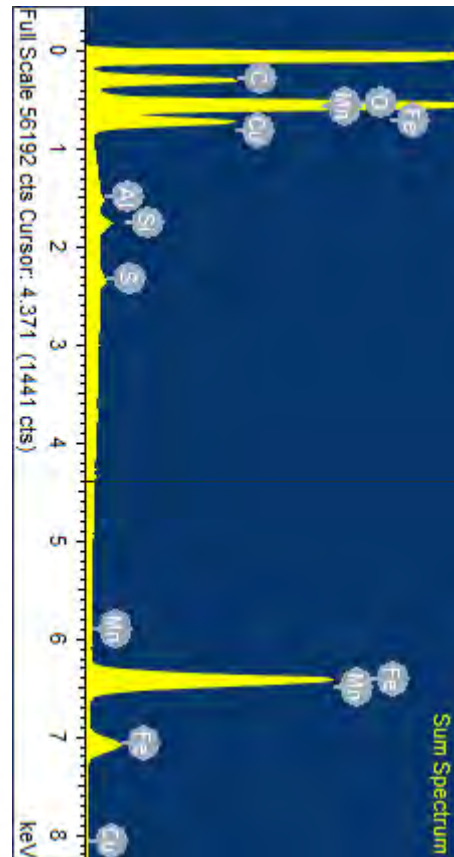
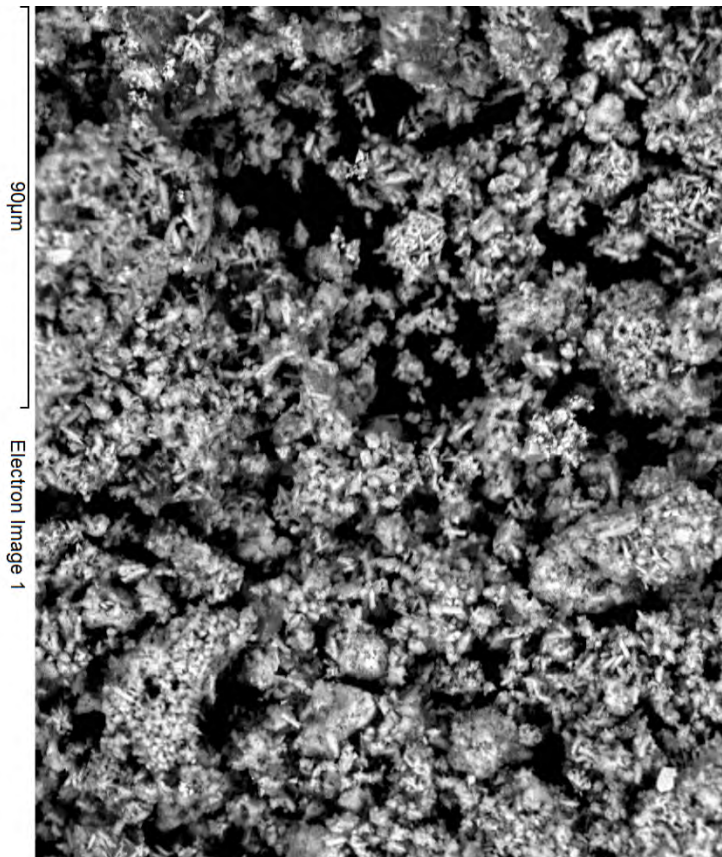
S Anhydrite 15-Sep-2017 02:09 PM

Mn Mn Metal 15-Sep-2017 10:35 AM

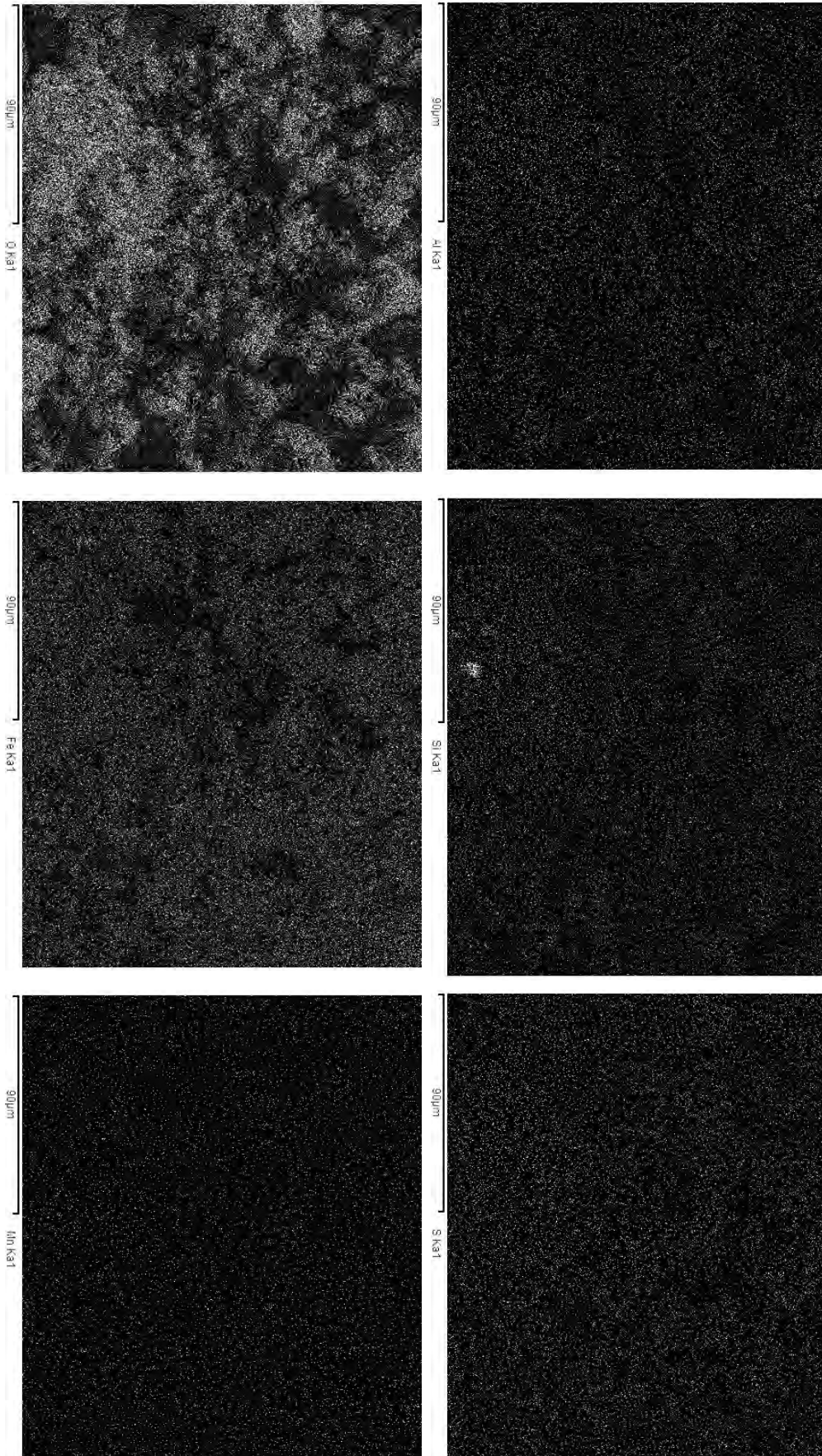
Fe Fe Metal 15-Sep-2017 10:25 AM

Cu Cu 1-Jun-1999 12:00 AM

Element	Weight%	Atomic%	Compd%	Formula
C K	11.44	21.17	41.91	CO2
Al K	0.09	0.07	0.17	Al2O3
Si K	0.26	0.21	0.56	SiO2
S K	0.17	0.12	0.42	SO3
Mn K	0.22	0.09	0.28	MnO
Fe K	43.93	17.48	56.52	FeO
Cu L	0.12	0.04	0.15	CuO
O	43.78	60.82		
Totals	100.00			



Elemental mapping of AÅ1

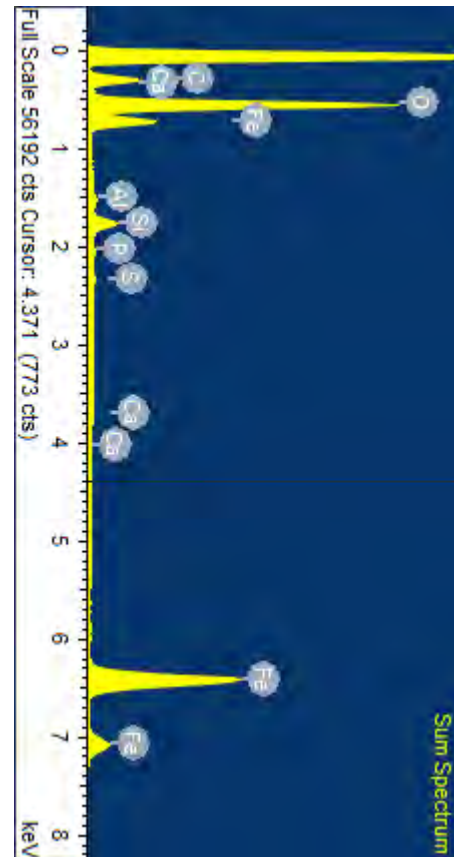
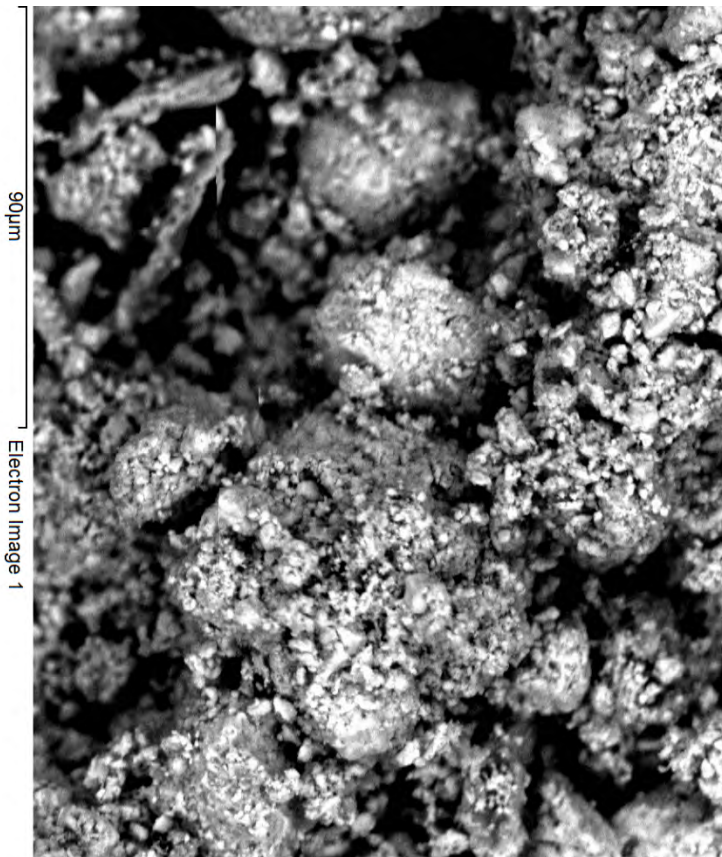


## Backscattered electron images and EDX-result of SR2 0°C

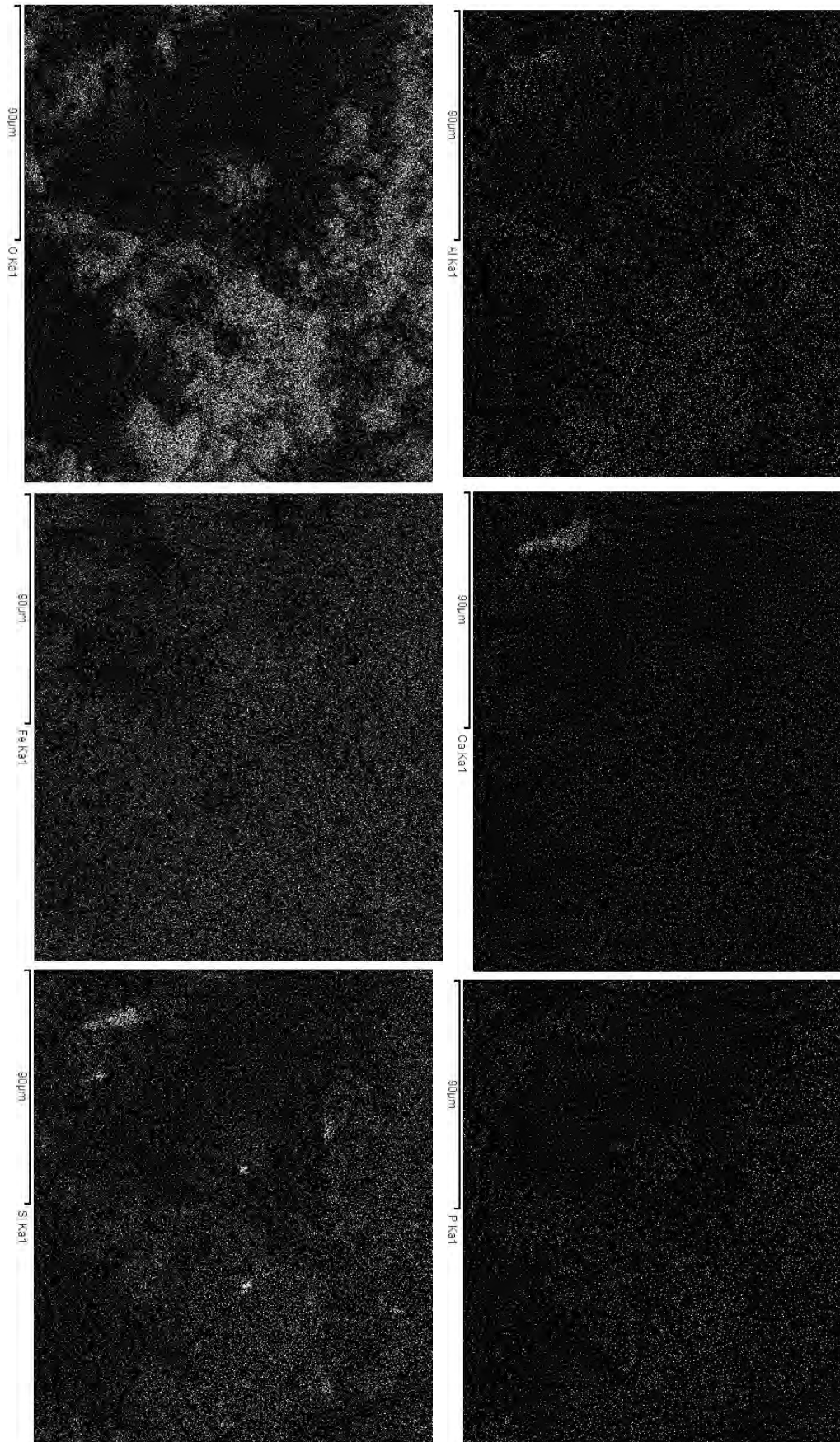
14/02/2018 11:44:26

Spectrum processing :  
 Peak possibly omitted : 4.501 keV  
 Processing option : Oxygen by stoichiometry (Normalised)  
 Number of iterations = 3  
 Standard :  
 C Calcite 18-May-2017 02:38 PM  
 Al Corundum 15-Sep-2017 01:33 PM  
 Si MAC Wollastonite 15-Sep-2017 01:48 PM  
 P Apatite MAC 15-Sep-2017 02:01 PM  
 S Anhydrite 15-Sep-2017 02:09 PM  
 Ca MAC Wollastonite 15-Sep-2017 01:48 PM  
 Fe Fe Metal 15-Sep-2017 10:25 AM

Element	Weight%	Atomic%	Compd%	Formula
C K	8.15	16.72	29.85	CO <sub>2</sub>
Al K	0.16	0.15	0.30	Al <sub>2</sub> O <sub>3</sub>
Si K	1.13	0.99	2.41	SiO <sub>2</sub>
P K	0.09	0.07	0.20	P <sub>2</sub> O <sub>5</sub>
S K	0.08	0.06	0.19	SO <sub>3</sub>
Ca K	0.18	0.11	0.25	CaO
Fe K	51.92	22.91	66.79	FeO
O	38.31	59.00		
Totals	100.00			



Elemental mapping of SR2



## Backscattered electron images and EDX-result of LOB 0\*C

10/04/2018 14:31:05

Spectrum processing :

No peaks omitted

Processing option : Oxygen by stoichiometry (Normalised)

Number of iterations = 3

Standard :

Al Corundum 15-Sep-2017 01:33 PM

Si MAC Wollastonite 15-Sep-2017 01:48 PM

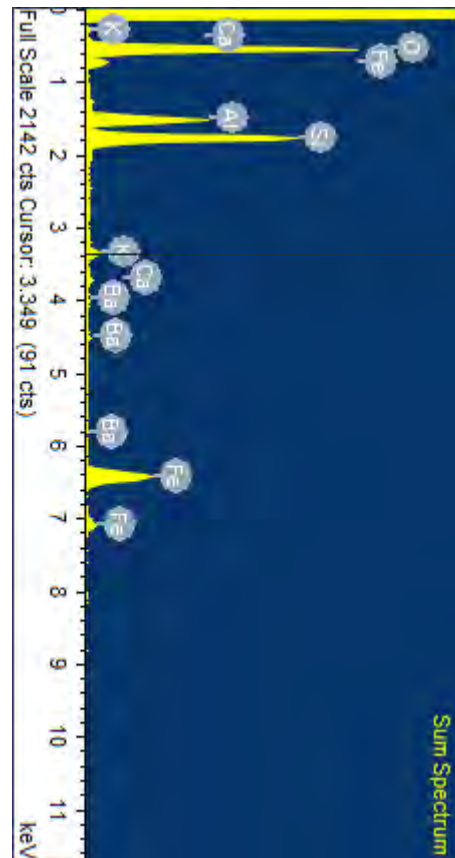
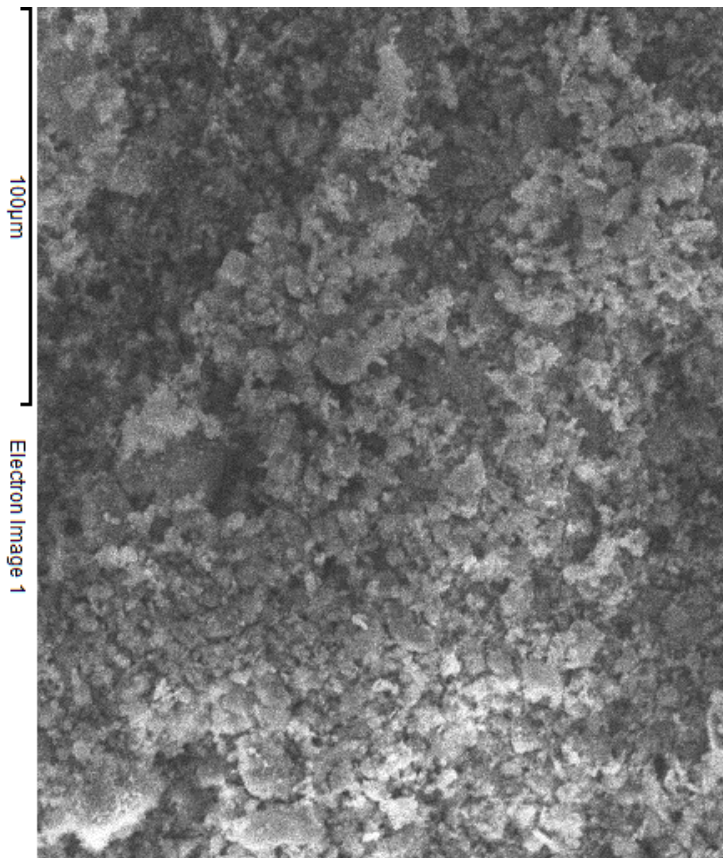
K MAC Orthoclase 15-Sep-2017 01:41 PM

Ca MAC Wollastonite 15-Sep-2017 01:48 PM

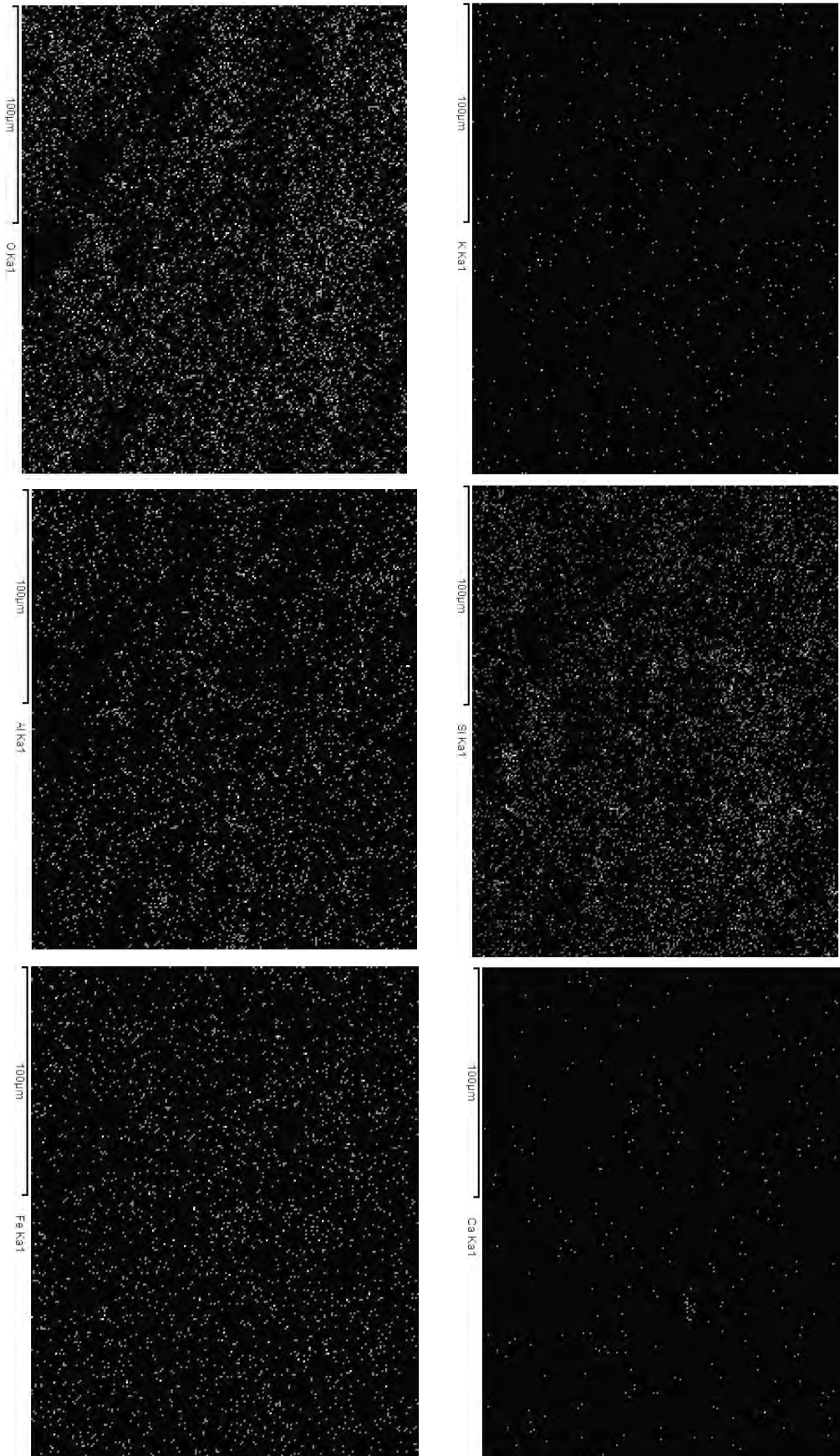
Fe Fe Metal 15-Sep-2017 10:25 AM

Ba BaF2 1-Jun-1999 12:00 AM

Element	Weight%	Atomic%	Compd%	Formula
Al K	11.46	10.18	21.66	Al <sub>2</sub> O <sub>3</sub>
Si K	19.90	16.98	42.58	SiO <sub>2</sub>
K K	1.55	0.95	1.86	K <sub>2</sub> O
Ca K	0.55	0.33	0.77	CaO
Fe K	24.50	10.51	31.52	FeO
Ba L	1.44	0.25	1.60	BaO
O	40.60	60.80		
Totals	100.00			



Elemental mapping of LOB



## Backscattered electron images and EDX-result of YAU 0\*C

10/04/2018 14:23:57

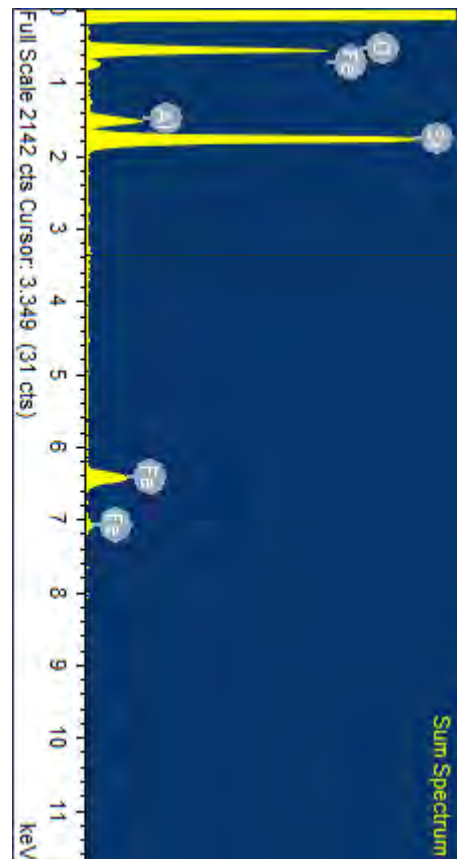
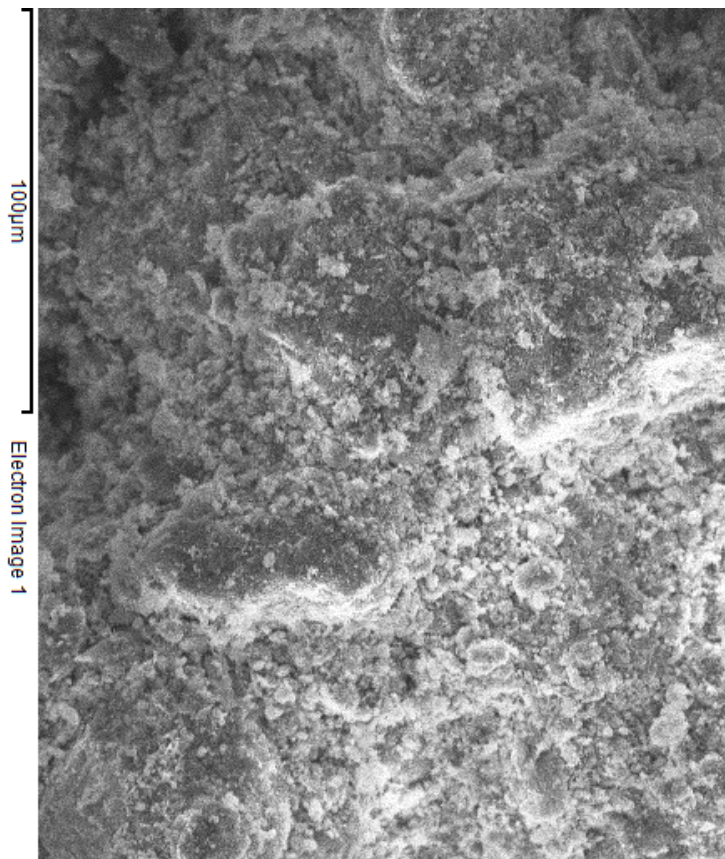
Spectrum processing :  
Peak possibly omitted : 8.010 keV

Processing option : Oxygen by stoichiometry (Normalised)  
Number of iterations = 3

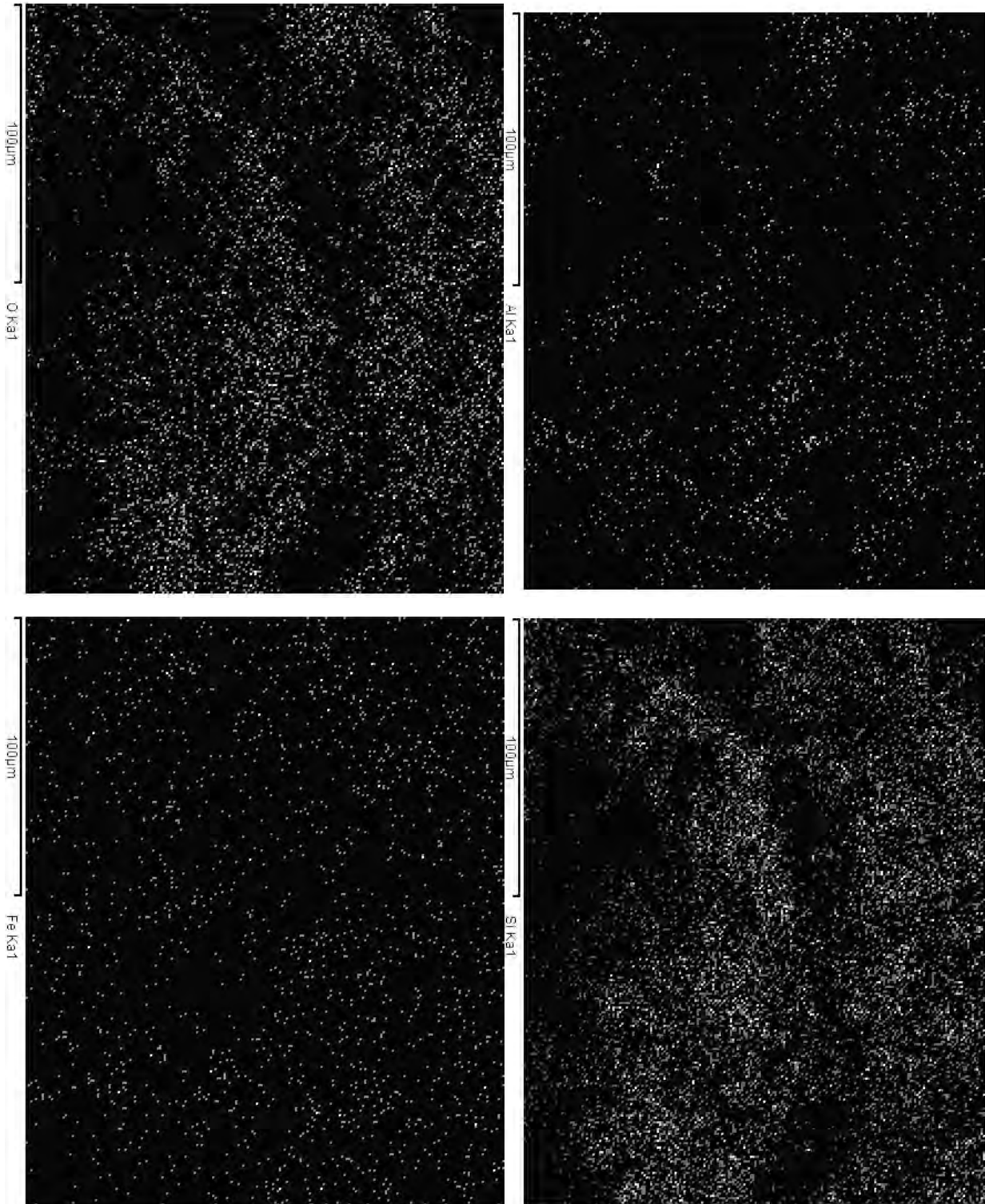
Standard :

Al Corundum 15-Sep-2017 01:33 PM  
Si MAC Wollastonite 15-Sep-2017 01:48 PM  
Fe Fe Metal 15-Sep-2017 10:25 AM

Element	Weight%	Atomic%	Compd%	Formula
Al K	5.21	4.32	9.85	Al <sub>2</sub> O <sub>3</sub>
Si K	31.41	24.98	67.20	SiO <sub>2</sub>
Fe K	17.84	7.13	22.95	FeO
O	45.54	63.57		
Totals	100.00			



Elemental mapping of YAU



## Appendix VII – Complimentary SCiO Images

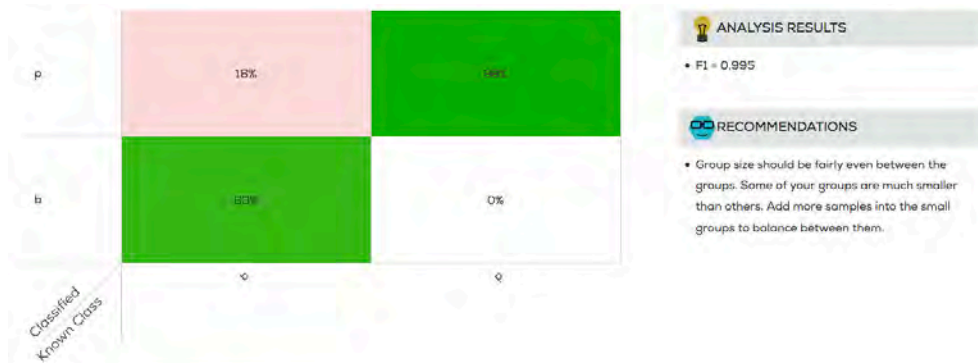


Fig. A: Model made with Subtract average-processing on background scans from the rough side of the rock surfaces (b) and paint on rock slabs (p).

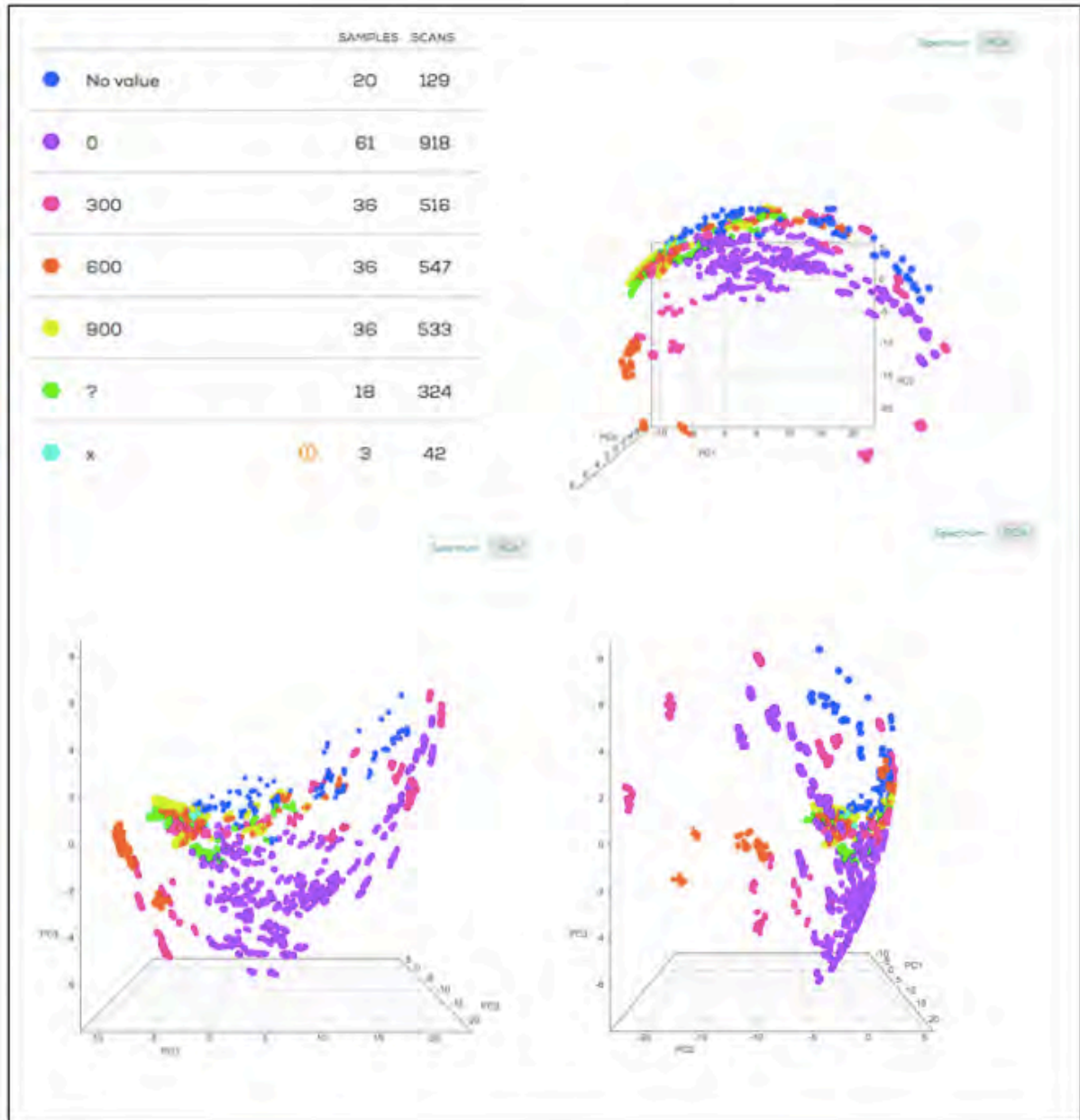


Fig. B: PC1-PC2-plot, PC1-PC3-plot and PC2-PC3-plot of all samples with SNV-processing. The samples are coloured by heating temperature. Blue/No value represent background/rock scans. Green/? represent samples where heating temperature is unknown. Turquoise/x represent HEM samples.

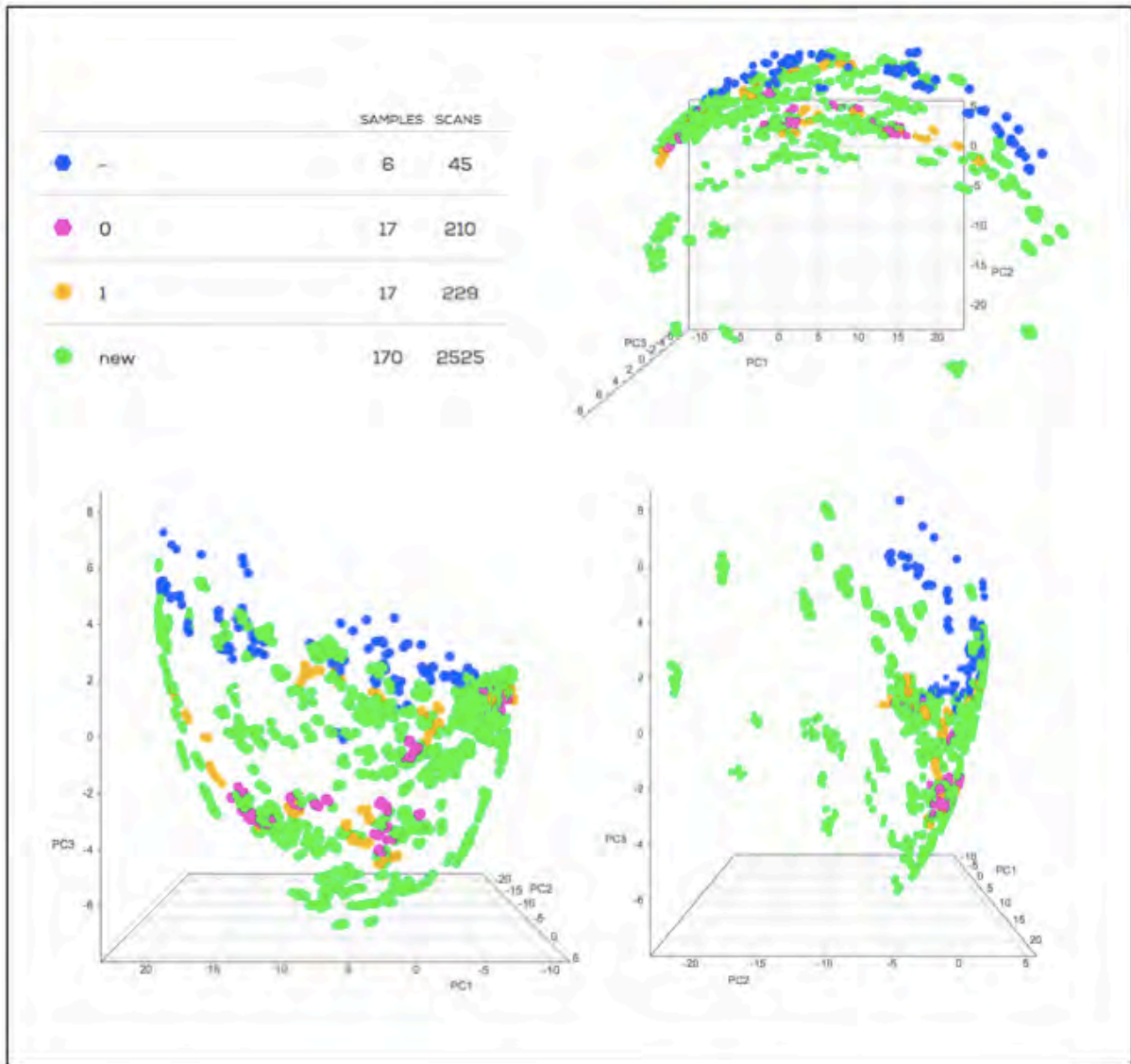


Fig. C: PC1-PC2-plot, PC1-PC3-plot and PC2-PC3-plot of all samples with SNV-processing. The samples are coloured by aging. Blue/- represent background/rock scans. Pink/O represent unexposed samples. Yellow/1 represent exposed samples. Green/new represent new samples.

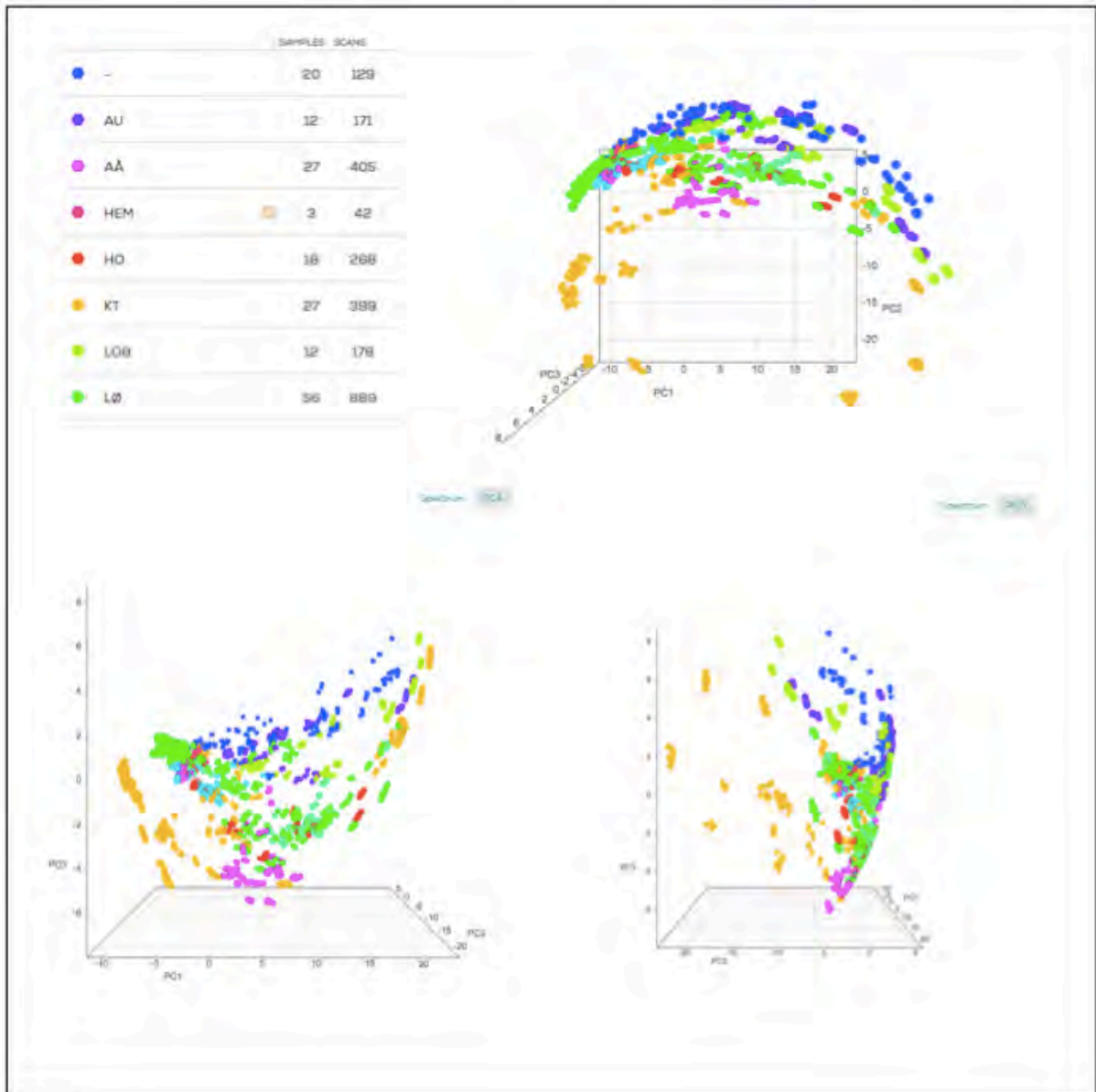


Fig. D: PC1-PC2-plot, PC1-PC3-plot and PC2-PC3-plot of all samples with SNV-processing. The samples are coloured by location. Blue/- represent background/rock scans.

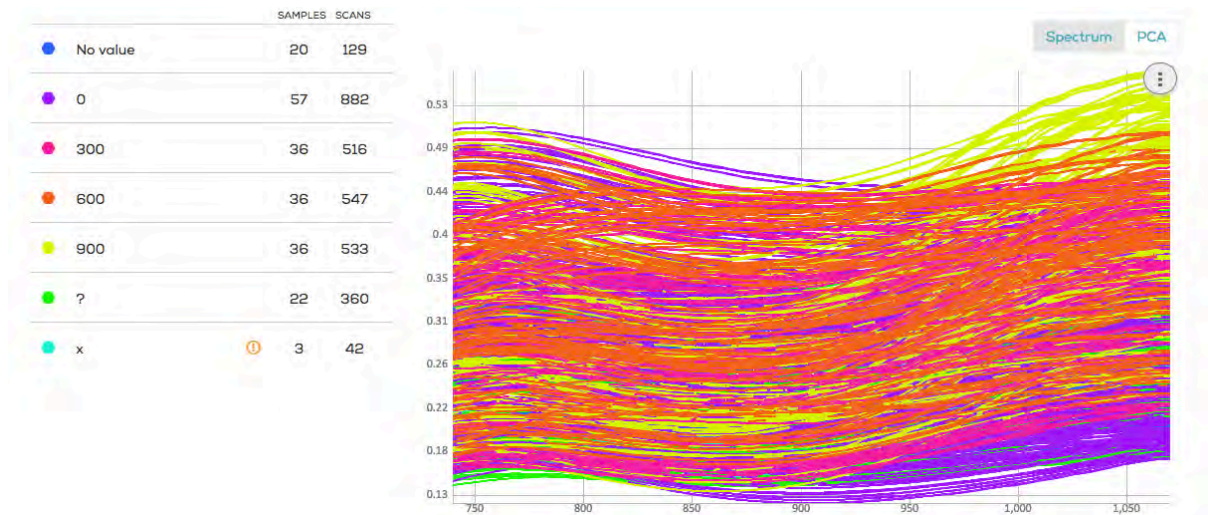


Fig E. Raw spectra of all samples coloured by heating temperature. Blue/No value represent background/rock scans. Green/? represent samples were heating temperature is unknown. Turquoise/x represent HEM samples.

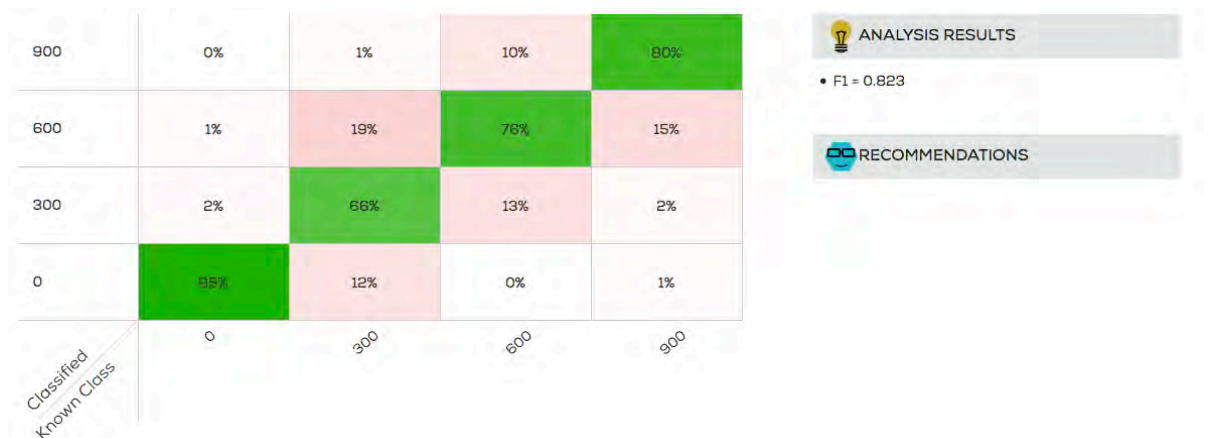


Fig. F: (12: Model made with Subtract average-processing on all painted samples, excluding samples with unknown heating temperature and HEM samples.

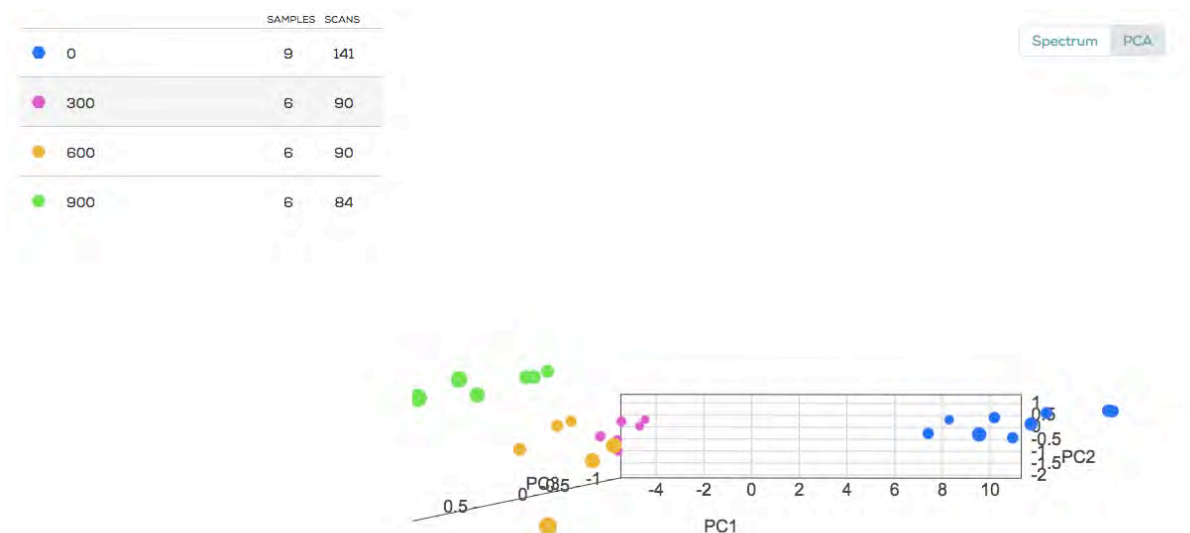


Fig. G 27: PC1-PC2-plot with AÅ samples. Scans have been averaged and log→1st Derivate→SNV-processing. Samples are coloured by heating temperature.

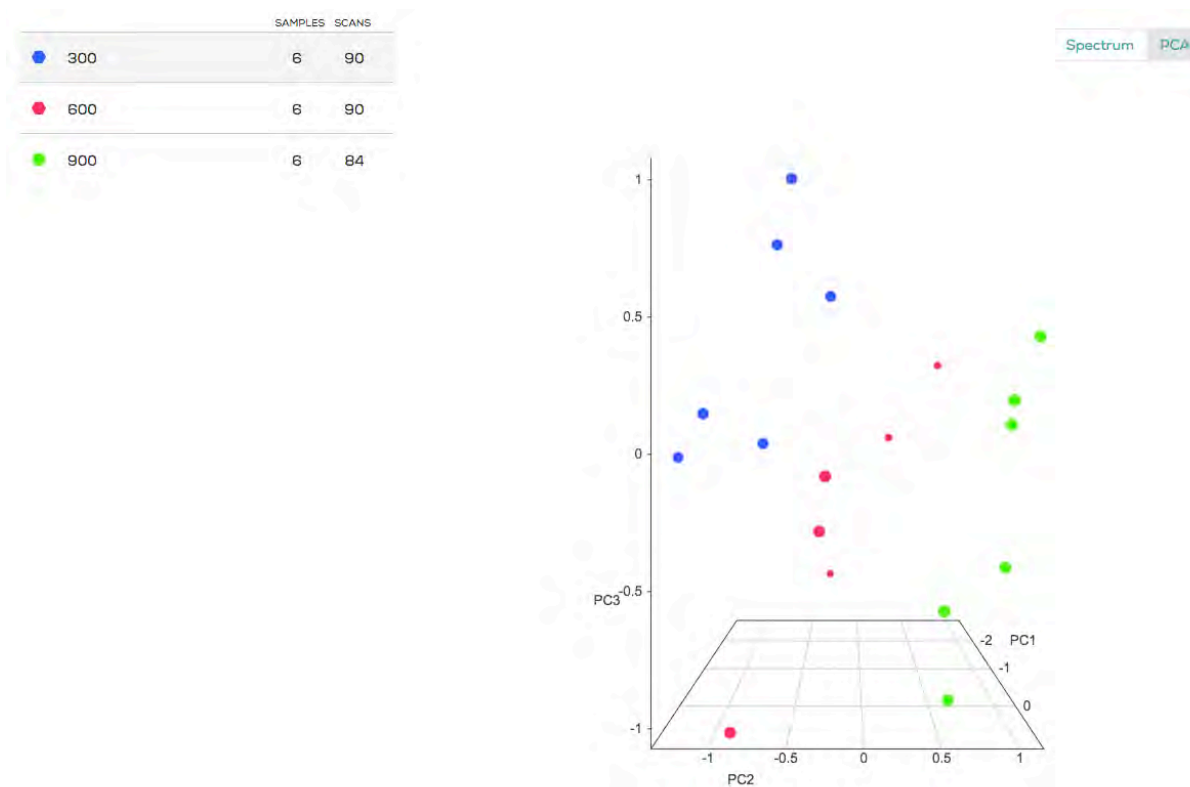


Fig. H: PC2-PC3-plot with AÅ samples. Scans have been averaged and log→1st Derivate→SNV-processing. Samples are coloured by heating temperature.

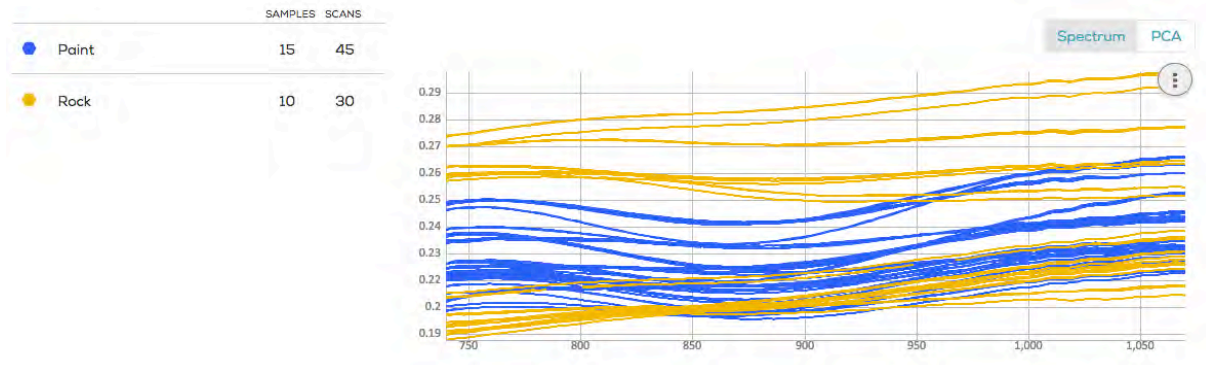


Fig I. Raw spectra Tumlehed scans.

## Appendix VIII – ÅÅ Temperature Model

	All ÅÅ, average scans		
	Colour codes		
	True		
	Makes sense		
	Number of samples used for model:	27	
	Target Attribute:	Heating temperature	
	Preprocessing used:	[Log, AggregateSpectra(aggregation_type='Mean', min_scans_per_batch=5), Derivative(order=1, window=35, poly_deg=2), SN V())]	
	Algorithm used:	RF	
Sample Number	Sample name	Known	Predicted
	y1-2	0	0
	y1-3	0	0
	y1-4	0	600
	y1-5	0	0
	y1-6	0	0
	y2-2	0	0
	y2-3	0	0
	y2-4	0	0
	y2-5	0	0
	y2-6	0	0
	g1	0	0
	g2	0	0
	r1-2	?	300
	r1-3	?	300
	r1-4	?	300
	r1-5	?	600
	r1-6	?	300
	r2-2	?	300
	r2-3	?	300
	r2-4	?	600
	r2-5	?	300
	r2-6	?	600
	h2	0	0
	h1	0	0
	a1	900	300
	a2	900	300
	a3	600	300

Appendix VIII

	a4	600	300
	a5	300	300
	a6	300	0
	a7	900	300
	a8	900	300
	a9	600	300
	a10	600	300
	a11	300	300
	a12	300	300
	a13	0	0
	a14	0	0
	a15	0	0
	a16	0	0
	a17	x	600
	a18	x	900
	b1	900	600
	b2	900	600
	b3	600	600
	b4	600	600
	b5	300	600
	b6	300	300
	b7	900	600
	b8	900	600
	b9	600	600
	b10	600	600
	b11	300	600
	b12	300	300
	b13	900	600
	b14	900	600
	b15	600	600
	b16	600	600
	b17	300	600
	b18	300	300
	c1	900	900
	c2	900	900
	c3	600	0
	c4	600	0
	c5	300	0
	c6	300	0
	c7	900	900
	c8	900	900
	c9	600	0
	c10	600	0
	c11	300	0
	c12	300	0

Appendix VIII

	d1	900	300
	d2	900	900
	d3	600	300
	d4	600	300
	d5	300	300
	d6	300	300
	d7	900	900
	d8	900	900
	d9	600	300
	d10	600	300
	d11	300	600
	d12	300	600
	e1	900	900
	e2	900	900
	e3	600	600
	e4	600	300
	e5	300	300
	e6	300	300
	e7	0	600
	e8	0	0
	e9	0	600
	e10	0	0
	e11	0	0
	e12	0	0
	e13	0	0
	e14	0	0
	e15	0	0
	e16	0	0
	e17	0	600
	e18	0	0
	e19	0	0
	f1	0	0
	f2	0	0
	f3	0	0
	f4	?	300
	f5	?	0
	f6	?	600
	f7	?	0
	f8	?	300
	f9	?	0
	f10	?	0
	f11	?	0
	f18	0	0
	f19	0	0
163	LØ1 powder	0	0

Appendix VIII

164	LØ2 powder	0	0
165	LØ3 powder	0	0
166	KT1 powder	0	0
167	HO1 powder	0	0
168	ST3 powder	?	0
169	AA1 powder	0	0
170	HEM powder	x	900
171	LØ3 powder	300	300
172	LØ3 powder	600	600
173	LØ3 powder	900	600
174	LØ3 powder	300	300
175	LØ3 powder	600	600
176	LØ3 powder	900	600
177	LØ3 powder	300	300
178	LØ3 powder	600	300
180	LØ3 powder	900	600
181	LOB powder	900	300
182	YAU powder	900	300
183	SR2 powder	900	900
184	KT1 powder	900	900
185	KT1 powder	900	900
186	HO1 powder	900	900
189	ST3 powder	900	900
194	KT1 powder	600	0
195	KT1 powder	300	0
196	KT3 powder	0	0
197	KT2 powder	0	0
198	KT1 powder	300	0
199	KT1 powder	600	0
200	HO2 powder	0	0
201	HO3 powder	?	0
202	HO1 powder	300	300
203	HO1 powder	600	300
210	ST1 powder	?	300
211	ST2 powder	?	300
212	ST3 powder	300	600
213	ST3 powder	600	600
214	LOB powder	0	0
215	LOB powder	300	0
216	LOB powder	600	300
218	YAU powder	0	0
219	YAU powder	300	300
220	YAU powder	600	300
221	SR1 powder	0	0
222	SR3 powder	0	0

Appendix VIII

223	SR2 powder	300	300
224	SR2 powder	600	600

F1 calculation	without samples used to make model				
Without temperature=? and x					
Class	0	300	600	900	Total predicted
Predicted 0	45	8	6	0	59
Predicted 300	0	15	12	7	34
Predicted 600	4	6	11	8	29
Predicted 900	0	0	0	15	15
Total 0,300,600 and 900	49	29	29	30	137
0 precision		0,763		0F1	0,833
0 recall		0,918			
300 precision		0,441		300F1	0,476
300 recall		0,517			
600 precision		0,379		600F1	0,379
600 recall		0,379			
900 precision		1,00		900F1	0,667
900 recall		0,5			
			F1	Regular average	0,589
			F1	Weighted average	0,625

## Appendix IX – LØ3 Temperature Model

All LØ avr water+blood			
Colour codes			
True			
Makes sense			
Number of samples used for model:	34		
Target Attribute:	heating temperature		
Pre- processing used:	[Log, AggregateSpectra(aggregation_type='Mean', min_scans_per_batch=5), Derivative(order=1, window=35, poly_deg=2), SNV()]		
Algorithm used:	RF		
Sample Number	Sample name	Known	Predicted
	y1-3	0	0
	y1-4	0	300
	y1-5	0	0
	y2-3	0	0
	y2-4	0	300
	y2-5	0	0
	g1	0	600
	g2	0	0
	r1-2	?	900
	r1-3	?	300
	r1-4	?	600
	r1-5	?	600
	r1-6	?	600
	r2-2	?	300
	r2-3	?	300
	r2-4	?	600
	r2-5	?	300
	r2-6	?	300
	h2	0	0
	h1	0	0
	a1	900	300
	a2	900	300
	a3	600	300
	a4	600	300
	a5	300	300
	a6	300	300
	a7	900	900
	a8	900	900

Appendix IX

	a9	600	900
	a10	600	900
	a11	300	900
	a12	300	900
	a13	0	300
	a14	0	0
	a15	0	300
	a16	0	0
	a17	x	900
	a18	x	900
	c1	900	900
	c2	900	900
	c3	600	0
	c4	600	0
	c5	300	0
	c6	300	0
	c7	900	900
	c8	900	900
	c9	600	0
	c10	600	0
	c11	300	0
	c12	300	0
	c13	900	300
	c14	900	300
	c15	600	300
	c16	600	300
	c17	300	300
	c18	300	300
	d1	900	300
	d2	900	300
	d3	600	900
	d4	600	300
	d5	300	300
	d6	300	300
	d7	900	300
	d8	900	300
	d9	600	300
	d10	600	300
	d11	300	300
	d12	300	300
	d13	900	300
	d14	900	300
	d15	600	300
	d16	600	300
	d17	300	300

Appendix IX

	d18	300	300
	e1	900	300
	e2	900	900
	e3	600	300
	e4	600	300
	e5	300	300
	e6	300	300
	e7	0	300
	e8	0	0
	e9	0	300
	e10	0	0
	e13	0	0
	e14	0	0
	e15	0	300
	e16	0	300
	e17	0	300
	e18	0	0
	e19	0	0
	f1	0	0
	f2	0	0
	f3	0	0
	f4	?	300
	f5	?	300
	f6	?	300
	f7	?	300
	f8	?	300
	f9	?	300
	f10	?	300
	f11	?	300
	f12	0	0
	f13	0	0
	f14	0	0
	f15	0	0
	f16	0	0
	f17	0	0
	f18	0	0
	f19	0	0
163	LØ1 powder	0	0
164	LØ2 powder	0	0
166	KT1 powder	0	0
167	HO1 powder	0	0
168	ST3 powder	?	300
169	AA1 powder	0	0
170	HEM powder	x	900
181	LOB powder	900	600

## Appendix IX

182	YAU powder	900	900
183	SR2 powder	900	300
184	KT1 powder	900	900
185	KT1 powder	900	900
186	HO1 powder	900	300
187	AÅ1 powder	900	300
188	AÅ1 powder	900	300
189	ST3 powder	900	300
194	KT1 powder	600	0
195	KT1 powder	300	0
196	KT3 powder	0	0
197	KT2 powder	0	0
198	KT1 powder	300	0
199	KT1 powder	600	0
200	HO2 powderder	0	0
201	HO3 powder	?	300
202	HO1 powder	300	300
203	HO1 powder	600	300
204	AÅ2 powder	0	0
205	AÅ3 powder	0	0
206	AÅ1 powder	300	300
207	AÅ1 powder	600	300
208	AÅ1 powder	300	300
209	AÅ1 powder	600	300
210	ST1 powder	?	300
211	ST2 powder	?	300
212	ST3 powder	300	300
213	ST3 powder	600	300
214	LOB powder	0	0
215	LOB powder	300	300
216	LOB powder	600	600
218	YAU powder	0	0
219	YAU powder	300	900
220	YAU powder	600	900
221	SR1 powder	0	0
222	SR3 powder	0	600
223	SR2 powder	300	300
224	SR2 powder	600	300

Appendix IX

F1 calculation	without samples used to make model				
Without temperature=? and x					
Class	0	300	600	900	Total predicted
Predicted 0	38	6	6	0	50
Predicted 300	10	18	16	16	60
Predicted 600	2	0	1	1	4
Predicted 900	0	3	4	10	17
Total 0,300,600 and 900	50	27	27	27	131
0 precision		0,765		0F1	0,76
0 recall		0,765			
300 precision		0,3		300F1	0,414
300 recall		0,667			
600 precision		0,25		600F1	0,065
600 recall		0,037			
900 precision		0,59		900F1	0,455
900 recall		0,370			
			F1	Regular average	0,423
			F1	Weighted average	0,482

## Appendix X – KT Temperature Model

All KT avr. model			
Colour codes			
True			
Makes sense			
Number of samples used for model:		27	
Target Attribute:		Heating temperature	
Pre-processing used:		[Log, AggregateSpectra(aggregation_type='Mean', min_scans_per_batch=5), Derivative(order=1, window=35, poly_deg=2), SNV()]	
Algorithm used:		RF	
Sample Number	Sample name	Known	Predicted
	y1-2	0	0
	y1-3	0	0
	y1-4	0	0
	y1-5	0	0
	y1-6	0	0
	y2-2	0	0
	y2-3	0	0
	y2-4	0	0
	y2-5	0	0
	y2-6	0	0
	g1	0	0
	g2	0	0
	r1-2	?	900
	r1-3	?	0
	r1-4	?	900
	r1-5	?	900
	r1-6	?	900
	r2-2	?	900
	r2-3	?	900
	r2-4	?	900
	r2-5	?	900
	r2-6	?	600
	h2	0	0
	h1	0	0
	a1	900	900
	a2	900	900
	a3	600	900
	a4	600	900
	a5	300	0

Appendix X

a6	300	0
a7	900	900
a8	900	900
a9	600	900
a10	600	900
a11	300	900
a12	300	900
a13	0	0
a14	0	0
a15	0	0
a16	0	0
a17	x	900
a18	x	900
b1	900	900
b2	900	900
b3	600	900
b4	600	0
b5	300	600
b6	300	900
b7	900	900
b8	900	900
b9	600	900
b10	600	900
b11	300	900
b12	300	900
b13	900	900
b14	900	900
b15	600	0
b16	600	900
b17	300	600
b18	300	900
c13	900	900
c14	900	900
c15	600	0
c16	600	0
c17	300	900
c18	300	900
d1	900	900
d2	900	900
d3	600	900
d4	600	900
d5	300	900
d6	300	900
d7	900	0
d8	900	0

Appendix X

	d9	600	900
	d10	600	900
	d11	300	0
	d12	300	0
	d13	900	900
	d14	900	900
	d15	600	900
	d16	600	900
	d17	300	900
	d18	300	900
	e1	900	900
	e2	900	900
	e3	600	0
	e4	600	0
	e5	300	900
	e6	300	900
	e7	0	0
	e8	0	0
	e9	0	0
	e10	0	0
	e11	0	0
	e12	0	0
	e19	0	0
	f1	0	0
	f2	0	0
	f3	0	0
	f4	?	0
	f5	?	0
	f6	?	0
	f7	?	0
	f8	?	0
	f9	?	0
	f10	?	0
	f11	?	0
	f12	0	0
	f13	0	0
	f14	0	0
	f15	0	0
	f16	0	0
	f17	0	0
	f18	0	0
	f19	0	0
163	LØ1 powder	0	0
164	LØ2 powder	0	0
165	LØ3 powder	0	0

Appendix X

167	HO1 powder	0	0
168	ST3 powder	?	0
169	AA1 powder	0	0
170	HEM powder	x	900
171	LØ3 powder	300	900
172	LØ3 powder	600	0
173	LØ3 powder	900	900
174	LØ3 powder	300	0
175	LØ3 powder	600	0
176	LØ3 powder	900	900
177	LØ3 powder	300	0
178	LØ3 powder	600	0
180	LØ3 powder	900	900
181	LOB powder	900	900
182	YAU powder	900	900
183	SR2 powder	900	900
186	HO1 powder	900	900
187	AA1 powder	900	900
188	AA1 powder	900	900
189	ST3 powder	900	0
200	HO2 powder	0	0
201	HO3 powder	?	0
202	HO1 powder	300	900
203	HO1 powder	600	900
204	AA2 powder	0	0
205	AA3 powder	0	0
206	AA1 powder	300	900
207	AA1 powder	600	0
208	AA1 powder	300	900
209	AA1 powder	600	900
210	ST1 powder	?	0
211	ST2 powder	?	0
212	ST3 powder	300	0
213	ST3 powder	600	900
214	LOB powder	0	0
215	LOB powder	300	0
216	LOB powder	600	900
218	YAU powder	0	0
219	YAU powder	300	900
220	YAU powder	600	900
221	SR1 powder	0	0
222	SR3 powder	0	0
223	SR2 powder	300	900
224	SR2 powder	600	0

Appendix X

F1 calculation without samples used to make model					
Without temperature=? and x					
Class	0	300	600	900	Total predicted
Predicted 0	39	4	5	2	50
Predicted 300	0	0	12	0	12
Predicted 600	0	2	0	0	2
Predicted 900	0	14	17	18	49
Total 0,300,600 and 900	39	20	34	20	113
0 precision		0,78		0F1	0,876
0 recall		1			
300 precision		0		300F1	0
300 recall		0			
600 precision		0		600F1	0
600 recall		0			
900 precision		0,37		900F1	0,522
900 recall		0,9			
			F1	Regular average	0,350
			F1	Weighted average	0,394

## Appendix XI – Blood versus Water Model

Water or Blood		
Colour code		
Makes sense		
Number of samples used for model:	122	
Target Attribute:	Binding media	
Preprocessing used:	[Log, AggregateSpectra(aggregation_type='Mean', min_scans_per_batch=5)]	
Algorithm used:	RF	
Sample Name and No	Known	Predicted

Sample Number	Sample Name	Known	Predicted
	y1-3	egg	blood
	y1-4	fat	blood
	y1-5	eggofat	blood
	y2-3	egg	blood
	y2-4	fat	blood
	y2-5	eggofat	blood
	r1-3	egg	blood
	r1-4	fat	blood
	r1-5	eggofat	blood
	r2-3	egg	blood
	r2-4	fat	blood
	r2-5	eggofat	blood
163	LØ1 powder	carbon tape	water
164	LØ2 powder	carbon tape	water
165	LØ3 powder	carbon tape	water
166	KT1 powder	carbon tape	water
167	HO1 powder	carbon tape	blood
168	ST3 powder	carbon tape	water
169	AA1 powder	carbon tape	water
170	HEM powder	carbon tape	blood
171	LØ3 powder	carbon tape	blood
172	LØ3 powder	carbon tape	blood
173	LØ3 powder	carbon tape	water
174	LØ3 powder	carbon tape	water
175	LØ3 powder	carbon tape	water
176	LØ3 powder	carbon tape	water
177	LØ3 powder	carbon tape	water
178	LØ3 powder	carbon tape	blood
180	LØ3 powder	carbon tape	water

Appendix XI

181	LOB powder	carbon tape	water
182	YAU powder	carbon tape	water
183	SR2 powder	carbon tape	blood
184	KT1 powder	carbon tape	water
185	KT1 powder	carbon tape	water
186	HO1 powder	carbon tape	water
187	AA1 powder	carbon tape	water
188	AA1 powder	carbon tape	water
189	ST3 powder	carbon tape	water
194	KT1 powder	carbon tape	water
195	KT1 powder	carbon tape	water
196	KT3 powder	carbon tape	water
197	KT2 powder	carbon tape	water
198	KT1 powder	carbon tape	water
199	KT1 powder	carbon tape	water
200	HO2 powder	carbon tape	water
201	HO3 powder	carbon tape	water
202	HO1 powder	carbon tape	water
203	HO1 powder	carbon tape	water
204	AA2 powder	carbon tape	water
205	AA3 powder	carbon tape	water
206	AA1 powder	carbon tape	water
207	AA1 powder	carbon tape	water
208	AA1 powder	carbon tape	water
209	AA1 powder	carbon tape	water
210	ST1 powder	carbon tape	blood
211	ST2 powder	carbon tape	blood
212	ST3 powder	carbon tape	water
213	ST3 powder	carbon tape	water
214	LOB powder	carbon tape	water
215	LOB powder	carbon tape	water
216	LOB powder	carbon tape	water
218	YAU powder	carbon tape	water
219	YAU powder	carbon tape	water
220	YAU powder	carbon tape	water
221	SR1 powder	carbon tape	blood
222	SR3 powder	carbon tape	blood
223	SR2 powder	carbon tape	water
224	SR2 powder	carbon tape	water

Appendix XI

F1 calculation without samples used to make model				
Class	blood	water		Total predicted
Predicted blood	12	9		21
Predicted water	0	47		47
Total blood and water	12	56		68
blood precision	0,571		dF1	0,727
blood recall	1			
water precision	1		sF1	0,915
water recall	0,839			
		F1	Regular average	0,820
		F1	Weighted average	0,880

## Appendix XII – 0°C Model

All 0°C			
Colour code			
True			
Number of samples used for model:		61	
Target Attribute:		dk,se or other	
Preprocessing used:		[Log, AggregateSpectra(aggregation_type='Mean', min_scans_per_batch=5), Derivative(order=1, window=35, poly_deg=2)]	
Algorithm used:		RF	
Sample Number	sample name	Known	Predicted
	r1-2	d	s
	r1-3	d	s
	r1-4	d	s
	r1-5	d	s
	r1-6	d	s
	r2-2	d	s
	r2-3	d	s
	r2-4	d	s
	r2-5	d	s
	r2-6	d	s
	a1	o	o
	a2	o	s
	a3	o	s
	a4	o	s
	a5	o	o
	a6	o	o
	a7	o	s
	a8	o	s
	a9	o	d
	a10	o	s
	a11	o	d
	a12	o	s
	a17	o	s
	a18	o	s
	b1	d	s
	b2	d	s
	b3	d	s
	b4	d	s
	b5	d	s
	b6	d	s
	b7	d	s

Appendix XII

	b8	d	s
	b9	d	s
	b10	d	s
	b11	d	s
	b12	d	s
	b13	d	s
	b14	d	s
	b15	d	s
	b16	d	s
	b17	d	s
	b18	d	s
	c1	s	s
	c2	s	s
	c3	s	s
	c4	s	s
	c5	s	s
	c6	s	s
	c7	s	s
	c8	s	s
	c9	s	s
	c10	s	s
	c11	s	s
	c12	s	s
	c13	s	s
	c14	s	s
	c15	s	s
	c16	s	s
	c17	s	s
	c18	s	s
	d1	s	s
	d2	s	s
	d3	s	s
	d4	s	s
	d5	s	s
	d6	s	s
	d7	s	s
	d8	s	s
	d9	s	s
	d10	s	s
	d11	s	s
	d12	s	s
	d13	s	s
	d14	s	s
	d15	s	s
	d16	s	s

Appendix XII

	d17	s	s
	d18	s	s
	e1	s	s
	e2	s	s
	e3	s	s
	e4	s	s
	e5	s	s
	e6	s	s
	f4	s	s
	f5	s	s
	f6	s	s
	f7	s	s
	f8	s	s
	f9	s	s
	f10	s	s
	f11	s	s
168	ST3 powder	s	s
170	HEM powder	o	s
171	LØ3 powder	d	s
172	LØ3 powder	d	s
173	LØ3 powder	d	s
174	LØ3 powder	d	s
175	LØ3 powder	d	s
176	LØ3 powder	d	s
177	LØ3 powder	d	s
178	LØ3 powder	d	s
180	LØ3 powder	d	s
181	LOB powder	o	d
182	YAU powder	o	s
183	SR2 powder	s	s
184	KT1 powder	s	s
185	KT1 powder	s	s
186	HO1 powder	s	s
187	AA1 powder	s	s
188	AA1 powder	s	s
189	ST3 powder	s	s
194	KT1 powder	s	s
195	KT1 powder	s	s
198	KT1 powder	s	s
199	KT1 powder	s	s
201	HO3 powder	s	s
202	HO1 powder	s	s
203	HO1 powder	s	s
206	AA1 powder	s	s
207	AA1 powder	s	s

Appendix XII

208	AA1 powder	s	s
209	AA1 powder	s	s
210	ST1 powder	s	s
211	ST2 powder	s	s
212	ST3 powder	s	s
213	ST3 powder	s	s
215	LOB powder	o	s
216	LOB powder	o	s
219	YAU powder	o	s
220	YAU powder	o	s
223	SR2 powder	s	s
224	SR2 powder	s	s

F1 calculation without samples used to make model				
Class	d	s	o	Total predicted
Predicted d	0	0	3	3
Predicted s	37	75	15	127
Predicted o	0	0	3	3
Total d, s and o	37	75	21	133
d precision	0		dF1	0
d recall	0			
s precision	0,591		sF1	0,743
s recall	1			
o precision	1		oF1	0,25
o recall	0,143			
		F1	Regular average	0,331
		F1	Weighted average	0,458

## Appendix XIII – 300°C Model

All 300°C			
Colour code			
True			
Number of samples used for model:		36	
Target Attribute:		dk,se or other	
Preprocessing used:		[Log, AggregateSpectra(aggregation_type='Mean', min_scans_per_batch=5), Derivative(order=1, window=35, poly_deg=2)]	
Algorithm used:		RF	
Sample Number	sample name	Known	Predicted
	y1-2	d	o
	y1-3	d	s
	y1-4	d	s
	y1-5	d	s
	y1-6	d	s
	y2-2	d	s
	y2-3	d	o
	y2-4	d	s
	y2-5	d	o
	y2-6	d	s
	g1	s	s
	g2	s	s
	r1-2	d	o
	r1-3	d	d
	r1-4	d	d
	r1-5	d	d
	r1-6	d	d
	r2-2	d	d
	r2-3	d	d
	r2-4	d	d
	r2-5	d	d
	r2-6	d	d
	h2	s	o
	h1	s	o
	a1	o	o
	a2	o	o
	a3	o	o
	a4	o	o
	a7	o	o
	a8	o	o
	a9	o	o

Appendix XIII

	a10	o	o
	a13	o	o
	a14	o	o
	a15	o	o
	a16	o	o
	a17	o	d
	a18	o	o
	b1	d	d
	b2	d	d
	b3	d	d
	b4	d	d
	b7	d	d
	b8	d	d
	b9	d	d
	b10	d	d
	b13	d	d
	b14	d	d
	b15	d	d
	b16	d	d
	c1	s	o
	c2	s	o
	c3	s	s
	c4	s	s
	c7	s	o
	c8	s	o
	c9	s	s
	c10	s	s
	c13	s	s
	c14	s	s
	c15	s	s
	c16	s	s
	d1	s	s
	d2	s	s
	d3	s	s
	d4	s	s
	d7	s	s
	d8	s	s
	d9	s	s
	d10	s	s
	d13	s	s
	d14	s	s
	d15	s	s
	d16	s	s
	e1	s	o
	e2	s	o

Appendix XIII

	e3	s	s
	e4	s	s
	e7	d	s
	e8	d	s
	e9	d	s
	e10	d	s
	e11	d	s
	e12	d	s
	e13	s	s
	e14	s	s
	e15	s	s
	e16	s	s
	e17	s	s
	e18	s	s
	e19	s	o
	f1	s	o
	f2	s	s
	f3	s	s
	f4	s	s
	f5	s	s
	f6	s	s
	f7	s	s
	f8	s	s
	f9	s	s
	f10	s	s
	f11	s	s
	f12	s	s
	f13	s	s
	f14	s	s
	f15	s	s
	f16	s	s
	f17	s	s
	f18	s	o
	f19	s	o
163	LØ1 powder	d	s
164	LØ2 powder	d	s
165	LØ3 powder	d	s
166	KT1 powder	s	s
167	HO1 powder	s	s
168	ST3 powder	s	s
169	AA1 powder	s	s
170	HEM powder	o	o
172	LØ3 powder	d	d
173	LØ3 powder	d	d
175	LØ3 powder	d	d

Appendix XIII

176	LØ3 powder	d	d
178	LØ3 powder	d	d
180	LØ3 powder	d	d
181	LOB powder	o	o
182	YAU powder	o	o
183	SR2 powder	s	s
184	KT1 powder	s	d
185	KT1 powder	s	d
186	HO1 powder	s	s
187	AA1 powder	s	s
188	AA1 powder	s	s
189	ST3 powder	s	s
194	KT1 powder	s	s
196	KT3 powder	s	s
197	KT2 powder	s	s
199	KT1 powder	s	s
200	HO2 powder	s	s
201	HO3 powder	s	s
203	HO1 powder	s	s
204	AA2 powder	s	s
205	AA3 powder	s	s
207	AA1 powder	s	s
209	AA1 powder	s	s
210	ST1 powder	s	s
211	ST2 powder	s	s
213	ST3 powder	s	s
214	LOB powder	o	o
216	LOB powder	o	o
218	YAU powder	o	o
220	YAU powder	o	o
221	SR1 powder	s	o
222	SR3 powder	s	s
224	SR2 powder	s	s

F1 calculation without samples used to make model				
Class	d	s	o	Total Predicted
Predicted d	27	2	1	30
Predicted s	16	71	0	87
Predicted o	4	13	20	37
Total d, s and o	47	86	21	154

Appendix XIII

d precision	0,9		dF1	0,701
d recall	0,574			
s precision	0,816		sF1	0,821
s recall	0,826			
o precision	0,541		oF1	0,690
o recall	0,952			
		F1	Regular average	0,737
		F1	Weighted average	0,766

## Appendix XIV – 600°C Model

All 600°C			
Colour code			
True			
Number of samples used for model:		36	
Target Attribute:		dk,se or other	
Preprocessing used:		[Log, AggregateSpectra(aggregation_type='Mean', min_scans_per_batch=5), Derivative(order=1, window=35, poly_deg=2)]	
Algorithm used:		RF	
Sample Number	sample name	Known	Predicted
	y1-2	d	o
	y1-3	d	s
	y1-4	d	s
	y1-5	d	o
	y1-6	d	o
	y2-2	d	o
	y2-3	d	o
	y2-4	d	o
	y2-5	d	o
	y2-6	d	s
	g1	s	s
	g2	s	o
	r1-2	d	o
	r1-3	d	s
	r1-4	d	d
	r1-5	d	d
	r1-6	d	d
	r2-2	d	d
	r2-3	d	s
	r2-4	d	d
	r2-5	d	s
	r2-6	d	s
	h2	s	s
	h1	s	o
	a1	o	o
	a2	o	o
	a5	o	o
	a6	o	o
	a7	o	o
	a8	o	o
	a11	o	o

Appendix XIV

	a12	o	o
	a13	o	o
	a14	o	o
	a15	o	o
	a16	o	o
	a17	o	d
	a18	o	s
	b1	d	d
	b2	d	d
	b5	d	d
	b6	d	d
	b7	d	d
	b8	d	d
	b11	d	d
	b12	d	d
	b13	d	d
	b14	d	d
	b17	d	d
	b18	d	d
	c1	s	s
	c2	s	d
	c5	s	s
	c6	s	s
	c7	s	s
	c8	s	d
	c11	s	s
	c12	s	s
	c13	s	s
	c14	s	s
	c17	s	s
	c18	s	s
	d1	s	s
	d2	s	s
	d5	s	s
	d6	s	s
	d7	s	s
	d8	s	s
	d11	s	s
	d12	s	s
	d13	s	s
	d14	s	s
	d17	s	s
	d18	s	s
	e1	s	s
	e2	s	s

Appendix XIV

	e5	s	s
	e6	s	s
	e7	d	o
	e8	d	s
	e9	d	o
	e10	d	o
	e11	d	o
	e12	d	o
	e13	s	o
	e14	s	o
	e15	s	s
	e16	s	o
	e17	s	s
	e18	s	s
	e19	s	o
	f1	s	o
	f2	s	s
	f3	s	s
	f4	s	s
	f5	s	s
	f6	s	s
	f7	s	s
	f8	s	s
	f9	s	s
	f10	s	s
	f11	s	s
	f12	s	s
	f13	s	s
	f14	s	s
	f15	s	s
	f16	s	s
	f17	s	s
	f18	s	o
	f19	s	o
163	LØ1 powder	d	o
164	LØ2 powder	d	d
165	LØ3 powder	d	o
166	KT1 powder	s	o
167	HO1 powder	s	o
168	ST3 powder	s	s
169	AA1 powder	s	s
170	HEM powder	o	s
171	LØ3 powder	d	o
173	LØ3 powder	d	d
174	LØ3 powder	d	d

Appendix XIV

176	LØ3 powder	d	d
177	LØ3 powder	d	d
180	LØ3 powder	d	d
181	LOB powder	o	o
182	YAU powder	o	o
183	SR2 powder	s	s
184	KT1 powder	s	d
185	KT1 powder	s	d
186	HO1 powder	s	s
187	AA1 powder	s	s
188	AA1 powder	s	s
189	ST3 powder	s	s
195	KT1 powder	s	s
196	KT3 powder	s	s
197	KT2 powder	s	s
198	KT1 powder	s	s
200	HO2 powder	s	o
201	HO3 powder	s	s
202	HO1 powder	s	s
204	AA2 powder	s	s
205	AA3 powder	s	s
206	AA1 powder	s	s
208	AA1 powder	s	s
210	ST1 powder	s	s
211	ST2 powder	s	s
212	ST3 powder	s	d
214	LOB powder	o	o
215	LOB powder	o	o
218	YAU powder	o	o
219	YAU powder	o	o
221	SR1 powder	s	o
222	SR3 powder	s	o
223	SR2 powder	s	s

F1 calculation without samples used to make model				
Class	d	s	o	Total predicted
Predicted d	16	5	1	22
Predicted s	8	66	2	76
Predicted o	16	14	14	44
Total d, s and o	40	85	17	142

Appendix XIV

d precision	0,727		dF1	0,516
d recall	0,4			
s precision	0,868		sF1	0,820
s recall	0,776			
o precision	0,318		oF1	0,459
o recall	0,824			
		F1	Regular average	0,598
		F1	Weighted average	0,691

## Appendix XV – 900°C Model

All 900°C			
Colour code			
True			
Number of samples used for model	36		
Target Attribute	dk,se or other		
Preprocessing used:	[Log, AggregateSpectra(aggregation_type='Mean', min_scans_per_batch=5), Derivative(order=1, window=35, poly_deg=2)]		
Algorithm used:	RF		
Sample Number	Sample name	Known	Predicted
	y1-2	d	o
	y1-3	d	o
	y1-4	d	o
	y1-5	d	d
	y1-6	d	o
	y2-2	d	o
	y2-3	d	o
	y2-4	d	o
	y2-5	d	o
	y2-6	d	d
	g1	s	o
	g2	s	o
	r1-2	d	o
	r1-3	d	d
	r1-4	d	d
	r1-5	d	d
	r1-6	d	d
	r2-2	d	d
	r2-3	d	s
	r2-4	d	d
	r2-5	d	d
	r2-6	d	d
	h2	s	o
	h1	s	o
	a3	o	o
	a4	o	o
	a5	o	o
	a6	o	o
	a9	o	o
	a10	o	o

Appendix XV

	a11	o	o
	a12	o	o
	a13	o	o
	a14	o	o
	a15	o	o
	a16	o	o
	a17	o	s
	a18	o	s
	b3	d	d
	b4	d	d
	b5	d	d
	b6	d	d
	b9	d	d
	b10	d	d
	b11	d	d
	b12	d	d
	b15	d	d
	b16	d	d
	b17	d	d
	b18	d	d
	c3	s	s
	c4	s	s
	c5	s	s
	c6	s	s
	c9	s	s
	c10	s	d
	c11	s	s
	c12	s	s
	c15	s	s
	c16	s	s
	c17	s	s
	c18	s	s
	d3	s	s
	d4	s	s
	d5	s	s
	d6	s	s
	d9	s	s
	d10	s	s
	d11	s	s
	d12	s	s
	d15	s	s
	d16	s	s
	d17	s	s
	d18	s	s
	e3	s	s

## Appendix XV

	e4	s	s
	e5	s	s
	e6	s	s
	e7	d	d
	e8	d	d
	e9	d	o
	e10	d	o
	e11	d	d
	e12	d	o
	e13	s	d
	e14	s	o
	e15	s	d
	e16	s	o
	e17	s	d
	e18	s	d
	e19	s	o
	f1	s	o
	f2	s	d
	f3	s	d
	f4	s	s
	f5	s	s
	f6	s	d
	f7	s	d
	f8	s	o
	f9	s	o
	f10	s	s
	f11	s	o
	f12	s	d
	f13	s	d
	f14	s	s
	f15	s	s
	f16	s	s
	f17	s	s
	f18	s	o
	f19	s	o
163	LØ1 powder	d	d
164	LØ2 powder	d	d
165	LØ3 powder	d	o
166	KT1 powder	s	d
167	HO1 powder	s	o
168	ST3 powder	s	d
169	AA1 powder	s	d
170	HEM powder	o	s
171	LØ3 powder	d	o
172	LØ3 powder	d	d

Appendix XV

174	LØ3 powder	d	d
175	LØ3 powder	d	d
177	LØ3 powder	d	d
178	LØ3 powder	d	d
194	KT1 powder	s	s
195	KT1 powder	s	s
196	KT3 powder	s	s
197	KT2 powder	s	d
198	KT1 powder	s	d
199	KT1 powder	s	s
200	HO2 powder	s	d
201	HO3 powder	s	s
202	HO1 powder	s	s
203	HO1 powder	s	s
204	AA2 powder	s	s
205	AA3 powder	s	s
206	AA1 powder	s	s
207	AA1 powder	s	s
208	AA1 powder	s	s
209	AA1 powder	s	s
210	ST1 powder	s	d
211	ST2 powder	s	d
212	ST3 powder	s	d
213	ST3 powder	s	s
214	LOB powder	o	o
215	LOB powder	o	o
216	LOB powder	o	o
218	YAU powder	o	o
219	YAU powder	o	o
220	YAU powder	o	o
221	SR1 powder	s	o
222	SR3 powder	s	o
223	SR2 powder	s	s
224	SR2 powder	s	s

F1 calculation without samples used to make model				
Class	d	s	o	Total predicted
Predicted d	32	20	0	52
Predicted s	1	50	3	54
Predicted o	14	16	18	48
Total d, s and o	47	86	21	154

Appendix XV

d precision	0,615		dF1	0,646
d recall	0,681			
s precision	0,926		sF1	0,714
s recall	0,581			
o precision	0,375		oF1	0,522
o recall	0,857			
		F1	Regular average	0,627
		F1	Weighted average	0,667